Online ISSN : 2249-4626
Print ISSN : 0975-5896
DOI : 10.17406/GJSFR

Global Journal

of Science Frontier Research: A

Physics and Space Science

Leave-Intercalation Theory

Phenomenon of the Fifth Cosmic Force

Highlights

Discussion of Quantum Theory

Storage Process of Lithium-ion Battery

Discovering Thoughts, Inventing Future

VOLUME 23 ISSUE 6 VERSION 1.0

Global Journal of Science Frontier Research: A
Physics & Space Science

Global Journal of Science Frontier Research: A
Physics & Space Science

Volume 23 Issue 6 (Ver. 1.0)

Open Association of Research Society

Incorporation No.: 0423089
License No.: 42125/022010/1186
Registration No.: 430374
Import-Export Code: 1109007027
Employer Identification Number (EIN):
USA Tax ID: 98-0673427

Global Journals Inc.

*(A Delaware USA Incorporation with "Good Standing"; **Reg. Number: 0423089**)*
Sponsors: Open Association of Research Society
Open Scientific Standards

Publisher's Headquarters office

Global Journals® Headquarters
945th Concord Streets,
Framingham Massachusetts Pin: 01701,
United States of America
USA Toll Free: +001-888-839-7392
USA Toll Free Fax: +001-888-839-7392

Offset Typesetting

Global Journals Incorporated
2nd, Lansdowne, Lansdowne Rd., Croydon-Surrey,
Pin: CR9 2ER, United Kingdom

Packaging & Continental Dispatching

Global Journals Pvt Ltd
E-3130 Sudama Nagar, Near Gopur Square,
Indore, M.P., Pin:452009, India

Find a correspondence nodal officer near you

To find nodal officer of your country, please email us at *local@globaljournals.org*

eContacts

Press Inquiries: *press@globaljournals.org*
Investor Inquiries: *investors@globaljournals.org*
Technical Support: *technology@globaljournals.org*
Media & Releases: *media@globaljournals.org*

Pricing (Excluding Air Parcel Charges):

Yearly Subscription (Personal & Institutional)
250 USD (B/W) & 350 USD (Color)

Editorial Board

Global Journal of Science Frontier Research

Contents of the Issue

i. Copyright Notice
ii. Editorial Board Members
iii. Chief Author and Dean
iv. Contents of the Issue

1. Research and Discussion of Quantum Theory. *1-23*
2. On Physical Parameters of the Stellarator Reactor with Regard to Recycling and Anomalous Diffusion Losses. *25-35*
3. Holographic Phenomenon of the Fifth Cosmic Force. *37-43*
4. Leave-Intercalation Theory and Conductive Mechanism during Charge-Discharge Process for Secondary Battery. *45-60*
5. Study on the Mechanism of Cycle and Storage Process of Lithium-Ion Battery. *61-81*
6. What does the Wave Function Represent?. *83-84*
7. Experimental and Numerical Determination of Limit Velocity for Plasma Thruster. *85-96*

v. Fellows
vi. Auxiliary Memberships
vii. Preferred Author Guidelines
viii. Index

Global Journal of Science Frontier Research: a Physics and Space Science
Volume 23 Issue 6 Version 1.0 Year 2023
Type: Double Blind Peer Reviewed Interenational Research Journal
Publisher: Global Journals
Online ISSN: 2249-4626 & Print ISSN: 0975-5896

Research and Discussion of Quantum Theory

By Zhi-Xun Huang

Communication University of China

Abstract- Quantum information technology mainly includes quantum communication, quantum radar, quantum computer these three aspects, in recent years, rapid development, many countries invested heavily in development. The awarding of the Nobel Prize in Physics in 2022 to three scientists for their work in quantum informatics has further stimulated people's interest in quantum theory, which has been studied and discussed. This paper not only reviews the historical situation, but also thinks and innovates in theory. The main contents of this paper are as follows: It is pointed out that there are fundamental contradictions between relativity and quantum mechanics; The wave function, quantum statistics and uncertainty principle are discussed in detail. The hidden variable theory is reviewed and the Bell inequality is discussed. The Aspect two-photon experiment was analyzed. The rationality of Bohm experiment scheme is discussed. The development of Bell type experiment is discussed. It is pointed out that the entangled state is not acting at a distance but propagating faster than the speed of light. Reviews the Copenhagen interpretation of quantum mechanics; Quantum communication and Wootters theorem are discussed. etc.

Keywords: *quantum mechanics, quantum entanglement states, Bell inequality, relativity.*

GJSFR-A Classification: *LCC: QC174.12*

Research and Discussion of Quantum Theory

Zhi-Xun Huang

Abstract- Quantum information technology mainly includes quantum communication, quantum radar, quantum computer these three aspects, in recent years, rapid development, many countries invested heavily in development. The awarding of the Nobel Prize in Physics in 2022 to three scientists for their work in quantum informatics has further stimulated people's interest in quantum theory, which has been studied and discussed. This paper not only reviews the historical situation, but also thinks and innovates in theory. The main contents of this paper are as follows: It is pointed out that there are fundamental contradictions between relativity and quantum mechanics; The wave function, quantum statistics and uncertainty principle are discussed in detail. The hidden variable theory is reviewed and the Bell inequality is discussed. The Aspect two-photon experiment was analyzed. The rationality of Bohm experiment scheme is discussed. The development of Bell type experiment is discussed. It is pointed out that the entangled state is not acting at a distance but propagating faster than the speed of light. Reviews the Copenhagen interpretation of quantum mechanics; Quantum communication and Wootters theorem are discussed. etc.

This paper holds that quantum mechanics has been finalized from 1926 to 1928, and its basic content has not changed much. But for some of the accusations, it is necessary to answer them theoretically. For example, we believe that the Copenhagen interpretation fundamentally changes our understanding of nature and marks a profound revolution in physics. And no other theory has since emerged that has such a profound understanding and wide application of microscopic phenomena as this interpretation. Another example is Bohm's two-particle correlation spin scheme in quantum entanglement experiments, which has been proved to be effective in a series of experiments, which is an important contribution in Bohm's life.

This paper holds that the so-called quantum field theory is a failure, and the original quantum mechanics should still be advocated today. Current theoretical research should pay great attention to quantum entangled states, because its nature is still unclear.Understanding this "first mystery of the physical world" not only has scientific significance, but also has great philosophical significance for understanding the universe.

Keywords: quantum mechanics, quantum entanglement states, Bell inequality, relativity.

I. Introduction

Quantum mechanics (QM) was established between 1926 and 1928.[1-4] In 1935, A. Einstein, B. Podolsky, and N. Rosen published an article entitled "Is Quantum Mechanics a complete description of physical reality?"[5] The principle of locality echoes Einstein's theory of special relativity (SR), but is inconsistent with quantum mechanics (QM). In 1951, D.Bohm[6] made a modern statement of EPR thinking, which actually started the study of quantum entangled states. On this basis, in 1965, J.Bell[7,8] proposed the hidden variable theory, which was later called Bell inequality, and in 1981-1982, A. Aspect[9,10] did A number of accurate experiments, and the results were inconsistent with Bell inequality, but consistent with QM. Therefore, there is a singular correlation of QM expectations in the two-particle system, but the hyperspace (overdistance) action is contradictory to EPR thinking. In the following decades, the Bell experiment flourished, and the interval of entangled photons gradually increased from 15m at Aspect time to 144km, and in 2017, the Chinese quantum satellite expanded to 1200km, which is very surprising.The errors of EPR papers provide profound lessons for scientific research. The development of quantum communication technology in recent years is based on quantum non-locality and quantum entanglement.

Quantum informatics (QIT) has three main research directions—quantum computing, quantum communication, and quantum radar. The key point of quantum communication is that there must be absolute confidentiality. But this is very difficult in practice, so we cannot say that the problem has been solved so far. The research and development of quantum computers has made great progress in the United States, Japan and China, which are already in a fierce competition with each other. As for quantum radar, the technology to design it entirely around photon entanglement does not yet exist.

In this context, quantum theory has attracted a lot of attention from the scientific community in recent years, and many people who are not physics majors want to understand the meaning of some proper terms— such as wave functions, entangled states, Bell inequalities, hidden parameters, and so on. And it has revived interest in questions about the history of science. It is no accident that the theory of quantum science and related application technologies are developing, and China has not only launched quantum satellites, but also invested huge resources in the research of quantum communication technology on the ground. As for quantum computers, together with artificial intelligence, they have become two hot spots in the world, and their development is related to the future of all mankind. If electricity, nuclear energy, computers, and the Internet are the landmark milestones that humanity has achieved in the past, then we must now

Author: Communication University of China, Beijing 100024.
e-mail: huangzhixun75@163.com

pay attention to the development of quantum information technology and artificial intelligence, because they are bound to dramatically change the face of society and human life.

The basic theory of quantum mechanics was formed in the early 20th century (1926-1928), and its theoretical system has not changed much. But there has always been a lot of theoretical debate, which has been stimulated by developments in recent years. In particular, in 2022, the Nobel Prize in Physics was awarded to three physicists who studied quantum oddities, a development that further boosted interest in studying quantum theory. This paper summarizes the author's views and opinions.

II. There is a Fundamental Contradiction between Relativity and Quantum Mechanics

Relativity (SR, GR)[11-13] and quantum mechanics (QM) are two of the most important scientific theories of the 20th century. Yet relations between the two have been strained. In 1998, UNESCO published the World Report on the Development of Science, with an introductory section entitled "What is the Future of Science?", in which it was stated: "The theory of relativity and quantum mechanics are two of the great academic achievements of the 20th century, but unfortunately the two theories have so far proved to be contradictory. This is a serious problem." It is rare for a disagreement between two scientific ideas to find its way into a UN document.

As we all know, E. Schrödinger created the wave mechanics of QM in the first half of 1926, the core of which is the basic motion equation of QM—Schrödinger equation (SE), which describes the motion change law of the microscopic particle system. According to M. Planck, this equation laid the foundation for quantum mechanics, just as the equations created by Newton, Lagrange, and Hamilton did for classical mechanics. It must be pointed out that SE is derived from Newton mechanics; This fact makes some relativists uncomfortable and therefore insist that SE "only applies to low speed cases (particle velocity v«c)". But they were wrong—the development of optical fiber technology is theoretically supported by SE, and the photons in the optical fiber travel at the speed of light (c), which is not a slow condition at all. Relativists are afraid that SR and GR will be negated one day, so they insist on "splitting the world equally": macroscopic and high-speed phenomena are governed by relativistic tubes, and microscopic and low-speed phenomena are governed by quantum theory. But what about the fact that quantum theory is also valid in the macro sense? !

Some physicists say that the fusion of SR and QM has long been solved in quantum field theory (QFT), with Dirac's successful derivation and application of the quantum wave equation (DE) in 1928. Our view is that these statements are not only false, but have been misleading for years.[14]Although DE's derivation is not directly based on Newton mechanics like SE, it does not really use SR's space-time view and world view. The derivation of DE is derived from two equations about mass, the mass-energy relation and the mass-velocity relation, but both of them can be derived from classical physics before the advent of relativity. The mass-energy relation was put forward by H. Poincare in 1900, and the mass-velocity relation was put forward by H. Lorentz in 1904.Therefore, DE is not actually derived from relativity. Since DE is not necessarily related to SR, it is unacceptable to say that it "represents the combination of SR and QM".

In this case, what reason is there to say that "the Dirac equation represents the establishment of relativistic quantum mechanics"? In fact, in-depth analysis has shown that SR and QM are opposing theoretical systems, and Einstein himself was indeed "lifelong" in his opposition to quantum mechanics. As a result, Weinberg's claim that "the only theory that can make quantum mechanics compatible with relativity is quantum field theory (QFT)" is empty.

Dirac's Nobel lecture, at the age of 31, exuded relief and triumph that he had solved what Schrödinger had failed to do and Klein and Gordon had failed to do, namely, "to derive the wave equations of microscopic particles under the guidance of relativity". But later, although in 1964 (Dirac was 62 years old) he still had the sense that SR was dominant and QM was subordinate, he clearly stated that "there are insurmountable difficulties in establishing relativistic quantum mechanics".[15] In 1978 (at the age of 76)Dirac showed a strong sense of confusion and dissatisfaction: he was fundamentally disenchanted with "the coherence and harmony of relativity and quantum mechanics"; No longer think quantum electrodynamics (QED) is a good theory; He called for a "really big change" in physics.[16]

In short, in his later years Dirac lost his fascination with relativity and gradually distanced himself. This is highlighted by the disparagement of QFT and QED. He said the success of QFT, which includes quantum electrodynamics, has been "extremely limited" and simply does not suffice to describe nature.

Quantum field theory (QFT) was proposed and shaped in the decades after 1927, when the physics community generally accepted relativity as a guiding theory. It was believed that both QM and QFT were subject to the requirements of relativity until 1982, when the famous physicist J. B. ell(among others) publicly criticized Einstein's views in 1985 and strongly supported QM. He also suggested that physics thinking should "go back to before Einstein."By this time, however, elementary particle physics had taken shape, and there was no further study of fundamental questions such as whether the interactions of microscopic

particles really had Lorentz transformation (LT) invariance. However, serious analysis and calculation can prove that LT transformation invariance may not exist in the process of particle physics, and there is a fundamental problem with QFT. The principle of relativity in SR does not hold.

A great debate about QM broke out in the 1920s and 1930s, and it was Einstein who started it. Einstein anticipated the crisis of relativity early on from the rise of QM, and began to deal with it. It is well known that W. Heisenberg won the 1932 Nobel Prize in Physics for his work on matrix mechanics and the uncertainty principle, which were important for the establishment of QM. Einstein, however, was against QM; This began to emerge in 1926 and culminated in 1935, when he published the EPR paper with B. Podolsky, N. Rosen. The localization principle in this paper corresponds to SR; For a separate system (I and II), there can be no out-of-range effect between them. N. Bohr refuted the EPR paper by pointing out that the effect of the uncertainty principle on I and II - II will react when I is measured, regardless of the distance between them. Of course, this discussion is all about microscopic particles.

The author has sorted out the situation of the great debate on quantum mechanics, in fact, only to give a partial contradiction and disagreement (in fact, more than these). Now let's list the two schools of thought on science; Q stands for quantum mechanics (Copenhagen School) view, R stands for relativity view.

a) Wave function

Q. It is believed that the wave function reflects the probability distribution and evolution of microscopic particles in space and time, and actually accurately describes the state of a single system (such as particles).

R. Objects to the notion that "wave functions accurately describe the state of individual systems," and to arbitrary, statistical explanations ("God does not play dice").

b) Uncertainty relation (Uncertainty principle)

Q. It is believed that the operation of microscopic particles has uncertainty that cannot be eliminated, and the law of uncertainty relationship is not only important but also causes unpredictability contrary to causality.

R. Rejects the uncertainty relation, arguing that quantum emission and absorption of light can one day be theorized on the basis of complete causality.

c) Quantum mechanical completeness

Q. That quantum mechanics is complete and correct; QM is a statistical theory, so it can only determine the probability of possible outcomes. There are no hidden variables. It is considered useless to use hidden variables, because these so-called hidden variables do not appear when describing the real process. In fact, no local hidden variable theory can derive all the statistical predictions of QM.

R. Believes that quantum mechanics is incomplete and that there may be deeper physical laws - for example, there may be undiscovered hidden variables that can determine the laws of individual systems. If hidden variables are found, causality still exists. In short, there must be deterministic descriptions of nature, and efforts should continue to pursue better (but now unknown) theories.

d) Wave-particle duality and complementary principle

Q. It is believed that all microscopic particles (whether they have mass or not) have wave-particle duality, sometimes manifested as particles (with a definite orbit), sometimes manifested as waves (can produce interference fringes);It depends on the experimental method of the observer. But it is impossible to observe both at the same time, in fact, the fundamental point is a mutually exclusive and complementary quantum relationship, and any experiment will lead to uncertainty about its conjugate variables; Therefore, the complementarity principle is consistent with the uncertainty relation.

R. As the originator of the photon theory, Einstein has long recognized that it is a contradictory phenomenon that light is both a wave and a particle. However, he did not agree with the uncertainty principle, and thus could not accept Bohr's complementarity theory, which saw uncertainty relations as an illustration and result of the complementarity principle.

e) Quantum entangled states

Q. Bohr immediately refuted the EPR paper after it came out; The author holds that QM has the same mathematical expression form at the beginning and the end, and accuses QM of being incomplete and unconvincing. The so-called "reality criterion" is not strict. It is suggested that the existence of the interaction of separate systems (I and II) is possible.

R. 1935 EPR paper, the first part of which argues that the QM hypothesis wave function determination contains a complete description of the physical reality of the system. The second part is intended to show that this assumption, together with the criterion of reality, will lead to a contradiction. In general, it denies the completeness of QM, and denies that the system will interact when divided into two parts.

From the above, it can be seen that the local description in relativity is incompatible with particle volatility in QM, and it is also incompatible with allowing particle transformation in QM. In particle physics, the non-relativistic QM is a logically self-consistent single-particle theory, but the premises of relativistic QM are logically inconsistent and difficult to use as an equation

of single-particle motion like SE. So what does relativistic local reality mean? It contains two aspects: physical realism and relativistic local causality. But quantum theory is essentially a non-local theory of space.

III. From Wave Functions, Quantum Statistics to the Uncertainty Principle

Max Born(1882-1970) was a German who taught at universities in Germany and the United Kingdom. In 1954, he was awarded the Nobel Prize in Physics for his work in quantum mechanics, particularly the statistical explanation of the wave function. Born's theory, which appeared in June and October 1926, states that the states of microscopic particles are mainly described by the wave function $\Psi(r,t)$, and the probability of finding a particle in the volume element $d\tau$ at space r at time t is given as $|\Psi(r,t)|^2 d\tau$ given as the probability density of the particle given as (r,t) given as the probability of the particle occurring $|\Psi(r,t)|^2$. Therefore, waves describing microscopic particles are probability waves. In short, when calculating the scattering process, Born realized that the probability of finding a microscopic particle is proportional to the square of the modulus of the wave function, so the wave of a microscopic particle is described as a probability wave. Born's statistical interpretation of the wave function can be applied both to the single behavior of a large number of particles and to the repeated behavior of a single particle many times. Born's theory has been supported by numerous experiments, and also well embodies the wave-particle duality of microscopic particles.

In the first half of 1926, E. Schrödinger proposed non-relativistic quantum wave mechanics. In 1953, Born recalled: "When Schrödinger wave mechanics appeared, I immediately felt that it required a non-deterministic explanation. I guess it Ψ^2 was the probability density, but it took a while to figure out the physical basis. Obviously, a return to determinism is no longer possible.""It is impossible to determine the position of the particle according to the Schrödinger equation, because it is a group of waves with blurred boundaries."

Born realized that the new QM did not allow for deterministic interpretation. Uncertainty relations also emphasize this point. This does not mean that there is no causal relationship in some aspect of nature, but that it cannot be calculated quantitatively. I note, incidentally, that P. Dirac made a similar argument - causality only applies to undisturbed systems (such systems are usually expressed in differential equations); However, under microscopic conditions, it is impossible to disturb the object carelessly while observing (measuring), and the expected causal link cannot be expected.

In "Letter 71" of his 2005 book 《The Born-Einstein Letter》, Einstein said, "I still do not believe that the statistical approach to quantum theory is the final answer, but I am the only one who holds this view."[17]Born commented: "At the end of the letter Einstein again rejects the quantum theory of statistics, but admits that on this point he is isolated.I was pretty sure I was right about that. All theoretical physicists at that time were in fact working in terms of statistical concepts, especially for N.Bohr and his school, which made an important contribution to the clarification of concepts."

In Letter 88 (April 5, 1948), Einstein wrote:

"I am sending you a short article, which I have sent to Switzerland for publication in accordance with Pauli's suggestion. I implore you to overcome your long-held aversion in this regard and read this short article as if you were a guest who had just arrived here from Mars and had not yet formed any opinions of your own. I ask you this not because I am under any illusion that I can influence your opinion, but because I think this essay will help you to understand my main motivation better than any other article of mine you know. ... In any case, I shall listen to your counter-argument with great interest."

Einstein's essay, titled "Quantum Mechanics and Reality," does not contain any mathematical analysis, but rather, in a speculative manner, implicitly criticizes uncertainty relations and proposes that physical ideas are established by such things as objects and fields, and that they are real beings independent of perceptual subjects. Objects separated from each other in space maintain their independence; For example, for two objects (A and B), the outside world acting on A has no direct influence on B, which is the principle of contiguity. However, the interpretation of QM is incompatible with this principle. For a physical system S (S consists of two local subsystems S_1 and S_2), they may have been interacting earlier. At the end of the action, when describing the system in terms of wave functions Ψ, it can be seen in the analysis that it is impossible to maintain both the QM principle and the independent existence of two separate parts in space. Einstein has stated that he insists on the independent existence of different parts of physical reality in space, and that QM is an incomplete description of physical reality. That is to say, the quantum mechanical approach is fundamentally unsatisfactory.

Einstein's essay is similar to the EPR paper in that it's not very new. Only in 1935 it was with N.Bohr, and now (1948) it is with M. Born. Born's reply of May 9 was lengthy, stating: "It seems to me that your axiom of 'the mutual independence of spatially separated objects A and B' is not as convincing as you understand it."It does not take into account the fact of coherence.

Spatially distant objects are not necessarily independent of each other if they have a common origin."

Born added: "At the root of Einstein's and my differences of opinion is the axiom that events at different locations A and B are independent of each other, in the sense that an observation of A state of affairs at B tells us nothing about A state of affairs at A. My argument against this assumption is taken from optics and is based on the concept of coherence. When A beam of light is split by reflection, birefringence, etc., the two beams take different paths, and one can deduce the state of a beam of light at distant point B by observing it at point A. It is strange that Einstein did not recognize this objection to his axioms as valid, even though he had been one of the first theorists to recognize the significance of de Broglie's work on wave mechanics."

Born's scientific work is closely related to Heisenberg's. Born was 19 years older than Heisenberg, who had been his research assistant. The quantum conditions of the old quantum theory were laid down by N.Bohr and A. Sommerfeld, which defined momentum p and position q for the motion of particles. In ordinary mathematics multiplication is subject to exchange rate — $p \cdot q = q \cdot p$;However, now (July 1925) a breakthrough new formulation of quantum conditions was proposed, in which quantum multiplication does not obey the exchange rate — $p \cdot q \neq q \cdot p$, which is called non-commutativity. Heisenberg proposed the bizarre quantum multiplication rule, which comes from the product of the amplitudes of two quantum transitions. Born realized that this could be the key to creating new mechanics (QM), and that this was nothing more than the case of two matrices multiplied together. Born helped create the fundamental relations of QM matrix mechanics, and it is definitely quantized; The following formula is actually the same as (2):

$$[p]\cdot[q]-[q]\cdot[p]=\frac{h}{j2\pi}[\mathrm{I}] \qquad (1)$$

Here [] denotes the matrix, but the $[\mathrm{I}]$ identity matrix; In the Planck constant of zero ($h=0$), i.e., non-quantized conditions, $p \cdot q = q \cdot p$, return to the familiar situation. For this contribution, Born was inscribed （1） on his tombstone when he died in 1970.

Werner Heisenberg (1901-1976) was a German physicist who taught at the University of Gottingen in 1923 at the invitation of M. Born, and later went to Denmark to study at the University of Copenhagen. It should be said that he learned a lot from the guidance of Bohr and Born. In 1927, Heisenberg proposed matrix mechanics to explain the spectrum of hydrogen atoms, and discovered and explained the strange double-line phenomenon. In March 1927 he sent out a paper entitled "Kinematic and Mechanical Contents of Quantum Theory", which contained one of the most attractive principles, the indeterminacy principle, also known as the uncertainty relation. Published in Zeitschrift fur Physik, Vol.43, 1927, 172-198, the paper shook up causality and remains a matter of debate today.

Heisenberg's uncertainty principle is a fine theory. and let's see what he says. In his 1933 Nobel Prize citation, Heisenberg stated that in the study of atomic phenomena, the unverifiable part of the measurement of disturbances to the system prevented the precise determination of classical properties, but permitted the application of QM. The analysis shows that there is a relationship between the accuracy of determining the position of a particle and the accuracy of simultaneously determining its momentum:

$$\Delta p \cdot \Delta q \geq \frac{h}{4\pi} \qquad (2)$$

Where Δp、Δq is the error when the two are measured, and h is the Planck constant. In this case, p、q are the regular conjugate variable. Since the uncertainty relation specifies the range of these accuracies, there is no visual picture of an atom that is completely unambiguous. Heisenberg stresses that the pattern of QM is statistical. The uncertainty relation provides an example of how accurate knowledge of one variable in QM excludes accurate knowledge of another variable. He therefore highly values Bohr's principle of complementarity —the complementary relationship between different aspects of the same physical process that characterizes QM as a whole.

For microscopic particles, any experiment to measure momentum or coordinates inevitably leads to uncertainty about their conjugate variable information. Therefore, it is impossible to know the coordinates and momentum of the particle at the same time. The uncertainty relation shows that the smaller the uncertainty of the coordinates, the greater the uncertainty of the momentum, and vice versa. Therefore, it is impossible to accurately measure the coordinates and velocities of particles at the same time. In other words, a particle with a definite velocity does not have an exact position in space. From this, it can be further proved that the probability of finding a free particle at any place in space is the same, so the position coordinates of the free particle are completely uncertain.... Moreover, the inverse relationship between the inaccuracies of this measurement holds true for other conjugated variables such as energy and time, Heisenberg said, because nature has such a precision limit that causality is no longer true. The Nobel

Committee praised Heisenberg's work at the time; They pointed out that the new theory (QM) has greatly changed people's understanding of the microcosmic world composed of atoms and molecules; In particular, here QM must abandon the requirement of causation and accept that the laws of physics express the probability of an event.

For the EPR paper, Heisenberg argues that quantum mechanics itself is complete, that it describes the most fundamental laws of nature, that reality and local nature are non-existent physical properties, and that studying them is as worthless as studying the age-old question of how many angels can stand on the tip of a needle....Heisenberg, however, avoids positive criticism of Einstein.

IV. Hidden Variable Theory and Bell Inequality in Quantum Mechanics

The term "hidden variables" was first proposed by de Broglie in 1928 to describe situations in QM that are difficult to explicitly describe analytically. After the publication of the EPR paper in 1935, the physics community was full of opinions, and did not know whether to support the article's criticism and severe attack on QM. The physicist D. Bohm came forward and did two things: First, he proposed the thought experiment model of EPR thinking as a singlet particle, which was done in 1952, and he did not know that he could actually do the experiment successfully. The other is to use hidden variable theory to explain QM causally under the encouragement of Einstein. Although Bohm does not explicitly say that he opposes QM, his bias is on Einstein's side. In addition, Bohm introduced the concept of quantum potential and participated in discussions in the physics community.

A. Einstein pursued a definitive theory of complete representation of physical realities. He still gave a classical statistical interpretation of the quantum mechanical concept of probability. In this case, it seems to imply unknown variables, that is, hidden variables exist; The current probability is the result of some average of these hidden variables.

The EPR paper of 1935 is a challenge to the Copenhagen school, and its core contents include physical reality, completeness, and localization. Locality refers to the fact that if the two systems are no longer interacting at the time of measurement, no intervention in one of them will affect the other system, so the separable system has the paradox of distance correlation. From this, EPR determined that quantum mechanics is incomplete. In 1951, D. Botham changed the momentum-position correlation in the EPR experiment to the correlation between two spin 1/2 particles. In 1952, D.Bohm proposed hidden variables in quantum mechanics.

The term quantum potential also first comes from de Brogle(1927), but Bohm gave the analytical expression; He takes the wave function

$$\Psi = \mathrm{R}\, e^{j 2\pi S/h} \tag{3}$$

Then write the Schrödinger equation (SE):

$$\nabla^2\Psi + \frac{8\pi^2 m}{h^2}\left(\frac{jh}{2\pi}\frac{1}{\Psi}\frac{\partial\Psi}{\partial t} - \mathrm{U}\right)\Psi = 0 \tag{4}$$

Where h is the Planck constant, and $\Psi(x, y, z, t) = \psi(x, y, z) f(t)$.By substituting the wave function defined by Bohm into SE, we get two equations, one of which is

$$m\frac{dV}{dt} = -\frac{\partial}{\partial t}(\mathrm{U} + \mathrm{Q})$$

Where $V = m^{-1}(\partial S/\partial t)$, and Q is the quantum potential function:

$$\mathrm{Q} = -\frac{\mathrm{h}^2}{8\pi^2 \mathrm{m}}\frac{\nabla^2 \mathrm{R}}{\mathrm{R}} \tag{5}$$

Bohm's quantum potential is supported by some physicists.

Although quantum mechanics continued to be confirmed by experimental observations, the "EPR paradox" continued to plague quantum mechanics until the next generation of physicists came along and put an end to one of the most enduring and famous debates in the history of science. The man who solved this problem was the Irish physicist John Bell, whose "Bell inequality" has been described as "one of the greatest scientific discoveries in human history."

Bell has been a staunch supporter of Einstein's belief in the reality and locality of physics. Bell was unimpressed by N.Bohr's statement that "any fundamental quantum phenomenon is only a phenomenon after it has been recorded", saying, "Have cosmic functions been waiting for eons of time for a monomeric organism to appear before collapsing?" "Or will it have to wait a little longer until a qualified observer with a doctorate becomes available?" He believes that the mysterious action at a distance in quantum mechanics is determined by "hidden variables" that are not yet understood.

Bell argues that for at least one QM state (singlet), the statistical prediction of QM is incompatible with the divisibility hypothesis; In other words, no local hidden variable theory can reproduce all the statistical

predictions of quantum mechanics. This is called Bell's theorem. It will be recalled that in a previous article Bell suggested that EPR thinking could be refuted only by finding impossible proof of local conditions or divide ability of distant systems. In the latter article, it is actually possible to deal with a two-particle system such as two reverse photons emitted from a common source, and the possible correlations between the results of the simultaneous measurement of the two particles. For example, when the polarization of two photons is measured separately, the Bell theory states that there is a limit to the correlation.

In summary, Bell proposed an inequality that observations of particles must avoid, thereby proving the incompleteness of quantum mechanics. Most importantly, this inequality is not a thought experiment; it can be proven experimentally. Let us now elaborate.

In his 1964 paper "On the EPR Paradox," J.Bell stated that "no single theory of hidden variables can reproduce all the predictions of quantum mechanics," and Bell was enamelled with the idea of introducing hidden variables to make up for what was then thought to be a "major deficit" in QM.

Let two identical particles with a spin of $\hbar/2$ form a singlet with a total spin of zero and a wave function is

$$\psi = \frac{1}{\sqrt{2}}[\alpha(\mathrm{I})\beta(\mathrm{II})—\beta(\mathrm{I})\alpha(\mathrm{II})] \qquad (6)$$

Where α(i) and β(i) are the eigen functions of the spin S of the i th particle taking the value $\hbar/2$ and($-\hbar/2$) in a certain direction. Since S=$\frac{\hbar}{2}\sigma$, they also represent the eigen functions for which the projection operator σ_n(i) of σ in the direction n takes values of 1 and (-1).When the two particles move away from each other, each maintains its own spin, so that the product of the two is (-1) forever. Therefore, if the spin measured for particle i is 1 in the direction n, the particle must have a value of (-1) in the same direction. If (-1) is measured for particle I, the value of particle II must be 1; This means that the value of particle Ⅱ depends on the measurement of Ⅰ. But they have been separated to no interaction, EPR paper believes that should be unrelated to each other, the measurement of Ⅰ should not affect the state of Ⅱ; This is a contradiction!

In order to study the correlation of pairs of singlet particles, the average value of the product of spin projections of particle I in the a direction and particle II in the b direction can be calculated

$$P(\boldsymbol{a},\boldsymbol{b})=\langle\psi|\sigma_a(\mathrm{I})\cdot\sigma_b(\mathrm{II})|\psi\rangle=-\boldsymbol{a}\cdot\boldsymbol{b}=-\cos\theta \qquad (7)$$

σ is the projection operator in the *a* and *b* directions, and θ is the angle between the unit vectors *a* and b. This is an indication that the two particles are related. If *a*=*b*, P(*a*, *a*)=-1, this is the case discussed above. If *a*=*b*, θ=0, P(*a*, *b*)=-1.

In order to solve the problem, Bell introduced a set of hidden variables based on local realism, i.e., |λ|, as a description of the state. The measurement result can be determined by a single value. It is assumed that there is a probability distribution ρ(λ) for different hidden variable states. At this point, Bell's tools for inference are in place.

Bell's purpose is to prove with the local hidden variable theory that the local requirement is inconsistent with the statistical prediction of QM. He starts with the following three premises:

- In a system consisting of two spin binaries, the measurement of the spin components $\sigma_1\cdot a$ and $\sigma_2\cdot b$ of each particle in a pair of correlated particles has only two possible values:

$$A(\boldsymbol{a},\lambda)=\pm1,\ B(\boldsymbol{b},\lambda)=\pm1$$

Where *a* and $\boldsymbol{b}$ are unit vectors and λ is hidden variables; Latter satisfaction

$$\int\rho(\lambda)d\lambda=1$$

- The ideal correlation conditions of the total spin singlet exist in any direction is:

$$A(\boldsymbol{a},\lambda)=-B(\boldsymbol{a},\lambda)$$

- The locality hypothesis is that when two particles are separated without interaction, the measurement result A(*a*, λ) of particle I does not depend on the measurement orientation *b* of particle II; Similarly, the measurement B(*b*, λ) for particle II does not depend on *a*. It must be noted that the derivation of Bell inequality is based on Bohm's spin dependent scheme (spin two-valued particle system).The premise ① assumes that there are only two possible values for the spin components of the related particles. The premise ② is that, under ideal correlation conditions, A(*a*, λ)=-B(*a*, λ) in any direction. Premise 3 assumes the independent properties of the two particles when measured after they are separated. So, the three premises are actually three assumptions—spin two state system, perfect correlation, and locality condition. The following correlation functions are also defined:

$$P(\boldsymbol{a},\boldsymbol{b})=\int\rho(\lambda)A(\boldsymbol{a},\lambda)B(\boldsymbol{b},\lambda)d\lambda$$

Where ρ(λ) is the probability distribution function for λ; From the above, Bell derives the following inequality:

$$|P(\boldsymbol{a},\boldsymbol{b})-P(\boldsymbol{a},\boldsymbol{c})|\leq|1+P(\boldsymbol{b},\boldsymbol{c})| \quad (8)$$

$\boldsymbol{c}$ is the unit vector.

This is one of the great inventions in the history of science—John Bell's inequality can be used to test whether the QM or EPR paper is correct. In other words, in a contest between quantum physicists and Einstein, who would win? Although there was still a long way to go, J. Bell had blazed a trail and made his name enter the history of physics. Figure 1 shows the Irish-born physicist giving a talk at an academic conference, with his famous inequality written on the blackboard.

Now let's do a simple test using equation (7). There are 3 unit vectors *a*, *b* and *c* coplanar, and the angle between *a* and *b* is 60°, and the angle between *b* and *c* is 60°, according to formula (7), there is

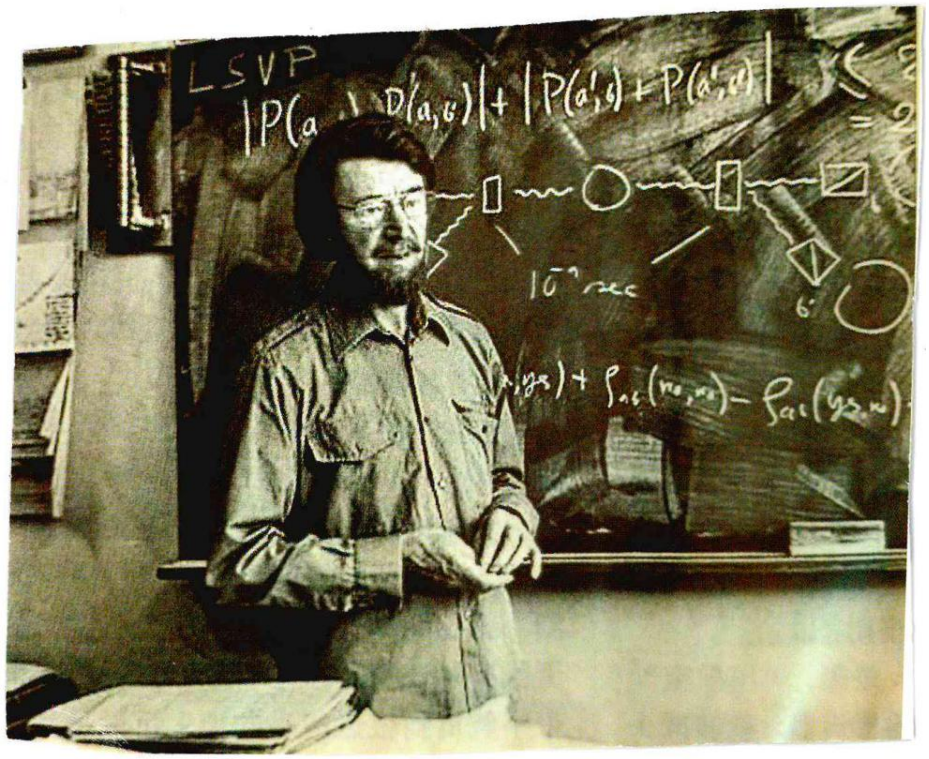

FIG. 1: Dr. J. Bell giving an academic presentation
(Handwritten inequalities on the board)

$$P(\boldsymbol{a},\boldsymbol{b})=P(\boldsymbol{a},\boldsymbol{c})=-\frac{1}{2}$$

$$P(\boldsymbol{a},\boldsymbol{c})=\frac{1}{2}$$

If you plug in the Bell inequality, you get

$$1\leq\frac{1}{2}$$

This is clearly not true; It can be seen that the inequality is inconsistent with QM.

Inspired by Bell's work, other physicists have derived different inequalities. However, later experimental progress has proved that the Bell inequality is the best result, and no further derivation is needed.

V. Bell Inequality Transition from Theory to Experiment

Obviously, inequality means that local realism limits the degree of correlation so that the correlation lies in a certain interval; QM's prediction of the degree of correlation, on the other hand, is a strict formula, and it falls on a cosine curve. So it would seem to be expected that the Bell inequality would be easier to satisfy.

The transition from theory to experiment is not a simple process. The initial experimental attempt was 7 years after Bell's paper was published (that is, in 1972), Dr. John Clauser of the United States did a real test following Bell inequality at UC-Borkeley. John Bell was a theorist who didn't know how to design experiments to test his theories. This transition was spearheaded by J. Clauser, another scientist is A. Aspect, who is better known than Clauser for his later elaboration of the experiment. Born in 1942, Clauser will be 80 years old when he wins the Nobel Prize in 2022, which is not easy! …… In college, he was a student of renowned physicist

Richard Feynman, but Feynman was not enthusiastic about the subject of EPR and Bell's theorem. In 1967 Clauser came across J.Bell's paper, which immediately caught his attention. In order to develop the experimental plan, Clauser read the paper of D Bohm ten years ago and visited the Chinese-American physicist Jianxiong Wu (J.X.Wu), both of whom had experience with two-photon experiments, but these activities did not bring about the experimental plan he needed. But these readings and visits are beneficial, because Bohm has long believed that entanglement occurs between two twin photons, which is the opposite of EPR!

To verify the Bell inequality, it is necessary to measure the pair by pair polarization correlation. In 1969, Clauser made a breakthrough in his approach, and the showdown between locality, hidden variables (on behalf of Einstein) and quantum mechanics (on behalf of many people) was approaching. The experiment must be carried out under many different polarization angles. Figure 2 is a theoretical comparison, where the ordinate is the correlation and the abscissa is the polarization angle; HV stands for hidden variables and QM stands for quantum mechanics.

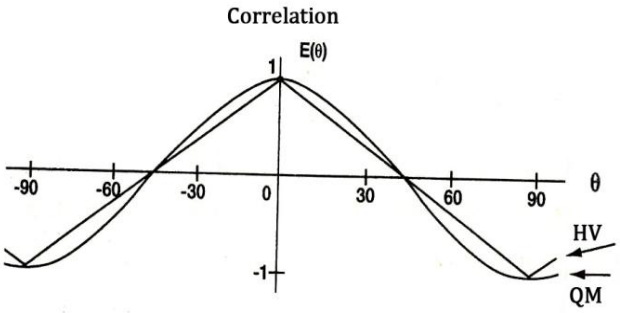

Fig. 2: Relation between correlation and polarization angle

As you can see from Figure 2, the difference between quantum theory and hidden variable theory is very slight. Only by accurately measuring the correlation of pairs of photons at different angles of polarization can researchers tell which theory is correct.

In summary, the polarization angle of each photon in the entangled photon pair must be measured. A 1969 paper with Clauser as the first author opened the door to experimental research. At this time, though, Clauser actually believed in Einstein, not quantum mechanics!

In a series of experiments, Dr Clauser emitted thousands of photons to measure polarization properties, which can only have two values—up or down. The detector results are a series of seemingly random ups and downs. But when the results of the two detectors are compared, the fluctuations have a compatibility that neither classical physics nor Einstein's laws can explain. Something strange is at work in the universe, and entanglement seems to be a real thing.

In a 2002 interview with the American Physical Society, Dr. Clauser admitted that he himself thought quantum mechanics was wrong and Einstein was right. He said: "Obviously we got the 'wrong' result. I had no choice but to report what we saw, and you know, 'This is the result.' But it went against my instincts, and I thought my instincts must be right." He added: "I hope we can overturn quantum mechanics."

One of the quirks of Dr Clauser's findings, and of the quantum-mechanical description of this strange effect, is that the correlation only emerges when individual particles are measured - that is, when physicists compare their measurements after the fact.

Dr Clauser spent much of that decade trying to figure out what holes he might have overlooked. One possibility is called a "positional vulnerability."

And now, Dr. Alain Aspect. began to research; He was born in 1947 and was 76 years old when he won the Nobel Prize in Physics in 2022.In 1982, Dr. Aspect and his team at the University of Paris tried to plug Dr. Clauser's hole by changing the direction in which the photon's polarization was measured every 10ns.He also thought Einstein was right.

Dr. Aspect's results have made entanglement famous, making it a real phenomenon that physicists and engineers can exploit. The quantum prediction holds true, but Dr Clauser has found other possible holes in the Bell experiment that would need to be plugged if quantum physicists were to declare victory over Einstein.

Dr Aspect's experiments, for example, change the direction of polarization in a regular, and therefore theoretically predictable, way that a photon or detector can sense.

It was then that Anton Zelinger, a professor at the University of Vienna, picked up the baton. In 1998, he added more randomness to the Bell experiment by using a random number generator to change the direction of polarization measurements while entangled particles were in flight.

Quantum mechanics has once again decisively defeated Einstein, closing the "positional loophole." Still, there are other possible sources of criticism or prejudice. In recent years Dr Zelinger and his collaborators have been experimenting with "cosmic clocks", which use fluctuations in light from distant objects called quasars, billions of light years away, as random number generators to set the detector's direction.

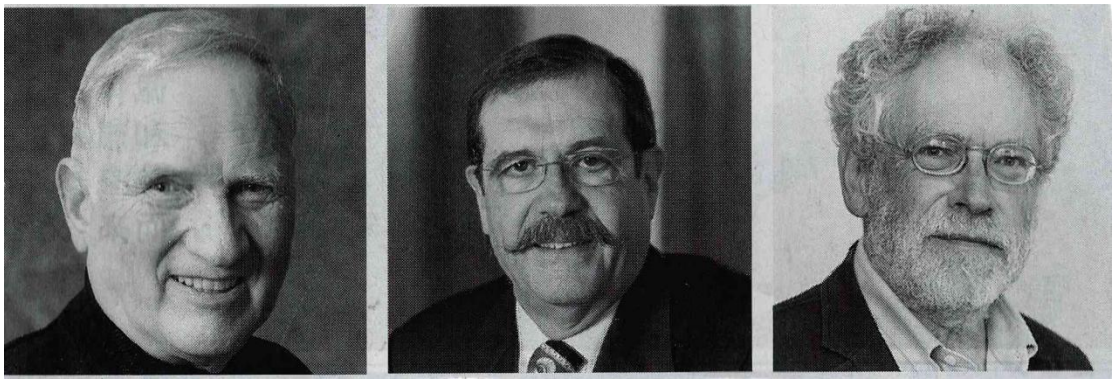

Fig. 3: The Three Musketeers who won the 2022 Nobel Prize in Physics

(From left to right: American J. Clauser, French A. Aspect, Austrian A. Zelinger)

The "Three Musketeers" of quantum entanglement who won the 2022 Nobel Prize in physics are given in Figure 3, and they are well deserved. Now, let's go back to the 1970s. Early experiments could be done with two-photons, as well as with other subatomic particles. The tests that have been done fall into three categories. One is the singlet proton-on-spin correlation experiment, which is very similar to the original thought experiment. A low-energy proton is hit at a target composed of hydrogen atoms, and the incident proton and the hydrogen nucleus, the proton, enter a single state after a brief interaction. Then both protons leave the target, they're still in a singlet state, and the protons are measured. The second is the experiment of polarization correlation between two gamma photons produced by annihilation radiation. Because annihilation radiation photons are not only emitted in opposite directions, their polarization (corresponding to the spin component) is also opposite, respectively expressed as ± 1. The third is the experiment of photon polarization generated by atomic cascade radiation. When an atom of an element rises to an excited state by absorbing laser light, and then returns to the initial energy level in two steps, each step radiates a photon, which leaves in opposite directions and has opposite polarization, denoted by ± 1.

The earliest experiments, published in 1972 by S. Freedman and J.Clauser (Freedman was Clauser's graduate student), used calcium atoms to radiate cascades of photon pairs. Since then, most experiments have used photon pairs, with only a few experiments using the singlet proton pair method. ... The results of this first experiment violate the Bell inequality and are consistent with QM.

Between 1973 and 1976, there were eight published experiments. Of these, two are consistent with Bell inequality and support EPR, and six violate Bell inequality and agree with QM.

A. Aspect et al. published three experimental results between 1981 and 1982, all using the calcium atomic cascade radiation photon pair method. These experiments prove with high precision that the results violate Bell inequality and agree with QM.

Aspect's experiment is the most famous. The design of the experiment (FIG. 4), tested by checking whether the photons emitted simultaneously in a single atomic transition follow the Bell inequality, uses a pair of lasers to excite calcium atoms (two-photon excitation) to the ground state to become a light source, with an acousooptic switch at 7.5m on each side of the source. The polarizer passes through or blocks photons with a certain probability. The fate of photons is monitored by electrons and the level of association is assessed. The results show that there is a strong correlation between the measurements of photons, even though there is a distance of 15m between the two measuring instruments. Aspect is very serious and makes the experimental components himself.

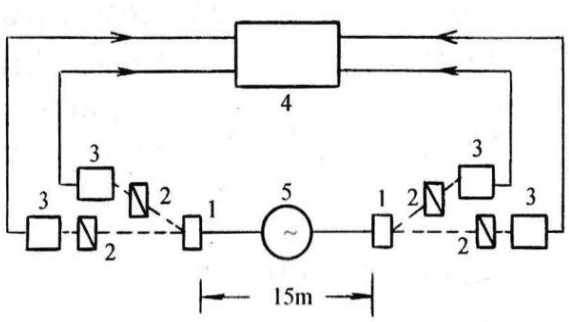

1 -- Switch 2 -- Polarizer 3 -- Photomultiplier
4 - Electronic coincidence monitor 5 -Two-photon source

Fig. 4: Aspect experiment layout

To sum up the above situation, it is no doubt that the experimental results negate the inequality and support quantum mechanics. Because there are only two experiments that meet the inequality, and it is still early, the precision is not high enough. Later experiments, especially the last three, were more accurate and reliable. Moreover, it is no coincidence that 10 independent experiments not only violate the inequality, but also violate it in exactly the same way that quantum mechanics predicts. Such an outcome would be expected for quantum mechanics, and would seem to shake little, but it would be an unexpected event for physics as a whole and for philosophy as a whole.

It is said that the relevant experiments of Aspect from 1982 to 1986, a total of 15 cases. At the time, it was believed that his experiments provided evidence against EPR.

Aspect's experimental results vindicated the correctness of quantum mechanics and prompted a change in Bell's thinking. In the past, he has called quantum mechanics "expedient and ambiguous"; By the 1980s, he said quantum mechanics was "so accomplished that it's hard to believe it's wrong." As for faster-than-light, Bell said in response to a question from the BBC that the EPR experiment does "contain something faster than light"; To his dismay, this would violate the law of causality: at this point, he said he disagreed with Einstein's worldview. As for the Aspect, he said in response to a BBC question that a simple picture of Einstein's concept of separability could no longer be maintained and could also contain some kind of faster-than-light entity. Apparently, both Bell and Aspect were cautious in 1985, given the mainstream status of relativity. I think it's important for Bell to say that physics should go back to before 1905, to Poincare and Lorenz's theory. In fact, whether Bell decided and abandoned relativity (SR)! He also said that he "wanted to go back to the etheric concept"; The attitude of this distinguished scientist could not have been clearer. J. Bell died in 1990, D. Bohm in 1992; This makes it impossible for these two famous scholars to consider and evaluate the subsequent series of new faster-than-light experimental advances, which is regrettable!

So what do other physicists think? Nobel Prize-winning physicist B. Josephson says that perhaps one part of the universe "knows" another, a distant correlation. P. Coveny and R. Highfield say that Aspect experiments show that two particles that are far apart in the universe can form a system, and there does appear to be a faster-than-light connection at work in distant spacetime. In short, after Aspect proved that quantum mechanics was correct and that the limitations of the Bell inequality did not hold, most of the international scientific community agreed that Einstein's local realism was wrong. For example, B.d'Espagnat says "Einstein's separability assumption must be abandoned, which Bohr has long criticized". K.Copper said; "The possibility of action at a distance should be considered. If action at a distance existed, it would have opposed the special relativistic interpretation of formal systems in favour of the Lorentz interpretation and Newton's 'absolute space'. Therefore, these new experiments based on Bell's theorem can be seen first and foremost as conclusive experiments between Lorentz's theory and Einstein's special theory of relativity."

VI. Rationality of Bohm Experimental Scheme

During World War II, theoretical physics was at a standstill. For example, N. Bohr also came to the United States to participate in the development of the atomic bomb so that the Allies could defeat the fascist countries. After the end of World War II, the relevant research was again paid attention to, for example, in 1951 D. Bohm gave a new interpretation of the expression of EPR (D. Bohm, Phys Rev, 1952, 85:166, 180): A microscopic particle with spin zero in a proper position M is separated by decay into two spin 1/2 particles, i. e. I and II. Assume that they immediately fly away in the opposite direction and are detected at the same distance but opposite directions (A and B). According to quantum mechanics, when the spin of I(or II) is measured at A(or B), the probability of the measured value being $\pm 1/2$ is each 0.5;However, if the spin of I is measured as 1/2, then II must be in the eigenstate of spin (-1/2). Although I and II can be very far apart, the measurement of I can determine the state of II, or the correlation between I and II.

However, some have questioned whether Bohm's improved description is indeed representative of the EPR paper, and here it is repeated to quote Bohm's book 《Quantum Theory》 : "Let us now describe the hypothetical experiment of Einstein-Rosen Podolsky." We have modified the experiment slightly, but the form is essentially the same as what they proposed, although it is much easier to work with mathematically. Let's say we have a diatomic molecule in a state where the total spin

is equal to zero, and let's say the spin of each atom is equal to I /2. Now suppose that a molecule is broken down into atoms in a process in which its total angular momentum remains constant. The two atoms then begin to separate and soon cease to interact significantly."

The EPR thinking described by D.Bohm suggests a strange quantum correlation. When two spinning particles interact far apart, their spins are equal and opposite, so one can be inferred from the other. According to quantum mechanics, the spin of both is uncertain until measured. The measurement determines the spin direction of one particle, and the quantum correlation causes the other particle to immediately accept the determined spin. This is true even when the two are light-years apart. This long-distance interaction suggests that there is a faster-than-light interaction between the particles. This was unacceptable to Einstein — it was the sort of thing that turned him against quantum mechanics. Einstein famously referred to this phenomenon disparagingly as "spooky action at a distance." The scientist, of course, does not recognize celestial spirits, so he thinks such a situation is impossible.

Notably, Bohm's system targets any microscopic particle, not just photons. That is, it could be two electrons, or two atoms that were originally part of the same molecule, and so on. This is important for researchers today. ... Now to the accusation: the EPR paper is saying that I and II no longer have any interaction after separation, whereas Bohm is saying that there is no significant interaction. In the language of modern physics, "there is no longer any interaction" is called local, and "there is no significant interaction" implies the possibility of non-local between particles. After all, the EPR experiment must be thoroughly relativistic, while the Bohm experiment must be non-relativistic. It follows that Bohm's thought experiments are not, as he claims, "essentially the same form as they propose." His subsequent non-local interpretation of quantum potential is in line with this thought experiment. In the interpretation of quantum potential, the expression of the wave function $\psi = R\exp(\frac{j}{\hbar}S)$ does not contain 'significant' interactions between quantum particles, but there are indeed non-local interactions between quantum particles due to the existence of quantum potential $Q = -\frac{h^2}{2m}\frac{\nabla^2 R}{R}$.

Our answer to this accusation is as follows: Einstein has long studied gravitational and electromagnetic interactions, and was aware of both the weak interaction proposed by E. Fermi (1932) and the strong interaction proposed by Hideki Yukawa (1934); when he published his EPR paper. Therefore, the "no interaction" in the EPR paper refers to any of the above four kinds of effects; Since EPR is a local realist, he will never acknowledge the existence of any other non-local non-force action. However, D.Bohm is a holist who, in addition to understanding the above four kinds of actions, also acknowledges the existence of non-force interactions (or mutual influences, correlations) in quantum systems, and he proposes that the quantum potential theory is the proof, although the effects of this non-force interaction are not as significant as the above four kinds of effects. Bohm made a distinction, calling those four "significant interactions." In fact, from the EPR paper and Bohm's argument, whether it is' any 'or' significant ', it says the same thing. In other words, there is no difference between what Einstein and Bohm are claiming. ... It would be futile to deny Bohm's contribution for the purpose of "defeating quantum mechanics." Moreover, many developments since Bohm have proved EPR wrong after all. Theoretically speaking, when a certain part (subsystem) of a composite system with many degrees of freedom is measured, it is incomplete. In this case, the quantum state of the subsystem is described by reduced density matrix; For a two-particle system with spin 1/2, after the spin measurement of I, the above matrix is used to describe I, and the result is a completely unpolarized spin state.The same is true when the system is entangled in other spin states. In summary, the key is that the measurements made on the subsystems of a composite system are incomplete measurements. Therefore, EPR's accusation that "quantum mechanics is not self-consistent" is untenable.

At the EPR thesis stage, the whole thing is very abstract. Bohm made a major contribution to the theoretical visualization of quantum entanglement between microscopic particles; This is undoubtedly a good thing!

One might say, why do we have to choose Bohm's proposal? Why does it have to be ideally related? Let's wait. I don't think it's appropriate to ask questions like this. Bell made some assumptions and derived the results; One can do experiments, and if the experimental results of a two-particle (two-photon or otherwise) system agree with the inequality, then the EPR paper is correct, QM is an incomplete theory, and entangled states (as Schrödinger calls them) do not exist. If the experimental results do not agree with the inequality, then the EPR paper is wrong, QM is complete, and the entangled state exists. So Bell, while subjectively inclined to agree with EPR, is objectively rigorous and impartial. If the experiment can be carried out, then these assumptions are valid. If the experiment doesn't work, then Bell's theoretical work is meaningless. In fact, it has been passed down to posterity, so that we still have to recount it today.

VII. Development of Bell Type Experiments

A. Einstein's opposition to quantum mechanics (QM) began in 1926 and culminated in his 1935 joint paper with B.Podolsky and N. Rosen, and the EPR paper later promoted the development of science from the opposite side. This paper is based on the theory of special relativity (SR), and both SR and EPR deny the possibility of faster-than-light. However, QM allows the existence of superluminal speed, and is consistent with the premise of the study of superluminal speed, that is, QM non-locality. In 1985, John Bell stated, "The Bell inequality is a product of the analysis of the EPR inference that there should be no action at a distance under the conditions of the EPR article; But those conditions lead to the curious correlations that QM predicts. The results of Aspect's experiment were expected, as QM has never been wrong and now knows it can't be wrong even under demanding conditions; Experiments have certainly proved Einstein's ideas untenable." Bell saw the dilemma as a return to Lorentz and Poincare, whose aether was a preferential reference frame in which things could travel faster than light.Bell pointed out that it was the EPR that gave the faster-than-light expectations.

For a long time, scientists have been puzzled by the phenomenon of "quantum entanglement," which seems to defy the classical laws of physics. The phenomenon seems to suggest that pairs of subatomic particles can be secretly linked together in a way that transcends time and space. "Quantum entanglement" describes how the state of one subatomic particle affects the state of another, no matter how far apart they are. This offended Einstein because it was considered impossible to transmit information faster than the speed of light between two points in space. ... Scientists are now acting — out of a sense of duty, but also out of intense curiosity.

The first problem with Bell type experiments is how to create the two-particle system required by Bohm's discussion. Nature seems ready for human experiments, and a common approach is to produce two-photons using atomic cascades of radiation. When an atom of an element descends two specific energy levels (e.g. by absorbing laser light from level $4S^{21}S_0$ straight up to the excited state $4P^{21}S_0$).It then drops to $4S4P'P_1$, then back to $4S^{21}S_0$), radiating one photon at each step, and the two appear on either side of the parent atom and leave in opposite directions, with opposite polarizations (±1). Such photon pairs are connected at birth, like human twins; It's an entangled photon pair. The two are forever entangled in each other, and if one changes, the other changes immediately (or almost immediately), even if they are light-years apart and in different places in the universe.

Another common method is to use positrons to produce double gamma photons, which are not only emitted in opposite directions, but also have opposite polarizations corresponding to the opposite components, expressed as ±1. Another method is to use a singlet proton pair - bombarding a hydrogen nucleus (proton) with low-energy protons, which briefly interact to become a singlet state; The two protons leave and remain singlet, effectively forming an entangled photon pair.

Let's look at what happened after the 1982 Aspect experiment. In 1996, G.Weihs conducted an experiment with two photons with a wavelength λ=702nm, which proved to violate the Bell inequality at 400m distance and was consistent with QM.Later, the Gisin team in Switzerland added the successful distance of 35m(1997), 10.9km(1998), 25km(2000), also technically using two photons.[18]In 2007, scientists from Austria, the United Kingdom, and Germany joined forces to achieve two-photon entanglement between two distant islands (144km) apart. In 2008, D. Salart achieved two-photon entanglement between two villages in Switzerland, at a distance of 18km.[19] In 2015, a team of researchers in the Netherlands conducted a close-range (200m) dual-electron experiment on a university campus, which is said to have filled the holes in two Bell experiments. In 2017, a team of Chinese scientists achieved thousand-kilometer quantum entanglement in an experiment, setting the highest record.

In the 25 years since 1982, the distance between the two particles in the entangled state experiment, from 15m→400m→25km→144km→1300 km, has made amazing progress. Most experiments rely on fiber-optic technology, but China's highest record is the use of quantum satellites. In a 2007 multinational experiment, the research team first created polarimetric entangled photon pairs on the island of La Palma in Spain's Canary Islands, and then left one photon in the pair on La Palma, while the other photon was transmitted via an optical path to Tenerife, 144km away. What is difficult to explain is that this interaction is independent of distance, reaching 144km.

The Dutch experiment is remarkable. The experiment is notable for two things; First, two electrons are entangled, and electrons are particles of matter. Second, although the two (I and II) were not far apart, the experiment closed a loophole that someone could use to attack the Bell experiment. So the experiment broke new ground, electrons have magnetic properties, the so-called "spin". This property causes the electrons to either face up or down. And until they are observed, there is no way to tell which of these two states they are in. In fact, due to the bizarre nature of quantum, they will be in an "overlapping" state facing both up and down at the same time. Facts are only revealed when they are observed. When two electrons get entangled. They all face up or down at the same time. But when observed, one is always facing down and the other is always

facing up. There is a complete correlation between them, and when you look at one electron, the other electron is always in the opposite position. The effect is immediate, even if the other electron is on the other side of the galaxy.

VIII. Quantum Entangled States do Not Act at a Distance but Propagate Faster than Light

The space-time representation of quantum theory does not conform to the spirit of SR, and Einstein is sensitive to this fact, which is why he stubbornly opposes QM. However, the wave function of the two-particle system in the EPR paper is an entangled state. This is a special form of (but also universal) quantum state, in addition to the properties of the general quantum state (such as similarity, uncertainty), but also its unique personality — related indivisibility, non-local and so on. N. Bohr had earlier pointed out in his debate with Einstein that separability does not hold in the quantum domain. Einstein would not accept that two subsystems in a system, even if separated, no longer exist independently of each other. The Bell inequality means that the local reality limits the degree of correlation to a certain interval, while the QM is a strict equality for the degree of correlation. The experiment yielded correlation results, which Aspect says "negates Einstein's simplistic picture of the world."

To get some insight, we refer again to a 1985 talk by J.Bell to the BBC.[16]He thinks QM is such an accomplished branch of science that it's hard to believe it could be wrong, so the results of Aspect's experiment were expected. "QM has never been wrong and now knows it can't be wrong even under very demanding conditions; To be sure, the experiment proves Einstein's worldview is untenable." ... At this point, the questioner said that the Bell inequality presupposes objective reality and local (indivisibility), the latter indicating that there is no faster-than-light transmission of signals. After the success of the Aspect experiment, one of the two must be discarded. "It's a dilemma," says Bell, "and the easiest way to do it is to go back to before Einstein, Lorentz and Poincare, who argued that the ether was a preferred frame of reference." It is possible to imagine such a frame of reference in which things move faster than light. There are many problems that can be easily solved by assuming the existence of ether."

Bell repeated, "I want to go back to the ether concept because there is this revelation in the EPR that there is something behind the scene that is faster than light, but this ether does not show up at the observation level."... "In fact, it is Einstein's theory of relativity that makes quantum theory so difficult."

One of Bell's sayings in 1985 was "be hind the scene something is going faster than light" (after the scene something is going faster than light).The remark was so striking that it is still quoted by researchers years later. ... J.Bell died in 1990, and there have been many advances in faster-than-light research since then that he failed to see. If he were alive today, he would be the world leader in faster-than-light research.

The fundamental difference between SR and QM is whether to admit the existence of non-local, whether to admit that the superluminal can exist. In recent years, a team of Swiss scientists has done an excellent job of answering with facts. We know that the Swiss physicist Nicholas Gisin(1952 -), who worked at CERN, was a great admirer of his predecessor J.Bell and believed that the Bell Principle was a major breakthrough in theoretical physics. His team first confirmed the violation of the Bell inequality by two-photon entanglement at a distance of 35m in the laboratory at the University of Geneva, thus proving the existence of quantum non-locality. They then extended the experiment to 10.9km in 1997, and were the first to use fiber optic technology in this Bell experiment.[18]Aspect in France congratulated themselves on the news - 10km is much better than the original 15m.Gisin firmly believes that quantum entanglement completely violates the spirit of relativity; Next, his team solved another prominent problem-in the theory of quantum entanglement, one particle can change the properties of another particle instantaneously, no matter how far apart they are;So how fast is "instantaneous"?

In 2000, Gisin's team used optical cables under Lake Geneva to send photons 25km away and found the opposite of Bell's inequality.[18]Gisin's group has a very interesting result - the experimental measurement of quantum entangled states (QES) acting at a speed of (10^4-10^7) .[19] This is an important case, indicating that the speed of action is not infinite, but faster than light. In short, Gisin believes that some kind of influence appears to be traveling faster than light; Gisin thinks this means that "relativity's description of spacetime is flawed." The 2008 paper says they performed a Bell type experiment with two entangled single photons spaced 18km apart (roughly east-west, with the source precisely in the middle). The rotation of the Earth allowed them to test all possible hypothetical superior reference frames in the 24h period. At all times of the day, two-photon interference fringes above the threshold determined by the Bell inequality are observed. From these observations, it is concluded that the observed non-local correlation is truly non-local, as shown by previous experiments. In fact, it should be assumed that this magic effect will spread even faster than the experimental results (10^4-10^7)c. That is, Salart et al. have consistently observed two-photon interference that is significantly higher than the Bell inequality threshold. Taking the advantages of the Earth's rotation allows a low limit of the acting speed to be determined for any

assumed superior frame of reference. If such a superior frame of reference exists and the earth's velocity is less than $10^{-3}c$, then the action velocity must be $\geq 10^{4}c$.

Until 2000, there were two hypothetical superior reference frames in the Swiss Bell experiment, one was the 2.7K microwave background radiation and the other was the Swiss Alps reference frame. The latter is not a cosmic reference frame, defined by the context of the experiment. In these analyses, the hypothetical superluminal influence is defined as the speed of quantum information (SQI), which differs from classical signaling; However, one should know how to obtain the limit (boundary) of SQI in any reference frame.

In an inertial reference frame on Earth, events A and B(in the case of the experiment, two single photons are detected) occur at time, in time t_{A}, and in time t_{B}, on the r_{A} and r_{B}, Consider another reference frame F(the assumed superior reference frame, moving at speed v relative to the Earth reference frame);When a correlation that violates Bell's inequality is observed, the SQI of the F system (denoted by symbols) creates a correlation with a bound of v_{qi}

$$v_{qi} \geq \frac{\left\| \boldsymbol{r}'_{B} - \boldsymbol{r}'_{A} \right\|}{\left| \mathrm{t}'_{\mathrm{B}} - \mathrm{t}'_{\mathrm{A}} \right|} \tag{9}$$

Where $(\boldsymbol{r}'_{A}, t'_{A})$ and $(\boldsymbol{r}'_{B}, \mathrm{t}'_{\mathrm{B}})$ are obtained by Lorentz transformation; by simplified it, we obtain:

$$\left(\frac{\mathrm{v}_{\mathrm{qi}}}{\mathrm{c}} \right)^{2} \geq 1 + \frac{\left(1-\beta^{2}\right)\left(1-\rho^{2}\right)}{\left(\rho + \beta_{0}\right)^{2}} \tag{10}$$

Where $\beta = v/c$, is the ratio of the speed of the Earth reference system in the reference system F to it, So from the above formula we know $\mathrm{v}_{\mathrm{qi}} > c$.

In Salart's experiment, the source of the signal, located in the laboratory in Geneva, was the generation of entangled photon pairs in a nonlinear crystal, using fiber Bragg gratings and light loops, each photon pair was separated with certain separation and sent to two villages via a Swiss fiber network system, with a linear distance of 18km. energy-time entanglement is used, which is a suitable state for quantum communication in standard telecommunications cables.

In short, the experiment was complex and sophisticated. Swiss scientists have shown that the speed at which quantum entangled states interact is not light speed, nor is it infinite, but superluminal — at least 10,000 times of c. Therefore, quantum entangled states are not acting at a distance (i.e., $v \neq \infty$), but rather superluminal broadcasting. Could quantum entanglement itself be considered a special form of faster-than-light communication? Some physicists think yes, some physicists think no. In 2010, physicist Prof. Zhiyuan Shen pointed out: "There is a faster-than-light interaction between two entangled photons, and when the spin of one photon is measured, the spin of the other photon at a distance immediately changes accordingly."[20] Einstein called this "weird action at a distance." Recently, a team at the University of Geneva in Swiss has measured the speed of photons in an entanglement experiment at at least 10,000 times the speed of light. Strangely enough, many authors of physics textbooks and papers say that this does not violate special relativity (SR) because people cannot be used to transmit information. But photons do transmit information, otherwise how would an entangled photon 'know' that another photon far away has changed its spin?

Physics is not anthropology, so why does it have to be people who transmit information to count? This view is actually another version of the humanistic principle, which takes the subjective role of man as the criterion of objective law. However, science, especially physics, is objective, and entangled photons have faster-than-light effects between them, which is proved by many experiments to exist objectively, which cannot be denied. We must abandon our subjective biases and accept faster-than-light transmission of information in entangled states as an objective fact."

These are very good words from Professor Shen; In my opinion, many objective laws (including faster-than-light information transfer between entangled particles) existed before there were humans on Earth. The problem is that we have not yet been able to use this phenomenon to enable human communication in space and space exploration. But not today doesn't mean never.

Quantum entanglement is the greatest mystery in physics, and for good reason.[21]quantum interaction may be called "the fifth fundamental physical interaction in addition to the four fundamental physical interactions (electromagnetism, gravity, weak force, and strong force)." The mistakes made in the EPR paper have profound lessons for people, reminding us that the world is stranger than we can imagine. The fact that entangled particles interact at faster-than-light speeds regardless of spatial distance is fundamentally lacking in theoretical explanation. Scientists know this is so, but they don't understand why it is so; In general, the strength of the effect varies with distance, but the expectation of quantum entanglement is that it will have the same strength no matter how far away; Why is this? No one can answer that at the moment. And this entanglement does not dissolve automatically after a period of time. ... Curiosity motivates us and is an inexhaustible source of thought and exploration.

Now, we say that superluminal signaling based on quantum nonlocality. We believe that this

phenomenon has always existed, and the question is only how to implement it in human communication. Although no one can be sure when they will succeed, it is certain that someone will keep trying. It must be pointed out that faster-than-light information transmission and faster-than-light travel are two major pursuits of human beings. If we take a broader view, we will not doubt the significance of studying the "remote transmission of faster-than-light information".

IX. About the Copenhagen Interpretation of Quantum Mechanics

The history of physics books tell us that the so-called Copenhagen interpretation (CI) of quantum mechanics consists of three main aspects: the Max Born probability interpretation of the wave function; Werner Heisenberg's uncertainty relation; Niels Bohr's principle of complementarity. The famous Bohr-Einstein debate took place at the 5th Solvy Conference in October 1927 and culminated in the 6th Solvy Conference.... Why are we bringing this up now? Because of the controversy surrounding the development of modern quantum communication technologies, some physicists have revived the argument that QM's Copenhagen interpretation is "problematic even today, and Einstein is not wrong." Some scholars logically conclude that "quantum communication is something that has no physical basis at all." If the foundation is not good, there must be something wrong with the house. In this way, the discussion and reflection take people back to 1927.

One theory is that Einstein is not against QM, but rather against the Copenhagen interpretation of QM;I don't agree with that. Because this interpretation of QM mainly comes from Bohr, Born and Heisenberg, and their theory is the main content of QM. In my opinion, the anti-QM and anti-QM Copenhagen interpretation are essentially consistent. While most physicists recognized the work of M. Born and W. Heisenberg, Einstein found the work of both men object able — he considered both Born's and Heisenberg's work "deviant from the normal path."He believed in the certainty of the objective world; For example, if the track is clearly visible through the cloud chamber, its orbit should not be ignored. In short, Einstein explicitly stated at the 5th Solvy Conference in October 1927 that "the certainty principle is not accepted." He also opposed the idea of quantum mechanics as a complete theory of a single process because it could act at a distance. Einstein said that he did not think of de Broglie-Schödinger waves as individual particles, but rather as ensemps of particles distributed in space. In effect, Einstein viewed waves as the average behavior of a large number of particles. On March 22, 1934, Einstein again objected to the probability interpretation in a letter to Born.

Einstein's 1948 article "Quantum Mechanics and Reality" published in the journal Dialectics can be seen as a statement of his later years. Although he acknowledged that quantum mechanics was "a significant, even decisive, advance in the knowledge of physics", he insisted that "the methods of quantum mechanics are simply not satisfactory". On the one hand, this contradictory statement is due to the fact that the depth and wide application of QM have made him unable to deny its significance, but he is unwilling to admit that he is wrong in academic opinion. Therefore, I do not believe that Einstein changed his attitude against QM in his later years. But some people still say that relativity (SR, GR) can be combined with QM, isn't that ridiculous?... More than 20 years after Einstein's publication, two leading physicists made sobering comments: P. Dirac, in his late years, said that "there is a real difficulty in reconcicating relativity with quantum mechanics"; According to S. Weinberg, "Theoretical physics has big problems, such as the requirement for Lorentz invariance that QM simply cannot meet." It should be said that these two statements are very clear and correct.

The years 1926-1927, when QM appeared, were 21-22 years after special relativity (SR) was proposed, and 11-12 years after general relativity (GR) was proposed. It can be said that relativity on the one hand achieved Einstein's great prestige, but at the same time made him tend to be conservative; This is regrettable.

The formation of QM's Copenhagen School has a process;[22] In the spring of 1912, N. Bohr went to work for the British physicist D. Rutherford, and returned to Copenhagen in the same year to think about the experimental law of the spectrum of the hydrogen atom. In 1913, Bohr proposed the theory of the quantized orbital motion of electrons in atoms orbiting the nucleus, and proposed two new concepts — light radiation or absorption is the result of quantum transitions in atoms and the angular momentum quantization of electrons in orbit, proving Bohr to be a very outstanding innovative scientist. In 1916 Bohr became Professor of theoretical physics at the University of Copenhagen. In 1920 he founded the Institute of Theoretical Physics, where many European scholars came to work. The entrance of W. Paul in 1922 and W. Heisenberg in 1924, both students of the famous A. Semmerfeld, was a landmark event. In addition, people who came to Bohr to do research were P. Dirac, P. Ehrenfest, L. Braillouin, L. Landau, G. Gamov, etc., as is well known, they all made important contributions later on. Of course, the fundamental point is that people under Bohr's leadership (especially W. Heisenberg and M. Born, etc.) proposed a new theoretical system — quantum mechanics (QM), whose unique mathematical expression and physical thinking are completely different from classical physics, and its correctness is gradually proved; This has made the

Copenhagen School famous and has many admirers and followers.

The leading figure of the Copenhagen school is N. Bohr, and the leading figure of the opposition is A. Einstein. When QM came out, Einstein was 47 years old and a world-renowned scientist. winner of the Nobel Prize in physics for explaining the photoelectric effect with his theory of photons. Einstein used classical physics to derive the theoretical formulation of photons, but he was able to refer to Planck quantum theory to complete the derivation of photons, which is a revolutionary work. But after the appearance of QM, he insisted on opposing it; His attitude remained unchanged until his death in 1955.

To deepen the understanding, the author proposes a formula:

$$QM \cong CI + SE + DE \tag{10}$$

QM at the left end of the above equation represents all that constitutes quantum mechanics; Right: CI represents the main content of the Copenhagen interpretation (Bohr, Heisenberg, Born), SE represents Schrödinger's quantum wave equation, and DE represents Dirac's quantum wave equation.

SE is one of the core theories of QM and is as important as Newton's equations of motion in classical physics. It has the ability to predict natural phenomena and is widely used. But Schrödinger is all about volatility; According to de Broglie and Schrödinger, the velocity of a moving particle is the same as the group velocity of a wave packet, so their theory implies that a wave packet and a particle are one and the same. It is wrong to view the relationship between microscopic particles and corresponding waves as exaggerating the status of waves. We start with non-relativistic free particles and make a simple derivation; It can be shown that the dispersion equation of de Broglie waves is:

$$\omega = \frac{\hbar}{2m} k^2$$

Where $\hbar = \frac{\mathrm{h}}{2\pi}$, $k = 2\pi / \lambda$. So we can find the group velocity

$$v_g = \frac{d\omega}{dk} = \frac{\hbar k}{m} = \frac{p}{m} = v$$

So the group velocity is equal to the particle velocity. The derivative of group velocity v_g with respect to wave number k is calculated from the above equation:

$$\frac{dv_g}{dk} = \frac{\hbar}{m} \neq 0 \tag{11}$$

Therefore, it is relevant to indicate that the wave packet will spread (gain weight) during transmission. But particles are stable in transit, so the scientific community rejected their idea; He joked that "Schrodinger's equation is smarter than Schrodinger".

It was Bohr who pointed out that the wave packet "gets fat" during the wave transmission process, while the particle has undoubted stability, so simply thinking of the particle as a wave packet does not make sense. Nevertheless, Schrödinger did not accept the "wave-particle duality" and "wave function collapse" of CI. It is said that Einstein encouraged him to design a thought experiment to disprove CI. In a 1935 article (Naturwissenchaften, 1935, Vol. 23, 807, 823, 844), Schrödinger proposed the so-called "Schrödinger cat state" paradox — a hypothetical device that triggers a small hammer with the decay of atoms, The vial containing the poison gas is broken, and the vial releases the poison gas to kill the cat. In which the decay of atoms is a random quantum event. The problem is that the decay of an atom is a superposition of multiple states, called super positions, which means that the cat is both dead and alive at the same time. Once the measurement is made, the quantum superposition state is destroyed. In other words, once we open the box to see the results, the cat is only in one state, that is, alive or dead. But this does not mean that the cat was already in this state before opening the box — before the observation, the cat was in a "life and death superposition" state, which is ridiculous. A quantum system in two states at the same time determines whether a cat lives or dies. This experiment shows that quantum theory goes against our intuition. The Schrödinger cat paradox is a blow to the Copenhagen school, because a cat cannot be "both dead and alive."[15]

But Schrödinger's thought experiment was based on the premise that wave functions could describe macroscopic objects (including living organisms), and this was not proven. However, this "cat paradox" discussion is not without merit, and it is intrinsically linked to the EPR paper published in the same year (1935).The inseparable state of a composite system (two-particle system) discussed in EPR is actually an entangled state, and this term happens to appear in Schrödinger's paper, so the entangled state problem is also called Schrödinger's cat paradox. Schrödinger used the term entanglement to describe superposition states of a composite system that could not be represented as direct products, and to illustrate with thought experiments that the wave-function probability interpretation would lead to absurd conclusions when applied to the macroscopic world.

Although Bohr's complementarity principle is widely used and not limited to the wave-particle duality of light, people are used to view the complementarity principle from this duality problem."Interpretation" holds

that both massless and massless particles have wave-particle duality; They sometimes appear as particles (with definite paths, but without interference fringes) and sometimes as waves (with no definite paths, but with interference fringes). It depends on how the experimenter observes, but it is impossible to observe both properties at the same time, i.e. not knowing the path of the particle and having interference fringes at the same time. The complementarity principle of N.Bohr is roughly the same. However, in 2014, the situation changed — recent advances in wave-particle duality research have demonstrated that it is possible to observe both particularity and volatility at the same time by installing two good measuring devices (path information and interference fringe detectors) in the same interferometer device, each of which performs different functions, does not interfere with each other, and works together in the right way.[16]This means that the traditional belief that "two properties are never observed at the same time" may be broken. Prof. Zhiyuan Li, a researcher at the Institute of Physics of the Chinese Academy of Sciences, has been doing research on the "wave-particle duality of microscopic particles and the possibility of violation of the complementary principle"....However, the author believes that even if the complementarity principle is not complete, it will not damage the QM as the physical basis of quantum communication (QC).

X. Quantum Communication and Wootters Theorem

Now we first give the definition of quantum entangled states in mathematical form; A composite system (I and II) is provided, where the common eigenstates of a complete set of mechanical quantities of I are, and the corresponding eigenstates of II are, and respectively represent quantum numbers. $|n\rangle_{\mathrm{I}}$ and $|m\rangle_{\mathrm{II}}$. If the quantum state of the composite system =, it is separable. $|\Psi\rangle_{\mathrm{III}} = |n\rangle_{\mathrm{I}} \otimes |m\rangle_{\mathrm{II}}$. If not, it is an inseparable state (or entangled state), written

$$|\Psi\rangle_{\mathrm{I,\,II}} = \sum_{xm} C_{xm} |n\rangle_{\mathrm{I}} \otimes |m\rangle_{\mathrm{II}} \qquad (12)$$

Here I and II are entangled quantum states, indicating that the measurement of I is related to the measurement of II, regardless of the distance between I and II. This is caused by the superposition of quantum states of the composite system. This quantum entangled state is one of the physical foundations of quantum informatics.

The age of quantum information seems to be suddenly upon us. Can we really use quantum communication methods in the same way as we use smartphones? Many people are asking that question. Since there are a large number of cases in which "physicists do not understand communication and communication experts do not understand quantum physics", people engaged in quantum communication experimental research should make a realistic explanation of their work results and international trends, and must not use the ignorance of the public to exaggerate propaganda and even mislead. In particular, one should not promote a "quantum theology" that would plunge oneself and others into the mire of idealism. For example, what is "quantum teleportation"?Caution should be exercised in presentation and promotion. In short, quantum communication (QC) must explain its existence and significance with the results of practice, the fundamental point of course is its security, confidentiality of the actual effect, and come up with the industry that is most concerned about communication security (such as military, banking) has accepted QC and achieved good results to prove themselves. Unfortunately, there doesn't seem to be any information on that at the moment.

Why is Quantum Communication Secure? The most popular explanation is this[23]: the Heisenberg uncertainty principle (uncertainty relation) causes the following situation, when the eavesdrover does not know the sender coding basis, it is impossible to accurately measure the information of the quantum state; In addition, the principle that quantum states cannot be cloned (Wootters' theorem) prevents eavesdroppers from making a copy of a quantum state to measure after knowing the coding base, so eavesdropping causes errors. At this time, the two parties knew that they were being bugged and stopped communicating.

Entanglement is not mentioned in the above statement; Actual quantum communication systems are diverse, and it seems that entangled photons were not used in QC technology until 2004.Thus entanglement appears to be a necessary condition for unsecured communication.... In conclusion, quantum communication researchers believe that it is Heisenberg's uncertainty principle and Wootters' quantum non-cloning theorem that guarantee the "unconditional security" of the BB84 protocol. It is assumed that the secretor intercepts the photon from the quantum channel and measures it, and this eavesdropping behavior will interfere with the quantum state, so that the operator at the sending and receiving end will feel that someone is eavesdropping and stop the communication. But instead of measuring, the secret keeper copies the same thing (with the cryptographic information).However, in 1982 W. Wolotters[24] proposed the "theorem that quantum states cannot be cloned", which denied the possibility of this method. This maintains the authority of quantum encryption and is considered unbreakable. To quote a document from the Chinese Academy of Sciences,

"Quantum key distribution uses single photons in a superposition state to ensure unconditional security between two parties that are far away from each other."

Wootters' theorem states: "In quantum mechanics, there is no physical process that achieves an exact copy of an unknown quantum state such that each copy is identical to the initial quantum state."By using the linear property of state space, we can simply prove the theorem that single quantum states cannot be cloned, which is very famous in quantum information. Two methods of proof are proposed:

① The input quantum state $|\psi\rangle$ and $|\phi\rangle$ are notexist, and the initial state is the standard pure state $|s\rangle$.

from $U(|\psi\rangle|s\rangle)=|\psi\rangle|\psi\rangle$, $U(|\phi\rangle|s\rangle)=|\phi\rangle|\phi\rangle$, obtain

$$U\left[\alpha(|\psi\rangle+\beta|\phi\rangle)|s\rangle\right]=(\alpha|\psi\rangle+\beta|\phi\rangle)(\alpha|\psi\rangle+\beta|\phi\rangle)$$

$$=\alpha^2|\psi\rangle|\psi\rangle+\beta\alpha|\phi\rangle|\psi\rangle+\alpha\beta|\psi\rangle|\phi\rangle+\beta^2|\phi\rangle|\phi\rangle \quad (13)$$

In addition, there are

$$U\left[\alpha(|\psi\rangle+\beta|\phi\rangle)|s\rangle\right]_{=}\alpha U(|\psi\rangle|s\rangle)+\beta U(|\phi\rangle|s\rangle)$$

$$=\alpha|\psi\rangle|\psi\rangle+\beta|\phi\rangle|\phi\rangle \quad (14)$$

The two are contradictory. So quantum states cannot be cloned.

② There are two quantum systems: A is the quantum state to be cloned, and the initial state is;$|\psi\rangle$. B means we started out in the standard pure state $|s\rangle$.Cloning is described by A unitary operator on a and B complex system, i.e. $U(|\psi\rangle\otimes|s\rangle)=U(|\psi\otimes|\psi\rangle)$ for $\forall|\psi\rangle$ is true, And for $|\phi\rangle\neq|\psi\rangle$, we obtain

$$U(|\phi\rangle\otimes|s\rangle)=U(|\phi\rangle\otimes|\phi\rangle)$$

Take the inner product and $U^{+}U=I$; for the pure state $|s\rangle$, from $\langle s|s\rangle=I$, so

$$(|\phi\rangle\otimes\langle s|)\,U^{+}U\,(|\psi\rangle\otimes|s\rangle)=(|\phi\rangle\otimes|\phi\rangle)\,(|\psi\rangle\otimes|\psi\rangle)$$

$$<=>\langle\phi|\psi\rangle\,\langle s|s\rangle=\langle\phi|\psi\rangle\,\langle\phi|\psi\rangle$$

$$<=>\langle\phi|\psi\rangle=\left(\langle\phi|\psi\rangle\right)^2 \quad (15)$$

now we see, $\langle\phi|\psi\rangle=0$ or $\langle\phi|\psi\rangle=I$, that is, the two states are orthogonal or equal.

The above derivation shows that a quantum cloning machine with a success rate of 1 can only clone a pair of mutually orthogonal quantum states. That is, if the cloning process can be represented as a unitary evolution, then unitary requires that two states can be cloned by the same physical process if and only if they are orthogonal to each other, that is, non-orthogonal states cannot be cloned.

However, in 2018, Xiaochun Mei[25] gave a proof that "the theorem that quantum states cannot be cloned is not true." In the original paper that proved the "theorem that quantum states cannot be cloned," Wootters first assumed that any quantum state could be cloned. Then a quantum state cloning operator is defined, and two conditions under which another quantum state can be cloned are derived. One is orthogonal and the other is non-orthogonal, that is, the integral of the product of these two quantum states is equal to zero or equal to 1. The quantum states that

meet these two conditions can be cloned, but cannot be cloned if they do not meet them. Therefore, there is no question of a quantum state that cannot be cloned, but of what quantum state can be cloned. The study also found that for a general quantum system, there can be an infinite number of quantum states satisfying these two conditions, the so-called quantum state can not be cloned is wrong.

In addition, the quantum state cloning operator defined by Wootters has serious problems. Apply this operator to a cloned wave function, and the result remains the same. Applying it to a standard pure state wave function can turn it into a cloned wave function. Such a result is obviously paradoxical, since the pure wave function is also a wave function, and therefore the quantum clone operator is mathematically untenable.

If Mei's derivation analysis is correct, the statement that "absolute secrecy can be obtained unconditionally by quantum communication" is not valid. However, some people think that Mei said in the article that "lasers can clone a large number of photons" is wrong, because although the laser uses stimulated radiation to work, it will inevitably emit spontaneously, so it cannot be said that it can be cloned. They believe that quantum states cannot be cloned for a long time.... The author has a different opinion on this matter — even if Wootters' theorem is impeccable, QC cannot be "absolutely confidential"; Otherwise, we would not have used decoy to build QC systems since 2004, because in that year science community use other method to build QC system!

XI. Discussion

Quantum mechanics (QM) has been proposed for nearly a hundred years. Now, it has become the foundation and core of modern physics, and its great influence is still expanding. A series of related experiments, such as discriminating experiments on Bell inequality, new experiments on wave-particle duality, experiments on faster-than-light properties presented by quantum tunneling, and recent experiments on the propagation speed of quantum entangled states, and various experiments on quantum communication, etc.; They have gone beyond the discussion of philosophical speculation, and revealed a series of new non-classical physical phenomena, which have aroused great attention. In recent years, not only are many scientists engaged in the research of QM basic theory and quantum information theory and experiment, but also new books on QM are published constantly. This is very welcome.

At the same time, there are some arguments, even fierce arguments; This is normal. However, some articles attempt to negate QM theory system without factual basis, so far do not recognize the greatness of QM theory, causing some confusion in the physical concept. In 1965, R. Feynman famously said, "I can safely say that nobody understands Quantum Mechanics," perhaps illustrating the difficulty of learning and understanding QM. However, if we do not hold the opinion of the family, we can have a definite grasp and correct understanding of the basic theory of QM. The progress and achievements of quantum information are also obvious and undeniable. This is the view of the vast majority of physicists. QM is a successful theory, Einstein's attitude is wrong, these are obvious facts. Even if it is not quite complete, it is enough to be the physical basis for QIT (including quantum communication QC).As for the publicity that QC is absolutely safe and confidential, we cannot agree!

The author emphasizes that the theory of QM is broad and profound, and its application is both extensive and fruitful. Only by acknowledging these two points can a calm and objective discussion take place. The author believes that the mathematical form of quantum mechanics has been established since 1926 to 1928, although it has been refined and generalized from time to time, it can withstand the test of theory and experiment, and has been finalized in theory. But the physical explanation, the physical reality behind the mathematical laws, has long been debated. de Broglie said, "Physicists today almost unanimously agree with Bohr and Heisenberg's explanation, because it seems to be the only one that fits all the known facts."These calm and objective comments should wake people up now. This article is positive about the Copenhagen interpretation.

However, we must also see that some people are still making criticisms at the basic theoretical level. Some claims are specious; For example, regarding the source of the non-locality of QM, some articles on the one hand say that this source is "due to the fact that the QM equation does not completely satisfy relativity", but then say that even the Klein-Gordon equation and the Dirac equation are also non-local, and these two equations are generally recognized as relativistic equations. This is paradoxical and contradicts Einstein's condemnation of "QM as non-local."Einstein never mentioned that non-locality refers to equations, and from his speech at the 5th Solvay Conference (1927) to the EPR paper (1935), he explained the non-locality caused by the way QM is described. It seems that some authors wanted to follow Einstein, but failed to understand the original meaning of Einstein.

The equation of QM is local, and the description is non-local, which is an inevitable result of the basic principle of QM. There are several principles that constitute the QM framework, which cannot be replaced by one equation. For example, the existence of entangled states is due to the following principles: (1) the wave function Ψ completely describes the particle state and its statistical interpretation;(2) Ψ satisfy the

principle of state superposition (which is the embodiment and requirement of volatility) and the measurement hypothesis; (3) The principle of homogeneity (identical particles are indistinguishable, requiring that the wave function of their system must be symmetric or antisymmetric). None of the above requirements is necessary, but it does not matter which QM equation it satisfies.

As for the article that "the other source of non-locality is from Fourier expansion", it is also incorrect. QM is only used with Fourier expansion. Apparently, he mistook the mathematical theorem for QM's superposition principle or measurement hypothesis. The expanded terms of mathematical theorems do not necessarily represent quantum states, whereas the terms of physical principles must be quantum states. It would be a mistake to confuse the two.

In addition, some people use the "Dirac story" to create the atmosphere that "QM is going to die."However, all mechanical quantities in QM are defined by operators, as is angular momentum ($\hat{\mathrm{L}} = \hat{\mathrm{r}} \times \hat{\mathrm{p}}$). Dirac does the same in his book. The so-called "Dirac story" does not mean that "the QM problem is serious" or "Dirac is incompetent."... In addition, we emphasize that "wavelength λ is a spatial range, not a local area", which is common sense.

XII. Improvements and Developments in Quantum Theory

Quantum mechanics is the crystallization of human wisdom and a great scientific creation. But logically, it also needs to be improved and developed. In the author's opinion, the serious problem is that there are always people who want to lead quantum theory with relativity and control quantum theory; However, QM is mainly devoted to the analysis and understanding of the micro world, and the theory of relativity can not deal with the problem of the micro world. Einstein himself developed SR and GR between 1905 and 1915, a period in which he was completely ignorant of the structure of the atom; So how is it possible to use relativity to rule quantum theory? Historically, it is the theory of relativity that has hindered the progress and development of quantum theory, and this is the view of many heavyweight physicists — one example is John Bell, another example is P. Dirac in his later years.

Some say that the combination of SR and QM leads to quantum field theory (QFT), which in turn gives rise to the so-called Standard Model. We do not share this view. This paper has pointed out that SR and QM have conflicting theoretical viewpoints on fundamental issues, which is not only impossible to "integrate with each other", but also incompatible with fire and water."Relativistic quantum mechanics" simply does not exist (see [14])! It is very ridiculous for someone to insist on such an impossible "marriage". As for the Standard Model, because it is built on the basis of "point particles", it is full of loopholes and unconvincing! The so-called "renormalization method" is to fix these loopholes, but it is also futile.

The problem of infinity used to exist in classical physics. For example, Coulomb's law in electromagnetism:

$$F = \mathrm{k}\frac{\mathrm{q}_1\mathrm{q}_2}{\mathrm{r}^2} \tag{16}$$

F is the electrostatic force between the charges q_1 and q_2, the distance r is distance between the charges; If you try to reduce it, F will keep increasing to an unreasonable degree. If $r = 0$, then F becomes infinite. In reality, of course, there is no such force. QFT is said to be an "improvement" on QM, but it is fraught with infinite divergence problems. As Professor Lingjun Wang said, this is a wrong theory, which deals with the infinite very casually and simply inexplicably. If one comes across infinite divergence in classical physics and asks QFT for advice, he will be disappointed! QFT takes relativistic covariance and gauge covariance as its basic principles, which makes it into confusion and cannot solve infinite divergence.

Professor Wang also said: "Another aspect of relativity's influence on QFT is to treat symmetry and covariance as the cornerstones of theoretical physics." Theorists "boldly assume" at the first sign of a problem that things are so absurd in QFT that they would rather have microscopic particles with no mass than stick to their canonical covariance. Yukawa Hideki later realized that there was a problem with QFT, I'm afraid it was too late!

For a long time, large-scale theoretical physics should abide by relativity and Big Bang cosmology, and small-scale theoretical physics should abide by QFT and Standard Model (SM).To do otherwise is heresy. This situation has seriously hindered the development of international theoretical physics — we might say it has not developed at all for many years. SM is also a hypothesis that is increasingly being questioned.... In short, here we advocate the original QM, oppose the use of relativity to interfere with everything, even Einstein himself does not understand high-energy particle physics, but also use relativity, QFT and other very suspicious theories to "guide";In this way, quantum theory will not only not improve and develop, it will only get worse!

Now let's talk about the so-called quantum theory of gravity. As we know, there is no separate time or space in relativity. There is only "space—time"; Although this is a concept that lacks physical meaning, one must accept it. Moreover, this "spacetime" is bendable, although no one knows what that "curved

spacetime" looks like. For gravity, relativity no longer recognizes it as a force, but as a manifestation of curved spacetime. In this way, GR turned physics problems into mathematics, and GR was even called geometro-dynamics.[26] This treatment gives relativity a cloak of mystery, but it does nothing to explain what gravity is. Einstein gravitational field equation (EGFE) is a problem, the author has a special article to discuss, here omitted.

The term quantum gravity implies that quantum theory is combined with GR. But this is impossible because there is no such thing as "bendable spacetime" in QM. Although there are treatises on quantum gravity, they do not solve practical problems. The so-called "gravitons" were nowhere to be found despite vigorous searches. The current talk of quantum gravity is formal and superficial.

After getting rid of the interference of relativity, I think there are two problems in particular that need to be studied. First of all, some people admit on the surface that "the essence of quantum non-locality is faster-than-light", but they insist on SR's "light-speed limit theory", in fact, they still adhere to Einstein's stuff. Second, what is the nature of quantum entangled states? It is not clear yet, and this is a big problem related to how we understand the universe! John Bell had intended to explore these two questions in depth, but died young (in 1990), leaving us to wonder.

XIII. Conclusion

Since the birth of quantum mechanics, it has been continuously doubted, criticized and suppressed. This is particularly true of Einstein, who has used his theory and his immense personal prestige to try to nip QM in the bud. If not, then it cannot be allowed to grow naturally, because the development of quantum theory is a threat to relativity. This self-interested critique of QM reached its climax in 1935.Einstein seems to have forgotten that he made some contributions in the early days of quantum theory; Einstein's theory of photons, for example, is still recognized today for his work on the field that earned him the 1921 Nobel Prize in Physics. His explanation of the photoelectric effect was beyond Maxwell's electromagnetic theory! ... But Einstein has forgotten this and spent 30 years criticizing and attacking QM, as if hoping to put it to death. However, the development of history shows another situation—QM continues to advance in theoretical depth and breadth, and its application continues to expand, and finally the world has entered a historical period of great development of quantum information (QIT).This reminds us of the saying, "He who laughs last laughs best!"

Bell's theorem is a general local theory with implicit supplementary parameters. The theorem assumes that quantum mechanics is "incomplete" and preserves Einstein's local view for the time being. It may be assumed, then, that there is a way to complete the quantum mechanical description of the world while satisfying Einstein's requirement that the physical reality occurring at A cannot affect the physical reality occurring at B unless B receives a signal from A (which, according to SR, cannot travel faster than light).In this case, completing the theory would mean discovering hidden variables and describing how they determine the behavior of particles or photons. (Einstein had suspected that distant particles were related to each other because their common origin gave them some local hidden variables.)These hidden variables are like instruction sheets; When there is no direct correlation between particles, they can show correlation as long as they act on instructions. If the universe is inherently local (that is, there is no faster-than-light communication or faster-than-light effects, as Einstein believes), then the information needed to make quantum mechanics complete must be conveyed by some predetermined hidden variable.

But by 1985, John Bell had completely abandoned these views. In effect, he abandoned both EPR and SR. Many physicists believe that entanglement violates the spirit of relativity because there is "something" (whatever it is) between two entangled particles that does indeed travel faster than the speed of light (even if its speed may be infinite), a view later held by J. Bell, which is the affirmation of faster-than-light.

In the past, many people in the international community believed that the theory of relativity was the highest achievement of Western science, which was wrong. The logic of relativity is so confusing and flawed that it is hard to trust. We believe that if we are to choose the highest achievement of Western science, it should be Newton's classical mechanics and quantum mechanics constructed by many people, their success is the triumph of human intelligence!

References Références Referencias

1. Schrödinger E. Quantisation as a problem of proper values. Ann d Phys, 1926,(4):1～9
2. Schrödinger E. Collected papers on wave mechanics. London: Blackie & Son, 1928.
3. Heisenberg W. Ueber die grundprinzipien der quantenmechanik. Forschungen und Forschritte, 1927, 3:83
4. Heisenberg W. The principles of quantum theory. Chicago: Univ. of Chicago Press, 1930
5. Einstein A, Podolsky B, Rosen N. Can quantum mechanical description of physical reality be considered complete. Phys. Rev, 1935, 47: 777～780
6. Bohm D. Quantum theory. London; Constable and Co., 1954.
7. Bell J. On the Einstein-Podolsky-Rosen paradox. Physics, 1964, 1: 195-200.

8. Bell J. On the problem of hidden variables in quantum mechanics. Rev. Mod. Phys, 1965, 38: 447～452
9. Aspect A, Grangier P, Roger G.The experimental tests of realistic local theories via Bell's theorem. Phys. Rev. Lett, 1981, 47: 460～465
10. Aspect A, Grangier P, Roger G. Experiment realization of Einstein-Podolsky-Rosen-Bohm gedanken experiment, a new violation of Bell's inequalities. Phys. Rev. Lett. 1982,49: 91～96
11. Einstein A. Zur elektrodynamik bewegter körper. Ann d Phys. 1905, 17:891～921. (English translation: On the electrodynamics of moving bodies, reprinted in: Einstein's miraculous year. Princeton: Princeton Univ Press, 1998).
12. Einstein A. The Field Equations for Gravitation. Sitzungsberichte der Deutschen Akademie der Wissenschaften. Klasse f'ur Mathematik, Physik und Technik, 1915: 844～847.
13. Einstein A. Die grundlage der allgemeinen relativitätstheorie. Ann. der Phys., 1916, 49: 769～822
14. Huang Z X Does the "Relativity Quantum Mechanics" really exist. Frontier Science, 2017, 11(4): 12～38.
15. Dirac P. Lectures on quantum mechanics. Yeshiva Univ. Press, 1964.
16. Dirac P. Direction in Physics. New York: John Wiley, 1978.
17. Born M. Einstein A. The Born-Einstein Letters. New York: Palgrave Macmillan, 2005.
18. Gisin N. L'impensable hasard, non-localitè, tèlèportation et autres merveilles quantiques. Genevai: Odile jacob, 2012.
19. Salart D, et.al. Testing the speed of "spoky action at a distance"[J]. Nature, 2008,454: 861～864
20. Shen Z Y. Three questions of physics. Science, 2010, 62(2): 3-4.
21. Aczel A. Entanglement——The Greatest Mystery in Physics. Avalon Pup., 2001.
22. Lu H F. Intepretation of Copenhagen group on quantum physics. Shanghai: Fudan Univ. Press, 1984.
23. Pai C X, et.al. Quantum Communication. Xian: Electronic Science and Technology Univ. Press., 2013.
24. Wootters W. Zurek W. A single quantum can not be cloned. Nature, 1982, 299: 802～803.
25. Mei X C, The proof that the non-cloning theorem of quantum states does not hold. Fund. Jour. of Mod. Phys., 2022,18(1): 27-44.
26. Kiefer C. Quantum Gravity. Oxford Sci. Publ., 2012.

Global Journal of Science Frontier Research: a Physics and Space Science
Volume 23 Issue 6 Version 1.0 Year 2023
Type: Double Blind Peer Reviewed Interenational Research Journal
Publisher: Global Journals
Online ISSN: 2249-4626 & Print ISSN: 0975-5896

On Physical Parameters of the Stellarator Reactor with Regard to Recycling and Anomalous Diffusion Losses

By V. A. Rudakov

Abstract- We present the results of numerical calculations of DT fusion modes in an experimental stellarator reactor operating under conditions of neoclassical transport processes taking into account recycling and the contribution of anomalous losses in the form of Bohm diffusion. The calculations were performed in the reactor with relatively small helical magnetic field corrugations when the effective values of helical magnetic field in homogeneity are less than toroidal in homogeneity ($\varepsilon_{eff} < \varepsilon_t$). Using a numerical code, a system of equations that describes the spatiotemporal behavior of plasma in a stellarator reactor under conditions of equal diffusion fluxes was considered. The influence of Bohm diffusion with a reduced coefficient of proportionality was taken into account. The reactor was modeled using heating sources with a capacity of tens of megawatts to bring it into a steady-state self-sustaining reaction mode. Stable modes of a self-sustaining fusion reaction were obtained while maintaining the plasma density at a constant level by simulating the injection of DT-fuel pellets into the plasma.

Keywords: *nuclear fusion, stellarator reactor, neo-classical diffusion, recycling, anomalous losses.*

GJSFR-A Classification: *ACM: J.2*

Strictly as per the compliance and regulations of:

On Physical Parameters of the Stellarator Reactor with Regard to Recycling and Anomalous Diffusion Losses

V. A. Rudakov

Abstract- We present the results of numerical calculations of DT fusion modes in an experimental stellarator reactor operating under conditions of neoclassical transport processes taking into account recycling and the contribution of anomalous losses in the form of Bohm diffusion. The calculations were performed in the reactor with relatively small helical magnetic field corrugations when the effective values of helical magnetic field in homogeneity are less than toroidal in homogeneity ($\varepsilon_{eff}<\varepsilon_t$).Using a numerical code, a system of equations that describes the spatiotemporal behavior of plasma in a stellarator reactor under conditions of equal diffusion fluxes was considered. The influence of Bohm diffusion with a reduced coefficient of proportionality was taken into account. The reactor was modeled using heating sources with a capacity of tens of megawatts to bring it into a steady-state self-sustaining reaction mode. Stable modes of a self-sustaining fusion reaction were obtained while maintaining the plasma density at a constant level by simulating the injection of DT-fuel pellets into the plasma.

Keywords: nuclear fusion, stellarator reactor, neo-classical diffusion, recycling, anomalous losses.

I. Introduction

Stellarator refers to the number of magnetic traps, on the basis of which it is possible to create a fusion reactor. An attractive feature of this type of fusion device is the possibility of a stationary, self-sustaining fusion reaction.

In the case of a conventional stellarator, in which the plasma-holding magnetic field is created by a system of continuous helical currents, the amplitude of the helical magnetic field in homogeneity turns out to be greater than the toroidal field in homogeneity $\varepsilon_h>\varepsilon_t$. In this case, the neoclassical plasma losses become quite high, which, combined with other loss mechanisms, can make it difficult to achieve modes of self-supported fusion reaction.

In recent years, ideas of creating quasi-symmetric magnetic configurations in stellarators have become popular [1]. The drift trajectories of trapped particles in such systems weakly deviate from magnetic a surface, which lead to reduced plasma losses. The trapping magnetic field in stellarators with quasi-symmetry properties is created by a system of deformed current coils. These traps include the W7-X stellarator. In case of W7-X a quasi-isodynamic configuration has been chosen – yields reduced neoclassical transport and, in particular, good fast ion confinement which is a prerequisite for any type of fusion reactor[2].

In expressions for diffusion fluxes loss reduction is provided by reduction of effective ripple of the helical harmonic ε_{eff}. Thus real values of harmonics of the helical field can remain large or decrease together with reduction of ε_{eff} depending on a way of creation of quasi-symmetry. In the present paper we consider a case when quasi-symmetry provides smallness not only of effective ripples, but also the amplitudes of the helical field harmonics.

In fusion plasma, many different transport mechanisms are present simultaneously, including diffusive, convective, radiation-related, and others. The large number of transport mechanisms does not allow us to unambiguously distinguish the functional dependences of transport flows on the physical and technical parameters of the plasma trap.

As a result of the analysis of experimental data obtained in plasma studies on various stellarators, it was found that the confinement properties of these devices obey certain dependences, which are commonly called scalings [3,4]. Scaling is quite good at predicting the confinement properties of next-generation fusion devices, the parameters of which do not differ much from the current traps. However, it is hardly possible to reliably predict the parameters of a fusion reactor using them. In a full-scale reactor, new energy sources and additional loss mechanisms are included. In addition, the parameters of operating experimental facilities are still far from the parameters of a fusion reactor. More realistic results can be obtained by numerical modeling of the processes taking place, taking into account, if possible, the main mechanisms of transfer and energy release in the reactor plasma.

At determination of diffusion transport fluxes in numerical codes the condition of their ambipolarity is laid, at which equality of fluxes is provided by the radial electric field arising due to quasi-neutrality of plasma. Under the conditions of neoclassical transport, the equality of fluxes can be realized at three values of the electric field. Depending on plasma parameters, flux

Author: Institute of Plasma Physics "National Science Center Kharkov Institute of Physics and Technology", Kharkov, Ukraine.
e-mail: rudakov@kipt.kharkov.ua

equality can arise either at one negative sign of E_r (the ionic root) or at a positive one (the electron root).

When the temperatures of electrons and plasma ions are close to each other, as a rule, ion transport fluxes are predominant and therefore the ion root is realized. In cases of preferential heating of electrons, for example by ECR methods, in sufficiently rarefied plasma the temperature of electrons can be much higher than the temperature of ions, at which the diffusion losses of electrons become larger than the ion losses. In this case, an electron root with positive values of E_r is realized.

The problem of determining the magnitude of the ambipolar electric field turns out to be more complicated when conditions for the realization of different roots of the electric field may occur at different radii of the plasma column. At that, the transition from one sign of the field to another sign occurs in a very narrow region of space with large values not only of the potential gradient, but also of the electric field gradient. For such cases there is no analytical description of diffusive transport flows.

In [5-7], to determine the sign and magnitude of the ambipolar field, the equation obtained in [8], which has the form of the diffusion equation, is used:

$$\frac{\partial E_r}{\partial t} - \frac{1}{V'}\frac{\partial}{\partial r} D_E V' r \frac{\partial}{\partial r}\frac{E_r}{r} = \frac{|e|}{\varepsilon}(\Gamma_e - Z_i\Gamma_i), \qquad (1)$$

where ε is the permittivity, V is the volume of the magnetic surface, D_E is the diffusion coefficient of the electric field. The condition of plasma quasi-neutrality gives enough grounds to consider the right side of the equation equal to zero. In this case, it is necessary to know the correct values of diffusion fluxes. The term with the time derivative in equation (1) does not play a real role. The flows are aligned in relaxation times of the order of ω_{pe}, so taking into account the diffusion of the electric field loses its meaning. The diffusion term on the left side of the equation is rather an additional contribution to one of the diffusion fluxes; however, the value of the diffusion coefficient D_E remains unknown. The main reason for taking into account the contribution of ∇E_r to particle fluxes is the need for a smooth transition from one sign of the root to another sign. The expression for D_E was not given in the publication [8]. In [9], such an expression was obtained, but it contains obvious errors and is unsuitable for application. Thus, the problem of determining the electric field and transport flows in regimes in which a change in the signs of the electric field inside the plasma is possible remains unresolved. It can be circumvented by choosing the plasma parameters at which the sign reversal of the ambipolar field is impossible.

In order to model transport processes in experimental stellarators and reactor plasma, several numerical codes have been developed and used. One of the well-known ones is the DKES (Drift kinetic equation solver) numerical code[10, 11]. This code was used to simulate transport processes in several experimental facilities, in particular, in the Vandelstein7-AS stellarator [12]. Numerical estimates of ambipolar fluxes performed using the DKES code in this work were based on experimental plasma temperature and density profiles. The solutions obtained with this code are not self-consistent and do not take into account the spatial distributions of sources and sinks of particles and energy changing in time.

In [13] the results of comparison of numerical calculations with experiments on determination of E_r in stellarator W 7-AS are presented. Several different estimations were used in calculations: with application of equation (1), in which value of diffusion coefficient E_r was chosen such that to get calculated electric field distribution close to experimental one; from equality of fluxes $\Gamma_e = Z_i\Gamma_i$, and also by zeroing of gradient combination in expression for neoclassical diffusion flux of ions. The last assumption proceeds from the fact that at a relation between diffusion coefficients $D_i >> D_e$, equality of fluxes can come only at small value of combination of gradient terms in the ion flux. Therefore, the magnitude of the potential gradient can be estimated by equating the above combination to zero. In experiments on W 7-AS, the maximum value of the electric field reached values of 50 kV/m when the ion root was realized. In the data presented in the paper, the greatest coincidence of the calculation and experimental results is observed in the estimates from the equality of fluxes at the experimental values of the density and temperature profiles.

In [14], using the DCOM numerical code [15], neoclassical transport in LHD under sufficiently dense plasma conditions was studied. The neoclassical transport coefficients in this code are calculated using the Monte Carlo method. In [14], the NNW (neural network) technique, which allows one to work in conditions of limited data, is also used. The cases are considered when the plasma density is of the order of $1.5 \cdot 10^{19}$ m^{-3}, and the T_e and T_i profiles differ little and have a maximum near 1.2 keV. It is shown that, in this case, only one ion root is realized in the transport fluxes. In this case, the calculation of the transport fluxes and the ambipolar field value was also carried out with the given (experimental) plasma density and temperature profiles.

Neoclassical losses in the TJ-II and LHD stellarators [16] were investigated using the PRETOR code. In the TJ-II stellarator, the plasma was heated by electron-cyclotron heating. The code uses experimental plasma density and temperature profiles. Two modes in terms of plasma density were calculated, small ($n \sim 7 \cdot 10^{18}$ m^{-3}) and large ($n \sim 1.2 \cdot 10^{19}$ m^{-3}). Positive

ambipolar field values at the center of the plasma were obtained in the calculations. In the case of LHD, the discharges in which a high temperature difference at the plasma center ($T_e >> T_i$) is observed and the density profile has a dip at the center of the plasma cord were chosen for the calculations. In these calculations, positive values of E_r were also obtained.

The publications cited present calculations of the profiles of plasma parameters in the formed stationary state. The temporal evolution of the discharges is absent. Note also that none of the mentioned codes solves the problem in a self-consistent way. For calculations of the electric field, fixed (experimental or model) plasma density profiles are necessarily used. Separate calculations were also carried out with fixed temperature profiles.

In [5] an attempt was made to analyze transport processes in several experimental facilities: LHD, TJ-II, and W7-AS, and to make predictions on the parameters of W7-X and on the scale of the fusion reactor. When analyzing the parameters of the experimental facilities, the publication uses model rather than experimental plasma density and temperature profiles. The transport code [6] is used in this work. In the calculations of transport processes in the LHD facility, the plasma density distribution is model-based. The temperature profiles are obtained as a result of solving the transport model under the assumption of ECR heating.

Calculations were made of the spatial distributions of the electric field and energy fluxes for the LHD facility and for a stellarator with twice the size of the LHD. The plasma density in these calculations is of the order of $1 \cdot 10^{20}$ m^{-3}, T_e maximum is 7 keV, and the ion temperature is close to 2 keV. At these parameters, an electron root is obtained in the center of the plasma, which is replaced by an ion root in the middle of the plasma radius. This result is given without any comparison with the results of the experiments at the LHD facility. In [17] the results of experimental measurement of the radial electric field in LHD are presented, in which it is noted that the electron root occurs only at density $n < 0.5 \cdot 10^{19}$ m^{-3}.

Experiments on the W7-X stellarator confirm the presence of transport processes close to neoclassical ones [18]. Under conditions of ECR heating in a relatively rarefied plasma $n < 0.5 \cdot 10^{19}$m^{-3} m^{-3} with a temperature $T_e > T_i$, an electron root is realized. At a higher density, the losses are determined by the ionic component of the plasma.

Designs of stellarator-based fusion reactors are being developed taking into account the design of existing stellarator-type experimental facilities. For example, the design of the Helias reactor [19] is based on the design of the W7-X stellarator, the design of the Heliotron H reactor is based on the design of the LHD stellarator. The physical parameters of the reactors are selected on the basis of stellarator scaling. Publications on calculations of the parameters of stellarator reactors, in which steady-state fusion modes would be achieved by using numerical codes with a self-consistent solution of a system of diffusion equations that takes into account transport processes in the reactor, are unknown to the author of this publication, except for publication [20] and his own works.

In [20] an attempt is made to calculate the parameters of the LHR-S reactor, the linear scale of which is four times larger than that of the LHD stellarator. For the analysis, both a zero-dimensional model based on scaling and a one-dimensional Transport Analysis Linkage code (TOTAL) based on the neoclassical transfer with the inclusion of semi-empirical anomalous losses associated with drift-wave turbulence are used. Using a zero-dimensional model, the plasma density and temperature profiles were given by parabolic distributions. In the one-dimensional transport code, the radial parameter profiles were calculated with anomalous transport coefficients, which were determined by adding the coefficient H=1.6, an improving correction to the ISS95 scaling.

The principle of introducing heating power into the plasma is not given in the publication. The constancy of the plasma density is maintained by injection of fuel pellets, but there is also no information about the order and method of their introduction. It is noted only that when using gas-puffing to implement a self-sustaining process, it is necessary to increase the "enhancement" factor H in proportion to the decrease in plasma density. Note also that in these calculations, the temperatures of the electrons and ions differ little and the sign of the ambipolar field corresponds to the negative ionic root.

The author of this publication performed a number of studies by numerically solving the problem determining the spatiotemporal processes in the plasma of fusion traps of the stellarator type [21-27]. In these works, the neoclassical plasma loss mechanism was assumed to be the main one. As a result of these works, the possibility of implementing both a self-supported thermonuclear reaction and a reaction using additional plasma heating in reactors with different values of the helical in homogeneity of the plasma-holding magnetic field was shown.

It is traditionally assumed that particles leaving the plasma as a result of diffusion will be removed from the reactor using a diverter. However, it is unlikely that such particles will be completely removed. Some of them will return to the plasma, which gives a certain contribution to the balance of energy and particles in the plasma. Publication [27] was made taking this effect into account.

In early studies of plasmas on stellarators it was found that plasma lifetime corresponded to Bohm diffusion [28, 29]. The Bohm diffusion was explained by

the influence of drift instabilities [30]. Possibilities of stabilization of instabilities by means of a shire and a "magnetic well" have been shown. Nevertheless, complete elimination of the influence of various instabilities on plasma losses is hardly possible, so there are reasons to assume the presence of some level of bomb-like diffusion in plasma.

The present work is devoted to the study of the physical parameters of the research reactor-stellarator, the calculations of which are based on the assumption of neoclassical losses in conjunction with anomalous losses caused by bohm-like diffusion with a reduced coefficient of proportionality. The influence of some recycling fraction was also taken into account.

II. Initial Parameters and Numerical Model

As in [24, 27], a stellar reactor with a holding magnetic field of 5 Tesla, a large torus radius of R=8 m, and a small plasma radius of r_p= 2 m were used for the calculations. The work was performed using the numerical code previously developed and described by the author in the publications [26, 27]. A system of four spatially one-dimensional equations is solved: thermal conductivities of electrons and ions, plasma diffusion, and diffusion of neutral atoms.

$$\frac{3}{2}\mathrm{N}\frac{\partial T_e}{\partial t} = -\frac{1}{r}\frac{\partial}{\partial r} r\Pi_e + \frac{K_f N^2 \langle\sigma v\rangle}{4} E_\alpha + Q_{he} - Q_{ei} - Q_b - Q_c + Q_E \quad (2)$$

$$\frac{3}{2} n \frac{\partial T_i}{\partial t} = -\frac{1}{r}\frac{\partial}{\partial r} r\Pi_i + Q_{ei} + Q_{hi} - Q_E \quad (3)$$

$$\frac{\partial n}{\partial t} = -\frac{1}{r}\frac{\partial}{\partial r} r S_e + S_\delta \quad (4)$$

$$\frac{\partial n_a}{\partial t} = -\frac{1}{r}\frac{\partial}{\partial r} r S_a - S_\delta , \quad (5)$$

The equation of thermal conductivity of electrons (2) in the right part, except for the term with thermal conductivity, takes into account the heating of electrons arising during braking of α-particles born in fusion, heating from external energy sources, losses by braking and cyclotron radiation, heat exchange with ions due to Coulomb collisions and due to an ambipolar electric field. Equation of heat conduction for ions (3), except for heat exchange with electrons contains a source of external heating of plasma. Diffusion fluxes and heat fluxes in the heat conduction equation for ions were represented as a sum of neoclassical and bohmian fluxes. The diffusion equations for plasma and neutral atoms of deuterium and tritium, except for diffusion terms, contain as source and sink terms taking into account ionization of atoms. In equations (4) and (5) $S_\delta = n_a\, n <\sigma\upsilon>_i$ the diffusion flux of electrons and the source, responsible for ionization of neutral particles in plasma, $S_a = n_a\, \upsilon_{T0}/\pi$ takes into account the flux of neutral atoms in plasma.

Equal amounts of deuterium and tritium were assumed in the reactor. The density was maintained at a constant level by modeling the injection of fuel pellets and by ionizing neutral atoms entering the plasma by recycling. The value of the radial electric field was found from the equality of the ion and electron diffusion fluxes at each node of the spatial grid along the small radius of the plasma. Different models of plasma heating by external sources were used in the calculations: separately heating of electrons, ions, or simultaneous heating of two components. It was also assumed that the specific heating power is proportional to the plasma density.

The maximum of neoclassical losses in the stellarator is in the region where the effective collision frequency $\nu_{\varepsilon\phi\phi} = \nu_\phi/\varepsilon_{eff}$ appears near the doubled plasma rotation frequency in the radial electric field ω_E [31]. Here ν_j is frequency of Coulomb collisions of ions or electrons of plasma; ε_{eff} is effective amplitude of helical magnetic field corrugations. According to [31], if ε_{eff} turns out to be larger than the amplitude of in homogeneity of the toroidal magnetic field ε_t, the diffusion coefficient to the left of the maximum is proportional to the root squared of ν_j, while in case of opposite inequality ($\varepsilon_{eff}<\varepsilon_t$), diffusion increases linearly with collision frequency - $D\propto\nu_j^1$. To the right of the maximum the diffusion losses decrease with frequency as the collisions $D\propto\nu_j^1$.

The possibility of creating a regime of a self-sustaining fusion reaction in a reactor for the case ($\varepsilon_{eff}>\varepsilon_t$) was considered in [22, 23]. In this work, as well as in [26], the calculations were performed for the case of a reactor with small corrugations of the helical magnetic field, when the inequality $\varepsilon_{eff}<\varepsilon_t$ is satisfied.

A decrease in ε_{eff} leads to an increase in ν_{eff}. In works [22,23,25] studied modes of reactor operation with plasma density $(7–8)\cdot10^{19}m^{-3}$, at which for ions practically always performed a condition $\nu_{eff} < 2\omega_E$, which corresponded to dependence on frequency of collisions of transfer coefficients for plasma ions $D\propto\nu^{1/2}$. At the same plasma parameters in stellarator with small ε_{eff} inequality may change on the opposite, therefore for calculations were chosen more high mean values of plasma density ($<n> = 1.9$, 2 и $2.1\cdot10^{20}m^{-3}$), as a result, almost always the diffusion coefficients of electrons and ions corresponded to the dependence $D\propto\nu_j^{-1}$.

In most cases, the dome-shaped model of fuel pellet ablation was used: $\delta n = n_\delta(1+x^4/\Delta^4-2x^2/\Delta^2)$, where Δ is the half-width of the evaporation region, which was equal to 0.5, 0.75, and 1 in different calculations relative to the plasma radius. The magnitude of the pellet varied within 1 to 2 percent of the total number of particles in the reactor plasma. When the number of particles in the plasma decreased below 0.99, another pellet was thrown into the plasma. The energy consumption for heating the injected particles was taken into account, and the energy losses for pellet evaporation and atom ionization were neglected due to their smallness.

The radius of the first wall of the vacuum chamber was taken to be $r_w = 2.3$m. Also, as in [26], the reactor was calculated with the helical magnetic field corrugation amplitudes $\varepsilon_{eff} = 0.008$, which approximately corresponds to the helical ripples of the W-7X stellarator. Note that in a conventional stellarator, the magnitude of the helical corrugation is an order of magnitude larger.

Under recycling conditions ionization of atoms occurs many orders of magnitude faster than diffusion processes, which need to be calculated simultaneously, so different time scales were used in the numerical model. Initially the problem is solved with small time step and, after establishing approximately constant profile of neutral atoms, the time step is increased so that in acceptable time diffusion processes can be considered.

Neutral particles in the surrounding plasma of the reactor will have a wide spectrum of energies, from a few to tens of electron-volts [32]. The numerical code does not allow taking into account the energy distribution of the particles involved in the recycling, so the calculations were carried out for fixed values of the energies of the neutral atoms. The fraction of particles participating in recycling, relative to the total number lost by plasma, was determined by the recycling coefficient k_r, which in most calculations was equal to 0.25 and in some cases - 0.5. The level of anomalousness in plasma losses was given by different value of the proportionality coefficient k_b in the expression for Bohm diffusion.

The calculations used different initial and boundary conditions for plasma density and temperature. Common to these conditions was the requirement of equality to zero of spatial derivatives in the center of the plasma and close to zero values of these parameters at its boundary. In different calculations, plasma heating was provided by different powers - from 50 to 120 MW. The source of plasma heating could switch off when the reactor's fusion power reached a predetermined level. In this case, the reactor could switch to a self-sustaining burning. At the same time, simultaneously with the stationary reactor power, stationary spatial profiles of plasma density, neutral atoms, ion and electron temperatures, and the ambipolar electric field, which did not depend on the power of external plasma heating sources and the initial distributions of its parameters, were established.

III. Results of Calculations

Figure 1 shows the behavior of the fusion power of the reactor in the process of bringing it to steady-state burning by using different heating powers supplied to the electron component of the plasma. The mean value of the plasma density - $<n>$, the recycling factor - k_r, the energy of neutral particles - E_n, and the half-width of the pellet ablation region - Δ are shown in the caption to the figure. In this case the influence of Bohm diffusion on plasma losses was not taken into account, and the recycling coefficient $k_r = 0.5$, which means that half of the particles that left the plasma are returned to it as a result of diffusion. The maximums on the curves correspond to the moments of switching off the heating power from external sources. After switching off the heating sources, the reactor reaches the same level of thermal power over time. At the same time, the spatial profiles of the plasma parameters also repeat. Some ripples in the curves are the result of fuel pellets injected into the plasma. The use of lower plasma heating powers leads to a slowing down of the reactor's exit to the self-supported reaction.

Figure 1 shows the behavior of the reactor's fusion power when recycling is taken into account. Consideration of recycling leads to a noticeable reduction in the fusion power of the reactor. Figure 2 shows the time dependences of the reactor's thermal power during its steady-state burning when recycling is taken into account and when it is not.

In contrast to Figure 1, the effect of anomalous losses with a coefficient of proportionality with respect to Bohm diffusion $k_b = 0.005$ was also taken into account here. Even a small fraction of particles involved in recycling ($k_r = 0.25$) leads to a significant decrease in

the reactor thermal power practically by 2.5 times. It also turned out that, for the chosen reactor parameters, anomalous losses in the form of a small fraction of the Bohm diffusion coefficient significantly affect the achievement of stable fusion in the reactor. Acceptable fusion reaction modes were obtained only at values of the proportionality factor in the expression for Bohm diffusion ($k_b \leq 0.01$). The time it takes for the reactor to warm up and enter stationary combustion mode is significantly delayed when the fraction of anomalous losses increases. At the same time, the reactor power level also decreases (Fig. 3).

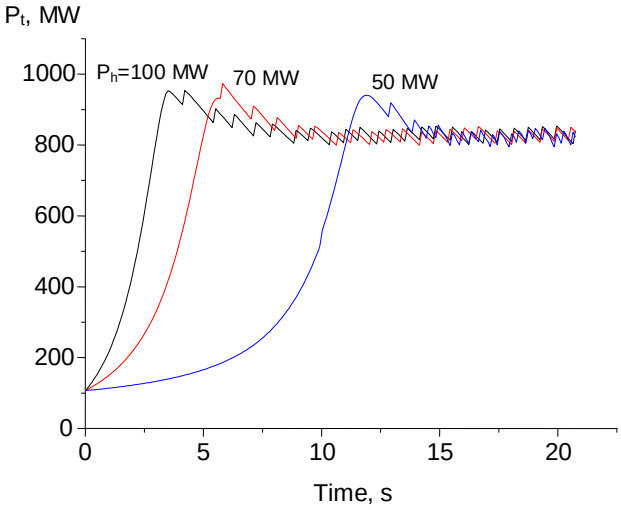

Figure 1: Time dependences of the fusion power of the reactor when using heating sources of different power. P_{he} = 50, 70, 100 MW, $<n>=1.9\cdot10^{20}m^{-3}$, k_r=0.5, E_n= 50 eV, $\Delta = 0.75$.

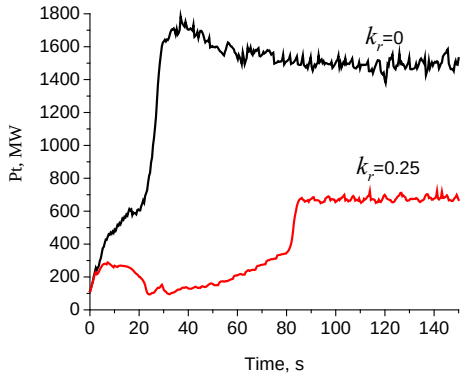

Figure 2: Time dependences of the fusion power of the reactor with and without recycling. P_{he} = 120 MW, $<n>=2.1\cdot10^{20}m^{-3}$, k_b=0.005, E_n= 7 eV, $\Delta = 1$.

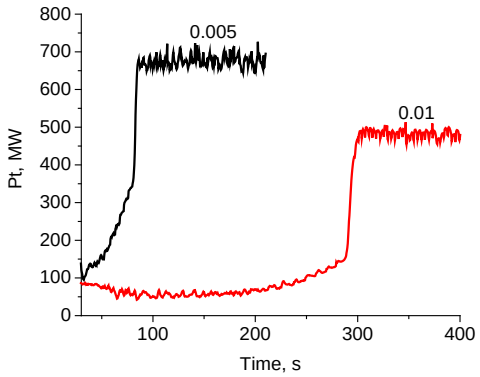

Figure 3: Time dependences of the fusion power of the reactor at various levels of anomalous losses. P_{he} = 120 MW, $<n>=2.1\cdot10^{20}m^{-3}$, k_b=0.005 and 0.01, E_n= 7 eV, k_r=0.25, $\Delta = 1$.

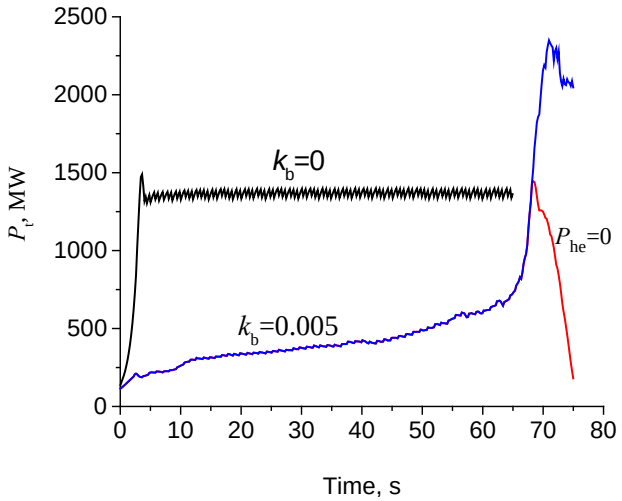

Figure 4: Time dependences of the thermonuclear power of the reactor at $k_b = 0.005$ and in the absence of anomalous losses- $k_b = 0$, $P_{he} = 120$ MW, $<n> = 2.1 \cdot 10^{20} m^{-3}$, $E_n = 7$ eV, $k_r = 0.25$, $\Delta = 0.75$.

Even at such small values of k_b, regimes with a self-sustaining fusion reaction cannot be obtained. Figure 4 shows the time dependences of the thermal power of the reactor for the cases of the absence of anomalous losses and when they are taken into account with k_b=0.005. In the absence of anomalous losses (k_b =0), turning off the heating when the thermal power of the reactor reaches P_t=1500 MW leads to stationary self-sustaining combustion. Atk_b =0.005, turning off the heating leads to a rapid decay of the reactor power (falling section of $P_t(t)$ at t>70 sec). The section of the dependence with k_b=0.005 at a thermal power of more than 1500 MW corresponds to the mode with the power of external sources of plasma heating turned on.

The reasons for the strong influence of anomalous losses on plasma confinement lie in the features of the formation of diffusion and heat fluxes. In this paper, we consider reactor operation modes that correspond to neoclassical losses with the dependences of the transfer coefficients of both plasma components $D \propto \nu^{-1}$. In this case the ion transfer coefficients turn out to be almost $\sqrt{M/m}$ times greater than the corresponding electron coefficients. However, diffusion and heat fluxes are determined by electrons. Diffusion fluxes are aligned due to the ambipolar electric field, which is included in the corresponding combination of density and temperature gradients. Fluxes determined by anomalous transfer coefficients do not depend on the electric potential gradient and, therefore, turn out to be anomalously high in the region of density and temperature gradients. Figure 5 shows the radial plasma density profile and Figure 6 shows the diffusion fluxes: neoclassical electron and bohmian. For the sake of clarity, the calculation was performed in the absence of recycling. In the central part of the plasma, where the density gradient is small, the Bohm flow is even smaller than the neoclassical one.However, in the region of a steep density gradient, there is a sharp jump in the anomalous flow, which is many times greater than the neoclassical one even at a small Bohm loss reduction factor (k_b=0.005).

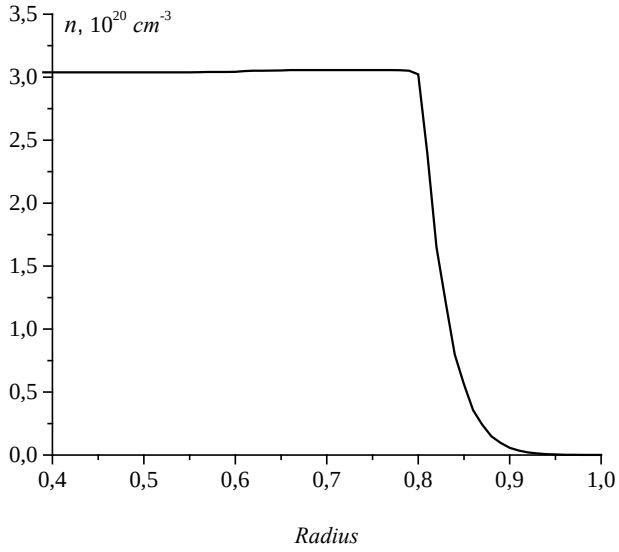

Figure 5: Spatial distribution of plasma density. <n>=2.1·10^{20}m^{-3}, k_b= 0.005, k_r=0, Δ = 1, P_{he}=60 MW , Pt=780 MW, <Te> =7.0keV, <Ti>=6.2 keV.

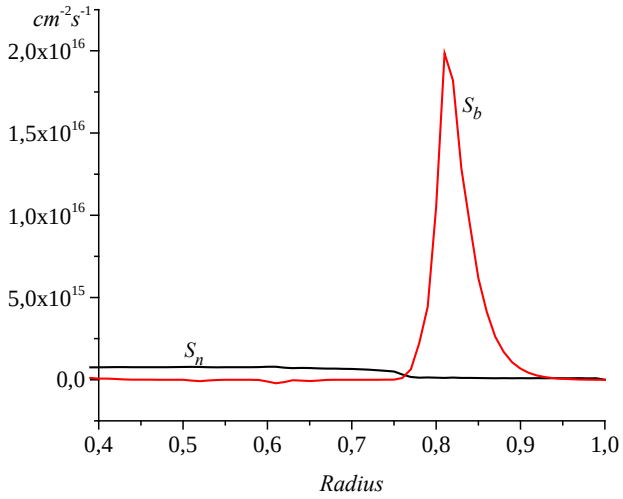

Figure 6: Diffusion fluxes depending on the plasma radius: S_n - neoclassical, S_b-bohmovs. <n>=2.1·10^{20}m^{-3}, k_b= 0.005, k_r=0, Δ = 1, P_{he}=60 MW, Pt=780 MW, <Te> =7.0keV, <Ti>=6.2 keV.

The density of neutral atoms in the space between the reactor wall and the plasma boundary turns out to be several orders of magnitude lower than the plasma density in the containment volume, grows as the fraction of particles involved in recycling increases (Fig. 7) and drops rapidly inside the plasma toward its center.

When the reactor is in the self-sustaining fusion reaction mode, its energy characteristics and the spatial distribution of plasma parameters do not depend on how it is brought into this mode. When additional heating is on, the plasma parameters also depend on the heating methods used. Thus, if additional heating is applied to plasma electrons, as a rule, there is a significant gap in the values of temperatures of electrons and ions at the periphery of the plasma cord. This is the result of weak collision energy exchange between plasma components under conditions of low plasma density. Figures 8-10 show plasma density, temperature, and ambipolar electric field profiles for two average values of plasma density.

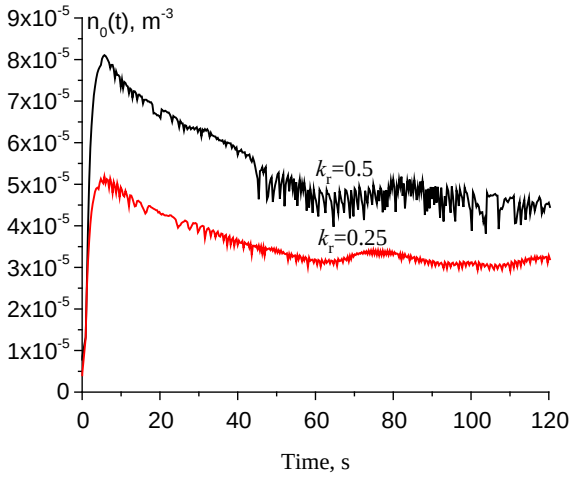

Figure 7: Time dependences of the density of neutral particles in the volume surrounding the plasma

$k_b = 0.005, \langle n \rangle = 1.9 \cdot 10^{20} m^{-3}$, $E_n = 1$ eV, $k_r = 0.25$ and 0.5, $\Delta = 1$, $P_{he} = 120$MW .

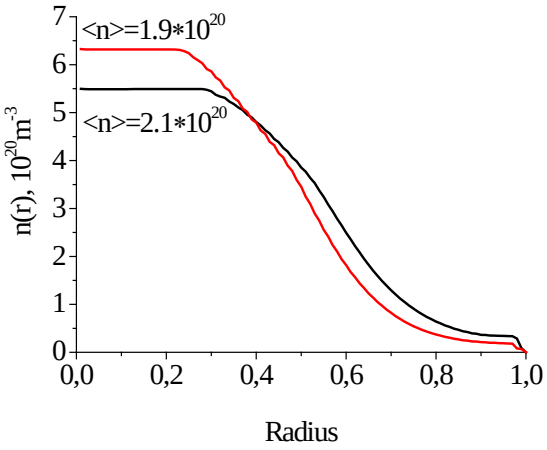

Figure 8: Spatial distributions of plasma density at two mean values

$\langle n \rangle = 1.9 \cdot 10^{20} m^{-3}$ and $\langle n \rangle = 2.1 \cdot 10^{20} m^{-3}$, $k_b = 0.005$, $E_n = 1$ eV, $k_r = 0.25$, $\Delta = 1$, $P_{he} = 120$MW

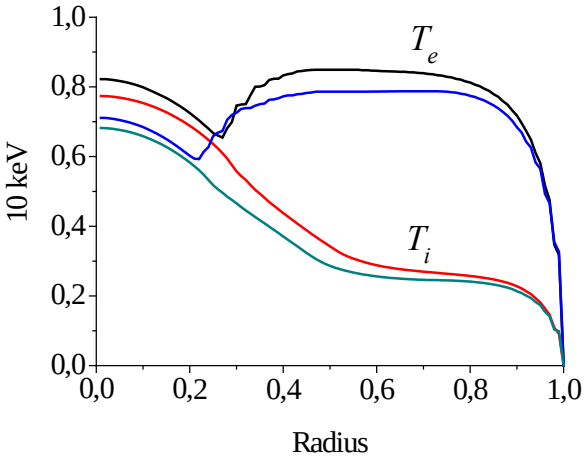

Figure 9: Spatial distributions of plasma temperature at two average plasma densities

$\langle n \rangle = 1.9 \cdot 10^{20} m^{-3}$ and $\langle n \rangle = 2.1 \cdot 10^{20} m^{-3}$, $k_b = 0.005$, $E_n = 1$ eV, $k_r = 0.25$, $\Delta = 1$, $P_{he} = 120$MW .

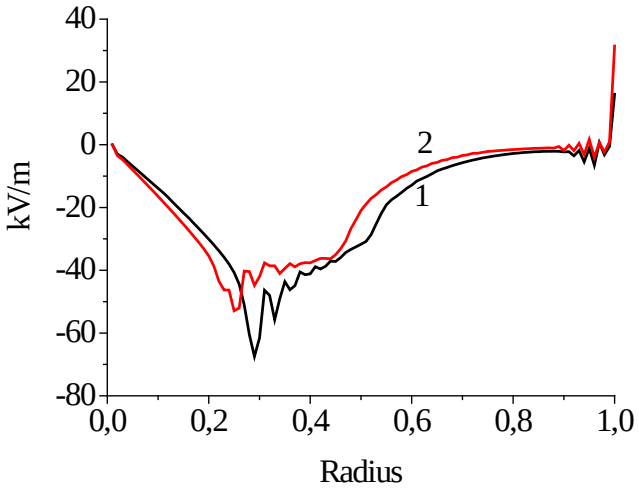

Figure 10: Spatial distributions of the ambipolar electric field at average values of the plasma Density

1 -<n>=1.9·10^{20}m^{-3}, 2 - <n>=2.1·10^{20}m^{-3}, k_b = 0.005, E_n= 1 eV.

IV. Conclusion

Calculations of the synthesis reaction modes in the stellarator reactor, carried out taking into account recycling and anomalous losses, showed their significant effect on the possibility of achieving a self-sustaining synthesis process. The effect of even a very small fraction of Bohm diffusion is especially destructive. In the parameters of the stellarator reactor adopted for calculations, it was not possible to obtain self-sustaining combustion even in the presence of a two-hundredth fraction of Bohm losses in the plasma.The recycling process significantly reduces the parameters of thermonuclear combustion. The results of the work indicate the need to take into account these processes when calculating the expected parameters of the stellarator reactor and take measures to reduce their destructive effect.

References Références Referencias

1. D. Shafranov, Phys. Usp. 42, 720 (1999).
2. T. Klinger *et al* 2019 *Nucl. Fusion* 59 112004 Overview of first Wendelstein 7-X high performance operation.
3. Yamazaki K., Mikhailov M., Sakibara S. et al. Neoclassical and anomalous transport analysis of Helical Reactor Plasmas.//Plasma Fusion Res. SERIES (2004) - Vol. 6. –P. 357-361.
4. Yamasaki K. et al. Global and Local Confinement Scaling Laws of NBI-heated Gas-puffing Plasmas on LHD // EPS-203, St. Peterburg, July 7-11- 2003.–P.3.16.
5. Y. Turkin, C.D. Beidler et al. Neoclassical transport simulations for stellarators//Physics of Plasmas, 18, 022505 (2011).
6. H. Ehmler, Y.Turkin, C.D. Beidler et al. Experimental check of neoclassical predictions for the radial electric field in a stellarator. //Nucl. Fusion 43 (2003), L11-L13.
7. Yu. Turkin, H. Maasβberg, C. Beidler et al// Fusion Science Technol. 50, 387 (2006).
8. D.E. Hastings, W.A. Houlberg, K.C. Shaing. Nuclear Fus. 25, 445 (1985).
9. D.E. Hastings Phys Fluids, 28, 334 (1985).
10. S.P. Hirshman, K.C. Shaing et al. Phys Fluids 29, 2951(1986).
11. W.I. van Rij, S.P. Hirshman// Phys Fluids B 1, 563 (1989).
12. H. Maaβberg, C.D. Beidler et al. The neoclassical "Electron Root" feature in the Wendelstein-7-AS stellarator// Physics of Plasmas, V. 7, #1.–P. 295-311 (2000).
13. H. Ehmler, Y.Turkin, C.D. Beidler et al. Experimental check of neoclassical predictions for the radial electric field in a stellarator//Nucl. Fusion 43 (2003) L11-L13.
14. A. Wakasa, S. Murakami et al. Study of Neoclassical Transport in LHD Plasmas by Applying the DCOM/NNM Neoclassical Database// Plasma and Fus. Res. Regular Articles, v.3, S1030 (2008).
15. A. Wakasa, S. Murakami et al// J. Plasma Fusion Res. SERIES 4, 408 (2001).
16. J. Garcia, K. Yamazaki et al. Neoclassical transport studies in stellarators using PRETOR code// J. Plasma Fusion Res. SERIES, v. 6 (2004).–P. 481-484.
17. K. Ida and LHD experimental group. Interactions between radial electric field, transport and structure in helical plasmas// Problems of Atomic Science and Technology, 2006, № 6. Series Plasma Physics (12).–P. 10-13.
18. T. Klinger *et al* 2019 *Nucl. Fusion* 59 112004.

19. J. Plasma Fusion Res. SERIES, Vol.3 (2000).–P. 135-139
20. K. Yamazaki, M. Mikhailov, S. Sakakibara et al. Neoclassical and anomalous transport analysis of Helical Reactor Plasmas// J. Plasma Fus. Res. SERIES, Vol. 6 (2004).– P. 357-361.
21. V. A. Rudakov O parametrakh reactor stellaratora v usloviyakh ambipolyarnosti neoclassicheskikh transportnykh potokov// Journal of Kharkiv National University, Physical series «Nuclei, Particles, Fields», 2012. – Vyp.2/54/. –P.15-23.(In rus).
22. V. A. Rudakov On physical parameters of the demonstration stellarator-reactor operating in the mode of self-supported thermonuclear reaction// Journal of Kharkiv National University, physical series «Nuclei, Particles, Fields», № 1017, 2012, issue 3/55/. – P.66 -74.
23. V. A. Rudakov About physical parameters of experimental reactor-stellarator in the conditions of ambipolarity of neoclassical transport fluxes// Problems of atomic science and technology, Series "Plasma Physics". –2012. – №6 (82). – issue 18. – P. 16-18.
24. V. A. Rudakov Distribution of plasma parameters in the stellarator at neoclassical transport under conditions of recycling// Problems of Atomic Science and Technology, Series: Plasma Physics 2015, №1 (21), –P. 41-44.
25. V. A. Rudakov The parameters of the stellarator as a neutron source for a subcritical reactor// Journal of Physical Science and Application. –2014. – 4(2). – P. 90-99.
26. V. A. Rudakov Physical parameters of a reactor-stellarator with small ripples of the helical magnetic field// Plasma Physics Reports. 2018, v. 44, №.9, P. 783–790.
27. V. A. Rudakov Effect of recycling for physical parameters of reactor-stellarator// Problems of Atomic Science and Technology, Series: Plasma Physics. 2018, №6, –P. 31-34.
28. Stodieck W., Ellis R.A., Gorman J.G. Loss of charged particles during ionization in stellarator discharges// Phys. Fluids, 1960. –3. –№6. – P. 1053-1056.
29. Stodieck W., Ellis R.A., Gorman J.G. Loss of charged particles in a stellarator// Nucl. Fusion, 1962. –Suppl. Pt. 1. – P. 193-198.
30. S.S. Moiseev, R.Z. Sagdeev. O coefficient diffuzii Boma//ZHETPh, 1963. –T. 44–P.763. (In rus)
31. Mynick H.E., Hitchon W.N.G. Effect of ambipolar potential on stellarator confinement// Nuclear Fusion. – 1983. – Vol. 23. – P. 1023.
32. R. Behrish, G. Federici, A. Kukushkin, D. Reiter// *Journal of nuclear materials*. 2003, 313-316. –P. 388-392.

This page is intentionally left blank

Global Journal of Science Frontier Research: a
Physics and Space Science
Volume 23 Issue 6 Version 1.0 Year 2023
Type: Double Blind Peer Reviewed Interenational Research Journal
Publisher: Global Journals
Online ISSN: 2249-4626 & Print ISSN: 0975-5896

Holographic Phenomenon of the Fifth Cosmic Force

By Yang I. Pachankis

Abstract- The letter reviews existing literature on fundamental particle processes in fusion, fission, and annihilation to reconstruct the causal inference from phenomenological evidence of the fifth cosmic force. The review is interlaced with the evidence obtained on the fifth cosmic force between the non-rigid bodies of black holes and white holes. The causal inference and evidence assessment use the Conformal Cyclic Cosmology as a framework, which is considered to be the most promising cosmological theory currently to incorporate the fifth cosmic force.

Keywords: annihilation; exotic fission; exotic fusion; grand unified theory; nuclear magnetic resonance; t-violation.

GJSFR-A Classification: FOR: 0201

Strictly as per the compliance and regulations of:

Holographic Phenomenon of the Fifth Cosmic Force

Yang I. Pachankis

Abstract- The letter reviews existing literature on fundamental particle processes in fusion, fission, and annihilation to reconstruct the causal inference from phenomenological evidence of the fifth cosmic force. The review is interlaced with the evidence obtained on the fifth cosmic force between the non-rigid bodies of black holes and white holes. The causal inference and evidence assessment use the Conformal Cyclic Cosmology as a framework, which is considered to be the most promising cosmological theory currently to incorporate the fifth cosmic force.

Keywords: annihilation; exotic fission; exotic fusion; grand unified theory; nuclear magnetic resonance; t-violation.

I. Introduction

Grand Unified Theory (GUT) looks to bridge the electromagnetic (EM) force with the weak force and strong force, so that the phenomenon of gravity can be properly explained. In theory, a GUT can deepen the causal explanations of quantum jump and quantum entanglement methodologically, and therein intersects particle physics and cosmology.

Black and white holes are often contextually understood as rigid bodies, but cosmological thermodynamics could have implied otherwise (Glazebrook, 1935; Penrose, 2006). The research with data analysis by nucleon recombination obtained evidence on the non-rigid body nature of the black hole and white hole asymptotic momentum (Pachankis, 2022a).

Inferentially from the non-imaging false-positive result from the experiment with the fifth cosmic force (Pachankis, 2022d), the missions behind the holographic raw data could have used thermonuclear-safe EM LASERs to induce the basic data collection and destructively interfered with the non-rigid body imaging with electrode data collection from cryogenic plates (Bardeen et al., 1973).

Albeit evidence on the fifth cosmic force is non-definitive, the holographic data have definitively and conclusively recorded the phenomenon ample for causal inference. The first question arises: does the fifth cosmic force separate electrons from positrons, shaping the fundamental asymmetry in the EM force? If strong force is exchanged between quarks, how it differs in protons and neutrons in relation to gluons and positrons? This led to the review and analysis of electron and positron conversion in pair production and pair conversion in cold fusion and hot fission behind the phenomenon of black hole and white hole thermonuclear binding (Pachankis, 2022c).

Author: S for Science, Current Address: 1001 Biqing N Rd, Chongqing, 402762, PRC e-mail: ypach@yangpachankis.us

II. Review

a) Electron-Positron Annihilation in Fusion And Fission

Glazebrook (1935) proposed measuring heat as energy for non-rigid EM quantities. The quantity of electrostatic EM force $\frac{mm}{r^2}$ was found to have a linear correlation $hv = 2mc^2$ with γ-quantum conversion (Wang, 1948), implying the Coulomb force is non-fundamental and hidden in the form of thermodynamics. The homogenous phenomenon was theorized in β-decay with the universal constant equivalent to gravitation, with implications in chiral anomaly during electron-positron annihilation by bombarding the former with protons (Bloch & Møller, 1935). The violation of time reversal invariance (T-violation) is implied in Standard Model (SM)-forbidden neutrinoless double β-decay (Dolinski et al., 2019; Vaccaro, 2011) with the detailed mechanisms of D-T fusion. If T-violation needs to be present with parity (P) violation for an elementary particle to possess electric dipole moment (EDM) (Commins), there must be a causal correlation between EM force and gravity by antimatter, except for positrons.

Modern neutron EDM experiments' use of ultra-cold neutrons in spin-dependent charge (C) violation inside EM field demonstrated plausible chirality between matter and antimatter (Dolinski et al., 2019). The chirality may be not only particulate but also cosmic, whereby the critical behavior of the 1d annihilation fission process was observed to differ by particle concentration in the directed percolation class (Odor, 2000). Conformal Cyclic Cosmology (CCC) inherited the cosmic geometry of the Big Bang (BB) theory, adding the chirality to the achiral presumptions of the BB (Gurzadyan & Penrose, 2016; Penrose, 2006, 2018), but just as the toroidalvortices experiment design in strong force pinch effect demonstrated, for the EM force to diffuse in space and function causally relevant in time, the strong force will have to connect both the past and future directions (Bostick et al., 1972), underlying the closed time curve in CCC. Strong force becomes the chiral basis of the EM force in CCC, and an achiral dimension is presumed in

the CCC to close the time curve between the past and the future. Weak force's intervention in the strong and EM forces causes gravity in the CCC model, with an unanswered question on the chirality of time between matter and its essential concept in the GUT.

b) Spin in the Fifth Cosmic Force

The chirality of matter and antimatter is best characterized by Rindler spacetime to the spin-mediated CCC model (Dabholkar, 2022). Figure 1 illustrates the infinitely extended chirality question in the CCC GUT with the geometric symmetry from the BB. However, the concentrated model of a GUT is beneficial for the focused discussions and inference on the fifth cosmic force concerning the cohesive heat flows by the second law of thermodynamics (Penrose, 2006).

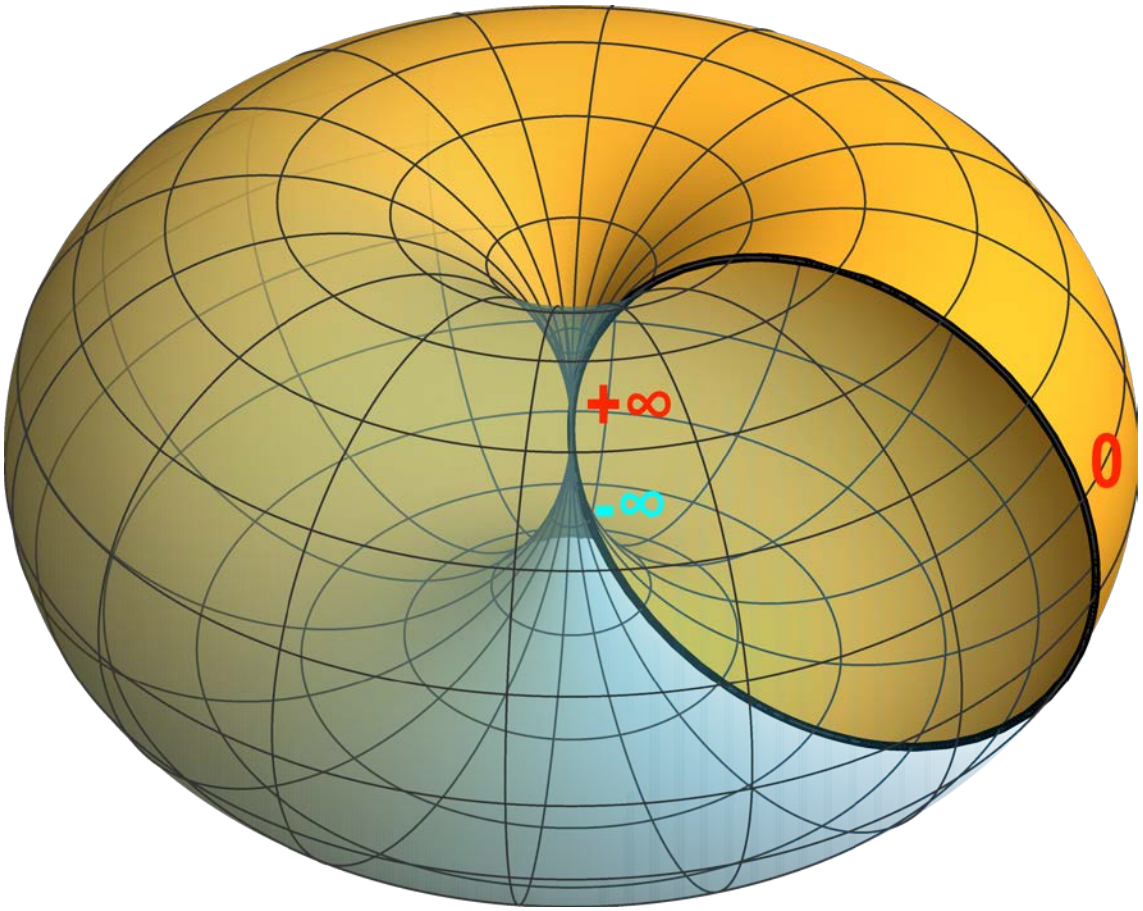

Figure 1: The geometric illustration of the CCC in Rindler spacetime

The spin-dependent chirality between $+\infty$ and $-\infty$ can be simplified to Hamiltonian $\hat{\vec{0}}$ (Pachankis, 2022b), effectively explaining T-violation in the cosmological context in post-BB discussions (Vaccaro, 2011). It was experimentally observed that the spin torque effect facilitates nucleation in annihilation by vortices density with the EM force (Kläui et al., 2006). PT violation is then inferably regulated by bremsstrahlung in the Higgs mechanism, where temperature dependence has been observed in various settings (Hsu et al., 2000; Pasechnik et al., 2015; Wilson, 2014). Between the spin factor and chirality, the energy source can only come from the fifth cosmic force. The inferences are conformable with the evidence obtained on the antimatter-saturated plasmas on the Kerr-Newman black hole and white hole surfaces seen in Figure 2 (Pachankis, 2022b).

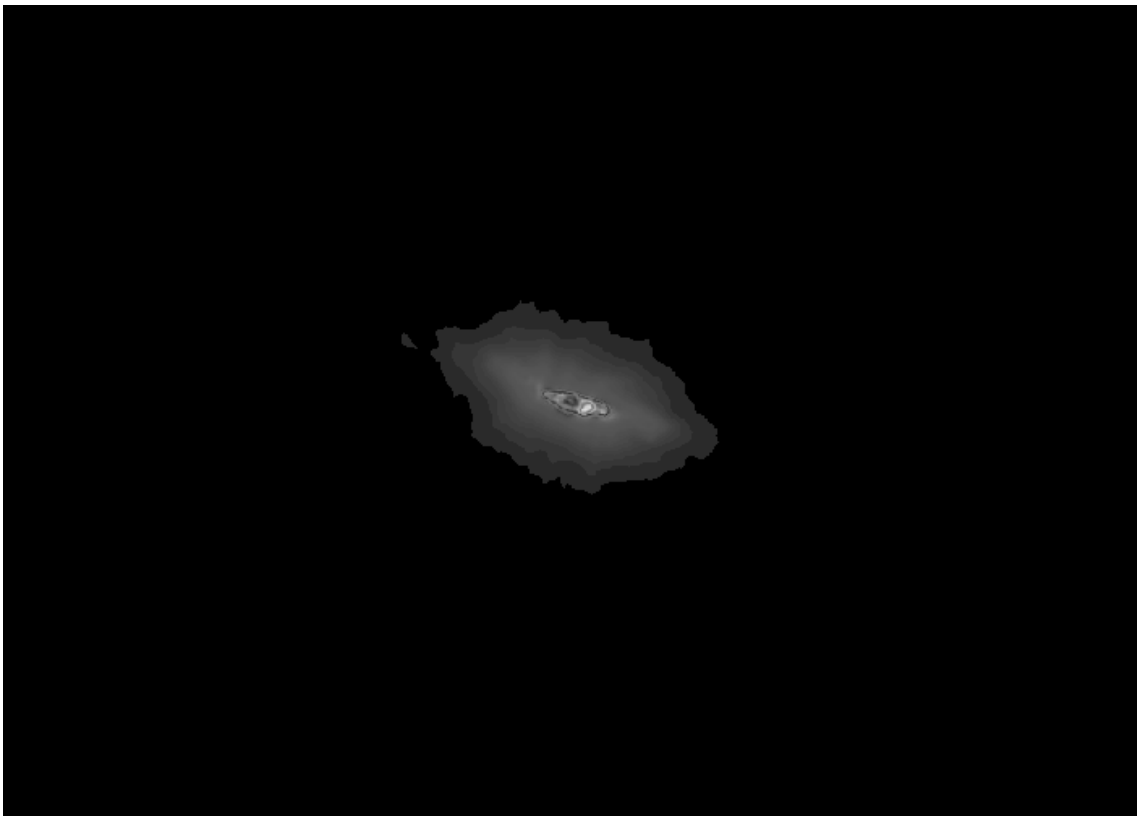

Figure 2: The monochrome multispectral recombination on the black hole and white hole on NGC 3034

Light seeds, namely the white hole seed seen in Figure 3, were predicted, but their cosmological relevance and implications with the CCC were not discovered (Ricarte & Natarajan, 2018). The CCC model concerning the $+\infty$ and $-\infty$ points effectively described the inverse correlations of the fifth cosmic force regarding the cosmic spins in String Theory, and aeons described the exotic metal-insulator formation from the collision momentum (Pachankis, 2022e). Therefore, the CCC is more astrophysical than cosmological, discarding its inheritance from the BB. However, it can also be transformed into observational cosmology with the astrophysical question on the formation of cosmic fields and resonance propagation, which puts the theoretical question on pair production in the cosmic context.

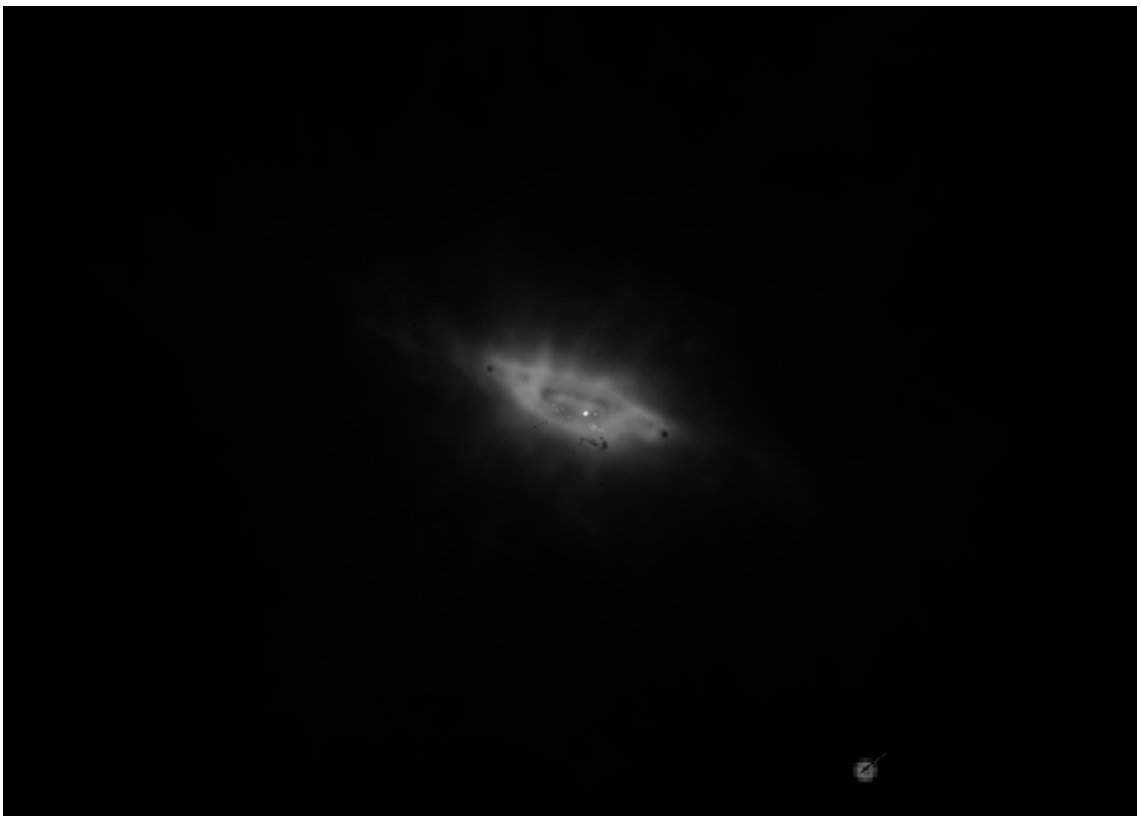

Figure 3: The black hole seed and white hole seed on NGC 3034.

Rainbowed flavor surrounding the Kerr-Newman Supermassive Compact Object (KNSCO) on NGC 3034 is observed on space-based and ground-based telescopes (Pachankis, 2021, 2022b). T + D muon-induced (catalyzed) fusion is effective in the description of the cold fusion process in the mix intersected by the fifth cosmic force (Holmlid, 2022). PT violation on the black hole front is effectively explained by bremsstrahlung between the muon and the electron in the electroweak interaction (Holmlid, 2022). With the differences in diffractive excitation between the space-based and ground-based observation data (Pachankis, 2021, 2022b), it is inferred that the strong force is elastic (Pasechnik et al., 2015; Penrose, 1965), and inelastic diffraction can only be induced by the fifth cosmic force with the boson, hadron, and fermion sets.

Quantum entanglement and Bell's inequality become the phenomenon of the fission interaction in the fifth cosmic force (Ruzbehani, 2021). T-violation is deterministic in the context of vortex annihilation and P violation (Bloch & Møller, 1935; Bostick et al., 1972; Hossenfelder & Palmer, 2020; Odor, 2000). Hot fission and cold fusion are both temperature-dependent by the involvement of positrons in the process (Hsu et al., 2000; Pachankis, 2022b), and nuclear magnetic resonance not only serves as the exterior current for nucleation (Kläui et al., 2006), but also serves for the cooling effect on the KNSCO (Wilson, 2014). Therefore, if the false-positive result seen in Figure 4 was not contributed by EM LASER, it could have been caused by T-violation in the momentum (Pachankis, 2022d).

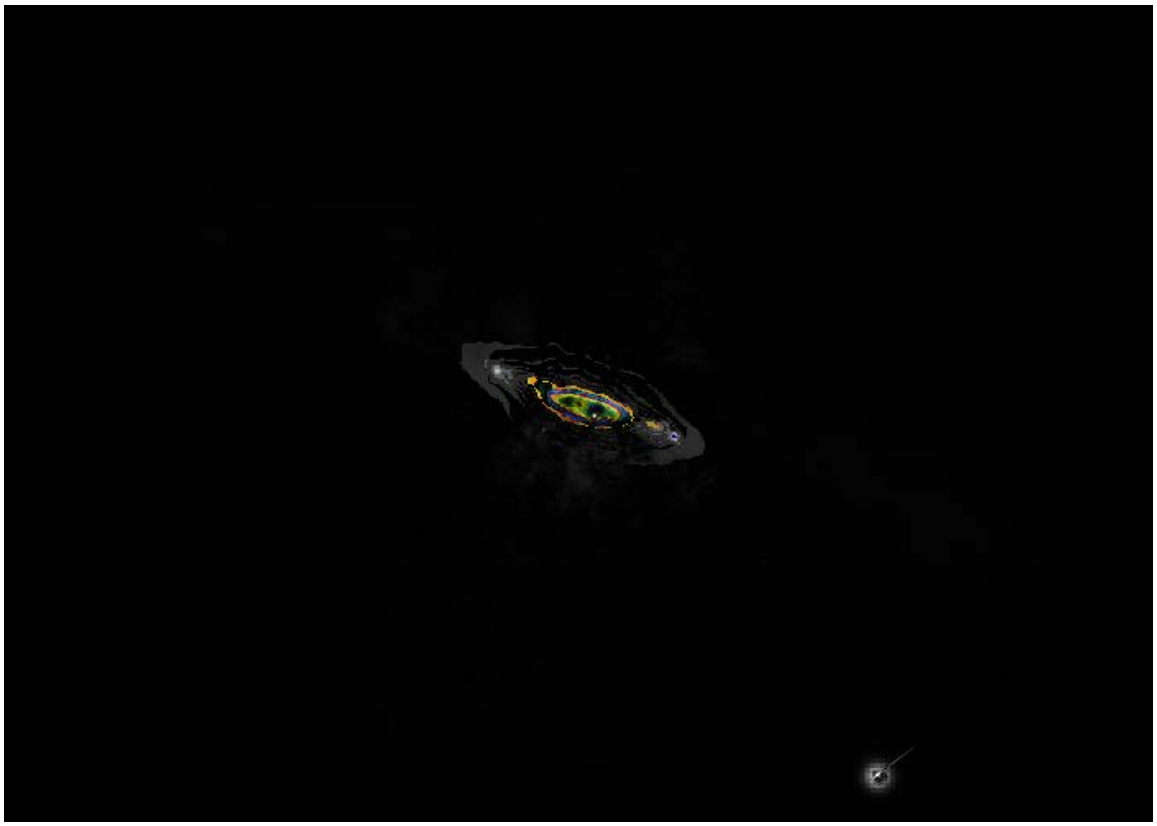

Figure 4: Multispectral material field recombination on the KNSCO on NGC 3034 with the outline of the fifth cosmic force

III. Conclusions

The holographic phenomenon of the fifth cosmic force falsifies all existing mainstream cosmological theories. T-violation concerning the second law of thermodynamics is key to the physical cause of falsification, and there is uncertainty if the law still holds in the fifth cosmic force. If not, the CCC can be the tested existing cosmological theory for further empirical validation and refinement.

Recently, Fermat's Library (2023) tweeted a logically and mathematically flawed equation seen in Figure 5. Proof that follows is a perfect demonstration of the mathematical basis of the falsification of the BB and CCC.

$$1 = \lim_{n\to 0} \sqrt{n + \sqrt{n + \sqrt{n + \dots}}}$$

Figure 5: The inequality is listed as equality in the tweet

Almost all proofs follow the logic that:

$$\lim_{n\to 0} \sqrt{n + \sqrt{n + \sqrt{n + \cdots}}}$$

$$Let\ m = \sqrt{n + \sqrt{n + \sqrt{n + \cdots}}}$$

$$\Rightarrow m^2 = n + \sqrt{n + \sqrt{n + \sqrt{n + \cdots}}}$$

Note that there is no proof that m^2 is a positive number, and the presumption followed, even with L'Hôpital's Rule, all added to the predisposition that the sequence is convergent. My revised proof follows:

$$\Rightarrow m^2 = |m + n|$$

$$\Rightarrow m^4 = (m + n)^2$$

$$\Rightarrow m^4 - m^2 - 2mn = n^2$$

$$\begin{cases} m \neq 0 \Rightarrow \left(\frac{n}{m} + 1\right)^2 = m^2 \Rightarrow \lim_{n\to 0} m = \pm 1 \\ m = 0 \Rightarrow \begin{cases} n = 0 \Longrightarrow contradicts\ with\ the\ definition\ n \to 0 \\ the\ limit\ diverges \Longrightarrow null\ result \end{cases} \end{cases}$$

Therefore, in a closed logic form, the inequality can only be expressed as:

$$1 \Leftrightarrow \lim_{n\to 0}\sqrt{n+\sqrt{n+\sqrt{n+\cdots}}} \Leftrightarrow -1$$

which can be the mathematical conceptual limit on the negative and positive cosmological constant; or else, the limit itself is the limit of the current dimensional construct. "Before" or infinitely many big bangs are mathematically no different from a singular big bang. As expressed from the derivation of the original form:

$$\lim_{n\to 0}\sqrt{n+\sqrt{n+\sqrt{n+\cdots}}} =$$

$$\lim_{n\to 0}\sqrt{n}\sqrt{\pm n^{1-2^0}+\sqrt{\pm n^{1-2^1}+\sqrt{\pm n^{1-2^2}+\sqrt{\pm n^{1-2^3}+\sqrt{\pm n^{1-2^4}+\cdots}}}}}$$

T-violation does not necessarily imply the unidirectionality of time but only the foundation of Bell's inequality. The physical equivalence of the concept of time is challenged by the fifth cosmic force and the hot fission process. There is a possibility that the organic and inorganic chemistry divide can be bridged by further knowledge in the fifth cosmic force or vice versa.

The fifth cosmic force is materialized by the exotic metalinsulator, possibly with the same connotation asaeons. Its materialization is closely associated with P violation and isospin, linking to the strong force. Fundamental (a) symmetry in the BB framework is astrophysically caused by the fifth cosmic force and may be related to the differentiation component of protons and neutrons.

Pair production in the known universe originates from the fifth cosmic force, and there is an uncertainty in the possible fundamental particle therein. The possibility is rendered by the non-quadruple structure with the fifth cosmic force and the KNSCO. Measurement bias in fermionic quantum jumps cannot be fully excluded without antimatter materials for instrumentation upgrades.

Acknowledgments

Yang I. Pachankis thanks NASA and the University of Arizona in their public outreach efforts that made the experiments possible. Yang deeply appreciates professor Chris D. Impey and his colleagues during the whole process. It is with the Global Journals Organisation the research is made available to the public, and Yang I. Pachankis thanks them for the publication support. Last but not least, Yang thanks the Fermat Library and the new math pal Steve Konrad met under the tweet. The discussions substantially helped the formation of the mathematics simplifying the argument.

Funding

There are no sources of funding to declare.

Conflict Of Interest

The author receives royalties from Eliva Press by the book *The Lenses of Quantum Physics on Earth to the Cosmos: From the Humanities to the Apocalyptic Inevitability* cited.

Data Availability

The raw data analyzed in the research was obtained from the publicly available NASA Data Challenge archive with the URL: https://waps.cfa.harvard.edu/eduportal/js9/softwareChallenge_Archive.php.

The processed data and observational experiment data are publicly available on Open Science Framework with the DOI: 10.17605/OSF.IO/WT5Z2.

References Références Referencias

1. Bardeen, J. M., Carter, B., & Hawking, S. W. (1973). The four laws of black hole mechanics. *Communications in Mathematical Physics*, *31*(2), 161-170. https://doi.org/10.1007/BF01645742
2. Bloch, F., & Møller, C. (1935). Production of Neutrons by Annihilation of Protons and Electrons According to Fermi's Theory. *Nature*, *136*(3451), 987-987. https://doi.org/10.1038/136987a0
3. Bostick, W. H., Nardi, V., & Prior, W. J. (1972). *Study of Vortex Annihilation and Neutron Production*.
4. Commins, E. D. *CP Violation in Atomic and Nuclear Physics*https://www.slac.stanford.edu/gen/meeting/ssi/1999/media/commins.pdf
5. Dabholkar, A. (2022). Quantum Entanglement in String Theory. In I. C. f. T. Physics (Ed.), *arXiv*: arXiv.
6. Dolinski, M. J., Poon, A. W. P., & Rodejohann, W. (2019). Neutrinoless Double-Beta Decay: Status and Prospects. *Annual Review of Nuclear and Particle Science*, *69*(1), 219-251. https://doi.org/10.1146/annurev-nucl-101918-023407
7. Glazebrook, R. T. (1935). Meaning of Certain Constants in Use in Physics. *Nature*, *136*(3451), 986-987. https://doi.org/10.1038/136986b0
8. Gurzadyan, V. G., & Penrose, R. (2016). CCC and the Fermi paradox. *The European Physical Journal Plus*, *131*(1). https://doi.org/10.1140/epjp/i2016-16011-1
9. Holmlid, L. (2022). Muon-catalyzed fusion and annihilation energy generation will supersede non-sustainable T + D nuclear fusion. *Energy,*

Sustainability and Society, *12*(1). https://doi.org/10.1186/s13705-022-00338-4
10. Hossenfelder, S., & Palmer, T. (2020). Rethinking Superdeterminism. *Frontiers in Physics*, *8*. https://doi.org/10.3389/fphy.2020.00139
11. Hsu, F. H., Choi, Y. J., & Hadley, J. H. (2000). Temperature dependence of positron annihilation lifetime spectra for polyethylene: positron irradiation effects. *Radiation Physics and Chemistry*, *58*(5-6), 473-477. https://doi.org/10.1016/s0969-806x(00)00202-4
12. Kläui, M., Laufenberg, M., Heyne, L., Backes, D., Rüdiger, U., Vaz, C. A. F., Bland, J. A. C., Heyderman, L. J., Cherifi, S., Locatelli, A., Mentes, T. O., & Aballe, L. (2006). Current-induced vortex nucleation and annihilation in vortex domain walls. *Applied Physics Letters*, *88*(23). https://doi.org/10.1063/1.2209177
13. Library, F. s. [@fermatslibrary]. (2023, July 05). *The Square Root of Zero* Twitter. https://twitter.com/fermatslibrary/status/1676578178297364481
14. Odor, G. (2000). Critical behavior of the one-dimensional annihilation-fission process 2A-->O, 2A-->3A. *Phys Rev E Stat Phys Plasmas Fluids Relat Interdiscip Topics*, *62*(3 Pt A), R3027-3030. https://doi.org/10.1103/physreve.62.r3027
15. Pachankis, Y. I. (2021). Research on the Kerr-Newman Black Hole in M82 Confirms Black Hole and White Hole Thermonuclear Binding. *Academia Letters*, *Article 3199*. https://doi.org/10.20935/al3199
16. Pachankis, Y. I. (2022a). Data-Driven Insights to Cosmology in the Dark Universe. *Journal of Plasma Chemistry and Plasma Processing Research*, *3*(1), 43-50. https://doi.org/10.33140/jpcppr.03.01.05
17. Pachankis, Y. I. (2022b). *The Lenses of Quantum Physics on Earth to the Cosmos: From the Humanities to the Apocalyptic Inevitability*. Eliva Press.
18. Pachankis, Y. I. (2022c). A Multi--wavelength Data Analysis with Multi--mission Space Telescopes. *International Journal of Innovative Science and Research Technology*, *7*(1), 701--708. https://doi.org/10.5281/zenodo.6044904
19. Pachankis, Y. I. (2022d). Physical Signals and Their Thermonuclear Astrochemical Potentials — A Review on Outer Space Technologies*. *International Journal of Innovative Science and Research Technology*, 7(5), 669–674. https://doi.org/10.5281/zenodo.6618334
20. Pachankis, Y. I. (2022e). White Hole Observation: An Experimental Result. *International Journal of Innovative Science and Research Technology*, *7*(2), 779–790. https://doi.org/10.5281/zenodo.6360849
21. Pasechnik, R., Kopeliovich, B., & Potashnikova, I. (2015). Diffractive Bremsstrahlung in Hadronic Collisions. *Advances in High Energy Physics*, *2015*, 1-20. https://doi.org/10.1155/2015/701467
22. Penrose, R. (1965). Gravitational Collapse and Space-Time Singularities. *Physical Review Letters*, *14*(3), 57-59. https://doi.org/10.1103/PhysRevLett.14.57
23. Penrose, R. (2006). Before the Big Bang: An Outrageous New Perspective and Its Implications for Particle Physics. European Particle Accelerator Conference, Edinburgh, Scotland.
24. Penrose, R. (2018). The Big Bang and its Dark-Matter Content: Whence, Whither, and Wherefore. *Foundations of Physics*, *48*(10), 1177-1190. https://doi.org/10.1007/s10701-018-0162-3
25. Ricarte, A., & Natarajan, P. (2018). The observational signatures of supermassive black hole seeds. *Monthly Notices of the Royal Astronomical Society*, *481*(3), 3278-3292. https://doi.org/10.1093/mnras/sty2448
26. Ruzbehani, M. (2021). Simulation of the Bell inequality violation based on quantum steering concept. *Scientific Reports*, *11*(1). https://doi.org/10.1038/s41598-021-84438-9
27. Vaccaro, J. A. (2011). T Violation and the Unidirectionality of Time. *Foundations of Physics*, *41*(10), 1569-1596. https://doi.org/10.1007/s10701-011-9568-x
28. Wang, M. H. (1948). Internal Pair Conversion. *Nature*, *162*(4111), 264-264. https://doi.org/10.1038/162264b0
29. Wilson, R. M. (2014). Nuclear magnetic resonance takes a reaction's temperature. *Physics Today*, *67*(1), 12-14. https://doi.org/10.1063/pt.3.2231

This page is intentionally left blank

Global Journal of Science Frontier Research: a Physics and Space Science
Volume 23 Issue 6 Version 1.0 Year 2023
Type: Double Blind Peer Reviewed Interenational Research Journal
Publisher: Global Journals
Online ISSN: 2249-4626 & Print ISSN: 0975-5896

Leave-Intercalation Theory and Conductive Mechanism during Charge-Discharge Process for Secondary Battery

By C. Z. Yang
Shanghai University

Abstract- The source of conductive ions in the charge and discharge process of AB_5/β-$Ni(OH)_2$, 2H-graphite/ $LiMeO_2$ and 2H-graphite/$LiFePO_4$ batteries is thought to be provided by the phase transition of positive active materials, so it is called phase transition theory. Through the detailed study of the charge and discharge processes of AB_5/β-$Ni(OH)_2$, 2H- graphite/ $Li(Ni_{1/3}Co_{1/3}Mn_{1/3})O_2$ and 2H-graphite/$LiFePO_4$, it is found that the source of conductive ions is the de-intercalation of H (nickel-hydrogen battery) and Li (lithium-ion battery) in positive and negative active materials, and the de-intercalation theory is proposed. On this basis, the conductive mechanisms of these three types of batteries are clarified: The directional migration and movement of conductive ions under the action of electric field.

Keywords: hydrogen-nickel battery; lithium-ion battery, phase transition theory, x-ray diffraction, de-intercalation theory, conductive mechanism.

GJSFR-A Classification: LCC: TK2941.D432

Strictly as per the compliance and regulations of:

Leave-Intercalation Theory and Conductive Mechanism during Charge-Discharge Process for Secondary Battery

C. Z. Yang

Abstract- The source of conductive ions in the charge and discharge process of AB_5/ β-$Ni(OH)_2$, 2H-graphite/ $LiMeO_2$ and 2H-graphite/$LiFePO_4$ batteries is thought to be provided by the phase transition of positive active materials, so it is called phase transition theory. Through the detailed study of the charge and discharge processes of AB_5/ β-$Ni(OH)_2$, 2H-graphite/ $Li(Ni_{1/3}Co_{1/3}\ Mn_{1/3})O_2$ and 2H-graphite/$LiFePO_4$, it is found that the source of conductive ions is the de-intercalation of H (nickel-hydrogen battery) and Li (lithium-ion battery) in positive and negative active materials, and the de-intercalation theory is proposed. On this basis, the conductive mechanisms of these three types of batteries are clarified: The directional migration and movement of conductive ions under the action of electric field.

Keywords: hydrogen-nickel battery; lithium-ion battery, phase transition theory, x-ray diffraction, de-intercalation theory, conductive mechanism.

I. Introduction

Colleagues in the chemical community know that the 2019 Nobel Prize in Chemistry is awarded to three scientists who have made great contributions to the research and development of lithium batteries. They are Professor John. Good enough in the University of Texas at Austin, Professor M Stanley Witt in gham in State University of New York, Binghamton, USA, and Professor Akira Yoshino in Nagoya University, Japan. This event itself shows that the invention, development and application of lithium-ion batteries are of great significance in science and technology, social progress and the improvement of human quality of life in today's world.

In the past 20 years, due to the development of mobile phones, electric bicycles and new energy vehicles, countries all over the world attach great importance to the research, development and application of renewable energy, and our country also attaches great importance to the research, development, industrialization and application of lithium-ion batteries.

After retiring in August 1999, from 2003 to 2011, he was invited to return to the Shanghai Institute of Microsystems and Information Technology (former Metallurgy), Chinese Academy of Sciences, which worked for 26 years (1963-1988). Under the leadership of Professor Xia Baojia, he participated in the study of X-ray diffraction characterization of active materials and the mechanism of charge-discharge, cycle and storage of secondary batteries [including Ni/MH, graphite/ $Li(Ni,Co,Mn)_2$ and graphite/$LiFePO_4$ batteries], and published a series of papers.

In 2011, he left the research group due to his wife's health, but did not give up this meaningful work. Yang Chuanzheng, Lou Yuwan, Zhang Jian, Xie Xiaohua and Xia Baojia published the Chinese version of the monograph 《Material characterization and electrode process Mechanism of green Secondary batteries》 [31] (Science Press, 2011). In 2022, the English version of 《Materials and Working Mechanisms of Secondary Batteries》 (Springer and Science Press in Beijing, 2022) [32] was published(See Attached). These research results belong to the research group. Not only five authors, but also many graduate students have made important contributions. Li Xiao-Feng, Li Jia, Liu Hui, Yan Jian, Liu Hao-Han, Li Yu-Xia and Wang Bao-Guo are worth mentioning. This is the result of the interdisciplinary study of electrochemistry, chemical power supply experts working closely with material physics and X-ray analysis experts.

This time, at the invitation of the Global Journal of Science Frontier Research, I would like to introduce the relevant research results to readers with two summary papers, so as to communicate and learn from their international counterparts. one is "The Leave-intercalation theory and conductive mechanism during charge-discharge process for secondary battery", the other is "Study on the mechanism of cycle and storage process of lithium-ion battery ".

There has been a classic introduction to how the battery works. However, there are few studies on the chemical and physical behavior and conductive physical mechanism in the process of charge and discharge.

Summarize the relevant experimental results, this paper comprehensively introduces a series of important results of X-ray diffraction studies on the charge and discharge processes of AB_5/ β-$Ni(OH)_2$, graphite/$LiMeO_2$ and graphite/$LiFePO_4$ batteries, including the de-intercalation theory of the source of

Author: Physics Department of Shanghai University.
e-mail: yangcz1939@163.com

conductive ions in the process of charge and discharge, and then clarifies the physical mechanism of the conductivity of secondary batteries.

II. Experimental Study on Charge and Discharge Process of Hydrogen-Nickel Battery

a) Phase transition during charge and discharge of hydrogen-nickel battery

In 1966, Bode et al. [1] described the working principle of the battery as follows:

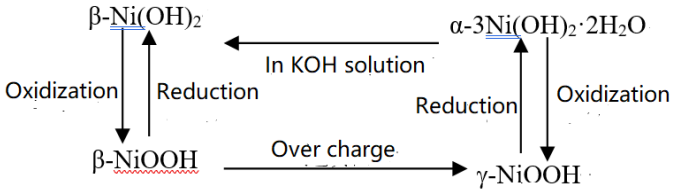

The working principle is written as the following chemical reaction formula [2]. Positive pole negative pole.

$$\text{Charge} \quad \beta\text{-Ni}(OH)_2 + OH \rightarrow \beta\text{-NiOOH} + H_2O + e \quad M + H_2O + e \rightarrow MH + OH^-$$

$$\text{Discharge} \quad \beta\text{-NiOOH} + H_2O + e^- \rightarrow \beta\text{-Ni}(OH)_2 + OH^- \quad MH + OH^- \rightarrow M + H_2O + e^-$$

$$\text{Total reaction} \quad M + \beta\text{-Ni}(OH)_2 \quad MH + \beta\text{-NiOOH}$$

The above description of how the battery works has been written into teaching books and academic monographs [3].

The above tells us that the chemical mechanism of conducting electricity is:

(1) The β-Ni$(OH)_2 \rightarrow \beta$-NiOOH phase transition occurs during charging, and the H^+ ion is supplied by this phase transition.

(2) The transition of AB_5 hydrogen AB_5H_x (hydride) occurs during the charging process.

(3) The above two phase transitions are completely reversible in the process of charge and discharge.

The above conductive mechanism can be called phase transition theory. It can also be seen from the above that under the action of electric field, the driving force of β-Ni$(OH)_2 \rightarrow \beta$-NiOOH phase transition is oxidation, and the driving force of β-NiOOH $\rightarrow \beta$-Ni$(OH)_2$ is reduction. It can be seen that oxidation-reduction is for Ni, and oxidation and reduction occur on the positive electrode and discharge respectively, which is not accordance with the principle that oxidation and reduction occur on the positive and negative electrodes respectively during charging (or discharging).

In 1999, Xing Zhengliang, Li Guoxun and Wang Chaoqun reported the results of charge-discharge in-situ XRD observations. The diffraction pattern of 1c charge for 3 h (300%) was identified as the coexistence of β-NiOOH and γ-NiOOH. This seems to give the experimental evidence of the conductive phase transition theory of MH/Ni battery. However, the experimental evidence of the coexistence of β-Ni$(OH)_2$+β-NiOOH or pure β-NiOOH phase before fully charged was not obtained. Therefore, it is very necessary to study the physical phenomena and physical conductive mechanism of charge-discharge process in detail, and it also has theoretical and practical significance.

b) In situ XRD study of β-Ni(OH)$_2$ on Nickel electrode during charging

In this study, the charge in situ observation was carried out by using the charge-discharge in-situ XRD device (patented product) provided by Rigaku Company in Japan. 1C the diffraction patterns of several stages of charging are shown in figure 1. We can see that in the characteristic diffraction spectrum of β-Ni$(OH)_2$ after 1C charging 50,100,150,480%, only when 1C is 480%, not only the characteristic diffraction pattern of β-Ni$(OH)_2$, but also the 003 and 006 diffraction peaks of γ-NiOOH are observed. The results show that (1) the charge depth of the observed surface is much smaller than that of the interior of the battery, that is, there is a serious hysteresis effect on the surface; (2) in the case of overcharge, β-Ni$(OH)_2$ + -NiOOH coexists rather than β-NiOOH + γ-NiOOH coexist.

c) Quasi-dynamic study of positive active material during charge and discharge of MH/Ni battery

The so-called quasi-dynamic is sampling at different stages of charging and discharging, in other words, some stages of charging or discharging of the battery (original, several intermediate and final states) stopped abruptly, and then the battery was dissected

and the positive and negative active materials were obtained as samples for XRD research and analysis. Figure 2 (a) shows the diffraction pattern of several charging stages.

i. *Phase structure change of β-Ni(OH)$_2$ during charge and discharge of MH/Ni battery*

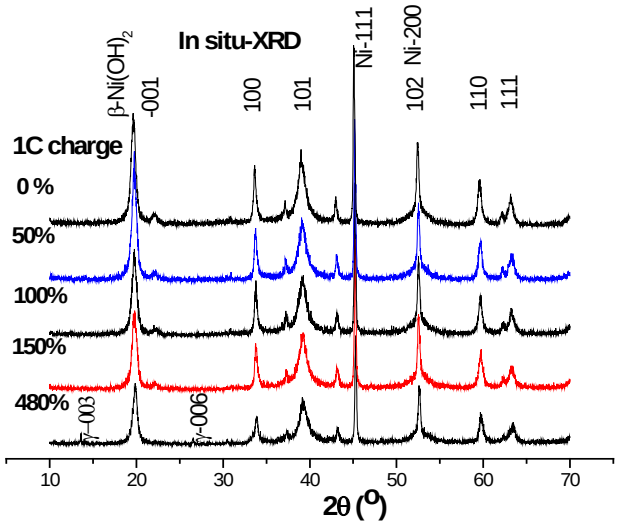

Fig. 1: 1C In situ XRD pattern of β-Ni(OH)$_2$ at different stages, Cuka

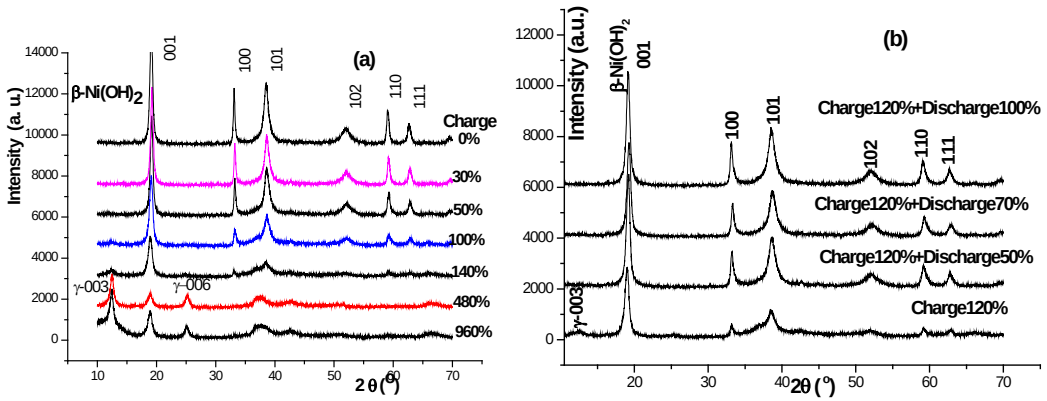

Fig. 2: 0.2c charge (a) discharge (b) XRD spectrum and CuK radiation of positive active material β-Ni(OH)$_2$ at several stages of charging

Know from figure 2 (a)

(1) When the charging depth is 0,30,50,100%, the positive active material still belongs to β-Ni(OH)$_2$.
(2) A small amount of γ-NiOOH is not precipitated until the charging depth reaches 100% and 120%.
(3) The content of γ-NiOOH phase increases with the increase of charging depth.

Now let's analyze the 0.2C charging 120% and 140% XRD patterns.The result of 140% charging is shown in figure 3.It can be seen that the positive active material with 140% charge at 0.2C belongs to the mixture of β-Ni(OH)$_2$ and γ-NiOOH, rather than a mixture of β-NiOOH and γ-NiOOH. Therefore, The pattern of 1C charge for 3 hours (300%) was identifiedby Xing Zhengliang, Li Guoxun and Wang Chaoqun as the mixture of γ-NiOOH and β-NiOOH, that is worth discussing.

From the relationship (see Fig.4) between $I_{\gamma\text{-NiOOH-003}}/I_{\beta\text{-Ni (OH)2-001}}$ and overcharge percentage, it can be seen that the content of γ-NiOOH phase increases with the increase of overcharge percentage.

β-Ni(OH)$_2$ belongs to hexagonal structure, P-3m (No.164) space group. There are 1 molecule, 5 atoms, namely 1 Ni atom, 2 oxygen atoms and 2 hydrogen atoms in the unit cell. The chemical bond between Ni and O is stronger, while that between H and O is much weaker. When there is no stacking disorder, the Ni-O layer presses ABAB ……Stacking in sequence.

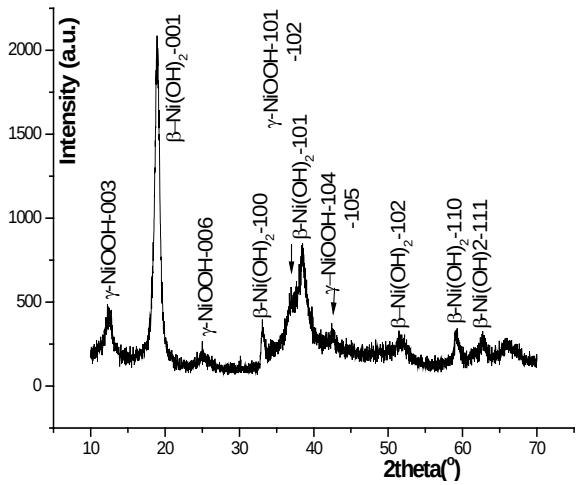

Fig. 3: 0.2 Phase analysis of XRD pattern of cathode chemical material after charging 140%

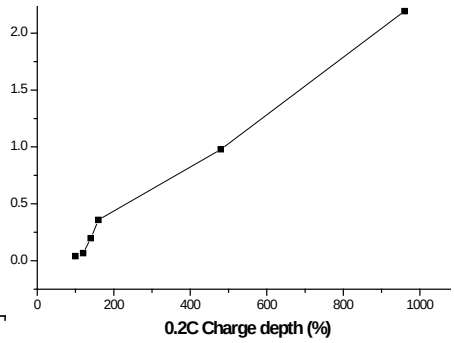

Fig. 4: Variation of $I_{\gamma\ NiOOH\ 003}/I_{\beta\ Ni\ (OH)2\text{-}001}$ with overcharge percentage

The experimental results in sections 2.2 and 2.1 have fully proved that there is no phase transition from β-Ni(OH)$_2$ to β-NiOOH during the charging process of MH/Ni battery. The hydrogen ion H^+ is not provided by this phase transition. The lattice parameters a and c of β-Ni(OH)$_2$ decrease with the charging process, which indicates that the hydrogen atom leaves the lattice position of β-Ni(OH)$_2$ and stay a vacancy, which leads to the lattice distortion of β-Ni(OH)$_2$ and the increase of stacking fault probability. Only when there are enough hydrogen atoms leaving the β-Ni(OH)$_2$ lattice for Ni: O: H to fall from 1:2:2 to 1:2:1 does NiOOH precipitate from β-Ni(OH)$_2$.

There is now a saying that when β-Ni(OH)$_2\rightarrow\beta$-NiOOH, the volume shrinks by 15%, and when β-Ni(OH)$_2\rightarrow\gamma$-NOOH, the volume shrinks by 18%. This 18% seems to be wrong. When β-Ni (OH)$_2\rightarrow\gamma$-NOOH, the cell volume increases by 262.9% (see Table 1).

Table 1: Related data of β-Ni(OH)$_2$, β-NiOOH and γ-NiOOH

Compound	β-Ni(OH)$_2$	β-NiOOH	-NiOOH
Structure system	Hexagonal	Hexagonal	Hexagonal
PDF card No.	03-0177	06-0141	06－0075
Valence state of Ni	Ni^{+2}	Ni^{+3}	Ni^{+3}
a (Å)	3.126	2.81	2.828
c (Å)	4.605	4.84	20.569
V (Å^3)	38.97	33.10	141.45
The rate of increase of cell volume (%)	0.00	-15.07	+262.98
Density (g/cm^3)	3.948	4.62	3.890
Number of molecules / unit cell	1	1	4
V(Å^3)/ molecule	38.97	33.10	35.36
The rate of change in the volume occupied by a molecule (%)	0.0	－15.0	－9.3

More reasonably, the change in the volume of each molecule in the unit cell should be taken into account.In this way, the cell volume of each molecule is reduced by 15.0% at β-Ni(OH)$_2\rightarrow\beta$-NiOOH and only 9.3% at β-Ni(OH)$_2\rightarrow\gamma$-NOOH, as shown in the last row of table 4. It can be seen that it is more reasonable to have β-Ni(OH)$_2$ transition γ-NOOH) rather than β-Ni(OH)$_2$ transition β-NiOOH phase transition.

The XRD patterns of several stages in the discharge state are shown in figure 2 (b). We can see that γ-NiOOH has been decomposed, and the phase structure of β-Ni(OH)$_2$ has not changed, but their fine structure has changed.

ii. *β-Ni(OH)$_2$ fine structure* [7, 11, 12]

The Refine in the Jade program has been used to determine the peak position and HWHM. The data were processed according to the method of reference [8, 9]. The lattice parameters a and c, the average grain size $D_{average}$, the micro-strain $\varepsilon_{average}$ and the total stacking fault probability (f_D+f_T) of β-Ni(OH)$_2$ are calculated.

The changing trends in the charge-discharge process are summarized in Table 2.

Table 2: Changes of fine structure of β-$Ni(OH)_2$ during charge-discharge process

Parameter of fine structure		Charge process	Discharge process
Lattice parameter	*a*	*a* decrease with the increase of charging depth.	It is roughly opposite to the charging process, but it is not completely reversible.
	c	*c* Begin to decrease, then increase	
$D_{everage}$		It thinning with the deepening of the charge and discharge process.	
$\varepsilon_{average}$		With the deepening of the charge and discharge process, it begins to increase, and then becomes smaller.	
(f_D+f_T)		With the deepening of the charging process, it begins to increase slowly, and then increases faster.	

d) Quasi-Dynamic study of negative electrode active material AB_5 during charge-discharge process

The XRD spectrum of the negative electrode active material AB5 in several stages of charge and discharge is shown in figure 5. On the whole, the structure of AB_5 alloy has no obvious change during charging, but the fine structure and microstructure also change. The changing trend with the charge-discharge process is summarized in Table 3. It can be seen that both an and c increase with the increase of charging depth, and the micro-strain ε also increases with the increase of charging depth. The discharge situation is just the opposite, but it returns to the original state, which indicates that there is some irreversibility in the charge-discharge process.

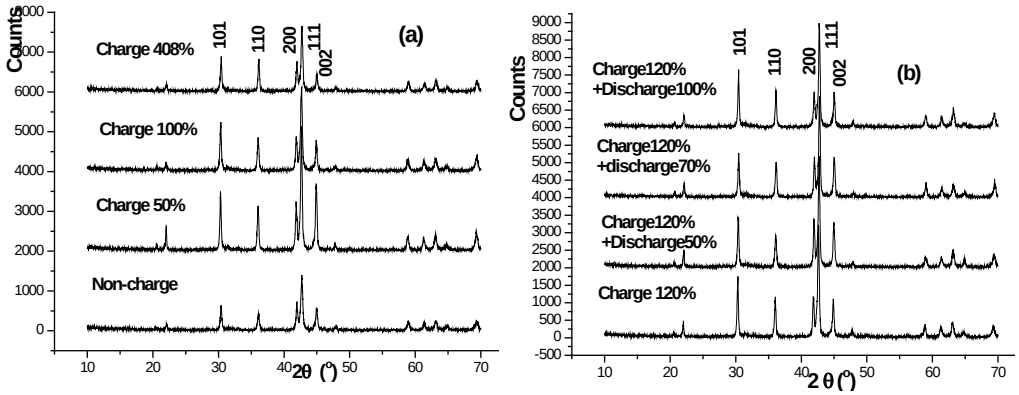

Fig. 5: XRD diagram of negative electrode active material AB5 alloy at several stages of charging (a) discharging (b)

Table 3: Changes of fine structure of AB_5 alloy during charge-discharge process

Parameter of fine structure		Charge process	Discharge process
Lattice parameter	*a*	Increase with the deepening of the charging process	It is roughly opposite to the charging process, but it is not completely reversible.
	c	Increase with the deep of the charging process	
Micro-strain ε		Increase with the deep of the charging process	

III. Experimental Study on Charge and Discharge Process of 2H-Graphite/Lime O_2 Battery

Lithium-ion battery is a new generation of green high-energy battery developed in the early 1990s, which has the characteristics of high energy density, high working voltage, long cycle life and low self-discharge rate, and has been widely used. It will become the preferred battery for electric vehicles and hybrid vehicles. As far as positive active materials are concerned, there are mainly four types of positive active materials: $LiCoO_2$, Li (Ni, Co)O_2, Li (Ni, Co, Mn)O_2 and $LiFePO_4$, but the negative active materials are all 2H-graphite with hexagonal structure, so there are various systems of 2H-graphite/$LiCoO_2$, 2H-graphite/ Li(Ni,Co) O_2, 2H-graphite/Li(Ni,Co,Mn) O_2 and 2H-graphite/ $LiFePO_4$. Moreover, there are different proportions in the

binary or ternary systems of $Li(Ni,Co)O_2$ and $Li(Ni,Co,Mn)$ O_2. However, $LiCoO_2$, $Li(Ni,Co)O_2$ and $Li(Ni,Co,Mn)O_2$ have the same crystal structure, so they can be written as general $LiMeO_2$.

a) Structural evolution of positive active materials during charge-discharge of 2H-graphite/$LiMeO_2$ battery

In 1992, Reimers and Dahn [14] used an on-line (in situ) X-ray diffraction device to find that when $LixCoO_2$ is in the charging process of x=0.5, due to lattice distortion, O-Li-O-Co-O-O., ABCABC... The rhombohedral structure $R\bar{3}m$ of the stack is transformed into a monoclinic structure; Amatucci et al. (1996) [15] considered that the positive terminal of the battery at full charge is CoO_2, which has a hexagonal structure. Yang and MeBreen et al. [16,17] studied the phase transition of $Li_{1-x}CoO_2$ during charging by means of on-line synchrotron radiation X-ray diffraction (λ = 1.195). It is concluded that $Li_{1-x}CoO_2$ changes into monoclinic M2 phase at $0.75 < x < 0.85$, and from hexagonal phase H2 of $CdCl_2$- type to O1A phase of $CdCl_2$- type at $0.77<x<1.00$, which belongs to P63mc space group. Finally, it becomes O1 phase, which is CoO_2.However, these studies only focus on the phase transition of $LiCoO_2$ materials during battery charging, and do not involve the changes of fine structure and microstructure; at the same time, they do not systematically study the fine structure changes of positive and negative active materials in the process of charge and discharge from the point of view of chemical physics. Therefore, in order to deeply understand the structural evolution of electrode materials in the actual battery operation process and explore the working mechanism of electrode materials in the real battery system, this section introduces the use of X-ray diffraction to study the crystal structure and microstructure changes of graphite/$LiCoO_2$ and graphite/$Li(Ni_{1/3}Co_{1/3}Mn_{1/3})O_2$ lithium-ion batteries during charge and discharge.

The XRD patterns of the cathode active material $LiCoO_2$ at different stages of charge and discharge are shown in figure 6. As can be seen from the figure, in the battery charging process, the change of the (006) peak in the cathode material XRD pattern is the most significant. At the initial stage of battery charging (10% charging), it splits at first, then moves to a low angle as the battery charge state continues to increase, and finally disappears; while other diffraction peaks have no other obvious changes except a small offset.

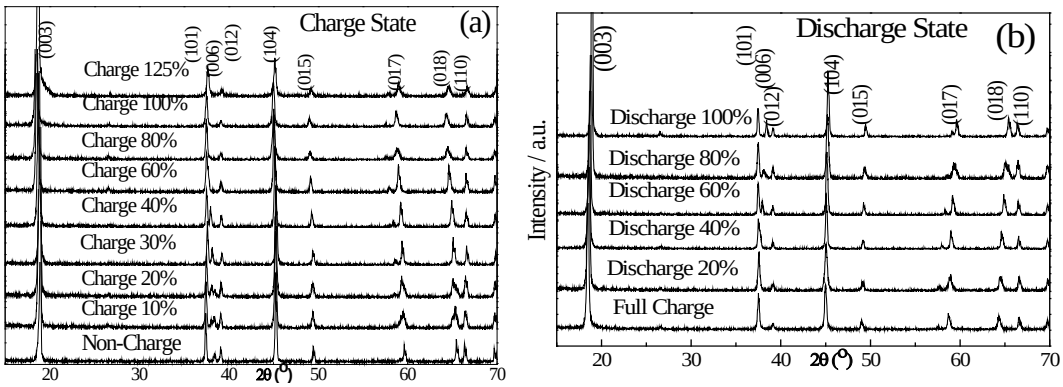

Fig. 6: X-ray diffraction patterns of cathode materials in several main stages of charge and discharge of 18650 graphite/$LiCoO_2$ battery

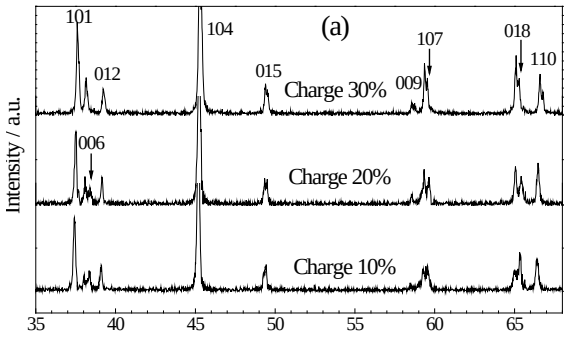

Fig. 7: XRD pattern of cathode material $LiCoO_2$ after removal of $K\alpha_2$ when the battery is charged at 10%, 20% and 30%.

In order to clearly investigate the structural changes of the cathode material $LiCoO_2$ when the battery was charged by 10% to 30%, the three diffraction patterns were magnified in figure 7 after removing $CuK\alpha_2$

components. As can be seen from figure 7, from the battery charge to 10%, in the spectrum (006), The four diffraction peaks of (015), (107) and (018) were all split into two peaks. At the same time, it was found that the intensity of the low angle peak (left peak) was lower than that of the high angle peak (right peak) after the split of each peak (006, 107, 018) at the initial charging stage (10% charging).

As the cell continues to charge (to 20%), the intensity of the low-angle peak increases, the intensity of the high-angle peak weakens, and the intensity of the two peaks is reversed.

The lattice parameters of the two peaks are calculated as two independent phases: when the battery is charged at 20%, the corresponding low-angle peak.

The lattice parameters of the high-angle peak are asides 2.8114, 14.1670, and the high-angle peaks are 2.8104, 14.0983, respectively. It can be seen that the lattice parameters of the two phases are different, but from the characteristic peak, both phases are still $LiCoO_2$ phase.

The above analysis results can be explained as follows: at the initial stage of battery charging (up to 10%), the lattice parameters of the material are changed due to the separation of Li from the $LiCoO_2$ lattice, and the $LiCoO_2$ lattice parameters of the unde-Li remain unchanged, so there are two phases, which is called the lithium-deficient phase; as the battery continues to charge, with the continuous removal of Li, the relative intensity of the two-phase characteristic peaks reverses, indicating that the content of the lithium-deficient phase increases and the content of the original phase decreases. This clearly shows that the de-Li of $LiCoO_2$ has a process from the surface of the electrode to the inner layer.

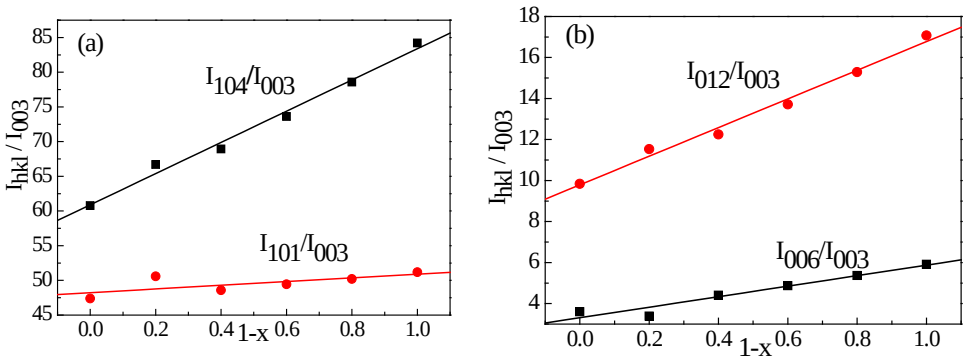

Fig. 8: The relationship between the intensity of the main diffraction lines of $Li_{1-x}CoO_2$ and 1-x

At the same time, as can be seen from figure 6 (a), when the battery is charged to 30% or 40%, the positive active material becomes single-phase again.

The data of the standard $LiCoO_2$ are roughly consistent, only the lines have some displacement; when the battery continues to charge to 60%, 80%, 100% and 125%, except for the disappearance of 006 lines, the other lines are still consistent with the data of the standard $LiCoO_2$, and no new phase is generated. This is different from the report of MeBreen et al. The reasons for the disappearance of 006 lines are as follows:

(1) The diffraction intensity of 006 decreases due to the removal of Li. For this reason, we use the Power Cell program to calculate the relative intensity of each diffraction line according to the $Li_{1-x}CoO_2$ model. The relationship between the relative intensity of each main diffraction line and 1-x is shown in figure 8.
It can be seen that when 1-x=0 is used, the diffraction intensity of 006 decreases very low and is not visible.

(2) lit is possible that 006 overlaps with 101 or 012 due to the change of lattice parameters.

(3) The mixed arrangement of Li/Ni atoms may occur in 2H-graphite/Li $(Ni_{1/3}Co_{1/3}Mn_{1/3})O_2$ battery during charge and discharge [17].

Comparing figs. 8 (a) and (b), it can be seen that the structural change of the positive material $LiCoO_2$ during the discharge of the battery is basically the reverse process of charging.

b) Structural evolution of negative active materials 2H-graphite

The XRD patterns of 2H-graphite/$LiCoO_2$ lithium-ion battery with hexagonal graphite as negative active material during the charge and discharge process are shown in Fig.9(a) and (b) respectively. The results of the analysis are listed in Table 4.

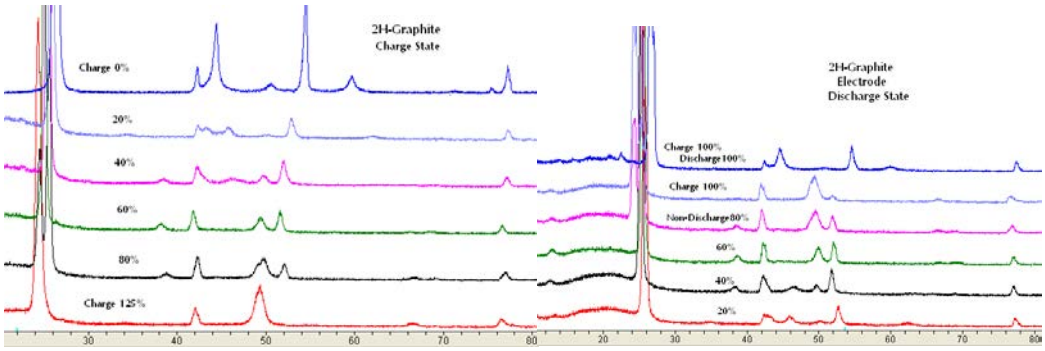

(a) 2θ (°) (b) 2θ (°)

Fig. 9: XRD pattern of negative active materials during charge and discharge of lithium-ion battery. (a) main stages of charging (b) main stages of discharge

Table 4: Results of phase analysis of negative active substances during charge and discharge

Charge state		Discharge state		
charge (%)	Existing phase	discharge (%)	no discharge (%)	Existing phase
0	2H-graphite	100	0	2H- graphite 1+2H-graphite 2
10	2H- graphite 1+2H- graphite 2			
20	2H- graphite	80	20	2H-graphite1+2H-graphite 2
30	2H- graphite			
40	2H- graphite	60	40	2H- graphite
60	2H- graphite	40	60	2H-graphite +LiC_{12}
80	LiC_{24} +LiC_6	20	80	LiC_{12}+LiC_6
100	LiC_6 + Li_2C_2 + LiC_{12} + LiC_{24}	0	100	LiC_6+ Li_2C_2 + LiC_{12} + 2H-graphite
125	LiC_6 + Li_2C_2			

As can be seen from figures 9 and Table 4, there is a gap between the hexagonal grids of carbon atoms embedded in the graphite lattice of Li atoms to form a solid solution, and then Li_{C24}, LiC_{12}, LiC_6 and Li_2C_2 are precipitated. As for when these compounds are precipitated, it is related to the system of lithium-ion battery and the ratio of positive and negative active materials.

IV. Experimental Study on Charge Discharge Process of 2H Graphite/LiFePO$_4$ Battery

a) Phase identification of 2H-graphite/$LiFePO_4$ battery during charge and discharge [23]

$LiFePO_4$ has become one of the most likely cathode active materials to replace lithium secondary battery [19]. This is because lithium secondary ion battery with lithium iron phosphate as cathode has the characteristics of high safety, long life, low cost and environment-friendly, so it has become the focus of development and research in the battery industry. At room temperature, the de-intercalation behavior of $LiFePO_4$ is actually a two-phase reaction process forming the two-phase interface between $FePO_4$ and $LiFePO_4$. Newman[20], Yamada[21] and Dodd[22] have systematically studied the phase transition during the charge-discharge process of $LiFePO_4$. During charging, the lithium ion migrates from the FeO6 layers and enters the negative electrode through the electrolyte, resulting in the oxidation reaction of $Fe^{2+} \rightarrow Fe^{3+}$. In order to maintain the charge balance, the electron arrives at the negative electrode from the external circuit. The reduction reaction occurs during the discharge, and the discharge is opposite to the above-mentioned process. However, the oxidation-reduction occurs on the positive electrode and corresponds to charge-discharge respectively. That is:

$$\text{Charge: } LiFe^{+2}PO_4 + xLi^+ + xe^- \rightarrow xFe^{+3}PO_4 + (1\text{-}x)LiFePO_4$$

$$\text{Discharge: } Fe^{+3}PO_4 + xLi^+ + xe^- \rightarrow xLiFe^{+2}PO_4 + (1\text{-}x)FePO_4$$

$LiFePO_4$ is a typical electron-ion mixed conductor with a band gap of 0.3eV, low electronic conductivity at room temperature and low ionic conductivity at room temperature (about 10~5S/cm). Therefore, in order to use LiFePO4 as cathode material for lithium-ion battery, it is necessary to improve its

electronic and ionic conductivity and improve its electrochemical interface properties.

Figure 10 shows the X-ray diffraction pattern of the positive plate at several stages of the charging (a) and discharging (b) process, and the Pnma orthogonal structure can be used to index $LiFePO_4$ and $FePO_4$, represented by the letters T and H, respectively. It should be noted that $FePO_4$ with orthogonal structure [Pnma (No.62), 34-0134] can only be used for 100% charging patterns,

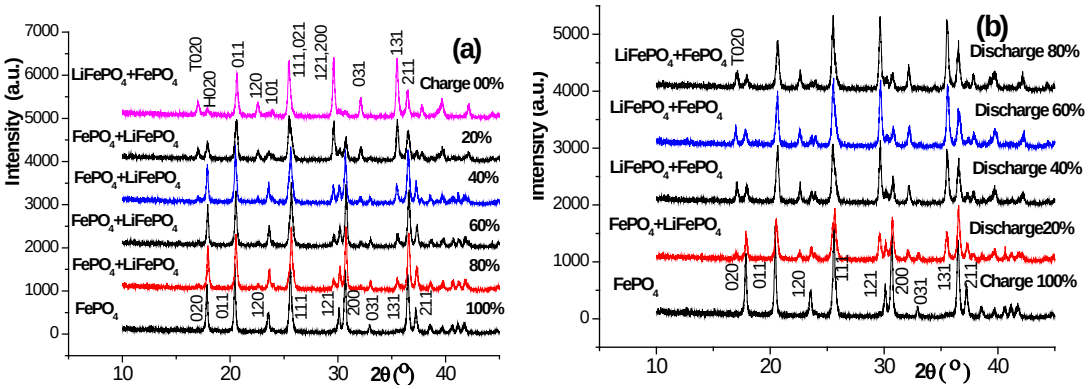

Fig. 10: XRD pattern of positive active material after 0.2C charging (a) and discharging (b) after active 2H-graphite/$LiFePO_4$ battery but not other structures [Cmcm]

The $FePO_4$ of (No.63) or $P_{22}2222$ (No.180)] is indexed. It can be seen that there are $LiFePO_4$ and $FePO_4$ in the positive active material after the aforementioned formation, and the content of the former is more. With the increase of the charging depth, the $LiFePO_4$ gradually decreases and the $FePO_4$ gradually increases. When the charge reaches 80%, there is still a trace of $LiFePO_4$, and it is not all $FePO_4$ until the charge reaches 100%.

From the diffraction pattern of several stages of the discharge process [figure 8 (b)], it can be seen that the positive electrode of the fully charged battery is composed of pure $FePO_4$, and $LiFePO_4$ appears at 20% discharge, and increases with the increase of discharge depth, until 80% discharge, although it is dominated by $LiFePO_4$, there is still a considerable amount of $FePO_4$. Comparing the phase composition of the positive active material of 80% discharge with that of the positive active material when charging 20%, there is an obvious difference between them, which shows that the positive active material is not completely reversible or called asymmetry in the charge-discharge process, but it indicates that there is a change of $LiFePO_4 \leftrightarrow FePO_4$ in the charge-discharge process.

However, based on the synchrotron radiation online (in situ) XRD method, Shin, Chung and Min et al. [24] found that the asymmetry of structural change was not observed in carbon-coated $LiFePO_4$ during 0.2 C charge/discharge, and but the asymmetry became serious when the magnification factor increased to 2C and 10C.

b) Quantitative analysis of phase study on the hysteresis effect of discharge

In order to further analyze the asymmetry of the phase transition of the positive active material during the charge and discharge of graphite/$LiFePO_4$ battery, the relative contents of $FePO_4$ and $LiFePO_4$ in the positive active material at each stage of charge and discharge were quantitatively determined by Zervin's non-standard method [26: 27]. The results are shown in figure 11. As can be seen from figure 9, (1) even in 0%SOC, the positive active material is not entirely $LiFePO_4$ phase, in which there is a small amount of $FePO_4$ phase (calculated to be about 8%), which is due to the formation of inactive $FePO_4$ shell during the first charge. (2) in the case of the same SOC, the content of $LiFePO_4$ in the discharge state is more than that in the charge state, on the contrary, the $FePO_4$ content in the discharge state is obviously low charge state, which obviously reveals that the asymmetry of charge and discharge is caused by the hysteresis effect of discharge.

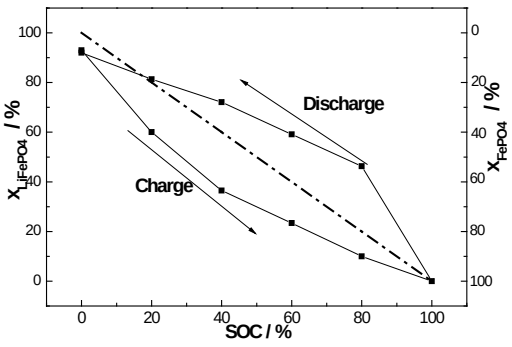

Fig. 11: Content change of $LiFePO_4$ and $FePO_4$ in positive active materials during charge and discharge of graphite/$LiFePO_4$ battery., —·—·—·— 45 degree line

c) The phase transition nature of $LiFePO_4 \rightarrow FePO_4$ [20]

Both $LiFePO_4$ and $Li_{1-x}FePO_4$ belong to triphylite orthorhombic system and Pnma (No.62) space group, while FePO4 belongs to heterosite orthorhombic system

and can only be indexed by Pnma (No.62) space group. The actual measured lattice parameters are:

	a(Å)	b(Å)	c(Å)	V(Å^3)	$(V_T-V_H)/V_T$
$LiFePO_4$	6.0157	10.3915	4.7207	295.101	0.00 %
$FePO_4$	5.8094	9.9222	4.8166	277.638	- 5.92 %

Each unit cell of crystalline $LiFePO_4$ contains four $LiFePO_4$ molecules, namely, 4 Li atoms, 4 Fe atoms, 4 phosphorus atoms and 16 oxygen atoms, with a total of 28 atoms. The atomic position is as follows[25]:

		x	y	z	
Li	4a	0	0	0	
Fe	4c	0.282	1/4	-0.023	+ 0 1/4 0;1/2 0 1/2;1/2/ 1/2 1/2
P	4c	0.095	1/4	0.418	
O1	4c	0.107	1/4	-0.268	
O2	4c	0.460	1/4	0.208	
O3	8d	0.165	0.043	0.288	

The $FePO_4$ unit cell also contains four $FePO_4$ molecules, namely, 4 Fe atoms, 4 phosphorus atoms, 16 oxygen atoms, a total of 24 atoms, and their atomic positions are as follows [26]

		x	y	z	
Fe	4c	0.277	1/4	0.9449	+ 0 1/4 0;1/2 0 1/2;1/2/ 1/2 1/2
P	4c	0.0935	1/4	0.3983	
O1	4c	0.1167	1/4	0.7131	
O2	4c	0.4417	1/4	0.1614	
O3	8d	0.1684	0.0461	0.2513	

The crystal structure model and chemical combination of $LiFePO_4$ and $FePO_4$ are shown in figs. 12 and 13, respectively.

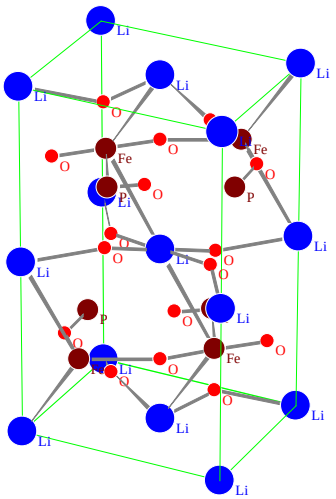

Fig.12: Crystal structure model and bonding of Pnma (No.62) olivine $LiFePO_4$

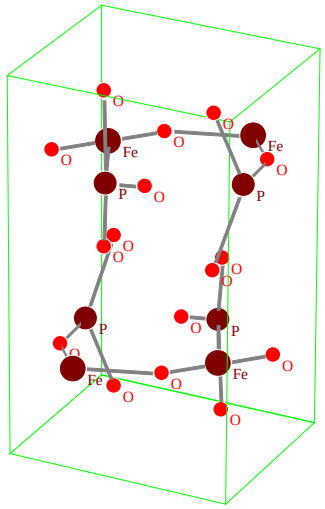

Fig.13: Structural model and bonding of $FePO_4$ of Pnma (No.62) space group structure

From the structural data of the two substances (including space groups, lattice parameters and atomic positions in the unit cell) and the structural models of Fig. 12 and Fig.13, it is known that the crystal structures of the two substances are almost the same. The change of $LiFePO_4$ $Li_{1-x}FePO_4$ $FePO_4$ (x=1) is not a real structural phase transition, only because the Li atom gradually leaves the 4a position of the $LiFePO_4$ crystal lattice under the action of electric field, which changes from $LiFePO_4$ to $Li_{1-x}FePO_4$ Lack Li, and then to $FePO_4$ without Li. However, the crystal structure remains basically unchanged, but only the crystallographic position of each atom moves slightly. Therefore, the change of $LiFePO_4 \rightarrow Li_{1-x}FePO_4 \rightarrow FePO_4$ is not the phase transition of real phase structure change, but can be called pseudo phase transition.

V. Leave-Intercalation Theory during Charge/Discharge Process for Secondary Battery [29]

a) Comprehensive analysis

On the basis of the above research results, the de-intercalation theory of ionic conductivity of secondary battery and the de-intercalation behavior of positive and negative active materials are described from an overall point of view.

The following reactions do not occur at the positive electrode during the charging and discharging process of the hydrogen-nickel battery.

$$\beta\text{-}Ni(OH)_2 + OH \Leftrightarrow \beta\text{-}NiOOH + H_2O + e$$

The following reactions occur at the positive electrode of 2H-graphite/$LiCoO_2$ lithium-ion battery during charge and discharge.

$$LiCoO_2 \Leftrightarrow Li_{1-x}CoO_2 + xLi^+ + xe^-$$

The following reactions occur at the positive electrode of 2H-graphite/ $Li(Ni,Co,Mn)O_2$ lithium-ion battery during charge and discharge.

$$LiMeO_2 \Leftrightarrow Li_{1-x}MeO_2 + xLi^+ + xe^- \text{ [Me represent (Ni,Co,Mn)]}$$

The following reactions occur at the positive electrode of 2H-graphite / LiFePO4 lithium-ion battery during charge and discharge.

$$LiFePO_4 + xLi^+ + xe^- \Leftrightarrow Li_{(1-x)}FePO_4 + xFePO_4$$

So people come to the conclusion that the conductive ions of the battery are provided by phase transition, which is called the phase transition theory of ionic conductivity.

After careful analysis, it is found that the oxidation reaction occurs at the positive electrode and the reduction reaction occurs at the positive electrode during discharge. in other words, the phase transition force during charging is oxidation reaction, and the driving force during discharge is reduction reaction, but this is not consistent with the following principle. that is, in the process of realizing the direct conversion of chemical energy into electric energy, the chemical power supply is in the process of directly converting chemical energy into electric energy. There must be two necessary conditions, one of which is that the process of losing electrons (oxidation) and obtaining electrons (reduction) in chemical reactions must be separated on positive and negative electrodes. Therefore, it is different from the general oxidation-reduction reaction.

Our experimental study found that: The above phase transition does not occur during the charging process of the hydrogen-nickel battery, and the following phase transition occurs only when the battery is fully charged and overcharged.

$$2\beta\text{-}Ni(OH)_2 \rightarrow \beta\text{-}Ni(OH)_2 + \gamma\text{-}NiOOH + H^+ + e^-$$

Although the following changes have taken place in 2H-graphite / LiCoO2 lithium-ion battery

$$LiCoO_2 \longleftrightarrow Li_{1-x}CoO_2 + xLi^+ + xe^-$$

However, the crystal structure of $LiCoO_2$ is the same as that of $Li_{1-x}CoO_2$, and the latter stay a vacancy in the lattice position of Li. Similar changes have taken place in 2H-graphite/$Li(Ni,Co,Mn)O_2$ lithium-ion batteries as follows

$$LiMeO_2 \Leftrightarrow Li_{1-x}MeO_2 + xLi^+ + xe^-$$

However, the crystal structures of $LiMeO_2$ and $Li_{1-x}MeO_2$ are also the same, and the latter stay a vacancy in the lattice position of Li.

The following changes occur during the charging process of 2H-graphite/$LiFePO_4$ lithium-ion battery

$$2LiFePO_4 \rightarrow LiFePO_4 + Li_{1-x}FePO_4 + xLi^+ \rightarrow Li_{1-x}FePO_4 + xLi^+ + FePO_4 \rightarrow FePo_4$$

However, the crystal structures of $LiFePO_4$, $Li_{1-x}FePO_4$ and $FePO_4$ are the same, and the phase transition belongs to pseudo-structure phase transition. The latter two are only lack of Li and no Li in the lattice position of Li.

Because of this, we put forward the de-intercalation theory of ionic conductivity of secondary battery, and clarify the conductive mechanism based on the de intercalation theory.

However, the de-intercalation mechanisms of different electrode active materials in secondary batteries are different. The de-intercalation mechanisms of the electrode active materials involved in this paper are summarized as follows:

b) The deintercalation mechanism of β-Ni(OH)$_2$

β-Ni(OH)$_2$ belongs to hexagonal structure, P-3m1 (No.164) space group, there are one molecule in the unit cell, that is, one Ni atom, two oxygen atoms and two hydrogen atoms, a total of five atoms. Their crystallographic positions in the unit cell are as follows:

Atom	position	x	y	z
Ni	1a	0	0	0
H	2c	0	0	±1/4
O	2d	1/3	2/3	±0.222

The crystal structure model and chemical bonding are shown in figure 16. As can be seen from the diagram, the chemical bond between Ni and O is stronger, while that between H and O is much weaker. When there is no stacking disorder, the Ni-O layer presses ABAB. The hydrogen is stacked sequentially, and the hydrogen is embedded in two layers between the Ni-O layers. The H atom in β-Ni (OH)$_2$ has two equivalent positions 0 0 ±1/4. The energy required for them to leave the β-Ni(OH)$_2$ lattice or re-embed into β-Ni(OH)$_2$ is almost the same, so there is only one charging platform.

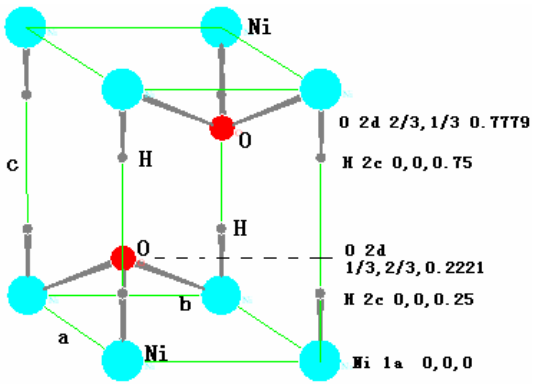

Fig. 16: Crystal structure model and chemical bonding of β-Ni(OH)$_2$

c) The de-intercalation mechanism of H in AB_5 alloy

There is one molecule in the $LaNi_5$ unit cell, that is, one La atom and five Ni atoms. The crystallographic position of the cell is:

Atom	position	Coordinate
La	1a	0 0 0
Ni-1	2c	1/3 2/3 0 ; 2/3 1/3 0
Ni-2	3g	1/2 0 1/2 ; 0 1/2 1/2 ; 1/2 1/2 1/2

The crystal structure model and chemical bonding are shown in figure 17.

Before the charging reaches a certain stage, the embedded hydrogen atom occupies the interstitial position of the $LaNi_5$ lattice and forms the AB_5-H_n solid solution. Hydride AB_5H_x can be formed only when the cell volume increases to a certain percentage due to the intercalation of hydrogen atoms. Of course, the formation of hydride has a process of nucleation and growth. The discharge process should be a reverse process in which the hydrogen atoms preferentially leave the hydride lattice and gradually decompose the hydride, and then the solid solution hydrogen atoms leave the AB_5-H_n solid solution alloy, The maximum value of n is 18. That is that maximum mass fraction of hydrogen storage of $LaNi_5$ is 1.379%[30].

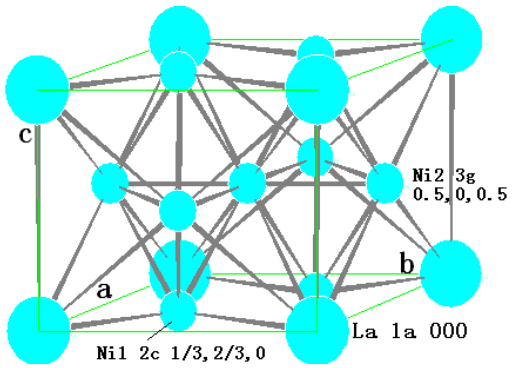

Fig. 17: Crystal structure model and chemical bonding of $LaNi_5$

d) Li intercalation mechanism of $LiMeO_2$ during charge and discharge

$LiCoO_2$ and $Li(Ni_{1/3}Co_{1/3}Mn_{1/3})O_2$ both belong to the (No.166) R-3m space group. There are three molecules in the unit cell. 12 atoms, and their occupancy in the cell is:

Li (3a) 000 ; 2/3 1/3 1/3 ; 2/3 1/3 1/3

Ni,Co,Mn (3b) 001/2 ; 2/3 1/3 5/6 ; 1/3 2/3 7/6

O (6c) 001/4 ; 2/3 1/3 7/12 ; 1/3 2/3 11/12 ; 00-1/4 ; 2/3 1/3 1/12 ; 1/3 2/3 5/12

The crystal structure model and chemical bonding are shown in figure 16.

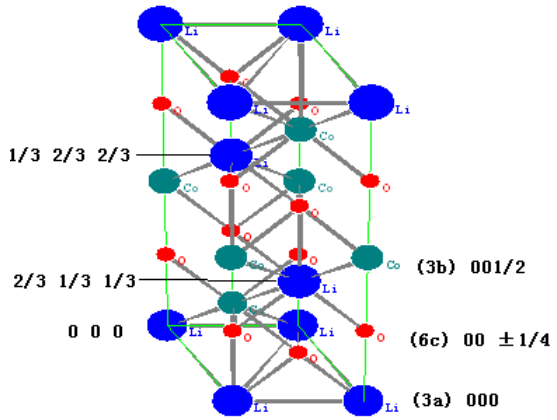

Fig. 16: Crystal structure model and bonding of $LiMeO_2$

As can be seen from the diagram, the chemical bond between the Li atom at position 000 and the neighboring atom is longer, and its binding force in the crystal cell is weak. When charging starts, The Li atom at position 000 is preferentially separated from the crystal lattice. The crystal lattice is followed by the Li atom at 2/3 1/3 1/3 ; 2/3 1/3 1/3 position of the crystal lattice, so it is in the charged state. When < 30%, the lattice parameters and lattice strain change slowly, and then the rate of change is larger. In the process of discharge, it is roughly the reverse process, but it is not completely reversible.

The appearance of two $Li_{1-x}CoO_2$ with different composition when charging in the range of 10-20% indicates that there is not a uniform de-Li of the whole cathode, but a process from the surface to the inside, and finally achieve a more uniform de-Li of the whole electrode. There is no phase transition during the whole charging and discharging process, but the fine structure (lattice parameters, micro-strain) and relative diffraction intensity, especially (006), of the positive active materials change most obviously due to de-Li and re-embedding Li.

e) The behavior of $LiFePO_4$ material during charge and discharge and the mechanism of Li deintercalation

Li atoms have four crystallographic positions in the $LiFePO_4$ lattice, namely:

000 ; 0 1/2 0 ; 1/2 0 1/2 ; 1/2 1/2 1/2

As can be seen from figure 12, the bonding force at position 000 is the weakest, and the bonding force at position 1/2 1/2 1/2 is the strongest, and that at position 0 1/2 0 is similar to that at position 1/2 0 1/2. Therefore, under the action of a smaller electric field, the Li atom at position 000 first leaves the $LiFePO_4$ lattice until it becomes $Li_{0.25}FePO_4$, and then the Li at position 0 1/2 0 and1/2 0 1/2 leave successively. Until it becomes Li-deficient $Li_{0.50}FePO_4$ and $Li_{0.75}FePO_4$, and finally, the Li atom at position 1/2 1/2 1/2 leaves until it becomes $FePO_4$ without Li. There may be four steps in the charge-discharge curve, the difference between the front and the last two steps is large, and the difference between the middle two steps is very small, the discharge process is on the contrary, which is proved by the experimental charge-discharge curve, as shown in figure 15.

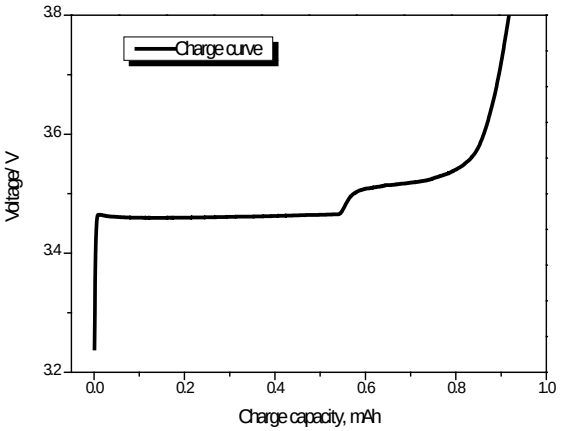

Fig. 15: Charging of Li/LiFePO4 and its differential curve [29]

f) Behavior of graphite during charge and discharge

The structure of graphite is characterized by the extension of the hexagonal grid surface composed of carbon atoms in the network plane and the ABAB along the normal direction of the network plane. Or ABCABC. The former belongs to P63/mmc (No.194) space group and the latter is 3R-graphite and belongs to R3 (No.146) space group [15]. Based on the experimental results of Section 3.2, some behaviors of graphite in the process of charge and discharge can be summarized.

With the beginning of the charging process, the Li atom is embedded in the graphite layer, and its priority is to enter the gap position between the graphite grid faces, so that the lattice parameters a and c as well as the micro-strain **ε** of the graphite, are increased, and the stacking disorder P is also changed. Because the ABAB sequential stacking is not as dense as the dense hexagonal structure, it has a large gap space and can hold a large number of interstitial atoms, so the Li-C compound will not be formed when the charge is less than 60%. Only when the battery charge is more than 60%, LiC_{24}, LiC_{12}, LiC_6 and Li_2C_2 phases will be formed successively. Due to the precipitation of the new phase, there is a process of nucleation and growth, so there will be two-phase or polyphase coexistence in this process. As for the percentage of charge in which Li-C compounds are precipitated, it depends on the system of lithium-ion batteries and the proportion of positive and negative active materials.

Similar to the positive electrode, the 002,100 peaks of 2H-graphite are separated when the charge is less than 20%, indicating that there are also two 2H-

graphite phases with different composition, indicating that the graphite electrode also has a surface-to-inside process of embedding Li.

VI. Physical Mechanism of Electrical Conductivity for Secondary Battery

At the beginning of charging, the migration of lithium ions (hydrogen ions) begins at the negative-electrolyte interface. Because lithium ion (hydrogen ion) is embedded in the negative electrode after obtaining (reducing) electrons at the negative electrode-electrolyte interface, the concentration of lithium ion (hydrogen ion) at the negative electrode-electrolyte interface decreases. In the solution, lithium ion (hydrogen ion) migrates from positive electrode to negative electrode like a relay race to make up for this concentration gap. Due to the directional migration of Li^+ ions (hydrogen ions), the concentration of Li^+ ions (hydrogen ions) is also reduced at the positive electrode-electrolyte interface. Under the action of electric field, the Li atoms in positive active materials ($LiCoO_2$, $Li(Ni,Co,Mn)O_2$, and $LiFePO_4$) leave the lattice position (the hydrogen atoms in the $\beta - Ni(OH)_2$ leave the lattice position), reach the positive electrode-electrolyte interface, lose electrons (that is, oxidation), and enter the electrolyte. To supplement the lithium ion (hydrogen ion) in the electrolyte. When the ion flow reaches dynamic equilibrium, it corresponds to the charging platform of the battery. When the battery is fully charged, the Li atom (hydrogen atom) in the positive electrode is exhausted, and the Li^+ ion (hydrogen ion) can only be provided by the electrolyte, so there must be Li^+ ion (hydrogen ion) in the original composition of the electrolyte.

The discharge process is contrary to the charging process. Under the action of the reverse electric field, the $Li^+(H^+)$ ion in the electrolyte is reduced to atoms at the positive electrode-electrolyte interface and embedded back into the lattice position of the positive active material. Then the $Li^+(H^+)$ ion migrates from the negative electrode to the positive electrode like a relay race, resulting in a decrease in $Li^+(H^+)$ ion concentration at the negative electrode-electrolyte interface. Then the Li(H) atom in the negative active material leaves the lattice, loses electrons and becomes $Li^+(H^+)$ ion, which enters the electrolyte through the negative electrode-electrolyte interface, thus forming the discharge conduction process that the negative side Li(H) atom leaves the crystal lattice of the negative electrode active material, the positive side Li(H) atom is embedded back into the crystal lattice position of the positive electrode active material, and the $Li^+(H^+)$ ion flows directionally from the negative electrode to the positive electrode.

In short, the physical conductive mechanism of secondary battery is the directional migration of conductive ions formed by de-intercalation and re-intercalation in positive and negative electrode active materials.

References Références Referencias

1. Bode H, Dehmel T K, Witte J. Zur kenntnis der nickelhydrox- idelktode , I. U ber das nickel (Ⅱ)-hydroxidhydrat [J] . Electrochim Acta, 1966, 11: 1079 ～1087.
2. Shukla A.K. Venugopalan S., Hariprakash et al., Nickel-based rechargeable batteries, J. Power Sources, 2001, 100:125～148
3. Li Guoxin, Editor-in-Chief, 2007, introduction to New Chemical Power supply Technology (Shanghai: Shanghai Science and Technology Press) 172～218.
4. Xing Zhengliang, Li Guoxun, Wang Chaoqun Xiao Jinsheng, XRD in situ observation of nickel electrode during charge and discharge, Power supply Technology, 1999 23 (2): 140～142.
5. Wang Chaoqun, Xing Zhengliang Wang Ning, Li Guoxun, Wu Burong, quantitative Phase Analysis of-NiOOH on Nickel electrode, Power supply Technology, 1999.
6. Ulrik Palmqvist, Lars Eriksson, Javier Garcia-Garcia et al, On the misuse of the structure model of the Ni electrode material, J. Powe Source, 2001, 25(1):15～25
7. Li Yuxia, Yang Chuanzheng, Lou Yuwan, Xia Baojia, study on the physical mechanism of conductivity in the charge-discharge process of MH/Ni batteries, Journal of Chemistry, 2009.67 (9): 901-909.
8. Qinpei Lou Yuwan Yang Chuanzheng Xia Baojia, a new method and calculation program for separating multiple broadening effects of X-ray diffraction lines, Journal of Physics 2006 55 (3): 1325-1335.
9. Yang Chuanzheng, Zhang Jian some advances in the study of microstructure of nanomaterials by X-ray diffraction, advances in physics, 2008, 28 (3): 280.～313.
10. Lou Yu-Wan, Yang Chuan-Zheng, Zhang Xi-Gui et al, Comparative study on microstructure of β-$Ni(OH)_2$ as cathode material for Ni-MH battery, Science in China: Series E: Tech. Sci., 2006, 49(3):297～312
11. Li Yu-xia (Master thesis of Shanghai Institute of Microsystems and Information Technology, Chinese Academy of Sciences): research on the relationship between the fine structure of electrode active materials and the function of Ni/MH batteries. P.53.
12. Yang Chuanzheng, Lou Yu-Wan, Li Yuxia, Xia Baojia, some advances in the study of the relationship between the performance of Ni/MH batteries with fine structure of electrode active materials, advances in Physics, 2009, 29 (1): 109, 126.

13. Reimers JN and Dahn JR, J. Electrom. Soc., 1992, 139(8):2091～2096.
14. Amatucci G G, Taracin J M and Klein L C, J. Electrochem. Soc., 1996, 143(3):1114～1123.
15. Yang XQ, Sun X, McBreen J, Electrochem. Cummun., 2000, 2:100～103
16. Sun X, Yang XQ, McBreen J,et al., J. Power Sources, 2001, 97-98:274～276
17. Li Jia, Yang Chuanzheng, Zhang Jian, Zhang Xigui, Xia Baojia, Journal of Chemistry, 2010 pr 68 (7): 646～652.
18. Li Jia, Yang Chuanzheng, Zhang Jian, Xia Baojia, Journal of Physics, 2009 58 (9): 6573～6581
19. Padhi A.K., Nanjundaswamy K.S. Goodenoigh J.B., J. Electrochem. Soc.1997,144:1188,
20. Srinivasan V., Newman J., Discharge model for the lithium iron-phosphate-electrode, J. Electrochem. Soc., 151(10): A1517-A1529
21. Yamada A., Koizumi H, Sonoyama N., Kanno R., Phase change in LixFePO4. Electrochem. Solid-State Letters.2005, 8(8): A409-A413
22. Dodd J.L., Yazami R., Fultz B., Phase diagram of LixFePO4, Electrochem. Solid-State Letters, 2006, 9(3): A151-A155
23. Qian Wang, Jian Zhang, Chuan-Zheng Yang, Bao-Jia Xia, J. Electrochem. Soc.,
24. Liu Haohan, Li Jia, Zhang Jian, Yang Chuanzheng, Xia Baojia, Phase transition Nature and Conductive Mechanism of Graphite / LiFePO4 Battery during charge and discharge, 2010, to be published
25. Destenay D., Mem.Soc. Roy. Sci., 1948,10(4)28; Wilson A.J.C., Structure Reports, 1950,13:319
26. Eventoff W, Martin R and Peacor D.R., Amer.Min., 1972,57:45～51 ; Structure Reports,1972,38A:314
27. Zhang Jian, Wang Qian, Xie Xiaohua, Yang Chuanzheng, Xia Baojia, strain Analysis and Conductive Mechanism of Lithium Ion Battery during charge and discharge, Journal of physical Science, 2012jue 1 (1): 72～86.
28. Jiang Chuanhai, Yang Chuanzheng, Internal stress diffraction Analysis, Chapter 14 stress Analysis and Conductive Mechanism of Green Secondary Battery Beijing: science Press, 2013.11.
29. Yang Chuanzheng, Lou Yuwan, Zhang Jian, Xie Xiaohua, Xia Baojia, material characterization and electrode process Mechanism of Green Secondary Battery, Science Press, 2015.9.
30. Yang Chuanzheng, study on Kinetic characteristics and Mechanism of hydrogen absorption/ Desorption of Alloy hydrogen Storage Materials, material Science, 2020 ～ (12): 1002 ～ 1026
31. Yang Chuan-Zheng, Lou Yu-Wan, Zhang Jian, Xie Xiao-Hua and Xia Bao-Jia, 《Characterization of Material and Mechanism of electrode process for green secondary Battery》, Science Press Beijing, 2015
32. Chuan-Zheng Yang, Yu-Wan Lou, Jian Zhang, Xiao-Hua Xie and Bao-Jia Xia, 《Materials and Working Mechanisms of Secondary Batteries》, Springer, Science Press in Beijing, 2022.

Table 1

Materials and Working Mechanisms of Secondary Batteries	
Authors	C. Z. Yang, Y. W. Lou, J. Zhang, X. H. Xie and B. J. Xia
Publisher	Springer and Science Press in Beijing
	2022
Content synopsis	This book is a monograph on material characterization and the mechanism study during charge-discharge, cycle and storage for secondary batteries by X-ray diffraction et al methods. whole book consists of 6 parts and 21 chapters. Part. 1(chap.1,2) describes the key experimental techniques and data analysis methods of X-ray diffraction. Part.2 (Chap.3～8) introduces the preparation methods and X-ray diffraction characterization of electrode active materials, including β-$Ni(OH)_2$, storage hydrogen alloy AB_5, $LiMeO_2$, $LiFePO_4$and 2-H graphite.et al. In this two parts, several new methods have been developed:(1) The least square method of separating the multiple broadening effect of diffraction lines and program for solving microstructure parameters; (2)A solution of mixed occupation parameters for Ni/Li atoms at 3a and 3b crystallographic sites of materials such as $LiNiO_2$, $Li(Ni,Co)O_2$, $Li(Ni,Mn)O_2$ and $Li(Ni,Co,Mn)O_2$; (3) A new technique for measuring the stacking disorder of hexagonal graphite. Part 3 (Chap.9～12) introduces the mechanism studies during charging and discharging for (Ni/MH), graphite/$LiMeO_2$ and graphite/$LiFePO_4$ batteries. Based on the phase transition theory, a new intercalation-de-intercalation theory and conduction mechanism of conductive ions are proposed; Part 4 (Chap.13～16) and part 5 (Chap.17～19) are the mechanism study of the of cycle process and storage process, respectively. In these two parts, through the comparative study of variation laws of battery performance and of fine structure and microstructure parameters of positive and negative active materials and diaphragm with cycle and storage process, the cycle and storage processes mechanism and battery performance decay mechanism are revealed; Part 6 (Chap.20 and 21) investigates the methods to improve the battery performance based on the understanding of decay mechanism of cycle and storage performances of batteries The research methods, contents and new results introduced in the book fully reflect the necessity and importance of interdisciplinary intersection and close cooperation between material physics and

	electrochemistry, X-ray diffraction analysis and battery experts in this kind of research.	
Chapter	Chapter Name	page
0	Preface, Catalogue and the author's introduction	38
1	Experimental methods of material characterization and the mechanism research	1
2	X-ray Diffraction analysis Methods of Materials Characterization and Mechanism Research	23
3	Characterization of active material β-$Ni(OH)_2$ and AB_5 alloy	61
4	Solid state reaction and formation mechanism in the synthesis of $LiMeO_2$ materials.	83
5	Mixed Occupation of Ni/Li Atoms in $LiMeO_2$ Materials	99
6	Ordered-Disordered of Ni, Co and Mn in (3b) position for $Li(Ni_{1/3}Co_{1/3}Mn_{1/3})O_2$	121
7	Preparation and X-ray Diffraction Characterization of $LiFePO_4$	139
8	Preparation and X-ray analysis of carbon electrode materials for lithium-ion batteries	159
9	Solid electrolyte Interface Film on Graphite Surface of Lithium-Ion Battery	207
10	Mechanism Research of Charge-discharge Process for MH/Ni Battery	227
11	Mechanism of charge-discharge process of Graphite/$LiCoO_2$ and Graphite/$Li(Ni_{1/3}Co_{1/3}Mn_{1/3})O_2$ batteries	247
12	Mechanism Research of Charge-Discharge Process for Graphite/$LiFePO_4$ battery	275
13	Mechanism Research of Cycle Process for MH/Ni Battery	297
14	Mechanism Research on the Cycle Process of 2H-Graphite/$Li(Ni,Co,Mn)O_2$ Battery	315
15	Cycle mechanism of graphite/$[Li(Ni_{0.4}Co_{0.2}Mn_{0.4})O_2+LiMn_2O_4]$	339
16	Mechanism of Cycle Process of Graphite/$LiFePO_4$ Battery	351
17	Mechanism research of Storage Process for MH-Ni Battery	365
18	Mechanism of Storage Process for Graphite/$LiCoO_2$ and Graphite/$Li(Ni_{1/3}Co_{1/3}Mn_{1/3})O_2$ batteries	379
19	Mechanism Research of Storage process for Graphite/$LiFePO_4$ Battery	417
20	Effect and Action Mechanism of β-$Ni(OH)_2$ Additive in MH/Ni Battery	443
21	The Method and Action Mechanism of Improving the Performance of Secondary Battery	461
The recommendation of three professorial experts		491
Subject index		495
The sum of the whole book	497 + 38 = 535	

Global Journal of Science Frontier Research: a Physics and Space Science
Volume 23 Issue 6 Version 1.0 Year 2023
Type: Double Blind Peer Reviewed Interenational Research Journal
Publisher: Global Journals
Online ISSN: 2249-4626 & Print ISSN: 0975-5896

Study on the Mechanism of Cycle and Storage Process of Lithium-Ion Battery

By C. Z. Yang
Shanghai University

Abstract- The changes of battery performance, crystal structure, fine structure and microstructure of positive and negative active materials in the processes of cycle and storage of lithium-ion battery were studied experimentally, and the change of battery performance was related to the structure change of positive and negative active materials. The mechanism of cycle and storage process was revealed, and the attenuation mechanism of battery cycle performance and storage performance was discussed. The method and action mechanism of improving cycle-storage performance are introduced.

Keywords: lithium-ion battery; x-ray diffraction; cycle process mechanism; storage process mechanism; attenuation mechanism of performance; methods to improve battery performance.

GJSFR-A Classification: LCC: TK7871.15.S5

Strictly as per the compliance and regulations of:

Study on the Mechanism of Cycle and Storage Process of Lithium-Ion Battery

C. Z. Yang

Abstract- The changes of battery performance, crystal structure, fine structure and microstructure of positive and negative active materials in the processes of cycle and storage of lithium-ion battery were studied experimentally, and the change of battery performance was related to the structure change of positive and negative active materials. The mechanism of cycle and storage process was revealed, and the attenuation mechanism of battery cycle performance and storage performance was discussed. The method and action mechanism of improving cycle-storage performance are introduced.

Keywords: lithium-ion battery; x-ray diffraction; cycle process mechanism; storage process mechanism; attenuation mechanism of performance; methods to improve battery performance.

I. Graphite/Li($Ni_{0.4}Co_{0.2}Mn_{0.4}$)O_2 Battery the Cycling Process Mechanism and Performance Degradation Mechanism [1,2-4]

The so-called cycle is that a time charge-discharge of the battery is one cycle period, which is the imitation of the working state of the battery, in order to observe the change of the battery performance with the increase of the cycle period and explore the stability and durability of the battery performance

a) Cycle performance of graphite/Li($Ni_{0.4}Co_{0.2}Mn_{0.4}$)O_2 battery

The battery is cycled at room temperature, 2C rate and 4.2-1.75V, and the cycle performance curve of the whole battery is shown in figure 1.It can be seen from the figure that the coating not only greatly improves the cycle stability of the battery, but also greatly improves the cycle performance. After 200 and 400 cycles, the capacity retention rate of uncoated batteries decreased by 89.2% and 81.1%, respectively, while that of Al_2O_3 coated batteries was 97.4% and 94.2%. respectively.

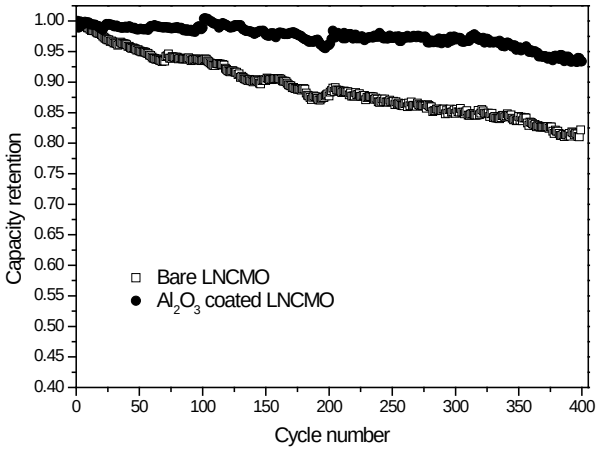

Fig. 1: Cycle performance of 18650 battery before and after coating at 25℃, 1.75V~4.2V, 2C rate

b) Changes of fine structure and microstructure of positive active material Li($Ni_{0.4}Co_{0.2}Mn_{0.4}$)O_2 during cycling

The XRD patterns of positive active materials before and after 2C charge-discharge cycle are shown in figure 2. At first glance, all the diffraction lines belong to structural Li($Ni_{0.4}Co_{0.4}Mn_{0.2}$)O_2, and there seems to be no change. However, after careful analysis, it is found that there are obvious changes in its fine structure.

Author: Physics Department of Shanghai University.
e-mail: yangcz1939@163.com

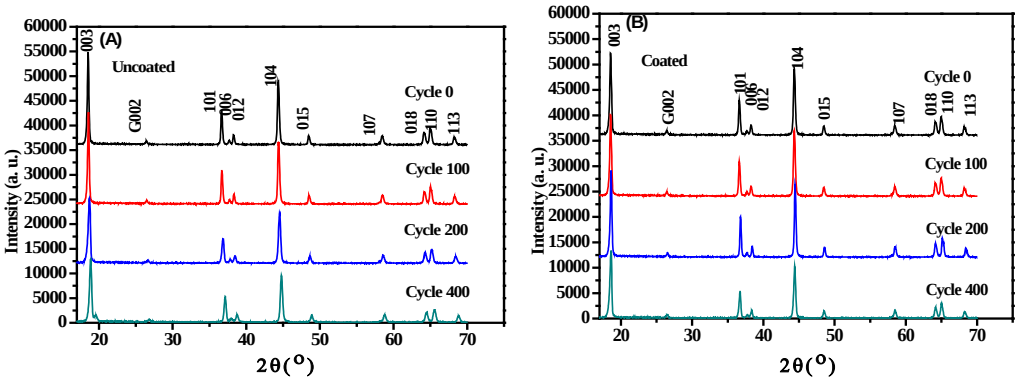

Fig. 2: XRD pattern of positive active materials before and after charge-discharge cycle (A) uncoated (B) coated with Al_2O_3

i. *Lattice parameters of positive active materials*

The variation of the lattice parameters of the positive active material with the cycle is shown in figure 3. It can be seen from figure 3 that the changing trends of a and c of the uncoated positive active materials are roughly the same, but the lattice parameters of the coated positive active materials are obviously different with the decrease of the cycle, a decreases with the increase of the cycle, while c increases at first and then decreases. This shows that after 100 cycles, the proportion of remaining Li atoms in the positive active material (NCM) is higher.

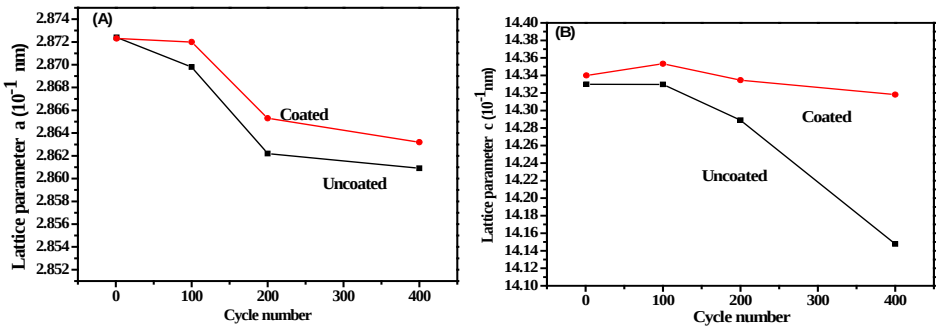

Fig. 3: 2C Variation of lattice parameters a (A) and c (B) of positive active materials with cycle before and after charge-discharge cycle

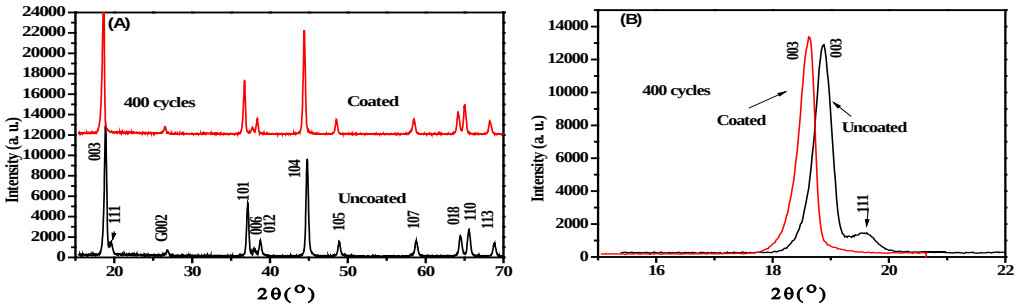

Fig. 4: XRD pattern (A) full spectrum of positive active materials after 400 cycles; (B) local magnification

Figure 4 shows the XRD pattern of the positive active material NCM after 400 cycles of the battery, in which figure 4(A) shows the full spectrum and figure 4(B) shows the amplification near the main diffraction peak of (003). It can be seen that the (003) peak of NCM changes after 400 cycles of uncoated battery, and the 111diffraction peak of spinel $Li_{1-x}Me_2O_4$ appears in the uncoated material.

The spinel phase is the product of the side reaction of NCM with electrolyte, but the peak is not seen in the coated material. The phase change is mainly due to the oxygen evolution and the dissolution of transition metal compounds during the cycle, and the reaction can be expressed as follows:

$$3Li_{1-x}MeO_2 - 2(1-x)e^- = MeO + Li_{1-x}Me_2O_4 + O + 2(1-x)Li^+ \quad (1)$$

Me is a transition metal element (Ni,Co,Mn). Li^+ enters the liquid phase, and MeO is easily dissolved in

the electrolyte, thus promoting the formation of spinel $Li_{1-x}Me_2O_4$.

ii. *Microcrystal size and micro-strain of positive active materials*

In order to calculate the microstructure parameters of positive active material, the FWHM of 003and 104diffraction lines were measured, and the average microcrystal size $\overline{D}$ and average micro-strain $\overline{\varepsilon}$ of the material were calculated according to the least square method of separating microcrystal-micro-strain effect. The results are shown in figure 5. It can be seen that (I) after charge-discharge cycle, the grain size is obviously refined and the micro-strain is obviously decreased, and the grain refinement of the coated cathode active material is greatly decreased; (ii) the micro-strain of the uncoated material decreases with the increase of the cycle, and finally changes from tensile strain to compressive strain, while the micro-strain of the coated material is larger than that of the uncoated material after the number of cycles is more than 100, especially the tensile strain is still maintained.

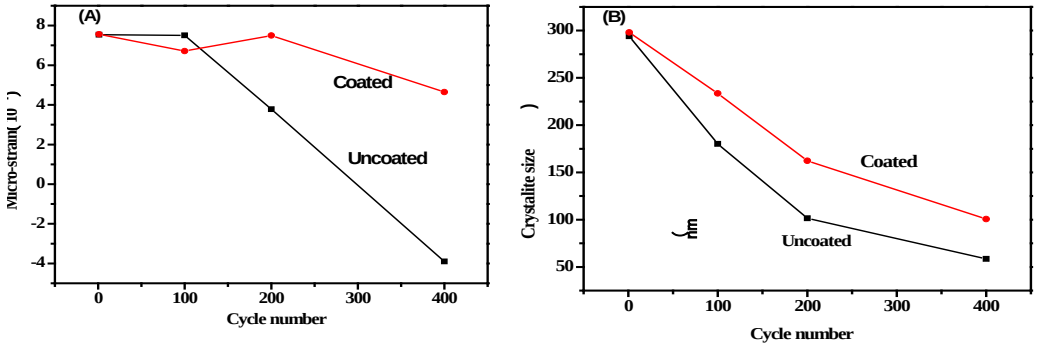

Fig. 5: Variation of microstructure parameters $\overline{D}$ and $\overline{\varepsilon}$ of positive active materials with cycle. Average micro-strain $\overline{\varepsilon}$ (B) average crystallite size $\overline{D}$

During the cycle of the battery, the strain of uncoated NCM starts to be tensile strain, which is mainly due to the fact that lithium ion enters into the lattice of NCM precursor during the crystallization process, which can be regarded as a kind of lattice expansion. With the progress of the cycle, the structure changes such as O precipitation appear in the uncoated NCM bulk phase, which leads to lattice contraction and compressive strain gradually. On the other hand, the coating can inhibit the precipitation of O, thus maintaining the state of compressive strain during the cycle. It is not difficult to see that the change law of micro-strain is consistent with the law of microcrystal refinement. This is mainly due to the accumulation and release of micro-stress caused by the change of micro-strain, which leads to the refinement of microcrystals. The coating suppresses the change of micro-strain, thus inhibiting the refinement of microcrystals.

c) *Fine structure of negative active materials*

The XRD pattern of the negative plate is shown in figure 6, which is partially magnified as in figure 7. It can be seen that the diffraction peak of graphite is obviously different in both peak position and half width. Because the negative electrode plate is directly used as the sample, the diffraction spectrum includes three diffraction peaks of 111,200,220 of the current collector Cu. We also measured the grain size of the extension c-axis direction [002] (see figure 8). Using Cu 111as the internal standard, the position of the 002 diffraction peak of graphite was accurately determined. According to the method [5~7], the value was determined by experiment, and the following formula was used.

$$2\theta_{correct}^{grap.} = 2\theta_{exp.}^{grap.} + (2\theta_{stand.}^{Cu} - 2\theta_{exp.}^{Cu}) \quad (2)$$

Obtain $2\theta_{correct}^{grap.}$ and then according to Bragg formula $2d_{002}\sin\theta_{corr.}^{grap.} = \lambda_{CuK\alpha 1} = 1.54056$ to calculate the exact value of graphite. The distance between the crystal planes in the c-axis direction is d002, and finally press the following formula:

$$P_{002} = \frac{d_{002} - 3.354}{3.440 - 3.354} \quad (3)$$

The stacking disorder degree P_{002} of graphite is calculated, and the results are shown in figs. 9 (a) and (b), respectively. It can be seen that: (i) when the number of cycles is more than 100, d_{002} decreases with the increase of cycles, indicating that the grains are obviously refined during the cycle; (ii) the lattice parameters c and stacking disorder P_{002} of graphite change obviously with the number of cycles, but there is no obvious difference between coated and uncoated.

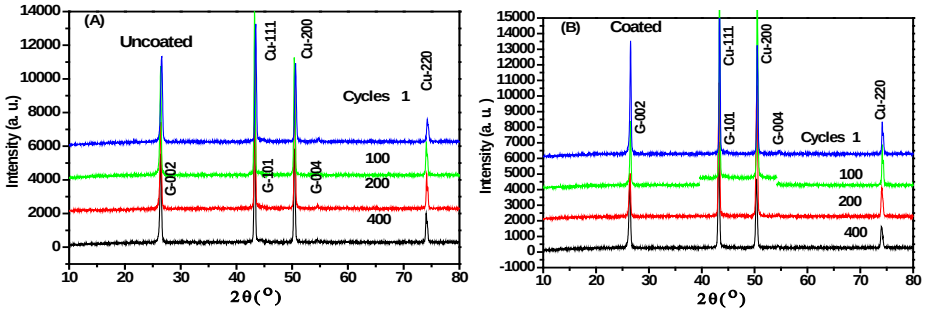

Fig. 6: XRD pattern of graphite before and after charge and discharge cycle, (A) uncoated (B) Al_2O_3 coating

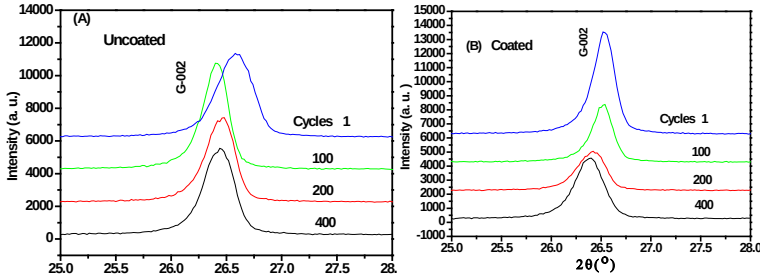

Fig. 7: Partial magnification of figure 6

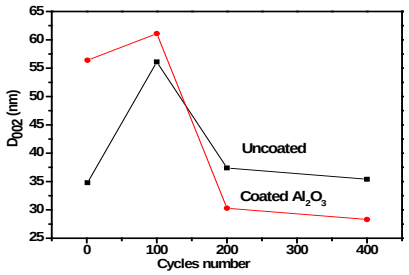

Fig. 8: Variation of grain size d_{002} of graphite along c-axis with cycle

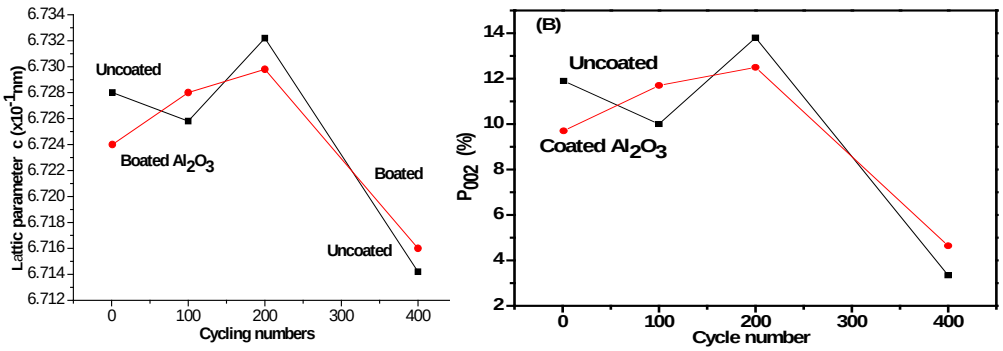

Fig. 9: Variation of lattice parameter c (a) and stacking disorder P_{002} (b) of negative electrode active material graphite with ring period

d) Changes in the fine structure of the diaphragm with the cycle [3]

The diaphragm of this kind of battery is composed of three layers of PP-PE-PP, PP is polypropylene film, belongs to monoclinic structure, P21 No.14 space group, PE is polyethylene, belongs to orthorhombic system, Pnam (No.62) space group. 2C the XRD pattern of the diaphragm before and after the charge-discharge cycle is shown in figure 10, in which the diffraction peaks have been indexed, it can be seen

that (1) the diffraction peaks of PP-131 and PE-110, PP-111 and PE-200 overlap; and (2) the positions of amorphous scattering peaks of PP and PE are at = 16.30C and 19.50C, respectively, indicating that the crystallinity of all samples is very high, and the amorphous part is very few; (3) the peak position shifts before and after the cycle, and the lines are obviously broadened; (4) compared with the uncoated ones, the broadening phenomenon decreases obviously.

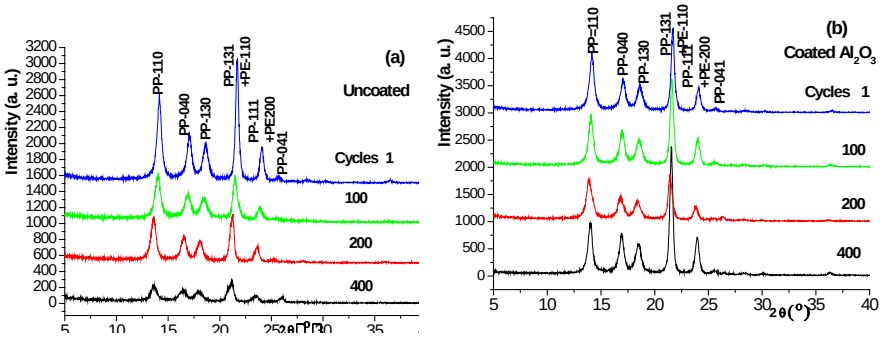

Fig. 10: 2C XRD pattern of the diaphragm before and after the filling and discharge cycle (a)uncoated (b) coated with Al_2O_3

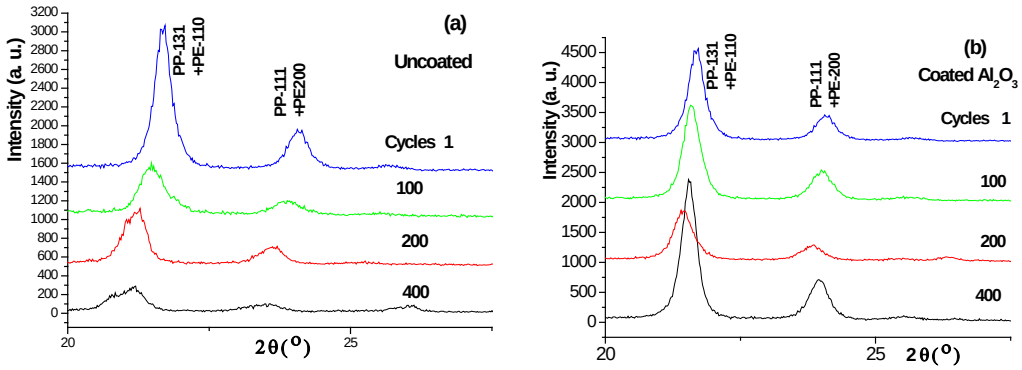

Fig. 11: 2C partial amplification of the XRD pattern of the diaphragm before and after the filling and discharge cycle, (a) uncoated (b) coated Al_2O_3

In order to investigate the situation of two pairs of overlapping peaks, the enlarged pattern is shown in figure 11, which shows that the coated and uncoated peaks are obviously different, and the latter peak displacement and broadening are much more serious; after 200,400 cycles, the PP-131 and PE-110 of the uncoated samples have obviously split, indicating that the surface of the diaphragm (PP) is seriously damaged and thinned during the cycle.

Because the diaphragm is two layers of polypropylene and one layer of polyethylene, the lattice parameters of polypropylene are calculated by using the peak position data of six diffraction peaks of PP. The results show that the three lattice parameters change with the increase of cycle, but the coated samples change more slowly than uncoated samples, an and b are smaller than uncoated ones, and c has a similar situation. This shows that the coating of positive active materials has a certain protective effect on the diaphragm.

There is an obvious difference in the broadening phenomenon of the observed diffraction peaks, especially between coated and uncoated, which indicates that there is an obvious difference in the microstructure (microcrystal size and / or micro-strain) of the diaphragm. The results show that the change of the uncoated data is irregular, but the effect of the coating is obvious: the coating of the positive active material slows down the grain refinement of the diaphragm, or the change of micro-strain is also reduced.

e) Degradation mechanism of cyclic performance of graphite/$LiMeO_2$ battery

Summing up the changing rules of the cycle performance, the positive and negative active materials and the fine structure of the diaphragm, we can see clearly that no matter whether the positive and negative active materials are coated or not, the attenuation of cycle performance has a good corresponding relationship with the changes of the positive and negative active materials and the fine structure of the diaphragm during the cycle. It also shows that the coating plays an important role in improving the cycle performance and slowing down the change of the positive and negative active materials and the fine structure of the diaphragm during the cycle.

In the discussion of the degradation mechanism of cycle performance of lithium-ion Secondary battery, many researchers attribute it to the effect of electrode surface, such as the chemical corrosion of electrolyte on electrode surface and diaphragm surface and so on. Of course, this kind of corrosion can not be ignored. First, let us focus on the changes of the positive and negative active materials and the internal structure of the diaphragm during the cycle, that is, the bulk effect, and first discuss the uncoated situation, and combine the results of surface analysis.

1) The positive lattice parameters a and c decrease with the increase of cycle period, indicating that there are more and more inactive Li atoms, and the grains and micro-strain of the positive active material decrease with the increase of the cycle period, and these two points are corresponding to each other. As a result, the activity of positive active materials will be reduced.
2) Negative lattice parameter c and stacking disorder increase at first and then decrease with the increase of cycle period, and the cycle refines the grain. Embedding Li atoms is unprofitable. In other words, the activity of graphite decreases with the increase of cycle period. Coating Al_2O_3 can obviously slow down the process of all kinds of changes mentioned above.
3) The three lattice parameters of the diaphragm change with the increase of the cycle period, especially with the increase of the cycle, the more serious the damage of the surface layer of the diaphragm.
   The combined action of the above three aspects is the main reason for the decline of cycle performance.
4) The performance degradation mechanism of 2025 graphite/$Li(Ni_xCo_yMn_{1-x-y})O_2$ battery was studied, which was caused by the increase of electrochemical impedance caused by the deposition of fluoride and NiO on the surface of $Li(Ni_xCo_yMn_{1-x-y})O_2$.
5) The capacity decay mechanism of 18650 graphite/$Li(Ni_xCo_yMn_{1-x-y})O_2$ battery was studied. The deposition of Ni, Co and Mn in the negative electrode during charge and discharge destroyed the integrity of SEI, and the regrowth of SEI film promoted the loss of active lithium during the cycle.
6) The decay mechanism of the rate performance of 18650 graphite/$Li(Ni_xCo_yMn_{1-x-y})O_2$ battery was studied, which was mainly caused by the deposition of fluoride and NiO on the surface of the positive electrode, and the electrochemical reaction impedance of the positive electrode increased faster than that of the negative electrode.
7) The mechanism of coating to improve the cycle performance of $Li(Ni_xCo_yMn_{1-x-y})O_2$ material and graphite/$Li(Ni_xCo_yMn_{1-x-y})O_2$ battery was studied.In order to reduce the deposition of fluoride and NiO on the surface of the positive electrode, and reduce the deposition of Ni, Co and Mn on the surface of the negative electrode, respectively.

It can be seen that in addition to the bulk effect of positive and negative active materials and diaphragm materials in the cycle process, the surface effect also plays an important role. The coating not only alleviates the surface effect, but also affects the bulk effect. It can be seen that the coating of positive active materials is very effective to improve and improve the performance of lithium-ion batteries.

II. Cycle Process Mechanism and Performance Decay Mechanism of Graphite/$LiFePO_4$ Battery[1,5,6]

a) 2H-graphite/LiFePO4 battery cycle performance

Figure 12 shows the discharge capacity curve (a) and capacity retention change (b) of 452340 2H-graphite/LiFePO4 battery under 25°C. It can be seen from the figure that the capacity increases with the increase of the cycle cycle, and its peak is at 186cycle, and then decreases slowly, until 1000 cycles, the capacity retention rate is still nearly 90%. Specific performance data are listed in Table 1. It can be seen that both the charging capacity and the discharge capacity increase, and then decrease gradually, and the maximum value is near the cycle 200 cycle; the charging platform voltage decreases at first and then increases slightly, and the minimum value is around the cycle 200 cycle, which corresponds to the change of the charging capacity; and the discharge platform voltage also increases at first and then decreases, which is consistent with the discharge capacity rising at first and then decreasing.

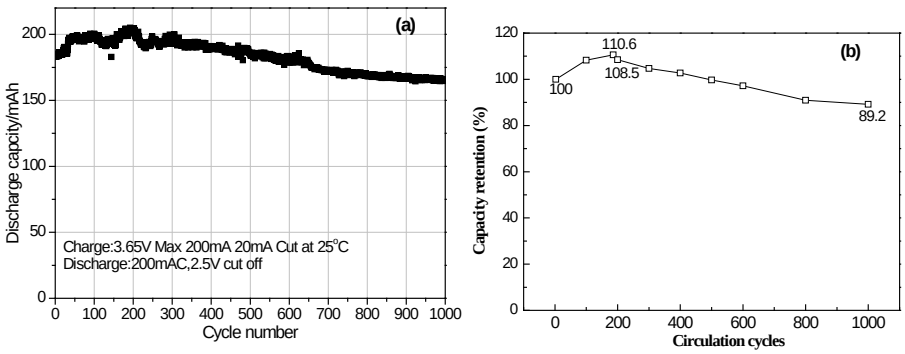

Fig. 12: 25°C cycle curve (a) and capacity retention curve (b) of 2H-graphite/$LiFePO_4$ 452340-typebattery

Table 1: Charge-discharge performance of 2H-graphite/$LiFePO_4$ battery after cycle

Number of cycles	Charging capacity mAh	Charging platform V	Discharge capacity mAh	Discharge platform, V
3	182.5	2.462	185.2	2.143
100	198.8	2.428	200.5	2.165
200	201.4	2.430	201.0	2.168
300	195.3	2.435	192.9	2.161
400	189.6	2.436	190.2	2.154
500	185.4	2.438	184.6	2.158
600	178.8	2.446	180.1	2.146
800	168.9	2.440	168.4	2.147
1000	164.8	2.435	165.2	2.150

b) *The relationship between the variation of cycle performance and the fine structure of positive and negative electrode and diaphragm material*

In order to explore the relationship between cycle performance and the fine structure of positive and negative electrodes and diaphragm materials, the experimental results are summarized in Table 2.It can be seen that the change law of cycle performance has a good corresponding relationship with the change of the relative content of $LiFePO_4$ in the positive electrode, the change of lattice parameters b and c, the change of disorder in negative graphite, and the change of lattice parameters a, b and micro-strain of PP in the diaphragm.

Table 2: Relationship between cycle performance and fine structure changes of positive and negative electrodes and diaphragm

Cycle performance	Positive active material	Negative active material	Diaphragm
Cycle performance and capacity retention increased at first and then decreased slowly with the cycle, with a maximum of about 200 cycles.	The relative content of LiFePO4 decreased at first and then increased with the cycle, and the maximum value was around 400th cycle.	The general change trend of stacking disorder is that it increases with the increase of cycle period.	The lattice parameters an and b of polypropylene increase with the increase of cycle period, but the change of c is irregular.
1.The charge capacity and discharge capacity obtained from the charge-discharge curve increase slightly with the increase of the cycle, and then decrease gradually, and their maximum values are both around 200 cycles. 2.The charging platform decreases at first, then increases slowly, while the discharge platform increases at first and then decreases.	1. The lattice parameters c and b of LiFePO4 increase slightly at first and then decrease with the cycle, and the maximum is around 300th cycle. 2. The general trend of D and ε of LiFePO4 is to increase.	1. The parameters of graphite lattice change little with the cycle. 2.The micro-structure parameters D and ε do not change much.	1.The micro-strain ε increases with the increase of cycle period. 2.After a long cycle, PP-113 and PE-110 split obviously, indicating that the surface of the diaphragm (PP) was seriously damaged and thinned during the cycle.

c) *Mechanism of cyclic performance degradation of 2H-graphite/$LiFePO_4$ battery*

From the chemical and physical study of the charge and discharge process of 2H-graphite/$LiFePO_4$ battery, it is known that there is a lag effect in the discharge process, or the asymmetry of charge and discharge, and from the study of the storage process of 2H-graphite/$LiFePO_4$ battery, it is known that the storage can greatly reduce the hysteresis effect of the discharge process.

The so-called cycle is that the charge-discharge cycle is one cycle at a time, so the tested samples are in the discharge state. Because of the hysteresis effect of discharge, how to change the hysteresis effect in the cycle is the first problem that should be paid attention to. It seems that this problem can be revealed from the change of the relative content of $LiFePO_4$ and $FePO_4$ with the cycle and the change of $LiFePO_4$ lattice parameters with the cycle. If the $LiFePO_4$ content after the subsequent cycle is greater than that in the previous cycle, the discharge lag effect is weakened, on the contrary, the discharge lag effect is enhanced.

1) After the beginning of the cycle, the relative content of $LiFePO_4$ increases and the content of $FePO_4$ decreases, indicating that there is more Li in the positive active materials, which increases the lattice parameters b and c of $LiFePO_4$, and can provide more Li ions, so the capacity after the cycle is increased, up to about 10%, resulting in a certain weakening of the discharge lag effect. However, when the cycle exceeds 200 to 300 cycles, the amount of Li embedded into LiFePO4 after discharge decreases, and the lattice parameters b and c of LiFePO4 begin to decrease, so the capacity decreases, and the discharge hysteresis effect increases until 1000 cycles, and some fluctuations may occur in the cycle.
2) The diaphragm is subjected to compressive strain at the beginning of the cycle, then becomes tensile strain, and increases with the increase of the cycle, and the lattice parameters an and b increase with the positive pole of the cycle. In the later stage, the two pairs of overlapping lines of PP and PE are obviously broadened and split. All these indicate that there are obvious changes in the diaphragm during the cycle, and reveal that: 1) the fine structure inside the diaphragm is not conducive to the passage of ions, and becomes more and more serious with the extension of the cycle, especially after 800 cycles; 2) the degree of damage to the surface of the diaphragm and the thinning of the surface PP layer become more and more serious with the increase of the cycle.

The combined effect of the above two reasons makes the cycle performance of graphite/LiFePO4 battery improve at the beginning and then gradually decline with the change of cycle cycle. Although the negative active material does not play a great role, it reflects the result of the first effect. Due to the decrease of the atomic weight of Li embedded in $LiFePO_4$ after discharge, in other words, there are more Li atoms dissolved in graphite, which increases the degree of disorder in graphite.

III. Mechanism Of Storage Process And Degradation Of Storage Performance Of 2H-Graphite/$LiMeO_2$ Battery[1,7~9]

a) *Storage performance of 2H-graphite/$LiMeO_2$ battery*[7~9]

Fig.13 (a) (b) respectively shows the variation of the 0.2C (240mA) capacity of 2H-graphite/$LiCoO_2$ and 2H-graphite/$Li(Ni_{1/3}Co_{1/3}Mn_{1/3})O_2$ batteries stored at 55 ℃ with different charged states. It can be found that: (I) the capacity of all batteries stored at high temperature (55°C) decays with the increase of storage days; (ii) the attenuation of battery capacity increases with the increase of the charge state during storage. The capacity decay rate of fully charged state (100%SOC) storage battery is significantly faster than that of other charged state batteries, and the attenuation is the most severe.

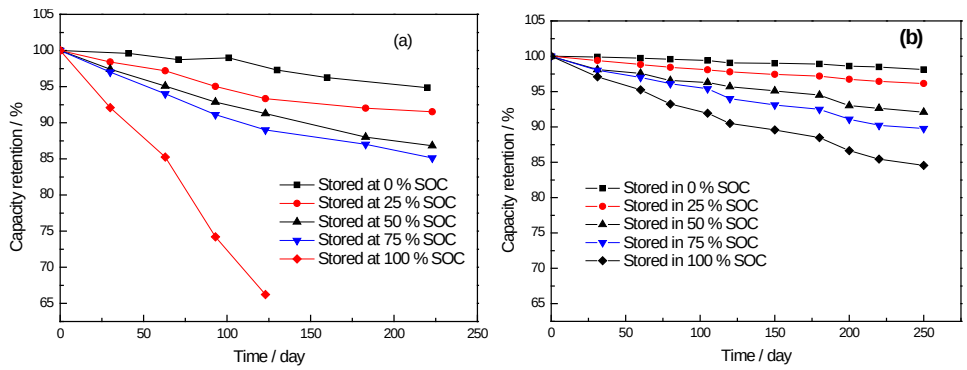

Fig. 13: 0.2C (240mA) capacity attenuation of A-type battery during storage at 25 55 ℃ with different charge states. (a) 2H-graphite/$LiCoO_2$ (b) 2H-graphite/$Li(Ni_{1/3}Co_{1/3}Mn_{1/3})O_2$

Compared with the two kinds of batteries, the storage performance of Graphite/Li($Ni_{1/3}Co_{1/3}Mn_{1/3}$)O_2 battery in full state is greatly improved. Figure 14 shows the relationship between the storage capacity decay rate and the degree of charge (SOC). It can be seen that the graphite/Li($Ni_{1/3}Co_{1/3}Mn_{1/3}$)O_2 battery can greatly improve the storage performance with high charge. These changes can be explained by the thickening of the passive film on the electrode surface after storage. The passivation film on the electrode surface is composed of the reaction products of lithium and electrolyte, and the increase of its thickness will consume the effective lithium removal amount of the positive electrode, resulting in the attenuation of battery capacity. At the same time, when Li^+ diffuses between the electrode and the electrolyte, it must pass through the passivation film on the electrode surface. It has been proved that the diffusion rate of Li^+ in this film is lower than that in the electrode and electrolyte. Therefore, the diffusion of Li^+ in this film becomes the speed control step of the whole process. With the increase of the thickness of the film, the diffusion resistance of Li^+ increases, which leads to the increase of the impedance of the electrode and the polarization of the battery in the process of charge and discharge.

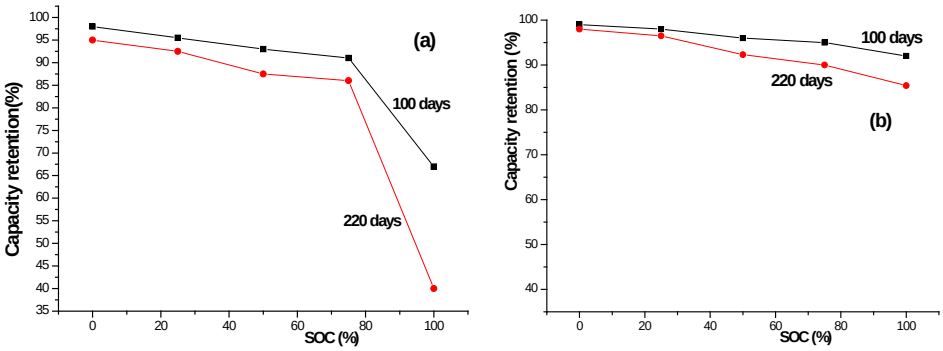

Fig. 14: Relationship between storage capacity decay rate and degree of charge (SOC). (a) 2H-graphite/$LiCoO_2$ battery, (b) 2H-graphite/Li($Ni_{1/3}Co_{1/3}Mn_{1/3}$)O_2 battery

b) Fine structure changes of battery positive and negative active materials before and after storage

In order to study the changes of the microstructure and surface morphology of the electrode active material during storage, the new battery and the battery stored under different conditions were discharged to 1.75V at 0.2C, so that the battery was in 0%SOC. In the glove box filled with argon, the battery was dissected, several positive and negative plates were removed, washed repeatedly with DMC solvent, and dried naturally. The positive and negative active materials were scraped off respectively, and the X-ray diffraction analysis was carried out on the Rigaku D/max-2200PC X-ray diffractometer. the contents of the analysis included phase structure identification, lattice parameters, microstructure and so on.

i. *Microstructural changes of negative active materials before and after storage*

Figs.15 (a) and (b) are 2H-graphite/$LiCoO_2$ battery and 2H-graphite/Li($Ni_{1/3}Co_{1/3}Mn_{1/3}$)O_2 with different charges, respectively. The XRD patterns of positive and negative active materials before and after storage at 55℃ for SOC.

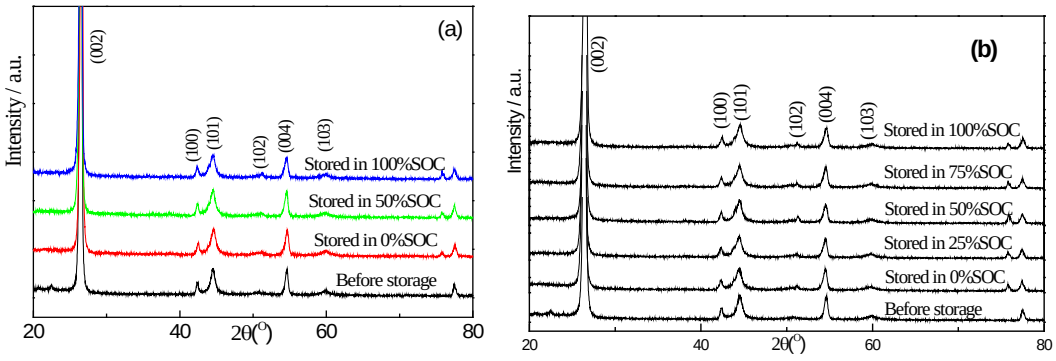

Fig. 15: XRD patterns of negative active materials before and after storage at 55 ℃. (a) before and after 100d storage of graphite / $LiCoO_2$ battery. (B) The XRD pattern of the material. positive and negative electrode activity of graphite / Li($Ni_{1/3}Co_{1/3}Mn_{1/3}$)O_2 before and after 250d storage (SOC) before and after storage at 55 ℃.

The lattice parameters, cell volume, microcrystal, microstrain and stacking fault of 2H-graphite, the negative electrode active material of graphite/$LiCoO_2$ and graphite/$Li(Ni_{1/3}Co_{1/3}Mn_{1/3})O_2$ battery, are calculated. The results are listed in tables 3 and 4, respectively. It can be found that the test results of the two kinds of batteries are similar, and the lattice parameters of the negative active material 2H-graphite have no obvious change after storage. at the same time, except for the slight increase of micro-strain after storage, there is no obvious change in microcrystals and stacking faults, indicating that storage has no significant effect on the bulk phase structure and microstructure of negative active material graphite. This once again shows that the decline in the storage performance of lithium-ion batteries is due to the positive electrode.

Table 3: Lattice parameters of negative electrode material 2H-graphite before and after storage in different charged states of graphite/$LiCoO_2$ battery. a, c, microcrystal D, micro-strain ε and stacking disorder P

		Before storage	0%SOC after storage	50%SOC after storage	100%SOC after storage
Lattice parameter/Å	a	1.4627	1.4538	1.4527	1.4517
	c	6.7207	6.6960	6.7196	6.7219
Micro-structure parameter	D (nm)	51.9	75.7	111.8	65.8
	ε(×10^{-3})	0.983	1.350	1.404	1.400
	P (%)	40.0	45.6	51.2	42.4

Table 4: Negative active materials of graphite/$Li(Ni_{1/3}Co_{1/3}Mn_{1/3})O_2$ battery before and after storage at 55℃ in different charged states. Microstructure parameters of 2H-graphite

		Before storage	0%SOC storage	25%SOC storage	50%SOC storage	75%SOC storage	100%SOC storage
Lattice parameter Å	a	1.4496	1.4486	1.4534	1.4520	1.4650	1.4528
	c	6.7115	6.7233	6.7338	6.7256	6.7213	6.7331
Micro-structure parameter	D (nm)	84.5	72.8	68.4	88.7	79.5	95.8
	ε(×10^{-3})	1.087	1.051	1.115	1.312	1.089	1.554
	P (%)	45.1	54.2	45.9	52.8	51.2	48.7

ii. *Microstructural changes of cathode active material $LiCoO_2$ before and after storage*[3]

Figure 16 shows the XRD map of the positive and negative active material $LiCoO_2$ before and after storage at 55 ℃ for 100 days. It can be seen from the figure that there is no obvious change in the diffraction peak position of the positive active material before and after storage, but it still clearly shows the characteristic peak of $LiCoO_2$, but the relative intensity of some peaks has changed. for example, the intensity of the peak is very high before storage, but its intensity decreases greatly after high temperature storage, which indicates that the phase structure of the material does not change after storage. At the same time, it is found that some of the XRD peaks (such as 003,101) of the positive active material LiCoO2 are broadened after high temperature and high charge storage. At the same time, it can be found that the X-ray diffraction peak shape and position of the negative active material are almost the same before and after storage, indicating that the bulk phase structure does not change after storage, but its fine structure changes. Tables 5 and 6 show the half-height widths and calculated results of (003), (101) and (104), respectively. It can be seen that the crystallite size decreases greatly with the increase of SOC, while the micro-strain changes from tensile strain to compressive strain after storage, and the compressive strain increases with the increase of SOC.

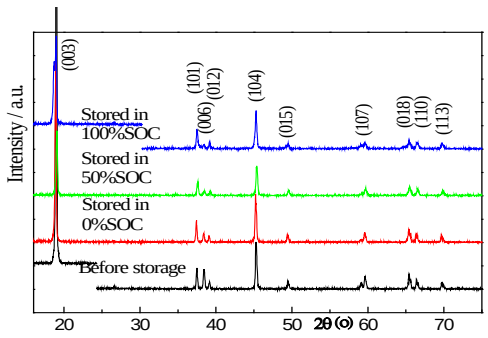

Fig. 16: XRD map of positive active material $LiCoO_2$ of battery before and after storage at 55 ℃ for 100 days

Table 5: Half peak width (o) of peaks of positive active materials $LiCoO_2$ (003,101) and (104) before and after storage

hkl		before	0%SOCafter storage	50%SOCafter storage	100%SOCafter storage
003	Half	0.134	0.161	0.206	0.364
101	peak	0.146	0.148	0.196	0.173
104	width(°)	0.153	0.154	0.195	0.204

Table 6: Lattice parameters, microcrystals and micro-strain of positive active material $LiCoO_2$ before and after storage in different charged states

		Before storage	0%SOC after storage	50%SOC after storage	100%SOC after storage
Lattice parameter (Å)	a	1.8156	1.8126	1.8119	1.8123
	c	14.0159	12.9975	12.9604	14.0072
Micro-structure parameter	D (nm)	336.1	116.9	67.2	19.4
	ε ($\times 10^{-3}$)	0.269	-0.187	-0.352	-2.447

c) *Microstructural changes of positive active material $Li(Ni_{1/3}Co_{1/3}Mn_{1/3})O_2$ before and after storage* [9]

Figure 17 shows the XRD diagram of the positive active material $Li(Ni_{1/3}Co_{1/3}Mn_{1/3})O_2$ before and after storage at 55 ℃ for 250d at different charge states (SOC) of the battery. It can be seen from the figure that there is no obvious change in the diffraction peak position of the positive active material before and after storage, but the characteristic peak of $Li(Ni_{1/3}Co_{1/3}Mn_{1/3})O_2$ is still clearly shown, which indicates that there is no new phase in the positive active material after storage, and its bulk phase structure does not change. However, after careful observation, it is found that the relative intensity of the diffraction peak of the sample seems to have changed slightly before storage, and some of the diffraction peaks have been broadened, which indicates that the fine structure of the sample may have changed after storage. The calculation results of the microstructure parameters are given in Table 7, which shows that the law of the microstructure parameters is similar to that of $LiCoO_2$, but the change rate slows down obviously.

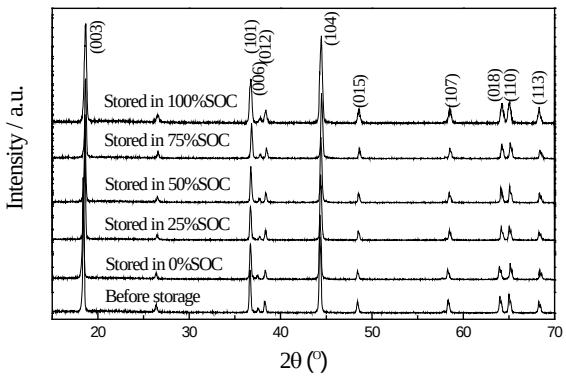

Fig. 17: XRD map of positive active material $Li(Ni_{1/3}Co_{1/3}Mn_{1/3})O_2$ of battery before and after 250 days storage at 55℃.

Table 7: Lattice and microstructure parameters of $Li(Ni_{1/3}Co_{1/3}Mn_{1/3})O_2$ before and after storage at different charge states at 55 ℃ for 250d

graphite/$LiNi_{1/3}Co_{1/3}Mn_{1/3}O_2$ battery		Before storage	0%SOC after storage	25%SOC after storage	50%SOC after storage	75%SOC after storage	100%SOC after storage
Lattice parameter (Å)	a	1.8610	1.8665	1.8661	1.8685	1.8643	1.8689
	c	14.2736	14.2720	14.3151	14.3127	14.4502	14.4196
Microstructure parameter	D (nm)	239.2	208.7	181.6	165.5	121.3	95.4
	ε ($\times 10^{-3}$)	0. 2367	-0. 1367	-0.1439	-0.2984	-0.468	-0.9641

It is found that for lithium-ion battery positive active materials containing Ni, such as $LiNiO_2$, Li $(Ni_{1-x}Co_x)O_2$ and $Li(Ni_{1-x-y}Co_xMn_y)O_2$, etc., due to the small difference between the radius of ions of Li^+ and Ni^{2+}, the phenomenon of cation mixing is easy to occur in these materials, that is, some Li^+ at 3a site and Ni^{2+} at 3b site change their positions. Once Li_+ enters the 3b site, it loses its deintercalation activity. Therefore, the mixed discharge of cations directly disturbs the detachment and intercalation of Li+ in the process of charge and discharge, resulting in the decline of the electrochemical performance of the materials [7].It is considered that the phenomenon of cationic mixed discharge may occur in the synthesis stage and charge-discharge cycle stage of the material, and this phenomenon may also occur in the storage stage of the battery due to the thermal vibration of lithium-nickel and the spontaneous re-intercalation of lithium ion. Therefore, it is necessary to determine the crystallographic occupation of Li and Ni in $Li(Ni_{1/3}Co_{1/3}Mn_{1/3})O_2$ before and after storage.

At present, based on the comprehensive study and analysis of the main diffraction characteristics of this kind of Ni-containing materials, we propose a new simulation method, that is, according to the addition and subtraction relationship of the contribution of 3a and 3b atoms to the diffraction intensity of each hkl crystal plane, we propose to use the diffraction integral intensity ratio of additive and subtractive lines to study the crystallographic occupation of Li and Ni in this kind of materials. The method for calculating the mixed occupancy parameter x of $Li(Ni_{1/3}Co_{1/3}Mn_{1/3})O_2$ is briefly introduced below[10,11].

According to the mixed occupancy model of $Li_{1-x}Ni_x(Li_xNi_{1/3-x}Co_{1/3}Mn_{1/3})O_2$, it is simulated with the help of Powder Cell1.0 calculation program. The curves of the relationship between the strength ratio I_{104}/I_{003}, I_{012}/I_{101}, I_{104}/I_{101} or $(I_{003}/I_{104})^{1/2}$, $(I_{101}/I_{012})^{1/2}$, $(I_{101}/I_{104})^{1/2}$ and the mixed space occupying parameter x are calculated, as shown in figure 18. It can be seen from the diagram that the relationship between $(I_1/I_2)^{1/2}$ and the mixed parameter x is a straight line, so the corresponding mixed occupying parameter x can be calculated, as shown in Table 8.

It shows that the synthesis process of this material is excellent, so it can be seen from the previous experiments that the performance of this material is also superior. After storage, the mixed space occupying parameters of the materials increase with the increase of SOC. This shows that the mixed discharge of cations occurs in the positive active material $Li(Ni_{1/3}Co_{1/3}Mn_{1/3})O_2$ after storage, and the amount of lithium-nickel ions mixed discharge increases with the increase of the charge state of the battery during storage. This phenomenon can correspond to the decline of the performance of the positive electrode and the whole battery after storage. The results show that the performance attenuation of positive active material $Li(Ni_{1/3}Co_{1/3}Mn_{1/3})O_2$ after storage is related to the increase of cationic mixed.

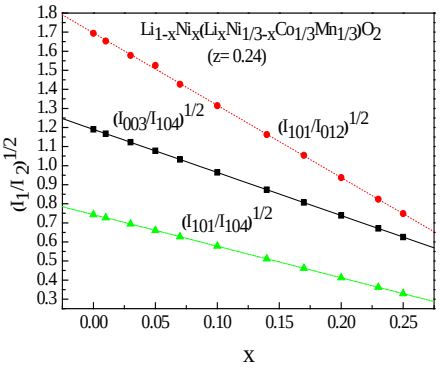

Fig. 18: The curve of the relationship between the $(I_1/I_2)^{1/2}$ and the mixing parameter x of $Li(Ni_{1/3}Co_{1/3}Mn_{1/3})O_2$ materials

Table 8: (I_{101}/I_{104}) of positive active material Li $(Ni_{1/3}Co_{1/3}Mn_{1/3})$ O_2 before and after storage and the calculated mixed space occupying factor x

	Before storage	0%SOC storage	25%SOC storage	50%SOC storage	75%SOC storage	100%SOC storage
I_{101}	4964	4967	5247	5129	5367	13277
I_{104}	8910	9151	10086	10529	11549	31423
I_{101}/I_{104}	0.5571	0.5428	0.5202	0.4871	0.4647	0.4225
x	0.0076	0.0136	0.0233	0.0378	0.0479	0.0676

d) Corresponding relationship between storage performance and fine structure of battery materials

Summarizing the previous research results, the The law change of performance changes for 2H-graphite / $LiCoO_2$ lithium-ion battery and 2H-graphite/$Li(Ni_{1/3}Co_{1/3}Mn_{1/3})O_2$ battery before and after storage are obtained.

1) It is found that the capacity, charge-discharge performance, cycle performance, power characteristics and safety of the battery stored at high temperature (55℃). All the properties attenuate, and the degree of attenuation attenuates with the increase of storage days, and the attenuation rate increases with the increase of charged state.

2) After storage at room temperature (25 ℃), the performance decay law of the battery is the same as that of 55°C storage, but the attenuation rate decreases obviously Slow.
3) After storage at low temperature (-20℃), the performance of the battery did not decrease obviously.
4) The storage temperature and the charge state of the battery have great influence on the storage performance of the battery. Performance retention of battery. The relationship between storage temperature, DC internal resistance increase rate and temperature is consistent with the $y = A \cdot \exp Bx + C$ described exponential relationship, and the relationship between battery performance retention rate and charge (SOC), DC internal resistance increase rate and storage charge state is also consistent with this exponential relationship.
5) It can be seen that graphite/Li($Ni_{1/3}Co_{1/3}Mn_{1/3}$)O_2 battery is better than graphite/$LiCoO_2$ battery in all aspects.

Summarize the previous results and compare the changes of positive and negative active materials and diaphragm structure of graphite/$LiCoO_2$ lithium ion battery and graphite/Li($Ni_{1/3}Co_{1/3}Mn_{1/3}$)O_2 battery before and after storage.

The main results are as follows:

1) Change of the microcrystal size and micro-strain of negative active materials change irregularly with the increase of storage charge after storage.
2) In the positive active material, D becomes smaller after storage and refines with the increase of storage SOC, and the positive electrode is subjected to tensile stress after storage. It changes into compressive stress and increases with the increase of storage SOC, and the increase rate of LiCoO2 is much faster than that of Li($Ni_{1/3}Co_{1/3}Mn_{1/3}$)O_2. The mixing parameter x of Ni and Li in Li($Ni_{1/3}Co_{1/3}Mn_{1/3}$)O_2 becomes larger after storage and increases with the increase of SOC.
3) SEI film is formed on the surface of negative electrode and thickens with the increase of SOC, but the SEI film of graphite / Li (Ni1/3Co1/3Mn1/3) O2 battery has obvious concavity and convexity.
4) Passivation film is also formed on the surface of positive electrode, and the surface of LiCoO2 is relatively dense. The surface of O2 is not dense, and the content of F in the film of the former medium battery is much larger than that of the latter.
5) The effect of the diaphragm on the negative side of the storage is not obvious, but the storage has a great influence on the diaphragm on the positive side, especially on the positive side of the graphite/$LiCoO_2$ battery.

By connecting the above two five points, it can be found that there is a good corresponding relationship between the storage performance attenuation and the fine structure of the electrode active material, especially with the fine structure change of the positive active material and the damage of the diaphragm on one side of the positive electrode.

e) Discussion on the decay mechanism of storage performance of battery

To sum up, the mechanism of storage performance degradation is discussed as follows: there are two functions of the battery during storage: (1) self-discharge of the battery; (2) Chemical/electrochemical interaction between the electrolyte and the positive and negative electrode surfaces and the two surfaces of the diaphragm. Let's first discuss the self-discharge effect.

1) In the process of storage, the battery will self-discharge. This leads to obvious changes in the fine structure of the battery materials, including positive and negative active materials and diaphragms, and makes the microcrystal refinement and micro-strain of positive active materials change from tensile strain to compressive strain, which obviously affects the de intercalation behavior of Li ions in the process of battery charge and discharge after storage, and causes a larger potential barrier for Li ion de intercalation, which hinders the de intercalation of Li ions, which shows the increase of DC internal resistance and the decrease of capacity.
2) This self-discharge phenomenon becomes more and more serious with the increase of the percentage of charge during battery storage. with the increase of the degree of battery charge, the grain refinement rate of the positive active material is accelerated, and the compressive strain increases rapidly, so the capacity decreases rapidly. the internal resistance also increases rapidly, so the performance change decays faster with the increase of the degree of charge, especially in the case of high charge.
3) The higher the storage temperature, the more serious the spontaneous discharge. At low temperature (-20°C), the performance attenuation is linear with a small slope, and at high temperature (55°C), it attenuates exponentially.
4) Graphite/Li($Ni_{1/3}Co_{1/3}Mn_{1/3}$)O_2 and graphite/$LiCoO_2$ batteries have the same negative electrode, different positive active materials, and different self-discharge effect during storage. The self-discharge phenomenon of the former battery is smaller than that of the latter battery, so the storage performance of the former battery is better than that of the latter. This is due to the fact that the fine structure of the negative active material does not change much, but there are obvious changes in the fine structure of

the positive electrode and the tissue structure of the surface film. The grain refinement rate of $LiCoO_2$ in 2H-graphite/$LiCoO_2$ battery is faster than that of $Li(Ni_{1/3}Co_{1/3}Mn_{1/3})O_2$ in 2H-graphite/$Li(Ni_{1/3}Co_{1/3}Mn_{1/3})O_2$, and the compressive strain of $LiCoO_2$ in 2H-graphite / LiCoO2 battery is much larger than that of $Li(Ni_{1/3}Co_{1/3}Mn_{1/3})O_2$ in 2H-graphite/$Li(Ni_{1/3}Co_{1/3}Mn_{1/3})O_2$.

Now the chemical/electrochemical interaction between electrolyte and positive and negative electrode surface and diaphragm surface is investigated.

The experimental results show that compared with the two kinds of batteries, the surface morphology of the negative electrode and the diaphragm on one side of the negative electrode do not change much, and there is no significant difference between the two kinds of batteries. However, the surface morphology and composition of the positive electrode are obviously different, the morphology of the diaphragm on one side of the cathode is also different, the content of F on the surface of $LiCoO_2$ is also higher, and the damage of the diaphragm on the positive side is also greater, so the graphite/$Li(Ni_{1/3}Co_{1/3}Mn_{1/3})O_2$ battery is superior to the graphite/$LiCoO_2$ battery in terms of capacity, cycle performance, storage performance and rate performance. This superiority is shown in the effect of storage charge and storage temperature.

In order to understand more clearly the effect of the change of the specific capacity of positive and negative electrodes on the capacity of the battery after storage, the capacity change rate of 0.20C of graphite/$Li(Ni_{1/3}Co_{1/3}Mn_{1/3})O_2$ battery and positive and negative electrodes after storage was calculated. The results are shown in Table 9.

Table 9: Capacity change rate of batteries and positive and negative electrodes 0.20 C after storage

	Capacity change rate / %		
SOC/ %	Full battery	Li($Ni_{1/3}Co_{1/3}Mn_{1/3})O_2$	graphite
0	98.10	98.44	99.21
25	96.05	96.02	98.06
50	91.03	91.03	94.46
75	89.71	89.71	91.41
100	84.49	84.49.	87.32

It can be seen from Table 15 that the capacity decay rate of battery, positive and negative electrodes after storage increases with the increase of SOC during storage. The capacity decay rate of the negative electrode is slower than that of the positive electrode, and the change of the positive capacity is very close to that of the battery capacity. It can be seen that after 55°C storage, the capacity attenuation of $Li(Ni_{1/3}Co_{1/3}Mn_{1/3})O_2$ positive electrode is larger, which is close to that of the whole battery; at the same time, the impedance increases, the dynamic performance decreases, and the performance attenuation of graphite negative electrode after storage is small. This shows that the performance attenuation of the battery after storage is mainly due to the positive electrode. The reason for the performance degradation of the battery after storage is that the $LiPF_6$ in the electrolyte is decomposed during storage, and the resulting HF erodes $Li(Ni_{1/3}Co_{1/3}Mn_{1/3})O_2$, resulting in capacity attenuation, and high impedance deposits such as LiF are formed on the surface of the positive electrode, which increases the impedance and decreases the dynamic performance.

It can be seen that in the lithium-ion secondary battery with graphite as the negative active material, the positive active material is the core and key of the problem in terms of increasing the capacity, improving the cycle performance and improving the storage performance. Therefore, the positive coating is advantageous [9].

IV. Study on the Mechanism of Storage Process and Energy Decay of Graphite/$LiFePO_4$ Battery[1,12,13]

a) 2H-graphite/$LiFePO_4$ battery storage capacity

Figure 19 shows the change curve of 0.2C capacity of 2H-graphite/$LiFePO_4$ battery during storage at 55℃. It can be found that the charge state of the battery also has a great influence on the storage performance of the lithium-ion battery with lithium iron phosphate as the cathode. However, it can be found that, different from the other two positive active materials, the capacity of 2H-graphite/$LiFePO_4$ battery does not decay monotonously with the extension of storage time. As can be seen in figure 19, the capacity of the battery increases at first and then decays during 25%～75%SOC storage, and this phenomenon is most obvious in 50%SOCstorage, when the storage time reaches 135d. Its capacity reached the highest value (increased to 101.4% of the original capacity). The capacity of the battery stored at 0% and 100%SOC decreases with the extension of storage time, but it can be found that the capacity decay rate of the battery with the other two positive active materials is also greatly reduced, and the capacity of the battery stored for 260d only attenuates 1.9% and 1.0% of the original capacity.

b) Structural changes of $LiFePO_4$ during charge and discharge of 2H-graphite /$LiFePO_4$ battery before storage

Figure 20 (a) shows the XRD spectrum of the positive active material $LiFePO_4$ in several stages of the charge and discharge process before and after battery storage.

The spectrum is indexed by $LiFePO_4$ and $FePO_4$ with orthogonal structure, represented by the letters T and H, respectively. It can be found that in the charging process, with the increase of charging depth, the content of $LiFePO_4$ phase gradually decreases, while the content of $FePO_4$ increases gradually; when the charge reaches 80%, there is still a trace of $LiFePO_4$, and until the charge reaches 100%, the peak of $LiFePO_4$ phase in the XRD spectrum completely disappears. During the discharge process, $LiFePO_4$ appears at 20% of the discharge, and its content increases with the increase of the discharge depth, up to 80% of the discharge, it is dominated by $LiFePO_4$ phase, but. There is still a certain amount of $FePO_4$.It can be seen that there is a phase transition of $LiFePO_4 \leftrightarrow FePO_4$ in the positive active material during the charge-discharge process. At the same time, it is found that after the formation of the battery, even the discharge positive active material is not a single phase of $LiFePO_4$, but contains a small amount of $FePO_4$ phase.

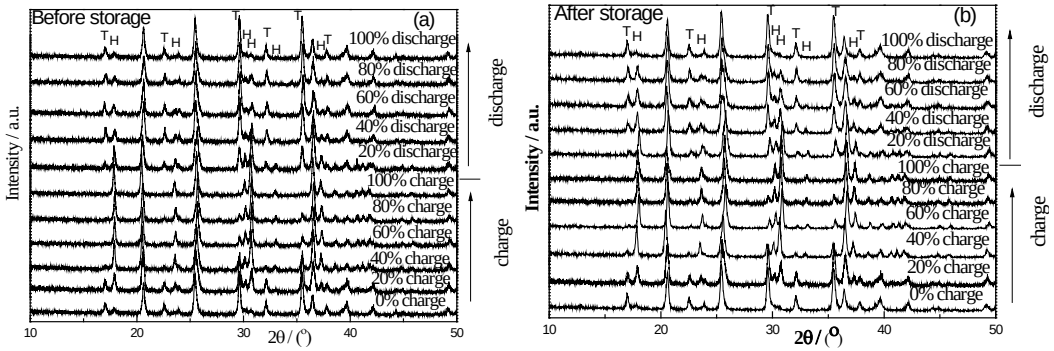

Fig. 20: XRD spectrum of $LiFePO_4$ in several stages of charging and discharging process of graphite/$LiFePO_4$ battery stored in 55°C 50%SOC 135days ago (a) after (b)

In order to show the changes of the two phases in the charge-discharge process more clearly, the characteristic peaks of the two phases in figure 20 (a) are locally magnified, and the XRD spectra of the same charged state in the charge-discharge process are compared, as shown in figure 21. It can be found that in the process of charge and discharge, even in the same charged state, there is an obvious difference in the relative intensity of the two phases in the XRD spectrum. In the same charged state, the strength of $FePO_4$ phase in the charged positive active material is higher than that in the discharge state, while the strength of the LiFePO4 phase in the discharged positive active material is higher than that in the charged state. This shows that in the process of charging, the disappearance rate of $LiFePO_4$ phase and the increase rate of $FePO_4$ phase are faster, while in the process of discharge, the disappearance rate of $FePO_4$ phase and the increase rate of $LiFePO_4$ phase are faster. This shows that there is a certain hysteresis or asymmetry in the phase change of $LiFePO_4$ positive active materials during charge-discharge[2].

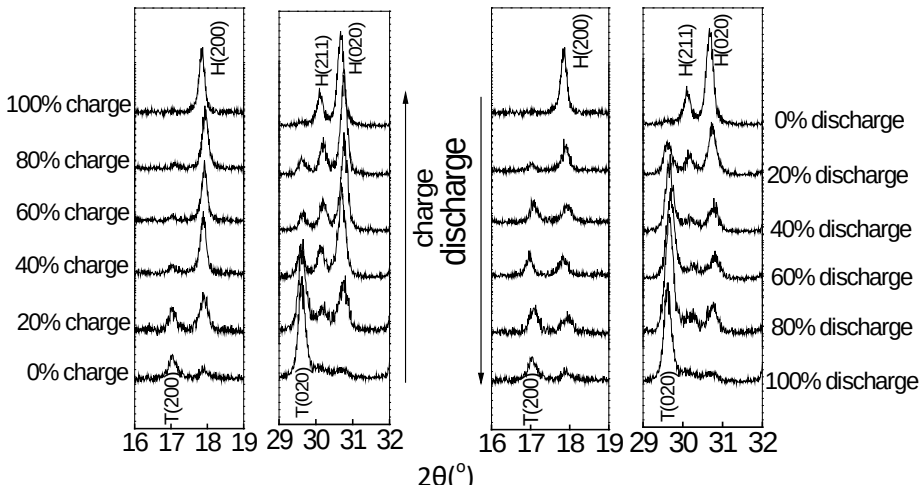

Fig. 21: Partial magnification of figure 18 (a)

c) *Structural changes of $LiFePO_4$ during charge and discharge of 2H-graphite/$LiFePO_4$ battery after storage*

The structural change of the positive active material of unstored graphite / $LiFePO_4$ battery during the charge-discharge process has been studied previously. It is found that the discharge process has an obvious lag compared with the structural change during the charging process, so will the structural change change during the charge-discharge process after storage?

Figure 20(b) shows the XRD pattern of the positive active material at the typical stage of charge and discharge of graphite/$LiFePO_4$ battery before storage and 135d after 50%SOC storage in 55°C. From the diagram, it can be found that, similar to that before storage, the structure of positive $LiFePO_4$ changes regularly during the whole charge and discharge process. With the increase of charging depth, the intensity of $FePO_4$ peak increases, the intensity of $LiFePO_4$ peak decreases, and the discharge process is opposite. From the surface, it is difficult to see the difference in the law of structural change before and after storage. However, by careful comparison, it can be found that the intensity ratios of $FePO_4$ and $LiFePO_4$ peaks in the diffraction patterns with the same charge-discharge state before and after storage are different, which seems to say that.

After bright storage, the hysteresis of the phase change of $LiFePO_4$ positive active materials changed during the charge-discharge process.

In order to further analyze the difference of hysteresis of phase transformation of positive active materials before and after storage, The relative contents of $FePO_4$ and LiFePO4 in positive active materials at each stage of charge and discharge were quantitatively calculated by Zevin's non-standard sample method. The following formula has The relative integral intensities of the two phases in the XRD diffraction spectra of each charge-discharge state are obtained by fitting the Jade6.5 software and substituted into the equation group (1). By solving them, the relative contents of $FePO_4$ and $LiFePO_4$ in the positive active materials in each charge-discharge state can be obtained. The results are shown in figure 22. It can be seen from the figure that before storage, even in the discharge state, the positive active material is not entirely $LiFePO_4$ phase, in which there is a small amount of $FePO_4$ phase (calculated to be about 8%), due to the low ion conduction capacity of LiFePO4 material itself.

$$\begin{cases} \left[\left(1-\frac{I_{LiFePO_4B}}{I_{LiFePO_4A}}\right)128.28x_{LiFePO_4A}\right]+\left[\left(1-\frac{I_{FePO_4B}}{I_{FePO_4A}}\right)128.25x_{FePO_4A}\right]=0 \\ x_{LiFePO_4A}+x_{FePO_4A}=1 \end{cases} \quad (3)$$

The first charge is caused by the formation of an inactive $FePO_4$ shell. However, it can be found that after 135days of 55oC storage in 50%SOC, the content of $FePO_4$ phase in the positive active material decreased to about 4% when it was in the discharge state, indicating that the inactive $FePO_4$ shell was reduced after storage. Comparing the curve of the relative content of $LiFePO_4$ and $FePO_4$ phase with the depth of charge and discharge before and after storage (the dotted line in the figure is the ideal curve of the relative content of $LiFePO_4$ and $FePO_4$ phase during charge and discharge (the equation is y=x), it can be found that before storage, the increase rate of $FePO_4$ phase content at the beginning of charge is obviously higher than the ideal value, and the disappearance rate of $FePO_4$ phase at the beginning of discharge is also significantly higher than the ideal value. There is an obvious difference in the content change of the two phases in the charge-discharge process, indicating that there is an obvious lag in the structural change of the cathode material in the charge-discharge process, and the reason for this phenomenon has been explained earlier. However, the change curve of the two phases after storage is close to the ideal curve, which indicates that the lag is reduced after storage. At the same time, in the XRD diagram of the positive electrode in the full state, because the $LiFePO_4$ is covered by the peak of $FePO_4$, the content of $LiFePO_4$ cannot be calculated, so the content of $FePO_4$ in the fully filled state is 100%, but this does not mean that the cathode is completely FePO4 phase at this time. By calculating the unit cell parameters of FePO4, it can be found that before storage, the unit cell volume of $FePO_4$ phase is V_{cell}=277.64, and after storage, the unit cell volume is V_{cell}=274.12 and the V_{cell}=272.75 given by the standard PDF card. It can be understood that when the cell volume of the positive pole is larger than the standard value before storage, it is due to the existence of undetached Li in the positive electrode, while when the fully charged state is stored, the content of undetached Li in the positive electrode decreases, which makes the cell volume decrease, close to the standard value. This shows that the content of unexfoliated Li in the positive electrode after storage decreases when it is in the full state, that is, the content of inactive $LiFePO_4$ mentioned above decreases. The above phenomena indicate that there may be some changes in the positive active material during the storage of graphite / $LiFePO_4$ battery

with 50%SOC, which leads to the decrease of the hysteresis of the phase transition of the positive active material, the inactive $FePO_4$ phase in the discharge material and the inactive $LiFePO_4$ content in the fully charged material.

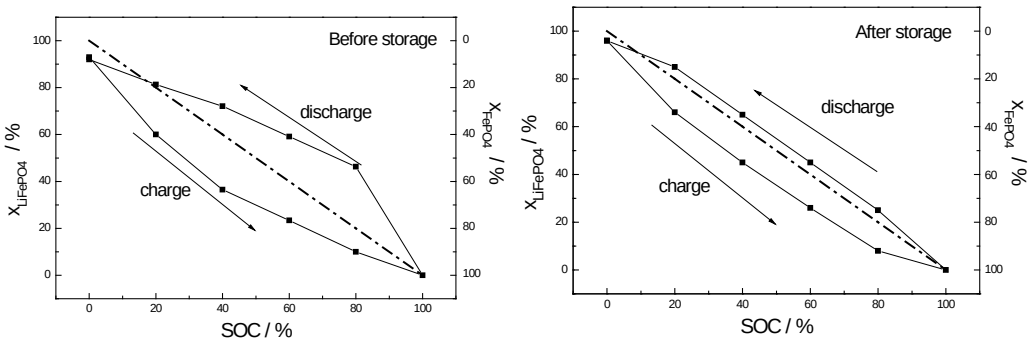

Fig. 22: During the charge and discharge of LiFePO4 electrode before and after 135d 55oC 50%SOC storage. Relative content change of LiFePO4 and FePO4 phases

d) The relationship between the performance change of 2H-Graphite/$LiFePO_4$ Battery and the Fine structure change of Battery active material

In order to reveal the law of storage performance decline, it is not difficult to summarize the results of 4.1-4.3:

1) After storage at high temperature (55℃), the storage performance of graphite/$LiFePO_4$ battery is also higher in the charged state of the battery. Great impact, similar to the above-mentioned lithium cobalt and ternary material batteries.
2) However, the difference is that the capacity of graphite/$LiFePO_4$ battery increases at first and then decreases during 25%~75%SOC storage, and this phenomenon is the most obvious during 50%SOC storage; during storage, the highest point of battery capacity appears at 135d, at which time, the power performance and safety of the battery have been improved to some extent. During storage at 0% and 100%SOC, the capacity of the battery decreases with the extension of storage time, but its capacity decay rate is also much lower than that of the other two types of batteries.
3) After storage, the capacity change rate of the positive electrode and the whole battery is very close. At the same time, the impedance of the positive electrode of the battery decreases and the dynamic performance improves after 25%~75% SOC storage, while after 0% and 100%SOC storage, the impedance of the positive electrode of the battery increases and the dynamic performance decreases, which is consistent with the performance change of the battery, indicating that the $LiFePO_4$ positive electrode plays a decisive role in the performance change of graphite / $LiFePO_4$ battery after storage.
4) The surface morphology of $LiFePO_4$ electrode after storage was observed, and the composition was determined. It was found that, similar to lithium cobalt oxide and ternary materials, a small amount of fluorine-containing precipitates also appeared on the surface of $LiFePO_4$ particles after storage, which was the main reason for the decline of battery performance after storage at 0% and 100%SOC. At the same time, it was found that microcracks appeared in the particles of positive active materials after 25~50%SOC storage. It is found that this phenomenon has a lot to do with the improvement of battery performance after storage
5) There is an obvious hysteresis effect in the phase transition of $LiFePO_4$ positive active material during charge and discharge before storage, but this hysteresis effect is greatly reduced after storage.
6) During the charged storage of $LiFePO_4$, the two phases of $LiFePO_4$ and $FePO_4$ coexist in the material particles, and there is a volume difference between the two phases. The internal stress on the interface makes the grains of the two phases split along the interface direction, which leads to cracks. The crack will produce a fresh interface and make the inactive core which originally exists in the active material particles have lithium removal activity again, so the dynamic performance of the positive electrode is improved and the capacity is increased; at the same time, the particle size will be reduced after cracking, which leads to the lag of $LiFePO_4$/$FePO_4$ phase transition of the cathode material during charge and discharge after storage.

e) Discussion on the mechanism of storage performance change of battery

The self-discharge and the chemical / electrochemical interaction between the positive electrode surface, the negative electrode surface, the two surfaces of the diaphragm and the electrolyte also occur during battery storage, which can solve the change of 0% and 100%SOC storage

performance. However, the storage performance of 25% to 75% of the charge cannot be explained, which is discussed below.

As mentioned earlier, when the $LiFePO_4$ electrode is not transformed into $LiFePO_4$ single-phase, after the first charge, the single-phase $LiFePO_4$ is transformed into two-phase $LiFePO_4$ / $FePO_4$, and then the residual $FePO_4$ phase appears in the electrode after discharge. this phase can not be reversibly de-intercalated lithium in the subsequent charge-discharge cycle, thus reducing the capacity of the battery. When the battery is stored in the charged state, the two phases of $LiFePO_4$/$FePO_4$ coexist in the positive electrode. It is found from the manual that LiFePO4 belongs to the orthorhombic, Pnma (No.62 space group of lithium iron phosphate, while $FePO_4$ belongs to the orthorhombic Pmna (No.62) space group of ferromanganese. The lattice parameters are listed in Table 10.It can be seen that the lattice parameters of $LiFePO_4$ and $FePO_4$ are quite different. The an and b values of $LiFePO_4$ are larger than those of $FePO_4$, but the c values are smaller.

Table 10: Lattice parameters and cell volumes of $LiFePO_4$ and $FePO_4$

	Lattice Parameters / Å				
	a	b	c	V	$(V_T-V_H)/V_T$
$LiFePO_4$	6.018	10.34	4.703	292.65	0.00 %
$FePO_4$	5.824	9.821	4.786	273.75	- 6.46 %

After calculating the cell volume of the two phases, it is found that there is a large volume difference between the two cells, and $LiFePO_4$ is 6.46% larger than $FePO_4$. From the lithium removal model of $LiFePO_4$ charge and discharge process proposed by Andersson [8], it can be known that the value is greater than $FePO_4$, and its c value is less than $FePO_4$. After calculating the cell volume of the two phases, it is found that there is a large volume difference between the two cells, and $LiFePO_4$ is 6.46% larger than $FePO_4$. From the lithium removal model of $LiFePO_4$ charge-discharge process proposed by Andersson [8], it can be known that in the charged $LiFePO_4$ particles, $LiFePO_4$ and $FePO_4$ form continuous phases with layered or mosaic distribution, respectively, so that the volume difference between the two cells will be further accumulated, resulting in a larger volume difference between the two phases, when a sharp interface will be formed between the two phases, and there is a strong internal stress on the interface. In the process of storage, the interface stress will split the two-phase grains along the interface direction, resulting in cracks. The crack will produce a fresh interface, so that the inactive core that originally exists in the active material particles will be exposed and come into contact with the electrolyte, thus making it have lithium removal activity again, so that the positive electrode will have a new discharge platform after storage. to increase the capacity of the battery. The appearance of the fresh interface will increase the electrochemical reaction activity of the electrode, reduce the RCT, of the positive electrode as shown in Table 20.3, and improve the kinetic performance of the electrode, thus reducing the polarization of the battery during charge and discharge (especially at high current). At the same time, the cracking of the particles will reduce the particle size and shorten the diffusion path of lithium ions in the material, so that the thickness of the FePO4 (charging) and $LiFePO_4$ (discharging) phases preferentially formed in the outer layer of the particles is reduced during the charge and discharge process, so that the blocking effect on the X-ray diffraction of the inner $LiFePO_4$ (charging) and $FePO_4$ (discharge) phases is reduced in the X-ray diffraction experiment, so that the barrier effect on the X-ray diffraction of the inner $LiFePO_4$ (charging) and $FePO_4$ (discharge) phases is reduced. After storage, the hysteresis or asymmetry of the phase change in the charge-discharge process was observed in the XRD pattern of the positive active material.

At the same time, it can also be found that when the battery is 50%SOC, the ratio of $LiFePO_4$ to $FePO_4$ in the positive active material is about 1 $FePO_4$, the interface between the two phases in the positive electrode is the largest, the particles of the positive active material have the most microcracks after storage, and the fresh surface area inside the particles is the largest, so the battery performance is improved the most after storage. When the battery is 25% and 75%SOC, the ratio of two-phase content in the positive active material is about 3:1 and 1v3, and the interface area between the two phases in the two-electrode active material is similar, but smaller than that in the 50%SOC positive active material, so the improvement of battery performance is small after storage.

However, when the battery is stored at 0% or 100%SOC, the positive active material is basically single-phase, so the particles will not crack. at this time, the interaction between the electrolyte and the positive active material leads to the deposition of F-containing material on the cathode surface, thus changing the surface characteristics of the positive electrode becomes the main factor affecting the performance of the electrode. therefore, after storage at 0% or 100%SOC, the positive electrode impedance increases and the dynamic performance decreases. This results in a decline in the performance of the battery.

Comparing the storage performance of three different positive active materials, graphite/$LiCoO_2$, graphite/$Li(Ni_{1/3}Co_{1/3}Mn_{1/3})O_2$ and graphite/$LiFePO_4$, it can be found that the capacity decay of graphite / $LiFePO_4$ battery is the slowest in the process of storage, the performance decline is the smallest after storage, and the storage performance is the best, and the storage performance can be improved when the charge is 25% to 75%, especially when the charge is 50%.

V. The Method and Action Mechanism of Improving the Performance of Lithium-Ion Battery [17]

According to the above understanding of the relationship between the changes of charge-discharge performance, cycle performance, storage performance and the structure of battery positive and negative active materials, also experimentally studied the methods to improve battery performance, and studied the effect and mechanism of these methods. Here is only a brief introduction.

As far as positive active materials are concerned, there are positive additives, coating, doping, nanometer of materials, etc.

As far as the anode materials of lithium-ion batteries are concerned, most of the commercial anode materials for lithium-ion batteries use a variety of lithium-intercalated carbon materials, such as artificial graphite or mesophase carbon microspheres (MCMB). However, there are still some shortcomings when used as anode materials for lithium-ion batteries, such as low first charge and discharge efficiency, and the potential of carbon material is very close to that of lithium metal. Metal lithium may precipitate on the surface of carbon electrode to form lithium dendrite and cause short circuit, obvious voltage lag with electrolyte, complicated preparation method and so on. Compared with carbon negative electrode materials, alloy anode materials have higher specific capacity, but alloy electrodes have large volume effect in the process of repeated intercalation and stripping of lithium, so the cycle performance is poor. Compared with the above anode materials for lithium-ion batteries, spinel lithium titanate ($Li_4Ti_5O_{12}$) shows its unique advantages as anode materials for lithium-ion batteries[14,15].

In the single solvent DMC electrolyte system, the oxidation potential of several lithium salts changes according to the following law: LiPF6 > LiBF4 > LiAsF6 > LiClO4; in EC/DMC electrolyte system, the electrical conductivity decreases in the order of LiAsF6 ≈ LiPF6 > LiClO4 > LiBFO4. In order to further improve the low temperature performance of lithium ion battery, Zhangjiagang Guotai Huarong 5160A electrolysis is used as low temperature co-solvent (PA). Its core is to reduce the content of EC in the electrolyte system and get better results [16].

Although various methods have been mentioned above to improve the performance of color recording battery, there are many researches on positive active materials because they play a leading role in the performance degradation. It plays a leading role, so there are many researches on positive active materials.

a) Summary of research on additives

Based on the research in this area, the following main conclusions are drawn.

1) As an additive, $Al(OH)_3$ can inhibit the decline of capacity and charge-discharge performance during storage; however, it has a certain adverse effect on the initial charge-discharge performance of the battery.
2) The amount of $Al(OH)_3$ has a great influence on the initial performance and storage performance of the battery. With the increase of the amount of $Al(OH)_3$, the impedance of $Li(Ni_{1/3}Co_{1/3}Mn_{1/3})O_2$ electrode increases, the initial charge-discharge performance of the battery decreases, and the improvement effect on the storage performance of the battery increases, but when the addition amount is more than 2wt%, the improvement effect on the storage performance of the battery is basically unchanged.2wt% was determined as the best addition amount of $Al(OH)_3$.
3) Before and after storage, the surface morphology of $Li(Ni_{1/3}Co_{1/3}Mn_{1/3})O_2$ electrode containing $Al(OH)_3$ changes little, while F element is concentrated on the surface of $Al(OH)_3$ particles, indicating that $Al(OH)_3$ self-sacrifice reacts with HF in the electrolyte, thus reducing the concentration of HF near the positive electrode and reducing the corrosion of positive active materials, which is the reason for the improvement of battery storage performance.
4) The addition of other additives (Al_2O_3, ZrO_2, ZnO, MgO) has a certain effect on the initial performance of graphite/$Li(Ni_{1/3}Co_{1/3}Mn_{1/3})O_2$ battery, but it is not obvious. Similar to $Al(OH)_3$, the addition of these additives can also inhibit the decline of the capacity and charge-discharge performance of the battery during storage, improve the cycle performance of the battery after storage, reduce the increase of DC internal resistance of the battery after storage, and restrain the increase of positive impedance. The results show that this method can improve the storage performance of graphite/$Li(Ni_{1/3}Co_{1/3}Mn_{1/3})O_2$ battery.

b) Study on the Mechanism of Surface coating Modification of cathode Materials

The failure mechanisms of various cathode materials are different, but the causes of failure are often similar. It can be attributed to two aspects: 1) the enrichment of surface fluoride hinders the conduction of

lithium ions and electrons; 2) the surface structure collapse caused by the surface reaction including dissolution or oxygen evolution.

Taking the layered LiMe (Me=Ni, Co, Mn) O2 materials as an example, the main mechanisms of coating modification are as follows:

1) The coating materials reduce the production of HF and consume HF in the electrolyte, and inhibit the change of the surface structure of cathode materials and the deposition of LiF and other substances. Myung et al. [42] studied the changes of surface composition and morphology of $Li(Li_{0.05}Ni_{0.4}Co_{0.15}Mn_{0.4})O_2$ before and after cycling by Al_2O_3 coating, XPS, TOF-SIMS and other means. It is found that Al_2O_3 coating reduces the production of HF, while Al_2O_3 coating consumes HF, which is the main reason for coating to improve the cycle performance of cathode materials.
2) The physical isolation of the coating reduces the direct contact between the electrolyte and the cathode active material, thus protecting the cathode material. Sun et al. [43] improve the cycle performance and thermal stability of $Li(Ni_{1/3}Co_{1/3}Mn_{1/3})O_2$ at high potential by AlF_3 coating, and think that AlF_3, as a physical barrier layer, hinders the direct contact between electrolyte and cathode material is the key to improve performance.
3) Due to the Lewis acid characteristics of the coating material, the surface of the positive active material is corroded and the fresh surface is constantly exposed, which reduces the conduction impedance of lithium ion. Bai et al. [44] soaked the Al_2O_3 particles in the electrolyte and found that the battery assembled with the soaked electrolyte had better cycle stability. Through SEM observation, it was found that the surface of the cathode $LiCoO_2$ was smoother after the cycle of the battery assembled with the soaked electrolyte. From this, it was inferred that the key to improving the performance of the cathode material was the acid characteristics of the coating layer, which was caused by the continuous corrosion of the cathode material surface.

To sum up, there is no consistent view on the modification mechanism of positive coating at present. The existing viewpoints have some limitations, and the study of the mechanism of positive coating modification is the key to further guide the related work, so the research on it is still of great significance.

c) Graphite / Al_2O_3 coated Li $(Ni_{0.4}Co_{0.2}Mn_{0.4})O_2$ battery

The comparative study results of graphite/Al_2O_3 coated $Li(Ni_{0.4}Co_{0.2}Mn_{0.4})O_2$ battery are summarized as follows:

1) There is little difference in specific surface area, vibrating density and diffusion coefficient of $Li(Ni_{0.4}Co_{0.2}Mn_{0.4})O_2$ before and after coating. The coating of Al2O3 on the surface reduces the basicity of $Li(Ni_{0.4}Co_{0.2}Mn_{0.4})O_2$, which is beneficial to the coating of electrode active materials.
2) There is a 10.9% difference in discharge capacity attenuation at 1C after 4.5-2.8V, 1C and 100 cycles of 2025 battery before and after coating, but the difference of 0.2C discharge capacity is only 3.1%. It shows that the key to the cyclic attenuation of the battery lies in the increase of impedance. SEM observed that the surface of the cathode active material of the uncoated battery was rougher than that of the coated one after cycling, indicating that there were more attachments on the surface. The EDS results show that the fluoride content on the surface of the uncoated cathode is higher. The XPS results show that more NiO is formed on the uncoated surface, which is one of the main reasons for the increase of impedance in the process of coating reduction cycle.
3) After 400 cycles of 4.2-2.75V and 2C current of 18650 battery before and after coating, the capacity of uncoated battery decreased by 17.8%, but the capacity attenuation of positive and negative electrodes was 7.1% and 3.4% respectively, which was much less than 17.8% of that of batteries. It shows that the attenuation of battery capacity is due to the mismatch between positive and negative charge and discharge capacities. The ICP detection of active lithium shows that the loss of active lithium is the key to its capacity attenuation during the cycle. The ICP test of the negative electrode material showed that the deposition amount of Ni, Co and Mn which promoted the formation of SEI film and the loss of active lithium in the coated anode was significantly lower than that in the uncoated battery, which was the reason for improving the cycle performance of the battery.
4) The measurement results of the positive and negative electrode impedance of the 18650 battery during the cycle show that the key to the decline of the rate performance lies in the positive electrode, and the coating reduces the impedance of both positive and negative electrodes, thus improving the rate retention ability of the battery.
5) The results of the 18650 battery stored at 60 ℃ for 60 days showed that the positive coating improved the storage performance of the battery, the capacity retention increased from 94.7% to 97.6%, and the increase of Ni, Co and Mn in the negative electrode decreased from 3.27 times to 1.27 times.

References Références Referencias

1. Yang Chuanzheng, Lou Yuwan, Zhang Jian, XieXiaohua, Xia Baojia, 《Material characterization and electrode process Mechanism of Green Secondary Battery》, Beijing: science Press, 2015, 560000 words.; 《Materials and Working

mechanisms of secondary Batteries》 2022. Springer and Science Press Beijing
2. Zhang Jian, Liu Haohan, Yang Chuanzheng, Xia Baojia, Research on cycle process of Graphite / Li $(Ni_{0.4}Co_{0.2}Mn_{0.4})O_2$+$LiMn_2O_4$ Battery, Power Technology, 2013, (2): 60:~64
3. Liu Hao-han, Zhang Jian, Lou Yu-wan, Yang Chuan-zheng, Xie Xiao-hua and Xia Bao-jia, Structure Evolution and Electrochemical Performance of Al_2O_3-coated $Li(Ni_{0.4}Co_{0.2}Mn_{0.4})O_2$ During Charge-discharge Cycling, Chem. Res. Chinese University, 2012, 28(4), 686—690.
4. Liu Haohan, study on failure Mechanism and coating Modification of Li $(Ni_xCo_yMn_{1-x-y})O_2$ material, Ph. D. thesis, Shanghai Institute of Microsystems and Information Technology, Chinese Academy of Sciences, 2011.6.
5. Zhang Jian, Liu Haohan, Yang Chuanzheng, Xia Baojia, "study on the cycle process of Graphite / $LiFePO_4$ Battery", Power Technology, 2012, 36 (2): 165~168.
6. Wu Xuefeng, Wang Zhenbo, Research on cycle performance and Safety performance of $LiFePO_4$/C Battery, Battery Industry, 2010 Magol 15 (3):156 to 159.
7. Jia Li, Jian Zhang, Xigui Zhang, Chuanzheng Yang, Naixin Xu, Study of the Storage Performance of a Li-ion Cell at Elevated Temperature,Electrochimica Acta, 2010, 55: 927–934.
8. Li Jia Zhang Jian Zhang Xigui Yang Chuanzheng Xia Baojia, "study on the performance of 2H-Graphite/$LiCoO_2$Lithium Ion Battery after Storage", Power Technology, 2009, 33 (7): 552-572.
9. Li Jia XieXiaohua Xia Baojia, Gao Xuefeng, "Mechanism of performance degradation of graphite/Li $(Ni_{1/3}Co_{1/3}Mn_{1/3})O_2$ Battery after Storage", Battery, 2011, 41 (6): 293-296.
10. Li Jia, he Liangming and du Yun, Safety performance of Lithium Ion Battery after High temperature Storage, Battery, 2010 pr 40 (3): 158 min 160.
11. Li Jia, "Research on Storage performance of Lithium Ion Battery", (Ph. D. thesis, Shanghai Institute of Microsystems and Information Technology, Chinese Academy of Sciences), 2010.
12. Zhang Xigui, Zhang Jian, Yang Chuanzheng, Xia Baojia, Simulation and Experimental study of mixed arrangement of Lithium and Nickel in $LiMeO_2$ Materials, Journal of Inorganic Materials, 2010, 25 (1): 8~12.
13. Li Jia, Zhang Xigui, Zhang Jian, Yang Chuanzheng, Xia Baojia, study the mixed occupation of Li/Ni atoms in Li $(Ni,Me)O_2$. New methods and applications, rare Metal Materials and Engineering, 2011, 40 (8): 1348-1354.
14. Liu Wei, preparation and Properties of Lithium Titanate, Ph. D. thesis, Shanghai Institute of Microsystems and Information Technology, Chinese Academy of Sciences, 2014.
15. Wang Qian, Development and inflation Mechanism of Lithium Titanate Lithium Ion Battery, Shanghai Microsystem and Information Technology, Chinese Academy of Sciences. Doctoral thesis, 2015.
16. Xie Xiao-hua, study on the performance of low temperature organic liquid electrolytes for lithium-ion batteries, doctoral thesis of Shanghai Institute of Microsystems and Information Technology, Chinese Academy of Sciences, May 2008.
17. Chuan-ZhengYang, Yu-WanLou, JianZhang, Xiao-HuaXie, Bao-JiaXia《Materials and Working mechanisms of secondary Batteries》,Chapter 21, 2022. Springer and Science Press Beijing.

This page is intentionally left blank

Global Journal of Science Frontier Research: a
Physics and Space Science
Volume 23 Issue 6 Version 1.0 Year 2023
Type: Double Blind Peer Reviewed Interenational Research Journal
Publisher: Global Journals
Online ISSN: 2249-4626 & Print ISSN: 0975-5896

What does the Wave Function Represent?

By Spiros Koutandos

Abstract- As was Einstein s original idea we suppose that the speed of light is altered in the presence of mass by a change in its dielectric susceptibility. Our explanation of the phenomena of quantum mechanics is a continuation of Einstein search for hidden variables. Mass induces a curvature in spacetime. This has two effects. New volume is created and this would mean that there is not exactly a point particle but matters in a way occupies some volume. Another result is that spacetime becomes cyclic and quantities like the action are quantized because they depend on angles through which the observer witnesses the events.

Keywords: *quantum thermodynamics; hidden variables of quantum mechanics; general relativity.*

GJSFR-A Classification: *LCC: QC174.12*

WHATDOESTHEWAVEFUNCTIONREPRESENT?

Strictly as per the compliance and regulations of:

What does the Wave Function Represent?

Spiros Koutandos

Abstract- As was Einstein s original idea we suppose that the speed of light is altered in the presence of mass by a change in its dielectric susceptibility. Our explanation of the phenomena of quantum mechanics is a continuation of Einstein search for hidden variables. Mass induces a curvature in spacetime. This has two effects. New volume is created and this would mean that there is not exactly a point particle but matters in a way occupies some volume. Another result is that spacetime becomes cyclic and quantities like the action are quantized because they depend on angles through which the observer witnesses the events.

Keywords: quantum thermodynamics; hidden variables of quantum mechanics; general relativity.

I. Introduction

There are plenty of reports in the scientific literature [1,2,3,4,5] regarding a possible interpretation of the wave function as a spacetime wave. The recent trend is to adopt a fifth axis of imaginary time. In that case this axis would have blurred past and future. This would help explain the ability of the wave particle to foresee which trajectory it is going to follow. The scientists also report on closed time like curves as solutions of general relativity. We give a different explanation by assuming closed spacetime curves in our work[6,7,8,9]

II. Main Part

Action is defined as:

$$S = \int \boldsymbol{p}\, d\boldsymbol{q} = \int mc^2 d\tau \qquad (1)$$

In equation (1) p is the momentum and q is the coordinate. Tau is the element of spacetime. Through a transformation the cyclic coordinates are used in what is called angle variables and then the action is defined as:

$$S = \oint p dq \qquad (2)$$

In our case of interest, that is in quantum mechanics we know that momentum is defined as ih times the gradient of psi, the wave function. We shall use equation (2) and implicate it to find action around a closed loop which may be the orbit of the particle. The only difference is that we are going to multiply by the complex conjugate of psi:

$$S = \oint \psi^* \nabla\psi d\vec{l} = \iint \vec{\Omega}\, d\vec{S} = \oint |\psi|^2\, d\phi = K\delta\tau = \delta\Omega \qquad (3)$$

In equation (3) we define as the vorticity Omega the following:

$$\vec{\Omega} = \frac{d\vec{F}}{dV} \times \frac{d\vec{r}}{dt} = \nabla \times \vec{J} \qquad (4)$$

So in short description what is happening is that the flux of vorticity even when taken through a closed surface is equal to the area of that psi describes in the complex plane of psi=a+ib which in turn equals to the change in spacetime value and the solid angle of the observer.

Next we represent some relationships we have discovered to hold true and which will be necessary:

$$dS = \frac{\hbar}{mN} dmdV = \frac{dm}{dV} dV^2 = dPdV = dTdS \qquad (5)$$

In equation (5) S on the left stands for action and indeed the S on the final right member of the equation stands for entropy.

The other useful formula is the following one:

$$\frac{\hbar^2}{2mN} \Delta|\psi|^2 = \frac{VdP}{dV} = \frac{|\psi|^2 V}{N^2} mc^2 = \hbar \frac{dm}{d\tau} = mc^2 \frac{d\Omega}{dV} = \frac{dL}{dV} \qquad (6)$$

In equation (6) Omega stands for the solid angle of spacetime. As we have mentioned in our previous work during the absorption of a photon from the atom a quantum thermodynamic engine is working which transforms the transverse photon which is a surface phenomenon to a longitudinal wave of polarization in which case we have dilation and rarefaction of the volume. The coefficient of efficiency is:

$$\eta = K \frac{dV}{dS} = \frac{E-U}{E} \qquad (7)$$

In equation (7) S stands for surface and K is the constant curvature of the space which is induced by the mass and is the inverse of the relativistic radius of the atom.

We conclude from the aforementioned that by combining equations (6) and (3) we get an extra formula regarding the cyclic procedure:

$$\oint |\psi|^2 d\phi = K\delta\tau = \delta\Omega = \oint \frac{VdP}{mc^2} \qquad (8)$$

Yet another useful formula from previous work [10] which we are going to apply is the following:

Author: e-mail: skoutandos1@gmail.com

$$\frac{\hbar}{m}\nabla\phi = \frac{d\vec{r}}{dt} \quad (9)$$

Equation (9) is valid in the absence of magnetic field and this case we are going to study for simplicity. The other useful outcome of our research is that the spacetime distorted by the mass becomes fluid. The following equation is valid then:

$$\frac{d\phi}{dt} = \frac{\hbar}{m}\nabla\phi \cdot \frac{d\vec{r}}{dt} = \frac{dr^2}{dt^2} \rightarrow d\phi dt = dr^2 \quad (10)$$

Spacetime metric is altered because the speed of light changes in the presence of mass as was Einstein s original idea. Inserting the dielectric susceptibility chi it becomes:

$$d\tau^2 = dr^2 - \frac{c^2}{\chi}dt^2 \quad (11)$$

Multiplying equation (11) by psi squared and taking a closed integral around a loop we find out that action may be quantized because the solid angles are periodic with period 4pi:

$$\oint|\psi|^2\left(\frac{d\tau}{dt}\right)^2 dt = \oint|\psi|^2 d\phi - \oint\nabla(\Delta|\psi|^2)d\vec{r} = K\delta\tau = \delta\Omega \quad (12)$$

From equation (12) we deduce that:

$$\frac{dS}{dt} = |\psi|^2\left(\frac{d\tau}{dt}\right)^2 \quad (13)$$

$$\oint dS = \delta\Omega \quad (14)$$

III. Discussion

It is one of the results of the implementation of general relativity that angles are quantized around a massive object. Our system differs from general relativity although we foresee curvature of spacetime in that in quantum mechanics force is the gradient of the potential energy rather than mass times acceleration. Besides it is the very fact that we have a variable mass that distinguishes this system.

We still have not precisely answered the question of what is the wave function. We believe, that as is being dictated by a rich literature it is possible that we may have a blurring of the axes with an imaginary component of time. If there is a fifth (non existing) imaginary axis of imaginary time then the complex conjugate of the wave function would proceed backwards in time. This may be seen for example by following the fact that momentum changes to negative by psi star and goes back. By taking the radial Schrodinger equation and applying vector calculus we find:

$$-\frac{\hbar^2}{2m}\Delta(\psi\vec{r}) = \frac{l(l+1)}{2mr^2}\psi\vec{r} \quad (15)$$

Equation (15) gives a picture of what may be happening. The radius vector is waving under complex multiplication with psi. General relativity foresees that a spinning object would attract space time like a warp.

IV. Results

Quantum mechanics describes a thermodynamic system inspired by the principles of general relativity. We give a possible answer to the long search for the quantum of action. After all h bar does have dimensions of action and angular momentum. The careful reader may observe that the talk is not only on closed loops but the same loop may be trans versed the other way since the phase is not single valued and we may have flux of vorticity through a closed surface. Indeed if there is a surface charge and mass as described by a polarization we should have vorticity flow.

We hope we have contributed to the field of research of hidden variables in quantum mechanics.

References Références Referencias

1. Wick rotation and supersymmetry, Arthur J.Mountain, TMR Meetings, Paris , 1999
2. Riemann surface and quantization, Perepelkin E.E., Sadovnikov B.I., Inozemtseva N.G., Article *in* Annals of Physics , June 2016
3. The Matter Wave Is Space-Time Wave, Xiaohan Deng, Zhiyong Deng, Hyperscience International Journal, HIJ, Vol 2, No 3, pp 60-75, Sep 2022
4. Relating a System's Hamiltonian to Its Entropy Production, Using a Complex Time Approach, Michael C. Parker, Chris Jeynes, Entropy 2023, 25, 629. Contact interactions between particle world lines, JHEP, 01(2016)033.
5. Closed timelike curves and causality violation, Francisco S. N. Lobo, arXiv:1008.1127v1
6. Enhanced comprehension of the quantum mechanical variables, Journal of Modern and Applied Physics, Spiros Koutandos, Vol.6, issue 1, 2023
7. Spacetime and the observer in quantum mechanics Journal of Modern and Applied Physics, Spiros Koutandos, Vol.6, issue 1, 2023
8. Are matter waves longitudinal photons? Spiros Koutandos Journal of Modern and Applied Physics In press
9. Regarding Schrodinger s equation, Spiros Koutandos, Journal of Modern and Applied Physics In press
10. About a possible derivation of the London equations, Spiros Koutandos, Physics essays.

Global Journal of Science Frontier Research: a Physics and Space Science
Volume 23 Issue 6 Version 1.0 Year 2023
Type: Double Blind Peer Reviewed Interenational Research Journal
Publisher: Global Journals
Online ISSN: 2249-4626 & Print ISSN: 0975-5896

Experimental and Numerical Determination of Limit Velocity for Plasma Thruster

By Milovan Pavlovic
Belgrade University

Abstract- The measurement of a mechanical impulse of the plasma thruster has been performed using by the well-known magnetoplasma compressor assembly (MPC) and features of the convergence nozzle. Based on previous research [6], hydrogen had selected as a working gas, from the reason that it can produce the highest velocity of plasma. Because of the magneto hydrodynamics model (MHD), it is entirely possible to perform rules for fluid dynamics to electromagnetism, with appropriate analog. Using all the mentioned tools, it can be determined limit value for plasma speed like analogue to sound speed, and according to, define the value of the analog Mach number for plasma. Such that would have far-reaching consequences because it would greatly facilitate feature research and the construction of plasma thrusters. Occurrence of velocity saturation indicates congestion of the nozzle, which arises as a consequence of the convergence of the nozzle, and this saturation is the velocity value corresponding to the limiting speed of plasma at a current circumstance. As the result is in agreement with the initial hypothesis, and the dependence is also confirmed with the derived formula, we can conclude that exists uniform relation between occurrences; also this occurrence are universal law of nature. Also, it is necessary to emphasize the importance of finding formula for the velocity field, which have been proved by numerical methods.

GJSFR-A Classification: *UDC: 533.9*

Strictly as per the compliance and regulations of:

Experimental and Numerical Determination of Limit Velocity for Plasma Thruster

Milovan Pavlovic

Abstract- The measurement of a mechanical impulse of the plasma thruster has been performed using by the well-known magneto plasma compressor assembly (MPC) and features of the convergence nozzle. Based on previous research [6], hydrogen had selected as a working gas, from the reason that it can produce the highest velocity of plasma. Because of the magneto hydrodynamics model (MHD), it is entirely possible to perform rules for fluid dynamics to electromagnetism, with appropriate analog. Using all the mentioned tools, it can be determined limit value for plasma speed like analogue to sound speed, and according to, define the value of the analog Mach number for plasma. Such that would have far-reaching consequences because it would greatly facilitate feature research and the construction of plasma thrusters. Occurrence of velocity saturation indicates congestion of the nozzle, which arises as a consequence of the convergence of the nozzle, and this saturation is the velocity value corresponding to the limiting speed of plasma at a current circumstance. As the result is in agreement with the initial hypothesis, and the dependence is also confirmed with the derived formula, we can conclude that exists uniform relation between occurrences; also this occurrence are universal law of nature. Also, it is necessary to emphasize the importance of finding formula for the velocity field, which have been proved by numerical methods.

I. Introduction

There is two types of object motion, when the distance between particles doesn't change, and move, when the distance between particles varies. Objects where the distance between the particles can vary are fluids or elastic objects. Fluids are objects that has no fixed shape, sometimes neither volume, because particles that make them can move freely, constantly changing their mutual distance. [1] Properties of fluid are strictly determined by the properties of the particles from which they are made, such as size, mobility, charge, etc. [2]

If considering a fluid low mobility of charge carriers, that means with low conductivity, and now start to energize this fluid. The mobility of charge carriers is rising, and as a consequence rise level of conductivity, the energy gap is shrinking more and more until this fluid becomes a conductor. [3] From the other side, energized fluid particles become faster, and therefore the velocity of fluid rises. If we continue to bring energy to fluid, and now we can initiate the movement of ions, and now this fluid we call "plasma" we can consider that plasma is fluid with the ability of good conductivity. Plasma presents ionized gas, which consists of ions, atoms that are separate with their orbital electrons, and free electrons. [2] [4]

The following is necessary to connect fluid dynamics and plasma dynamics; it is most suitable to do it through equations. It can be achieved by combining continuity equations, Maxwell equations, and Navier-Stokes equations. The model that connects these equations and rules is the Magnetic Hydrodynamics plasma model (MHD), and the sub-model in MHD responsible for plasma propulsion is the Magnetic Hydrodynamics accelerator. [3]

Magneto hydrodynamics is a model of electrically conducting fluids that treat all interpenetrating particle species together as a single continuous medium. It is primarily concerns with the low-frequency magnetic behavior in plasmas and liquid metals. [5] A partially ionized gas is a three-component mixture of electrons, ions, and neutral particles. Its behavior in a field can be described in terms of the ordinary equations of gas dynamics. We will consider here a simplified and more frequently used, for discharge condition, version of equations, assuming the gas to be at rest as a whole, weakly ionized, and quasineutral. It is sufficient to write the equations only for the electron gas. Its state is characterized by the charge density, the vector of macroscopic velocity, temperature, or pressure. [3].

According to research performed during 2019 and 2020 year in the laboratory of the Physics Faculty, Belgrade University, we find that plasma propulsion is possible to generate using a magnetoplasma compressor (MPC). Then we only performed an assay, using a ballistic pendulum in order to prove that propulsion is possible, and the result was enchanting. The plasma beam from the MPC was so intense that the probe plate was broken into several pieces and scattered inside the chamber. This scene also envisages difficult conditions for designing an experiment, that is, performing specific measurements.

To determine parameters for a plasma propulsor, it is necessary to know specific properties, such as the field of velocity, temperature distribution, and mass flow. A fluid is observed as a mixture of particles with different properties, such as mass, velocity, size, etc. - so the mass flow isn't constant. In the beginning, we can determine the velocity of the

Author: Physics Faculty, Belgrade University, Faculty of Mechanical Engineering, Belgrade University, Konelek Aero, Belgrade.
e-mail: milovan.pavlovic93@gmail.com

plasma, using the Rogovski coil, and roughly determine that the temperature is of the order of magnitude $\sim 10^4\ ^\circ K$. [6] This means that we are working with a complex fluid, without the possibility to measure any physics quantity, except velocity directly.

A Rogowski coil is an electrical device for measuring alternating current or high-speed current pulses; it registers particle drift relative to the primary direction. It sometimes consists of a helical coil of wire with the lead from one end returning through the center of the ring to the other end so that both terminals are at the same end of the coil. Since the voltage that is induced in the coil is proportional to the rate of change (derivative) of current in the straight conductor, the output of the Rogowski coil is a change in the number of particles through the contour, and that ultimately gives flow rate - velocity. [7]

In such situations, when the conditions for measurements are non-exceeding, and mass flow is unsteady, we can perform a rule for a boost of convergence nozzle, the relation between the flow coefficient and Reynolds number. Convergence nozzle has the property that it cannot produce supersonic flow, i.e., it gives a maximum Mach number of approximately one $(M = 0.99999)$. For values of Mach number close to one, the ratio between the flow coefficient and Reynolds number is constant, which will ultimately mean that the mass flow is continuous in such a flow. [8] [9]

In the further part of the text, the theoretical and experimental settings, the derivation of the formulas, and the result will be presented, with a discussion related to the derived formulas.

II. Experimental Setup and Equipment Properties

The experiment is carried out using a plasma accelerator, which is placed inside a steel chamber in which there is a vacuum, there no heavy particles. The plasma accelerator is an assembly in the center of which a cathode is placed, around which eight-rod anodes are arranged concentrically. The electrodes (cathode and anode) are made of copper, solid material, so the cathode is $5\ cm$ long with, $3\ cm$ radius, while the anodes are $14\ cm$ long, with and $0.8\ cm$ radius. [6]

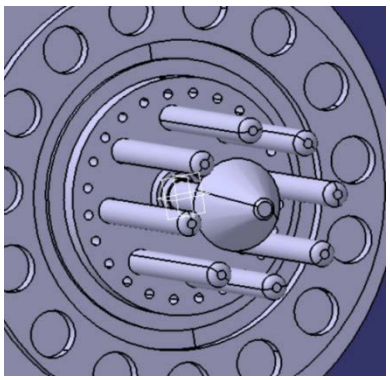

Figure 1: Model of the used equipment, built in the program CATIA V5

The equipment consists of a high-voltage generator from $1kV$ to $5kV$ and a high current of up to $5000A$, intended for powering a plasma accelerator or a magnetic plasma compressor (MPC). Inside the generator, there is a system for the periodic discharge of particles of the working gas, coordinated with the voltage pulse that is transmitted to the electrodes. There is a high-capacity capacitor in series with the source, which has the role of providing a pulse signal to the accelerator. A Rogowski coil is attached to the back of the accelerator, which protrudes from the steel chamber. Opposite the plasma accelerator is another Rogowski coil; with cooperation with the first coil, we can determine the speed of the plasma. The Rogowski coils are connected to an oscilloscope whose role is to register the recorded signals and, based on the comparison of those signals provide information on the plasma velocity distribution. [10]

The Rogowski coil usually consists of a torus coil with a large number of windings; the density of the winding, the diameter of the winding, and the stiffness of the windings are circular for maintaining resistance to external fields and a low sensitivity limit. For this case and similar cases, it is particularly suitable to use the torus geometry for the Rogowski coil, because it works with very high voltages and high currents. Toroidal geometry has the advantage of central excitation, which doesn't excite standing waves in the coil, thus reducing the probability of resonance. Standing waves and resonance, in this case, are harmful, because they can cause the coil to oscillate constantly, an excitation that takes a long time to stop; this can also cause the Rogowski coil to malfunction. [7]

As the voltage induced in the coil is proportion to the rate of change of the current in the plasma jet, the output of the Rogowski coil is most often connected to an electrical integrated circuit, an amplifier circuit, and a stabilizer circuit, to obtain an output signal that is proportional to the current. The voltage induced in the Rogowski coil, based on the dependencies mentioned in the previous text, can be expressed by the formula: [6] [10]

$$U(t) = -\frac{AN\mu_0}{l}\frac{dI(t)}{dt}, \qquad A = r^2\pi, \qquad l = 2\pi R$$

– where A represents the inside surface of the coil, N is the number of coil windings, l is the circumference of the coil's outer ring, $\frac{dI(t)}{dt}$ the level of charge in the strength of the electric current along the surface.

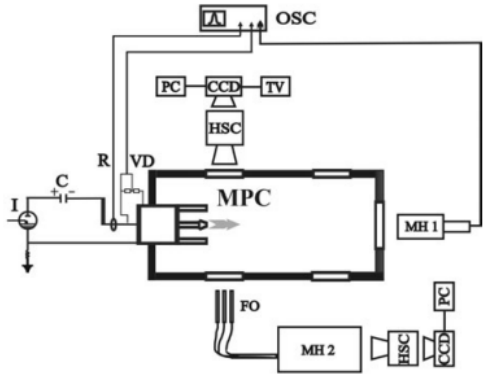

[6]

Figure 2: Experimental setup: C—capacitor, I—ignitron, OSC—oscilloscope for registration of signals from Rogowski coil (R), voltage divider (VD) and McPherson spectrometer (MH1), HSC—high-speed camera, FO—fiber optics, MH2—Jobin Yvon spectrometer

The anode, in this case, is not designed from one part, like a ring, but is intended as an assembly, which consists of 8 copper rods that are arranged concentrically around the cathode. The reason for this is the fact that the group of anodes and cathodes endure very high temperatures, over $20000°K$, which occurs as a result of the high current from the generator. In these conditions, the electrodes suffer a high degree of erosion, and copper wear occurs; if rod anodes are used instead of ring anodes, erosion on the anodes is almost completely neutralized. Ions are introduced into the accelerator through rod anodes, between which rods a "wiped" current is formed in a vacuum. The gas around the anode acts as a virtual electrode, and its magnetic field protects the rod anodes from erosion. [6] [11]

Reduction of erosion is a multiple gain, in addition to reducing wear of electrodes, providing them with a longer lifespan, and reducing impurities in the plasma, which shows better performance than plasma with copper impurities. [11] On the support, between the anode and the cathode, there are working gas injectors, through which the working gas is released into the high-voltage environment that, at the moment, regains between the anode and the cathode, energizing that working gas, igniting it, the accelerator fires a plasma pulse. The working gas injectors are specially shaped and placed in an optimal position, concerning the anode and cathode, to prevent a possible breakdown of the discharge on the surface of the injectors, i.e., the support. [6]

This further enables high injection quality, which leads to the necessary stability of the ionization zone, avoiding measurement of the plasma jet according to the output of the working gas. The stability of the compression of the plasma jet flow is manifested by a symmetrical and homogeneous cylindrical discharge of the current propagated through the surface of the electrodes. The symmetry of the discharge is recorded as a specific section of the formation composed of energy storage cells according to the sphere and continuous input of the working gas through the electrodes. [10]

III. Experiment Description

Plasma is observed as a gas that doesn't have a constant mass flow and consists of charged particles, so it is subject to the laws of fluid mechanics and electromagnetism simultaneously. As already mentioned, the environment is vary unfavorable for measurement, in general, for conducting an experiment; therefore, we cannot work with a continuous stream of the plasma, because, in that way, we would endanger the apparatus, so the plasma must work in pulse mode. Also, because the principle of a convergent jet describes the change in speed concerning the difference in the area of the output cross-section, it is necessary to perform more measurements for the different distance between anodes rod, which can show the dependence of the output speed on the cross-sectional area. Several positions are provided on the support for each anode, so we get several exit cross-sectional surfaces. In this way, we simulate the narrowing of the cross-sectional surface of the convergent nozzle. In order for the experiment to show a positive result, it is necessary to demonstrate convergence velocity with a decrease in the distance between the anode rods, which should ultimately lead to velocity saturation. Velocity saturation, in this case, should represent jet congestion i.e., reaching the maximum Mach number for a convergent jet, which is approximately one. Based on the relation between the flow coefficient and the Reynolds number [8], in this case, magnetic Reynolds number, the mass flow can be considered constant.

The magnetic Reynolds number represents a quantity analogous to the ordinary Reynolds number. Unlike the Reynolds number, which means the ratio of inertial force and viscous force, the magnetic Reynolds number represents the ratio of the conventional $\left|curl\left(\vec{v}\times\vec{B}\right)\right|$ and diffusion $\left|v_m\Delta\vec{B}\right|$ factor in plasma. So we get an expression for the magnetic Reynolds number as: [3]

$$\frac{\left|curl(\vec{v}\times\vec{B})\right|}{\left|v_m\Delta\vec{B}\right|}\approx\frac{\frac{1}{D}VB}{v_m\frac{1}{D^2}B}=\frac{DV}{v_m}=Re_m$$

– where D is the characteristic dimension of the system, V is the characteristic velocity of motion (flow), and v_m is the speed of movement of charge carried in a magnetic field. Based on the Helmholtz equation, we observe that this equation measures the relative influence of the conventional and diffusion terms in the equation for the time evolution of the vorticity vector $\vec{\omega}=\frac{1}{2}curl\,\vec{v}$. [3]

On the support, it is possible to place rod anodes in the form of a concentric circle concerning the cathode in the center, with different radius values, without the residual harmful effects of one set compared to the other. This is important to note because one can get the impression that always the same positioned injector of the working gas can affect the results of the experiment, which is not the case here. The working gas injector is set to be most optimal for the most challenging case, the point when the distance between the anode and the cathode is minimal; the occurrence of anomalies such as the breakdown of the discharge on the surface of the injection of the working gas or the shift of the working gas or plasma towards the source can be fatal. In other cases, the working gas injector is further away from the anode, and the distance is greater than optimal; instead of the optimal, the term minimum is more suitable, because the primary spark starts from the anode.

When energizing the electrodes, to ignite the working gas, i.e., creating plasma, a magnetic field appears around the electrodes. As a consequence of the mutual action of magnetic fields that arise due to the flow of current through the anode and cathode, a concave magnetic lens is created, conditionally speaking, which collides with the plasma beam. As the anodes are closer to the cathode, the magnetic lens will be more robust, i.e., the more it compresses the plasma, which is analogous to the reduction of the exit cross-section area of the convergent nozzle. On the contrary, the farther the electrodes are, the magnetic leans that they bind is weaker, i.e., analogous to the increase in the outer cross-sectional area of the converging nozzle.

We will not go to the congestion of the converging nozzle experimentally. Still based on the several obtained values and using the appropriate form of extrapolation, the idea is to graphically arrive at the value at which the nozzle is congested. The reason for this is the high safety risk we are exposed to when the nozzle is clogged.

The complete experiment will be repeated several more times, at the same value of pressure, about $1000\ Pa$, because according to previous research [6], due to a reduction of pressure below $1000\ Pa$ there is an increased erosion of the cathode, which leads to a decrease in the velocity of plasma steam. This decrease in velocity is explained as a consequence of the impurity of the working gas in the plasma nozzle, which causes an increase in the mass of the working gas. Also, based on previous experiments [6] it was shown that hydrogen as a working gas can achieve the highest plasma output velocity, so that we will use hydrogen as a working gas.

a) Initial conditions and assumptions

The calculation of the specific thrust, that is, the mechanical impulse or any parameter that has a role to describe and explain the plasma as a propellant will be following the rocket engine. So, we look at the plasma thruster as a rocket engine and expect the plasma thruster equation to confirm the rocket engine equations, or at least the form of the thrust equation: $\vec{F}_P=\dot{m}_{ps}\vec{v}_i$. This idea is self-evident, because the plasma thruster, like the rocket engine, has no inlet, in the sense that there is no inlet mass flow of gas, but it is a consequence of the process that takes place inside the thruster itself.

The basic assumption is that due to the reduction of the outer cross-section of the nozzle, velocity saturation occurs, i.e., the appearance of a limiting velocity analogous to the ejection of air from the convergent nozzle.

Due to the excessive energies that will be developed during the performance of the experiment, the action of the high voltage and a very strong current, and due to the act of the very strong magnetic field, at the moment when the electrodes are very close, erosion of the cathode can be caused. This erosion will occur as a result of excess energy, will cause a decrease in velocity, and can be considered analogous to the congestion of the converging nozzle.

IV. Experimental Results

The experiment was carried out in the summer, of July 2020. The operating temperature was $27\ ℃\ (\sim 300\ °K)$, with a relative humidity of about 45%, while the atmospheric pressure was $993 mbar$ and the altitude was $110 m$. Based on the initial conditions of the experiment, we get that the speed of sound is

$$c=\sqrt{\frac{kRT_0}{\mathrm{M}}}=347\ \frac{m}{s}.$$

Based on the course of the experiment, the discharge time, that is, the duration of the plasma pulse, was recorded to be about $8\ \mu s$, and it doesn't change much with the charge of operating conditions. The deviations are about $\pm 2\ \mu s$. The only change that has a severe effect on discharge time is changing the working gas. However, the discharge time doesn't exceed $20\ \mu s$, which is a very short time to measure anything on that

pulse, especially not the flow rate distribution of the generated plasma.

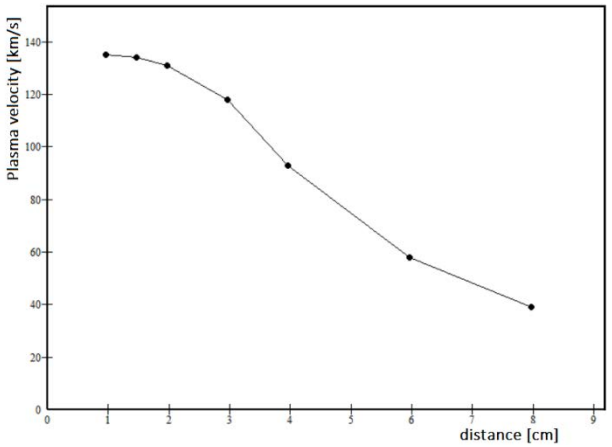

Figure 3: Plasma flow velocity for hydrogen (H_2) in the function of the distance between cathode and anodes, under the constant pressure $P = 1000Pa$

With the help of Rogowski's coil measured values, we obtained very high mean plasma velocities (Figure 3.) of the order of $\sim 10^2 \frac{km}{s}$, which will be shown in more detail later in the text, as well as the occurrence of convergence. As the velocity of the plasma steam increase, so does the heat radiated by the plasma. Regarding the heat, it is important to note that at a distance of $5\ cm - 7\ cm$ from the plasma nozzle outer, the plasma steam reaches its maximum in terms of energy, therefore the heat it radiates.

During the experiment, the zones responsible for the parameters of the plasma beam could be observed, ionization zone and compression zone.

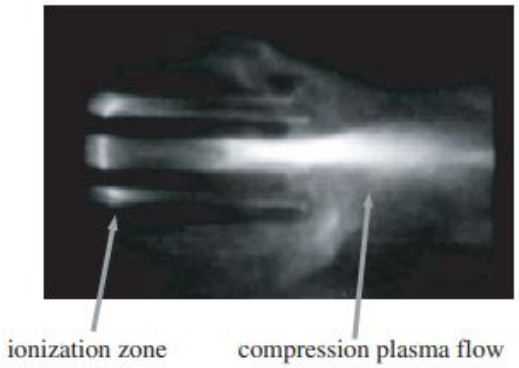

[6]

Figure 4: Plasma discharge, represented with ionization zone and compression plasma flow zone

After energizing the electrodes with a voltage of $\sim 10^3\ kV$, gas is automatically released into the ionization zone, which triggers the ignition of the plasma accelerator. The start of the plasma accelerator discharge depends on the pressure of the working gas, and accordingly, it can start from the place where the distance between the anode and the cathode is the smallest.

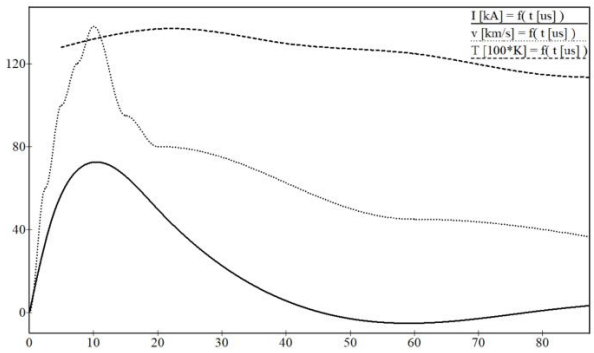

Figure 5: Distribution of electric current $I\ [kA]$, plasma velocity $v\ \left[\frac{km}{s}\right]$ and plasma temperature $T\ [100 \cdot K]$ in the function of time interval $t\ [\mu s]$

During discharge, the discharge current and magnetic field increase. The actual discharge begins at the movement when the electric filed is established within the entire volume through which the plasma steam will spread. Compression occurs under the influence of a magnetic field, which means that the magnetic field simulates the convergence of the nozzle. The increase of the magnetic field, i.e., the transfer of almost complete energy is established only at the entrance to the acceleration channel.

Further, the plasma formed in this way is compacted, and compressed, under the effect of the magnetic field that arises as a result of the flow of current through the electrodes. The plasma steam is compressed due to the interaction between the longitudinal component of the current caused by the discharge and the azimuthal magnetic field, as well as due to the dynamic pressure of the plasma steam converging towards the abscissa of the system. [4]

V. Numerical Solution, Equation of Convergence Nozzle

The Numerical calculation was performed in COMSOL Multiphysics, using the custom method DC discharge, described by the Navier-Stokes equation adjusted to electrodynamics. In this way, we could roughly confirm the experimental results, neglecting the numbers themselves, but paying attention to the occurrence of velocity saturation. The velocity saturation would unquestionably prove the validity of the convergent nozzle law in plasma propulsors. Nevertheless, even though we would obtain solutions for the ideal case, the numerical method is beneficial for finding the velocity field of plasma steam.

Due to the symmetry of the apparatus, we can consider that the two-dimensional system can adequately describe the situation. This approximation should not significantly affect on the velocity and magnetic field vector, i.e., the resulting velocity field should not deviate significantly from the real one.

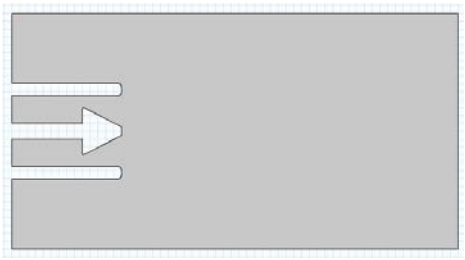

Figure 6: Model of Magneto Plasma Compressor for Numerical Method

For the description of fluid motion, some radical changes will have to be made to the standard equations of motion given in the program. The properties of working gas, and chemical reaction, will be used from the program's database, file (*H_xsecs*), for hydrogen H_2. [14] The significant factor for proper description of plasma flow is the existence of diffusion, i.e., ambipolar diffusion $D_a = \frac{D_+\mu_- + D_-\mu_+}{\mu_- + \mu_+}$; [4] ambipolar diffusion is included in the equation of motion with a vector of current density $\vec{j}$. The diffusion model will be the mixture-average model, which includes the migration of charged particles in the electric field, and plasma purpose – reduction of electrons during transportation properties. Although a DC discharge ultimately reaches a steady-state condition, the problem must be solved as a time-dependent problem so the plasma can naturally evolve into its equilibrium state. [14]

In purpose to import the influence of the magnetic field, as a crucial factor in this research, we will use AC/DC interfaces – electric current interfaces. As the magnetic field itself has no role other than plasma compression, i.e., the simulation of the convergent nozzle, the evolution of this physics quantity doesn't reflect in results, so we will assume that the magnetic field is stationary. [15]

a) The equation for numerical method

To purposely numerically describe plasma propulsion, it is necessary to start from the equation of motion, and it would find. Let's start with Newton's Second Law. According to the definition [12], a net of forces can represent a net of forces which acted on fractal and a net of forces which acted on fractal borders:

$$\vec{F} = \sum_{i=1}^{N} m_i \cdot \ddot{\vec{r}}_i = d\dot{m} \cdot \dot{\vec{r}} = \vec{F}_{fract} + \vec{F}_{bord}$$

– if $\dot{m} = \frac{d}{dt}(\rho \cdot V)$, and $\dot{\vec{r}} = \vec{v}$, thus,

$$d\vec{F} = d\dot{m} \cdot \dot{\vec{r}} = d\left(\frac{d}{dt}(\rho \cdot V)\right) \cdot \vec{v}$$

Mass flow can be expressed with a continuity equation:

$$\dot{m} = \iiint \frac{\partial \rho}{\partial t} \cdot dV + \iiint \nabla \cdot (\rho \cdot \vec{v}) \cdot dV$$

– follow, net of forces on fluid fraction written as $\vec{F}_{fract} = \vec{f}$, and according to [3] and [13], net of forces acted on fractal borders are described by Bernoulli's equation; consisting by pressure gradient on fractal borders ∇p, the influence of Lorentz force $\vec{j} \times \vec{B}$, component of viscosity $v_m \Delta \vec{v}$, and very significant factor for this calculation – compressibility $(\lambda + \frac{1}{3} v_m)\nabla(\nabla \cdot \vec{v})$.

$$\frac{\partial}{\partial t}(\rho \vec{v}) + \nabla \cdot [\rho \vec{v}, \vec{v}] = \rho \vec{f} - \nabla p + \vec{j} \times \vec{B} + v_m \Delta \vec{v} + \left(\lambda + \frac{1}{3} v_m\right) \nabla(\nabla \cdot \vec{v}) = 0$$

Volume force, the weight of fluid fraction, etc. – we can neglect $\vec{f} = 0$. The influence of Lorentz force describes magnetic pressure, significant factor in describing the compression of plasma steam. According to vector calculus identity and Ampere's law [13]:

$$\vec{j} \times \vec{B} = \nabla\left(\frac{1}{2\mu_0} B^2\right) + \frac{1}{\mu_0}(\vec{B} \cdot \nabla)\vec{B}$$

– where member $\frac{1}{2\mu_0} B^2$ represents magnetic pressure. Into the viscosity component, member v_m is the velocity of movement charge's carriers in the magnetic field, and represents analogous to the viscosity coefficient. This parameter can be expressed $v_m = -\frac{1}{\mu_0 \sigma}$. When it comes to the compressibility factor in the equation, it is necessary to perform vector calculus identity in purpose to solve $\nabla(\nabla \cdot \vec{v})$:

$$\nabla \times (\nabla \times \vec{v}) = \nabla(\nabla \cdot \vec{v}) - \Delta \vec{v} \rightarrow \nabla(\nabla \cdot \vec{v}) = \nabla \times (\nabla \times \vec{v}) + \Delta \vec{v}$$

– where $\nabla \times \vec{v} = 2\vec{\omega}$, and $\vec{\omega}$ is the time evolution of the vorticity vector, and this parameter is a consequence of the influence rotating magnetic field, representing the connection between the magnetic field vector and the Reynolds number. Now equation of motion has form:

$$\rho \cdot \left(\frac{\partial \vec{v}}{\partial t} + \vec{v}(\nabla \cdot \vec{v})\right) = \nabla p + \nabla\left(\frac{1}{2\mu_0}B^2\right) + \frac{1}{\mu_0}(\vec{B}\cdot\nabla)\vec{B} - \frac{1}{\mu_0\sigma}\cdot\Delta\vec{v} + \left(\lambda - \frac{1}{3}\cdot\frac{1}{\mu_0\sigma}\right)(\nabla \times 2\vec{\omega} + \Delta\vec{v})$$

– the substantial derivative of the velocity will be equal to zero:

$$\left(\frac{\partial \vec{v}}{\partial t} + \vec{v}(\nabla \cdot \vec{v})\right) = 0$$

– so finally equation of motion have form:

$$0 = \nabla p + \nabla\left(\frac{1}{2\mu_0}B^2\right) + \frac{1}{\mu_0}(\vec{B}\cdot\nabla)\vec{B} - \frac{1}{\mu_0\sigma}\cdot\Delta\vec{v} + \left(\lambda - \frac{1}{3}\cdot\frac{1}{\mu_0\sigma}\right)(\nabla \times 2\vec{\omega} + \Delta\vec{v})$$

b) Results

For the analysis of the numerical results, we will use a time-dependent study, as mentioned in the previous part of the text. For a time-dependent or transient simulation use a time-dependent solver for computing the solution over time. [14] This study type is also used for optimization problems that are constrained with a time-dependent partial differential equation (PDE) problem. Time-Dependent and Time Discrete study generates equations for transient (time-dependent) simulations, corresponding to a Time-Dependent Solver, Time Discrete Solver, or Time Explicit Solver. [16] [17]

The method for time stepping is the BDF operator. The BDF operator is used to approximating time derivatives in two or more steps $bdf(expr, i)$ when we work in a time discrete solver. The expression BDF results in a discretization of the time derivative of $expr$ using the backward differentiation formula. The second argument i, determines the order of accuracy of the discretization. As the calculation itself is roughly performed, without excessive details, but only to obtain approximate values and distributions, the selected values for the parameters will be 1 for minimum BDF order, and 2 for maximum BDF order. For event tolerance, we can use 0.01. The BDF operator can be implemented using the $prev$ operator, as $bdf(u,1) = \frac{u - prev\,(u,1)}{time\ \ step}$, this formula is also known as a backward Euler Method. [16] The Backward Euler method has a task to describe consistent initialization into algebraic variable settings, with a selected fraction of the initial step of 0.001. [17] As a result, we have to get the field of velocity (Figure 9.) and pressure field (Figure 8.), such as the distribution of electron density (Figure 7.), but only the purpose of proving the validity of the calculation. Namely, as we already know the dependence of electron density and time, for hydrogen (H_2) we can compare the diagram obtained by numerical calculation (Figure 7.), and the photography obtained experimentally [6].

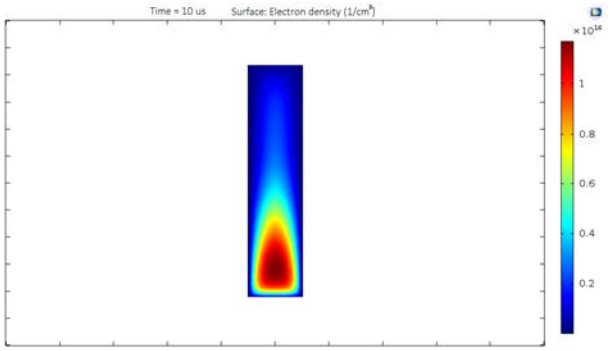

Figure 7: The electrons density time-dependence for hydrogen (H_2)

Given the diagram, and distribution, looks exactly what we expected. Maximum value hydrogen electron density is of the order of magnitude $\sim 10^{16} - 10^{17}$; we can consider it close enough [6] to take the model as a valid representation. As the velocity of plasma steam propagation and the pressure i.e., pressure distribution, depend on the number of particles, i.e., electrons as the most mobile, their mobility, and distribution, a proper electron density diagram guarantees a valid consideration of velocity and pressure.

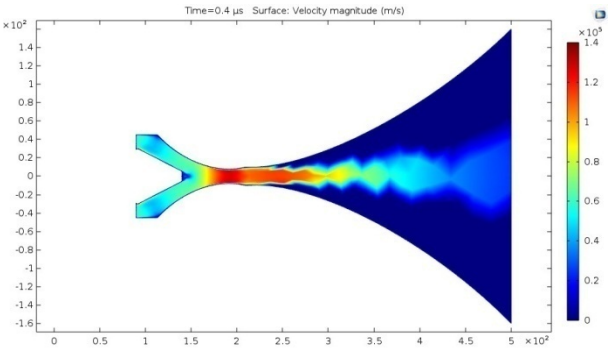

(a)

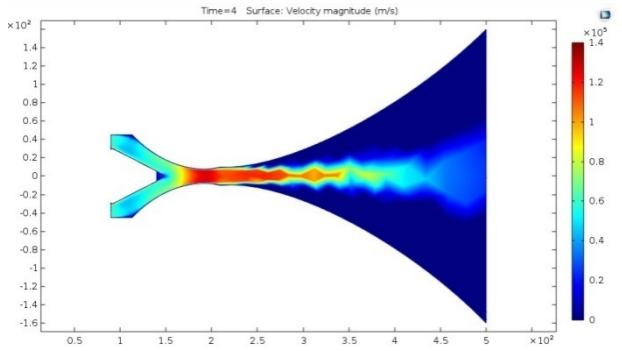

(b)

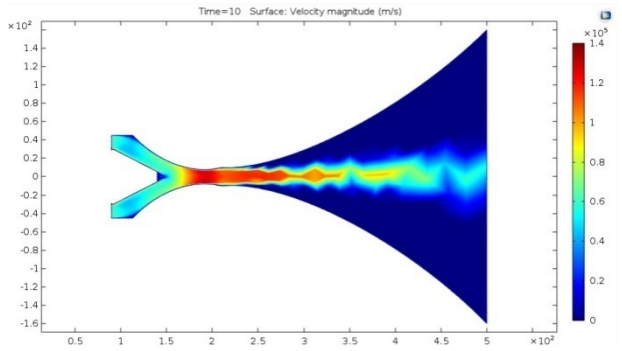

(c)

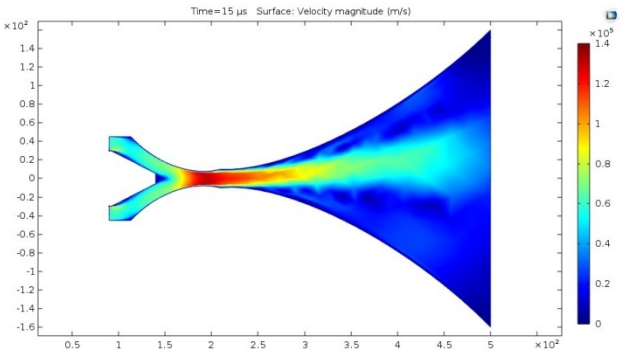

(d)

Figure 8: (a) (b) (c) (d) Velocity field in function of the displacement, during different time interval

The study was carried out in such a way that the magnetic field defines the shape of the trajectory and the way of transporting particles through space. The propagation of the particles that form the plasma steam is limited by the magnetic field so that none of the particles can leave the cone that creates the magnetic field around them. On the other hand, the mobility of those particles, as well as their distribution, are expressed using diagram Figure 8. and Figure 9. Based on the velocity distribution diagram during time intervals, we can observe different forms of particle behavior, follow the velocity field, as well as various phenomena that occur.

The results are presented in different time intervals. The calculation itself is designed to give results for a $15\,\mu s$ performed in steps of $0.5\,\mu s$. In this work, only diagrams depicting some exciting or unusual phenomenon will be shown, and described. An essential approximation of the plasma thruster analysis in our case is the assumption that no particles will leave the cone that creates the magnetic field; in the real possibility there is probably particle dissipation outside the magnetic field itself. In the actual point the particles will probably move outside the cone of the magnetic field, but this should not have significant effects on the calculation results we are currently observing.

Analyzing the diagrams for the velocity of plasma propagation in Figure 8, we notice that the velocity increase with increasing compression, which is a consequence of the influence of the magnetic field. Since before the nozzle is congested, there is a gradual formation of closures, the nature of which lies in the pressure distribution. Based on Figure 9, it is seen that the congestion of the nozzle occurs due to the pressure drop in the tear of the nozzle. This tells us that when the magnetic field increase, there is a gradual increase in velocity, and a gradual decrease in pressure, until the moment of saturation.

Based on the diagram of Figure 8. (d), we can notice an exciting phenomenon that is also characteristic of the congestion of a convergent nozzle in fluid dynamics. The appearance of fluid steam, which leaks during converging nozzle throttling, doesn't continue moving along the abscissa, but the steam gradually moves upward. The reason for this occurrence is probably a decrease in pressure inside the plasma steam; it is obviously Figure 9. (d).

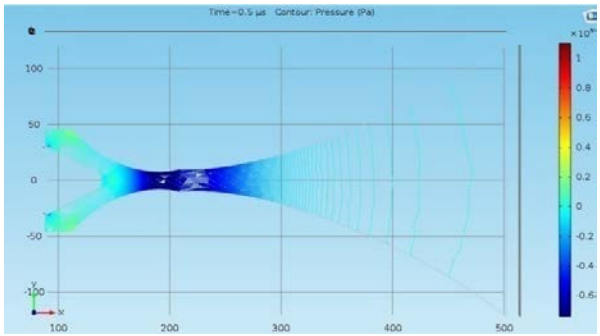

(a)

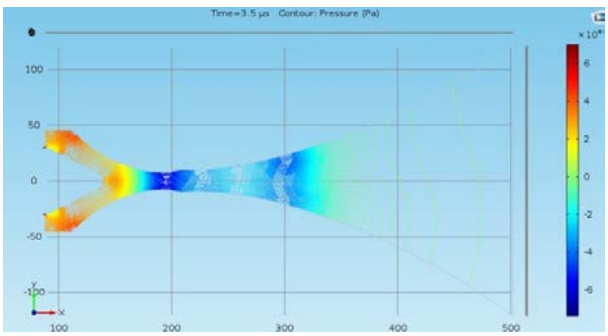

(b)

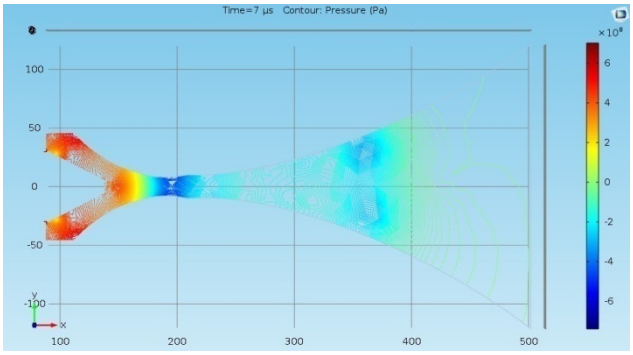

(c)

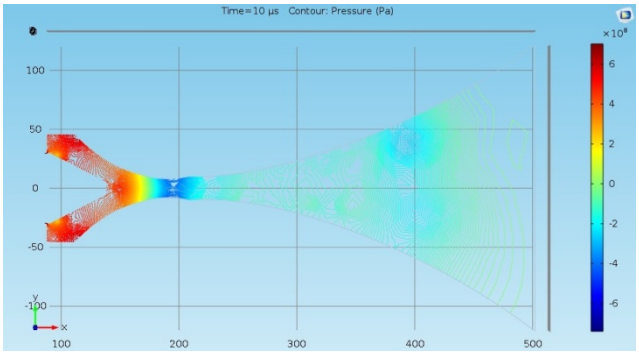

(d)

Figure 9: (a) (b) (c) (d) Distribution of Pressure in function of the distance, during time interval

Figure 9. (d) shows a decrease in pressure around the plasma impulse, and according to the distribution of pressure inside the cone, we can determine that pressure around the plasma impulse is lower than the pressure in the environment, so plasma flow starts to rise upward.

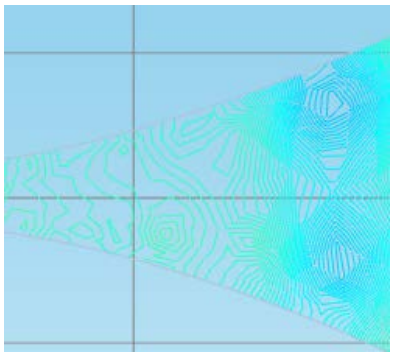

Figure 10: Pressure contour in turbulent regime obtained von Karman vortex streets

Also, it is vital to notice the presence of von Karman vortex streets in distributions of velocity (Figure 8. (b) (c)) and pressure (Figure 9. (b) (c) (d) and Figure 10) till the moment of congesting Figure 8. (d). This is an expected phenomenon for this flow type in fluid dynamics, which again proves the connection between fluid dynamics and plasma dynamics. After exiting at Mach number, less than or close to one, during exit from the nozzle, a transition will occur, and then turbulence, which appropriate values of the Reynolds number will generate von Karman vortex street.

VI. Discussion

For the case of gas leakage, when the Mach number is equal to one, or has small oscillations around one, based on the relation between the flow coefficient and Reynolds number, we can consider the mass flow as constant. Following, the total pressure is a sum of the pressure and the magnetic pressure $p + \frac{1}{2\mu_0}B^2$, the function of Mach number $\frac{M}{\left(1+\frac{\aleph-1}{2}M^2\right)^{\frac{\aleph+1}{2(\aleph-1)}}}$, and Reynolds number, mobility of charged particles are included in the equation by velocity.

$$\dot{m} = \aleph \cdot v \cdot \left(p + \frac{1}{2\mu_0}B^2\right) \cdot \frac{M}{\left(1+\frac{\aleph-1}{2}M^2\right)^{\frac{\aleph+1}{2(\aleph-1)}}} \cdot A_{iz} = const$$

The member A_{iz} represent cross-surface at the point where the point where the plasma steam is narrowest. Based on the experiment, at the point of maximum constriction of the plasma steam, the diameter is between $1\ cm$ and $1.2\ cm$, based on this, we can quickly determine the cross-section surface at the point of maximum constriction.

As already mentioned, the thrust, and the mechanical impulse of the plasma, will be calculated in the same way as a rocket engine; in the previous part of the text reason is explained. If using the previous formula for mass flow $\dot{m}$, use for combustion mass flow $\dot{m}_c$, the formula for plasma thrust:

$$\vec{F}_P = \dot{m}_c \vec{v}_i = \aleph \cdot \left(p + \frac{1}{2\mu_0}B^2\right) \cdot \frac{M}{\left(1+\frac{\aleph-1}{2}M^2\right)^{\frac{\aleph+1}{2(\aleph-1)}}} \cdot A_{iz} \cdot v^2 \cdot \vec{e}_x$$

For the limiting value of the congestion of the convergent nozzle, when the mass flow is constant, the Mach number is approximately one $M = 1$, thus

$$F_P = \left(p + \frac{1}{2\mu_0}B^2\right) \cdot \frac{\aleph \cdot A_{iz} \cdot v^2}{\left(1 + \frac{\aleph-1}{2}\right)^{\frac{\aleph+1}{2(\aleph-1)}}}$$

According to experimental results:

$$F_P = 1.62866 \cdot 10^5\ N \sim 163\ kN$$

- specific thrust:

$$F_{ST} = 1.36 \cdot 10^5 \frac{N\ s}{kg}$$

- and mechanical impulse:

$$I_p = \int_0^{10^{-5}} v\dot{m}dt = 2.443\ kg\frac{m}{s} \sim 2.45\ Ns$$

Based on [6], we notice that temperature and magnetic field are mutually dependent, leading us to the dependence of plasma velocity and temperature (Figure 11). For the reason that the magnetic field forms a convergent nozzle, while on the other hand, it depends of the temperature, we conclude that the Mach number for the plasma, directly depends on the temperature.

Since from fluid mechanics [1], we know that the Mach number depends on the ratio of the limiting velocity of the flow (sound speed) and the function of the square root of the temperature, which has the property of defining the current velocity of the flow. Compression for plasma flow can be expressed with $B^2 = 4\mu_0 nkT$ [6] and find that the magnetic field depends on temperature as a function of the square root, $B \propto \sqrt{T}$. As plasma velocity is directly proportional to magnetic field [3] $v \propto B$, we can conclude that velocity is proportional to square root of temperature $v \propto \sqrt{T}$, same as fluid mechanics, for $M = 1$, $v = \sqrt{kRT}$.

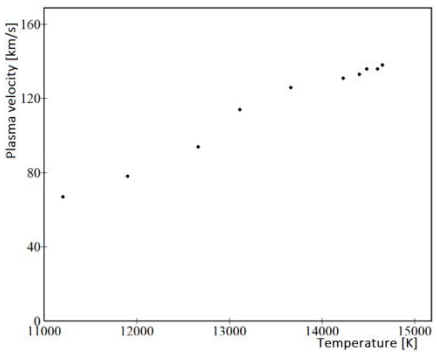

Figure 11: Plasma velocity in the function of temperature

According to experimental results in Figure 3, we notice that plasma velocity increase with the reduction of distance between the anode and cathode; we can easily conclude that the intensity of the magnetic field depends on distance between the anode and the cathode. This leads us to the fact that if we reduce the distance between the anode and the cathode, we increase the vector of the magnetic field. As the increase of the magnetic field vector leads to nozzle compression, the idea that the magnetic field can manipulate with a plasma nozzle, forming a convergent or convergence-divergence plasma nozzle, is founded. With an increase in the magnetic field vector, there is also an increase in the velocity of plasma discharge; according to the formula, the magnetic field vector is directly proportional to the velocity.

Of course, in specific moment, compression must reach a critical point, i.e., saturation of the flow rate, which will be analogous to the congestion of a convergent nozzle. According to that, we prove the initial hypothesis, and find another a critical correlation for the MHD model.

Also, I would like to point out another important observation, based on numerical results in Figure 9, as plasma velocity increase, fluid pressure decrease. However, as the pressure has its mechanical and magnetic components, and based on the previous formulas, as well as Alfven's speed [5], the magnetic pressure increases with the increase in the plasma velocity. Based on that behavior, we can conclude that the total pressure, the sum of mechanical and magnetic pressure, is a conserved quantity, i.e., if mechanical pressure increases, magnetic pressure must decrease, and vice versa.

It is necessary to emphasize that the numerical results are given only for the case when the Mach number for the plasma is equal or close to one. The formula for the velocity field, which is the basis of the numerical calculation, is derived so that the Mach number for the plasma is equal to one. This fact in no way diminishes the importance of research, on the contrary, this research helps to understand the properties of plasma better and gives us an excellent basis for further study. Because, if we have a limit value of plasma velocity, dependence of pressure, temperature, magnetic field, etc. – we can properly perform calculations for plasma nozzles.

If we continued to reduce the distance between the anode and the cathode, we would cause drop of the plasma velocity at a certain moment. With the reduction of the distance between the anode and the cathode, there would be an increase in energy of plasma, to such an extent that the cathode would begin to erode. The erosion of the cathode would be manifested as a drop in plasma velocity. Anode erosion would be minimal or doesn't exist at all, due to the geometry of the anode.

I would like to point out that we are nearing the end of making a cathode with compact geometry, which should completely neutralize the erosion of the system,

or minimize it as much as possible. One of the key problems is the conditions for the testing of such an assembly, because it can cause catastrophic consequences such as the explosion of the equipment, or even the release of neutrons, which would lead to catastrophic consequences for the environment. In our laboratory, we don't have the conditions for such an experiment. However, a positive result would have a multiple benefits. I am convinced that it is possible to create a sufficiently strong rotating magnetic field, which would be able to capture the plasma beam, and under the influence of such a strong magnetic field, could become a secondary particle accelerator perpendicular to the original direction. This accelerator would actually be the basis for a plasma reactor. Invention of plasma reactor is surely a capital discovery.

VII. Conclusion

According to the presented results, and compared with similar research, we can find the following conclusion. Based on the experimental results, all assumptions from the beginning proved to be accurate so that the experiment can be considered as positive.

A significant invention is undoubtedly the ability of a magneto-plasma compressor (MPC) to produce buoyant force, and trust, which leads us directly to the idea of a plasma thruster. But, this ability is not enough for itself; the essential thing is an equation that can describe this occasion, and closely explain the phenomenon. Based on experimental results, we proved the initial assumption that the plasma velocity, during the boost of the convergent nozzle, must reach a specific limit value. According to this value, we find the existence and approximate value of the Mach number for plasma. Helped by the presence of a limit value for plasma velocity in a convergent nozzle, we allowed every feature observation of plasma easier; using a value of one for Mach number, we can consider mass flow constant.

Also, we find that magnetic fields manipulate with plasma steam movement, field of velocity, pressure distribution, etc. – basically, we use magnetic fields to determine flow features. With the help of the magnetic field, we can define the shape of the nozzle, therefore the condition of the plasma flow, the concentration of particles per unit volume, and in this way the intensity of the electric current, the temperature, such as the velocity of the flow. Finding the values mentioned physics quantities, as well as a closer explanation of the specific phenomena that participate in plasma propulsion at $M \cong 1$, is the first step towards the realization of plasma thruster.

We can also conclude that the mechanical, thermodynamic, and electrical properties of the plasma thruster don't depend on the working gas. The exact relation will apply to different working gases, i.e., magnetic field, pressure, and temperature; they will have the same roles and dependencies, only the constant will be other. In addition to the gas constants that necessarily change with the change of the working gas, it is essential to note that the limiting value of the plasma velocity will be different, i.e., lower than the plasma velocity when the working gas is hydrogen.

Although the experiment was supposed to give us an approximate model for observing the plasma thruster, I think we got more than expected. Of course, this is only the first step toward the realization of a plasma thruster, but it is a significant step. We received outlines, ideas, how the plasma thruster should look, as well as guidelines for future experiments, which can be carried out based on this work.

In addition to the obtained results, the long-term relevance of this work can be seen in the opening of an ample space for new research and new ideas.

Acknowledgement

I owe a lot of thanks to dr Milorad Kuraica, dr Predrag Iskrenovic and dr Nikola Davidovic.

Work is dedicated to prof. Vasko Fotev and prof. Nikola Sisovic.

References Références Referencias

1. Cvetko Crnojevic – Mehanika Fluida (2014), Masinski Fakultet Univerziteta u Beogradu, Kraljice Marije 12, 11000 Belgrade, Republic of Serbia
2. Boza Milic – Osnovi Fizike Gasne Plazme (1989) Prirodno Matematicki Fakultet Univerziteta u Beogradu, Studentski Trg 13, 11000 Belgrade, SFRY
3. Yuri P. Raizer – Gas Discharge Physics (1987) The Institute for Problems in Mechanics, USSR Academy of Sciences, Varnadsky Street 101, SU-117526 Moscow, USSR
4. A. I. Morozov – Principles of coaxial (quasi) stationary plasma accelerators (1990) Sov. J. Plasma Phy., Moscow, USSR
5. Alfven H. (1942) – Existence of Electromagnetic-Hydrodynamics Waves, Nature, doi: 10.1038/150405d0
6. J. Puric, I.P. Dojcinovic, V.M. Astasinjski, M.M. Kuraica, B.M. Obradovic (2004) – Electirc and Tehrmodyniamic Properties of Plasma Flows Created by a Magnetoplasma Compressor, Plasma Sources Sci. Technol.
7. D. G. Pellinen, M. S. DiCipua, S. E. Sampayan, H. Gerbracht, and M. Wang (1980) – Rogowski coil for measuring fast, high level pulsed current, Rev.Sci.Instr 51, 1535; doi 10.1063/1.1136119

8. N. Nachev, M. Fedorov (1977) – Teorija aviacionih gazoturbinnih dvigatelei, Moskva, USSR
9. V. H. Abianc, (1953) – Teorija aviacionih gazovih turbin, Moskva, USSR
10. A. I. Morozov (1975) – The conceptual development of stationery plasma thrusters, Sov. J. Plasma Phys. 1 95, Moscow, USSR
11. Milovan A. Pavlovic (2020) – Numericko i eksperimentalno odredjivanje numerickog impulsa plasma propulsora, Master Rad - Masinski Fakultet, Univerziteta u Beogradu
12. Lj. Ristovski (1986) – Fizika kontinuuma – Fluidi, PMF Univerziteta u Beogradu, Jugoslovenski zavod za produktivnost rada, Beograd, SFRY
13. A. I. Morozov (1974) – Fizika i primenie plazmenjih uskoritelij, Nauka i Tehnika, Minsk, USSR
14. J. J. Lowke (1997) – A Unified Theory of Arcs and their Electrodes, J. Phys. IV France Vol. 7, C4-283-C4-294
15. G. Hauke and T. J. R. Hughes (1994) – A Unified Approach to Compressible and Incompressible Flows, Comp. Meth. Appl. Mech. Engineering, vol. 113
16. The NIST Reference on Constants, Units, and Uncertainty, http://physics.nist.gov/cuu/Constants/index.html
17. COMSOL Multiphysics Users Guide.

Global Journals Guidelines Handbook 2023

www.GlobalJournals.org

Memberships

Fellows/Associates of Science Frontier Research Council

FSFRC/ASFRC Memberships

Introduction

FSFRC/ASFRC is the most prestigious membership of Global Journals accredited by Open Association of Research Society, U.S.A (OARS). The credentials of Fellow and Associate designations signify that the researcher has gained the knowledge of the fundamental and high-level concepts, and is a subject matter expert, proficient in an expertise course covering the professional code of conduct, and follows recognized standards of practice. The credentials are designated only to the researchers, scientists, and professionals that have been selected by a rigorous process by our Editorial Board and Management Board.

Associates of FSFRC/ASFRC are scientists and researchers from around the world are working on projects/researches that have huge potentials. Members support Global Journals' mission to advance technology for humanity and the profession.

FSFRC

Fellow of Science Frontier Research Council

FELLOW OF SCIENCE FRONTIER RESEARCH COUNCIL is the most prestigious membership of Global Journals. It is an award and membership granted to individuals that the Open Association of Research Society judges to have made a 'substantial contribution to the improvement of computer science, technology, and electronics engineering.

The primary objective is to recognize the leaders in research and scientific fields of the current era with a global perspective and to create a channel between them and other researchers for better exposure and knowledge sharing. Members are most eminent scientists, engineers, and technologists from all across the world. Fellows are elected for life through a peer review process on the basis of excellence in the respective domain. There is no limit on the number of new nominations made in any year. Each year, the Open Association of Research Society elect up to 12 new Fellow Members.

Benefit

To the institution

Get letter of appreciation

Global Journals sends a letter of appreciation of author to the Dean or CEO of the University or Company of which author is a part, signed by editor in chief or chief author.

Exclusive Network

Get access to a closed network

A FSFRC member gets access to a closed network of Tier 1 researchers and scientists with direct communication channel through our website. Fellows can reach out to other members or researchers directly. They should also be open to reaching out by other.

Career | Credibility | Exclusive | Reputation

Certificate

Receive a print ed copy of a certificate

Fellows receive a printed copy of a certificate signed by our Chief Author that may be used for academic purposes and a personal recommendation letter to the dean of member's university.

Career | Credibility | Exclusive | Reputation

Designation

Get honored title of membership

Fellows can use the honored title of membership. The “FSFRC” is an honored title which is accorded to a person’s name viz. Dr. John E. Hall, Ph.D., FSFRC or William Walldroff, M.S., FSFRC.

Career | Credibility | Exclusive | Reputation

Recognition on the Platform

Better visibility and citation

All the Fellow members of FSFRC get a badge of "Leading Member of Global Journals" on the Research Community that distinguishes them from others. Additionally, the profile is also partially maintained by our team for better visibility and citation. All fellows get a dedicated page on the website with their biography.

Career | Credibility | Reputation

Future Work

Get discounts on the future publications

Fellows receive discounts on future publications with Global Journals up to 60%. Through our recommendation programs, members also receive discounts on publications made with OARS affiliated organizations.

Career | Financial

GJ Internal Account

Unlimited forward of Emails

Fellows get secure and fast GJ work emails with unlimited forward of emails that they may use them as their primary email. For example,
john [AT] globaljournals [DOT] org.

Career | Credibility | Reputation

Premium Tools

Access to all the premium tools

To take future researches to the zenith, fellows and associates receive access to all the premium tools that Global Journals have to offer along with the partnership with some of the best marketing leading tools out there.

Financial

Conferences & Events

Organize seminar/conference

Fellows are authorized to organize symposium/seminar/conference on behalf of Global Journal Incorporation (USA). They can also participate in the same organized by another institution as representative of Global Journal. In both the cases, it is mandatory for him to discuss with us and obtain our consent. Additionally, they get free research conferences (and others) alerts.

Career | Credibility | Financial

Early Invitations

Early invitations to all the symposiums, seminars, conferences

All fellows receive the early invitations to all the symposiums, seminars, conferences and webinars hosted by Global Journals in their subject.

Exclusive

Publishing Articles & Books

Earn 60% of sales proceeds

Fellows can publish articles (limited) without any fees. Also, they can earn up to 60% of sales proceeds from the sale of reference/review books/literature/ publishing of research paper. The FSFRC member can decide its price and we can help in making the right decision.

Exclusive | Financial

Reviewers

Get a remuneration of 15% of author fees

Fellow members are eligible to join as a paid peer reviewer at Global Journals Incorporation (USA) and can get a remuneration of 15% of author fees, taken from the author of a respective paper.

Financial

Access to Editorial Board

Become a member of the Editorial Board

Fellows may join as a member of the Editorial Board of Global Journals Incorporation (USA) after successful completion of three years as Fellow and as Peer Reviewer. Additionally, Fellows get a chance to nominate other members for Editorial Board.

Career | Credibility | Exclusive | Reputation

And Much More

Get access to scientific museums and observatories across the globe

All members get access to 5 selected scientific museums and observatories across the globe. All researches published with Global Journals will be kept under deep archival facilities across regions for future protections and disaster recovery. They get 10 GB free secure cloud access for storing research files.

ASSOCIATE OF SCIENCE FRONTIER RESEARCH COUNCIL

ASSOCIATE OF SCIENCE FRONTIER RESEARCH COUNCIL is the membership of Global Journals awarded to individuals that the Open Association of Research Society judges to have made a 'substantial contribution to the improvement of computer science, technology, and electronics engineering.

The primary objective is to recognize the leaders in research and scientific fields of the current era with a global perspective and to create a channel between them and other researchers for better exposure and knowledge sharing. Members are most eminent scientists, engineers, and technologists from all across the world. Associate membership can later be promoted to Fellow Membership. Associates are elected for life through a peer review process on the basis of excellence in the respective domain. There is no limit on the number of new nominations made in any year. Each year, the Open Association of Research Society elect up to 12 new Associate Members.

To the institution

Get letter of appreciation

Global Journals sends a letter of appreciation of author to the Dean or CEO of the University or Company of which author is a part, signed by editor in chief or chief author.

Exclusive Network

Get access to a closed network

A ASFRC member gets access to a closed network of Tier 1 researchers and scientists with direct communication channel through our website. Associates can reach out to other members or researchers directly. They should also be open to reaching out by other.

Career | Credibility | Exclusive | Reputation

Certificate

Receive a print ed copy of a certificate

Associates receive a printed copy of a certificate signed by our Chief Author that may be used for academic purposes and a personal recommendation letter to the dean of member's university.

Career | Credibility | Exclusive | Reputation

Designation

Get honored title of membership

Associates can use the honored title of membership. The “ASFRC” is an honored title which is accorded to a person’s name viz. Dr. John E. Hall, Ph.D., ASFRC or William Walldroff, M.S., ASFRC.

Career | Credibility | Exclusive | Reputation

Recognition on the Platform

Better visibility and citation

All the Associate members of ASFRC get a badge of "Leading Member of Global Journals" on the Research Community that distinguishes them from others. Additionally, the profile is also partially maintained by our team for better visibility and citation. All associates get a dedicated page on the website with their biography.

Career | Credibility | Reputation

Future Work

Get discounts on the future publications

Associates receive discounts on the future publications with Global Journals up to 60%. Through our recommendation programs, members also receive discounts on publications made with OARS affiliated organizations.

Career | Financial

GJ Internal Account

Unlimited forward of Emails

Associates get secure and fast GJ work emails with unlimited forward of emails that they may use them as their primary email. For example,
john [AT] globaljournals [DOT] org.

Career | Credibility | Reputation

Premium Tools

Access to all the premium tools

To take future researches to the zenith, fellows receive access to almost all the premium tools that Global Journals have to offer along with the partnership with some of the best marketing leading tools out there.

Financial

Conferences & Events

Organize seminar/conference

Associates are authorized to organize symposium/seminar/conference on behalf of Global Journal Incorporation (USA). They can also participate in the same organized by another institution as representative of Global Journal. In both the cases, it is mandatory for him to discuss with us and obtain our consent. Additionally, they get free research conferences (and others) alerts.

Career | Credibility | Financial

Early Invitations

Early invitations to all the symposiums, seminars, conferences

All associates receive the early invitations to all the symposiums, seminars, conferences and webinars hosted by Global Journals in their subject.

Exclusive

Publishing Articles & Books

Earn 30-40% of sales proceeds

Associates can publish articles (limited) without any fees. Also, they can earn up to 30-40% of sales proceeds from the sale of reference/review books/literature/publishing of research paper.

Exclusive | Financial

Reviewers

Get a remuneration of 15% of author fees

Associate members are eligible to join as a paid peer reviewer at Global Journals Incorporation (USA) and can get a remuneration of 15% of author fees, taken from the author of a respective paper.

Financial

And Much More

Get access to scientific museums and observatories across the globe

All members get access to 2 selected scientific museums and observatories across the globe. All researches published with Global Journals will be kept under deep archival facilities across regions for future protections and disaster recovery. They get 5 GB free secure cloud access for storing research files.

Associate	Fellow	Research Group	Basic
$4800 **lifetime designation**	$6800 **lifetime designation**	$12500.00 **organizational**	APC **per article**
Certificate, LoR and Momento **2** discounted publishing/year **Gradation** of Research **10** research contacts/day **1 GB** Cloud Storage **GJ** Community Access	**Certificate,** LoR and Momento **Unlimited** discounted publishing/year **Gradation** of Research **Unlimited** research contacts/day **5 GB** Cloud Storage **Online Presense** Assistance **GJ** Community Access	**Certificates,** LoRs and Momentos **Unlimited** free publishing/year **Gradation** of Research **Unlimited** research contacts/day **Unlimited** Cloud Storage **Online Presense** Assistance **GJ** Community Access	**GJ** Community Access

Preferred Author Guidelines

We accept the manuscript submissions in any standard (generic) format.

We typeset manuscripts using advanced typesetting tools like Adobe In Design, CorelDraw, TeXnicCenter, and TeXStudio. We usually recommend authors submit their research using any standard format they are comfortable with, and let Global Journals do the rest.

Alternatively, you can download our basic template from https://globaljournals.org/Template.zip

Authors should submit their complete paper/article, including text illustrations, graphics, conclusions, artwork, and tables. Authors who are not able to submit manuscript using the form above can email the manuscript department at submit@globaljournals.org or get in touch with chiefeditor@globaljournals.org if they wish to send the abstract before submission.

Before and during Submission

Authors must ensure the information provided during the submission of a paper is authentic. Please go through the following checklist before submitting:

1. Authors must go through the complete author guideline and understand and *agree to Global Journals' ethics and code of conduct,* along with author responsibilities.
2. Authors must accept the privacy policy, terms, and conditions of Global Journals.
3. Ensure corresponding author's email address and postal address are accurate and reachable.
4. Manuscript to be submitted must include keywords, an abstract, a paper title, co-author(s') names and details (email address, name, phone number, and institution), figures and illustrations in vector format including appropriate captions, tables, including titles and footnotes, a conclusion, results, acknowledgments and references.
5. Authors should submit paper in a ZIP archive if any supplementary files are required along with the paper.
6. Proper permissions must be acquired for the use of any copyrighted material.
7. Manuscript submitted *must not have been submitted or published elsewhere* and all authors must be aware of the submission.

Declaration of Conflicts of Interest

It is required for authors to declare all financial, institutional, and personal relationships with other individuals and organizations that could influence (bias) their research.

Policy on Plagiarism

Plagiarism is not acceptable in Global Journals submissions at all.

Plagiarized content will not be considered for publication. We reserve the right to inform authors' institutions about plagiarism detected either before or after publication. If plagiarism is identified, we will follow COPE guidelines:

Authors are solely responsible for all the plagiarism that is found. The author must not fabricate, falsify or plagiarize existing research data. The following, if copied, will be considered plagiarism:

- Words (language)
- Ideas
- Findings
- Writings
- Diagrams
- Graphs
- Illustrations
- Lectures

- Printed material
- Graphic representations
- Computer programs
- Electronic material
- Any other original work

Authorship Policies

Global Journals follows the definition of authorship set up by the Open Association of Research Society, USA. According to its guidelines, authorship criteria must be based on:

1. Substantial contributions to the conception and acquisition of data, analysis, and interpretation of findings.
2. Drafting the paper and revising it critically regarding important academic content.
3. Final approval of the version of the paper to be published.

Changes in Authorship

The corresponding author should mention the name and complete details of all co-authors during submission and in manuscript. We support addition, rearrangement, manipulation, and deletions in authors list till the early view publication of the journal. We expect that corresponding author will notify all co-authors of submission. We follow COPE guidelines for changes in authorship.

Copyright

During submission of the manuscript, the author is confirming an exclusive license agreement with Global Journals which gives Global Journals the authority to reproduce, reuse, and republish authors' research. We also believe in flexible copyright terms where copyright may remain with authors/employers/institutions as well. Contact your editor after acceptance to choose your copyright policy. You may follow this form for copyright transfers.

Appealing Decisions

Unless specified in the notification, the Editorial Board's decision on publication of the paper is final and cannot be appealed before making the major change in the manuscript.

Acknowledgments

Contributors to the research other than authors credited should be mentioned in Acknowledgments. The source of funding for the research can be included. Suppliers of resources may be mentioned along with their addresses.

Declaration of funding sources

Global Journals is in partnership with various universities, laboratories, and other institutions worldwide in the research domain. Authors are requested to disclose their source of funding during every stage of their research, such as making analysis, performing laboratory operations, computing data, and using institutional resources, from writing an article to its submission. This will also help authors to get reimbursements by requesting an open access publication letter from Global Journals and submitting to the respective funding source.

Preparing your Manuscript

Authors can submit papers and articles in an acceptable file format: MS Word (doc, docx), LaTeX (.tex, .zip or .rar including all of your files), Adobe PDF (.pdf), rich text format (.rtf), simple text document (.txt), Open Document Text (.odt), and Apple Pages (.pages). Our professional layout editors will format the entire paper according to our official guidelines. This is one of the highlights of publishing with Global Journals—authors should not be concerned about the formatting of their paper. Global Journals accepts articles and manuscripts in every major language, be it Spanish, Chinese, Japanese, Portuguese, Russian, French, German, Dutch, Italian, Greek, or any other national language, but the title, subtitle, and abstract should be in English. This will facilitate indexing and the pre-peer review process.

The following is the official style and template developed for publication of a research paper. Authors are not required to follow this style during the submission of the paper. It is just for reference purposes.

Manuscript Style Instruction (Optional)

- Microsoft Word Document Setting Instructions.
- Font type of all text should be Swis721 Lt BT.
- Page size: 8.27" x 11'", left margin: 0.65, right margin: 0.65, bottom margin: 0.75.
- Paper title should be in one column of font size 24.
- Author name in font size of 11 in one column.
- Abstract: font size 9 with the word "Abstract" in bold italics.
- Main text: font size 10 with two justified columns.
- Two columns with equal column width of 3.38 and spacing of 0.2.
- First character must be three lines drop-capped.
- The paragraph before spacing of 1 pt and after of 0 pt.
- Line spacing of 1 pt.
- Large images must be in one column.
- The names of first main headings (Heading 1) must be in Roman font, capital letters, and font size of 10.
- The names of second main headings (Heading 2) must not include numbers and must be in italics with a font size of 10.

Structure and Format of Manuscript

The recommended size of an original research paper is under 15,000 words and review papers under 7,000 words. Research articles should be less than 10,000 words. Research papers are usually longer than review papers. Review papers are reports of significant research (typically less than 7,000 words, including tables, figures, and references)

A research paper must include:

a) A title which should be relevant to the theme of the paper.
b) A summary, known as an abstract (less than 150 words), containing the major results and conclusions.
c) Up to 10 keywords that precisely identify the paper's subject, purpose, and focus.
d) An introduction, giving fundamental background objectives.
e) Resources and techniques with sufficient complete experimental details (wherever possible by reference) to permit repetition, sources of information must be given, and numerical methods must be specified by reference.
f) Results which should be presented concisely by well-designed tables and figures.
g) Suitable statistical data should also be given.
h) All data must have been gathered with attention to numerical detail in the planning stage.

Design has been recognized to be essential to experiments for a considerable time, and the editor has decided that any paper that appears not to have adequate numerical treatments of the data will be returned unrefereed.

i) Discussion should cover implications and consequences and not just recapitulate the results; conclusions should also be summarized.
j) There should be brief acknowledgments.
k) There ought to be references in the conventional format. Global Journals recommends APA format.

Authors should carefully consider the preparation of papers to ensure that they communicate effectively. Papers are much more likely to be accepted if they are carefully designed and laid out, contain few or no errors, are summarizing, and follow instructions. They will also be published with much fewer delays than those that require much technical and editorial correction.

The Editorial Board reserves the right to make literary corrections and suggestions to improve brevity.

Format Structure

It is necessary that authors take care in submitting a manuscript that is written in simple language and adheres to published guidelines.

All manuscripts submitted to Global Journals should include:

Title

The title page must carry an informative title that reflects the content, a running title (less than 45 characters together with spaces), names of the authors and co-authors, and the place(s) where the work was carried out.

Author details

The full postal address of any related author(s) must be specified.

Abstract

The abstract is the foundation of the research paper. It should be clear and concise and must contain the objective of the paper and inferences drawn. It is advised to not include big mathematical equations or complicated jargon.

Many researchers searching for information online will use search engines such as Google, Yahoo or others. By optimizing your paper for search engines, you will amplify the chance of someone finding it. In turn, this will make it more likely to be viewed and cited in further works. Global Journals has compiled these guidelines to facilitate you to maximize the web-friendliness of the most public part of your paper.

Keywords

A major lynchpin of research work for the writing of research papers is the keyword search, which one will employ to find both library and internet resources. Up to eleven keywords or very brief phrases have to be given to help data retrieval, mining, and indexing.

One must be persistent and creative in using keywords. An effective keyword search requires a strategy: planning of a list of possible keywords and phrases to try.

Choice of the main keywords is the first tool of writing a research paper. Research paper writing is an art. Keyword search should be as strategic as possible.

One should start brainstorming lists of potential keywords before even beginning searching. Think about the most important concepts related to research work. Ask, “What words would a source have to include to be truly valuable in a research paper?” Then consider synonyms for the important words.

It may take the discovery of only one important paper to steer in the right keyword direction because, in most databases, the keywords under which a research paper is abstracted are listed with the paper.

Numerical Methods

Numerical methods used should be transparent and, where appropriate, supported by references.

Abbreviations

Authors must list all the abbreviations used in the paper at the end of the paper or in a separate table before using them.

Formulas and equations

Authors are advised to submit any mathematical equation using either MathJax, KaTeX, or LaTeX, or in a very high-quality image.

Tables, Figures, and Figure Legends

Tables: Tables should be cautiously designed, uncrowned, and include only essential data. Each must have an Arabic number, e.g., Table 4, a self-explanatory caption, and be on a separate sheet. Authors must submit tables in an editable format and not as images. References to these tables (if any) must be mentioned accurately.

Figures

Figures are supposed to be submitted as separate files. Always include a citation in the text for each figure using Arabic numbers, e.g., Fig. 4. Artwork must be submitted online in vector electronic form or by emailing it.

Preparation of Eletronic Figures for Publication

Although low-quality images are sufficient for review purposes, print publication requires high-quality images to prevent the final product being blurred or fuzzy. Submit (possibly by e-mail) EPS (line art) or TIFF (halftone/ photographs) files only. MS PowerPoint and Word Graphics are unsuitable for printed pictures. Avoid using pixel-oriented software. Scans (TIFF only) should have a resolution of at least 350 dpi (halftone) or 700 to 1100 dpi (line drawings). Please give the data for figures in black and white or submit a Color Work Agreement form. EPS files must be saved with fonts embedded (and with a TIFF preview, if possible).

For scanned images, the scanning resolution at final image size ought to be as follows to ensure good reproduction: line art: >650 dpi; halftones (including gel photographs): >350 dpi; figures containing both halftone and line images: >650 dpi.

Color charges: Authors are advised to pay the full cost for the reproduction of their color artwork. Hence, please note that if there is color artwork in your manuscript when it is accepted for publication, we would require you to complete and return a Color Work Agreement form before your paper can be published. Also, you can email your editor to remove the color fee after acceptance of the paper.

Tips for Writing a Good Quality Science Frontier Research Paper

Techniques for writing a good quality Science Frontier Research paper:

1. Choosing the topic: In most cases, the topic is selected by the interests of the author, but it can also be suggested by the guides. You can have several topics, and then judge which you are most comfortable with. This may be done by asking several questions of yourself, like "Will I be able to carry out a search in this area? Will I find all necessary resources to accomplish the search? Will I be able to find all information in this field area?" If the answer to this type of question is "yes," then you ought to choose that topic. In most cases, you may have to conduct surveys and visit several places. Also, you might have to do a lot of work to find all the rises and falls of the various data on that subject. Sometimes, detailed information plays a vital role, instead of short information. Evaluators are human: The first thing to remember is that evaluators are also human beings. They are not only meant for rejecting a paper. They are here to evaluate your paper. So present your best aspect.

2. Think like evaluators: If you are in confusion or getting demotivated because your paper may not be accepted by the evaluators, then think, and try to evaluate your paper like an evaluator. Try to understand what an evaluator wants in your research paper, and you will automatically have your answer. Make blueprints of paper: The outline is the plan or framework that will help you to arrange your thoughts. It will make your paper logical. But remember that all points of your outline must be related to the topic you have chosen.

3. Ask your guides: If you are having any difficulty with your research, then do not hesitate to share your difficulty with your guide (if you have one). They will surely help you out and resolve your doubts. If you can't clarify what exactly you require for your work, then ask your supervisor to help you with an alternative. He or she might also provide you with a list of essential readings.

4. Use of computer is recommended: As you are doing research in the field of science frontier then this point is quite obvious. Use right software: Always use good quality software packages. If you are not capable of judging good software, then you can lose the quality of your paper unknowingly. There are various programs available to help you which you can get through the internet.

5. Use the internet for help: An excellent start for your paper is using Google. It is a wondrous search engine, where you can have your doubts resolved. You may also read some answers for the frequent question of how to write your research paper or find a model research paper. You can download books from the internet. If you have all the required books, place importance on reading, selecting, and analyzing the specified information. Then sketch out your research paper. Use big pictures: You may use encyclopedias like Wikipedia to get pictures with the best resolution. At Global Journals, you should strictly follow here.

6. Bookmarks are useful: When you read any book or magazine, you generally use bookmarks, right? It is a good habit which helps to not lose your continuity. You should always use bookmarks while searching on the internet also, which will make your search easier.

7. Revise what you wrote: When you write anything, always read it, summarize it, and then finalize it.

8. Make every effort: Make every effort to mention what you are going to write in your paper. That means always have a good start. Try to mention everything in the introduction—what is the need for a particular research paper. Polish your work with good writing skills and always give an evaluator what he wants. Make backups: When you are going to do any important thing like making a research paper, you should always have backup copies of it either on your computer or on paper. This protects you from losing any portion of your important data.

9. Produce good diagrams of your own: Always try to include good charts or diagrams in your paper to improve quality. Using several unnecessary diagrams will degrade the quality of your paper by creating a hodgepodge. So always try to include diagrams which were made by you to improve the readability of your paper. Use of direct quotes: When you do research relevant to literature, history, or current affairs, then use of quotes becomes essential, but if the study is relevant to science, use of quotes is not preferable.

10. Use proper verb tense: Use proper verb tenses in your paper. Use past tense to present those events that have happened. Use present tense to indicate events that are going on. Use future tense to indicate events that will happen in the future. Use of wrong tenses will confuse the evaluator. Avoid sentences that are incomplete.

11. Pick a good study spot: Always try to pick a spot for your research which is quiet. Not every spot is good for studying.

12. Know what you know: Always try to know what you know by making objectives, otherwise you will be confused and unable to achieve your target.

13. Use good grammar: Always use good grammar and words that will have a positive impact on the evaluator; use of good vocabulary does not mean using tough words which the evaluator has to find in a dictionary. Do not fragment sentences. Eliminate one-word sentences. Do not ever use a big word when a smaller one would suffice.

Verbs have to be in agreement with their subjects. In a research paper, do not start sentences with conjunctions or finish them with prepositions. When writing formally, it is advisable to never split an infinitive because someone will (wrongly) complain. Avoid clichés like a disease. Always shun irritating alliteration. Use language which is simple and straightforward. Put together a neat summary.

14. Arrangement of information: Each section of the main body should start with an opening sentence, and there should be a changeover at the end of the section. Give only valid and powerful arguments for your topic. You may also maintain your arguments with records.

15. Never start at the last minute: Always allow enough time for research work. Leaving everything to the last minute will degrade your paper and spoil your work.

16. Multitasking in research is not good: Doing several things at the same time is a bad habit in the case of research activity. Research is an area where everything has a particular time slot. Divide your research work into parts, and do a particular part in a particular time slot.

17. Never copy others' work: Never copy others' work and give it your name because if the evaluator has seen it anywhere, you will be in trouble. Take proper rest and food: No matter how many hours you spend on your research activity, if you are not taking care of your health, then all your efforts will have been in vain. For quality research, take proper rest and food.

18. Go to seminars: Attend seminars if the topic is relevant to your research area. Utilize all your resources.

19. Refresh your mind after intervals: Try to give your mind a rest by listening to soft music or sleeping in intervals. This will also improve your memory. Acquire colleagues: Always try to acquire colleagues. No matter how sharp you are, if you acquire colleagues, they can give you ideas which will be helpful to your research.

20. Think technically: Always think technically. If anything happens, search for its reasons, benefits, and demerits. Think and then print: When you go to print your paper, check that tables are not split, headings are not detached from their descriptions, and page sequence is maintained.

21. Adding unnecessary information: Do not add unnecessary information like "I have used MS Excel to draw graphs." Irrelevant and inappropriate material is superfluous. Foreign terminology and phrases are not apropos. One should never take a broad view. Analogy is like feathers on a snake. Use words properly, regardless of how others use them. Remove quotations. Puns are for kids, not grunt readers. Never oversimplify: When adding material to your research paper, never go for oversimplification; this will definitely irritate the evaluator. Be specific. Never use rhythmic redundancies. Contractions shouldn't be used in a research paper. Comparisons are as terrible as clichés. Give up ampersands, abbreviations, and so on. Remove commas that are not necessary. Parenthetical words should be between brackets or commas. Understatement is always the best way to put forward earth-shaking thoughts. Give a detailed literary review.

22. Report concluded results: Use concluded results. From raw data, filter the results, and then conclude your studies based on measurements and observations taken. An appropriate number of decimal places should be used. Parenthetical remarks are prohibited here. Proofread carefully at the final stage. At the end, give an outline to your arguments. Spot perspectives of further study of the subject. Justify your conclusion at the bottom sufficiently, which will probably include examples.

23. Upon conclusion: Once you have concluded your research, the next most important step is to present your findings. Presentation is extremely important as it is the definite medium though which your research is going to be in print for the rest of the crowd. Care should be taken to categorize your thoughts well and present them in a logical and neat manner. A good quality research paper format is essential because it serves to highlight your research paper and bring to light all necessary aspects of your research.

Informal Guidelines of Research Paper Writing

Key points to remember:

- Submit all work in its final form.
- Write your paper in the form which is presented in the guidelines using the template.
- Please note the criteria peer reviewers will use for grading the final paper.

Final points:

One purpose of organizing a research paper is to let people interpret your efforts selectively. The journal requires the following sections, submitted in the order listed, with each section starting on a new page:

The introduction: This will be compiled from reference matter and reflect the design processes or outline of basis that directed you to make a study. As you carry out the process of study, the method and process section will be constructed like that. The results segment will show related statistics in nearly sequential order and direct reviewers to similar intellectual paths throughout the data that you gathered to carry out your study.

The discussion section:

This will provide understanding of the data and projections as to the implications of the results. The use of good quality references throughout the paper will give the effort trustworthiness by representing an alertness to prior workings.

Writing a research paper is not an easy job, no matter how trouble-free the actual research or concept. Practice, excellent preparation, and controlled record-keeping are the only means to make straightforward progression.

General style:

Specific editorial column necessities for compliance of a manuscript will always take over from directions in these general guidelines.

To make a paper clear: Adhere to recommended page limits.

Mistakes to avoid:

- Insertion of a title at the foot of a page with subsequent text on the next page.
- Separating a table, chart, or figure—confine each to a single page.
- Submitting a manuscript with pages out of sequence.
- In every section of your document, use standard writing style, including articles ("a" and "the").
- Keep paying attention to the topic of the paper.
- Use paragraphs to split each significant point (excluding the abstract).
- Align the primary line of each section.
- Present your points in sound order.
- Use present tense to report well-accepted matters.
- Use past tense to describe specific results.
- Do not use familiar wording; don't address the reviewer directly. Don't use slang or superlatives.
- Avoid use of extra pictures—include only those figures essential to presenting results.

Title page:

Choose a revealing title. It should be short and include the name(s) and address(es) of all authors. It should not have acronyms or abbreviations or exceed two printed lines.

Abstract: This summary should be two hundred words or less. It should clearly and briefly explain the key findings reported in the manuscript and must have precise statistics. It should not have acronyms or abbreviations. It should be logical in itself. Do not cite references at this point.

An abstract is a brief, distinct paragraph summary of finished work or work in development. In a minute or less, a reviewer can be taught the foundation behind the study, common approaches to the problem, relevant results, and significant conclusions or new questions.

Write your summary when your paper is completed because how can you write the summary of anything which is not yet written? Wealth of terminology is very essential in abstract. Use comprehensive sentences, and do not sacrifice readability for brevity; you can maintain it succinctly by phrasing sentences so that they provide more than a lone rationale. The author can at this moment go straight to shortening the outcome. Sum up the study with the subsequent elements in any summary. Try to limit the initial two items to no more than one line each.

Reason for writing the article—theory, overall issue, purpose.

- Fundamental goal.
- To-the-point depiction of the research.
- Consequences, including definite statistics—if the consequences are quantitative in nature, account for this; results of any numerical analysis should be reported. Significant conclusions or questions that emerge from the research.

Approach:

- Single section and succinct.
- An outline of the job done is always written in past tense.
- Concentrate on shortening results—limit background information to a verdict or two.
- Exact spelling, clarity of sentences and phrases, and appropriate reporting of quantities (proper units, important statistics) are just as significant in an abstract as they are anywhere else.

Introduction:

The introduction should "introduce" the manuscript. The reviewer should be presented with sufficient background information to be capable of comprehending and calculating the purpose of your study without having to refer to other works. The basis for the study should be offered. Give the most important references, but avoid making a comprehensive appraisal of the topic. Describe the problem visibly. If the problem is not acknowledged in a logical, reasonable way, the reviewer will give no attention to your results. Speak in common terms about techniques used to explain the problem, if needed, but do not present any particulars about the protocols here.

The following approach can create a valuable beginning:

- Explain the value (significance) of the study.
- Defend the model—why did you employ this particular system or method? What is its compensation? Remark upon its appropriateness from an abstract point of view as well as pointing out sensible reasons for using it.
- Present a justification. State your particular theory(-ies) or aim(s), and describe the logic that led you to choose them.
- Briefly explain the study's tentative purpose and how it meets the declared objectives.

Approach:

Use past tense except for when referring to recognized facts. After all, the manuscript will be submitted after the entire job is done. Sort out your thoughts; manufacture one key point for every section. If you make the four points listed above, you will need at least four paragraphs. Present surrounding information only when it is necessary to support a situation. The reviewer does not desire to read everything you know about a topic. Shape the theory specifically—do not take a broad view.

As always, give awareness to spelling, simplicity, and correctness of sentences and phrases.

Procedures (methods and materials):

This part is supposed to be the easiest to carve if you have good skills. A soundly written procedures segment allows a capable scientist to replicate your results. Present precise information about your supplies. The suppliers and clarity of reagents can be helpful bits of information. Present methods in sequential order, but linked methodologies can be grouped as a segment. Be concise when relating the protocols. Attempt to give the least amount of information that would permit another capable scientist to replicate your outcome, but be cautious that vital information is integrated. The use of subheadings is suggested and ought to be synchronized with the results section.

When a technique is used that has been well-described in another section, mention the specific item describing the way, but draw the basic principle while stating the situation. The purpose is to show all particular resources and broad procedures so that another person may use some or all of the methods in one more study or referee the scientific value of your work. It is not to be a step-by-step report of the whole thing you did, nor is a methods section a set of orders.

Materials:

Materials may be reported in part of a section or else they may be recognized along with your measures.

Methods:

- Report the method and not the particulars of each process that engaged the same methodology.
- Describe the method entirely.
- To be succinct, present methods under headings dedicated to specific dealings or groups of measures.
- Simplify—detail how procedures were completed, not how they were performed on a particular day.
- If well-known procedures were used, account for the procedure by name, possibly with a reference, and that's all.

Approach:

It is embarrassing to use vigorous voice when documenting methods without using first person, which would focus the reviewer's interest on the researcher rather than the job. As a result, when writing up the methods, most authors use third person passive voice.

Use standard style in this and every other part of the paper—avoid familiar lists, and use full sentences.

What to keep away from:

- Resources and methods are not a set of information.
- Skip all descriptive information and surroundings—save it for the argument.
- Leave out information that is immaterial to a third party.

Results:

The principle of a results segment is to present and demonstrate your conclusion. Create this part as entirely objective details of the outcome, and save all understanding for the discussion.

The page length of this segment is set by the sum and types of data to be reported. Use statistics and tables, if suitable, to present consequences most efficiently.

You must clearly differentiate material which would usually be incorporated in a study editorial from any unprocessed data or additional appendix matter that would not be available. In fact, such matters should not be submitted at all except if requested by the instructor.

Content:

- Sum up your conclusions in text and demonstrate them, if suitable, with figures and tables.
- In the manuscript, explain each of your consequences, and point the reader to remarks that are most appropriate.
- Present a background, such as by describing the question that was addressed by creation of an exacting study.
- Explain results of control experiments and give remarks that are not accessible in a prescribed figure or table, if appropriate.
- Examine your data, then prepare the analyzed (transformed) data in the form of a figure (graph), table, or manuscript.

What to stay away from:

- Do not discuss or infer your outcome, report surrounding information, or try to explain anything.
- Do not include raw data or intermediate calculations in a research manuscript.
- Do not present similar data more than once.
- A manuscript should complement any figures or tables, not duplicate information.
- Never confuse figures with tables—there is a difference.

Approach:

As always, use past tense when you submit your results, and put the whole thing in a reasonable order.

Put figures and tables, appropriately numbered, in order at the end of the report.

If you desire, you may place your figures and tables properly within the text of your results section.

Figures and tables:

If you put figures and tables at the end of some details, make certain that they are visibly distinguished from any attached appendix materials, such as raw facts. Whatever the position, each table must be titled, numbered one after the other, and include a heading. All figures and tables must be divided from the text.

Discussion:

The discussion is expected to be the trickiest segment to write. A lot of papers submitted to the journal are discarded based on problems with the discussion. There is no rule for how long an argument should be.

Position your understanding of the outcome visibly to lead the reviewer through your conclusions, and then finish the paper with a summing up of the implications of the study. The purpose here is to offer an understanding of your results and support all of your conclusions, using facts from your research and generally accepted information, if suitable. The implication of results should be fully described.

Infer your data in the conversation in suitable depth. This means that when you clarify an observable fact, you must explain mechanisms that may account for the observation. If your results vary from your prospect, make clear why that may have happened. If your results agree, then explain the theory that the proof supported. It is never suitable to just state that the data approved the prospect, and let it drop at that. Make a decision as to whether each premise is supported or discarded or if you cannot make a conclusion with assurance. Do not just dismiss a study or part of a study as "uncertain."

Research papers are not acknowledged if the work is imperfect. Draw what conclusions you can based upon the results that you have, and take care of the study as a finished work.

- You may propose future guidelines, such as how an experiment might be personalized to accomplish a new idea.
- Give details of all of your remarks as much as possible, focusing on mechanisms.
- Make a decision as to whether the tentative design sufficiently addressed the theory and whether or not it was correctly restricted. Try to present substitute explanations if they are sensible alternatives.
- One piece of research will not counter an overall question, so maintain the large picture in mind. Where do you go next? The best studies unlock new avenues of study. What questions remain?
- Recommendations for detailed papers will offer supplementary suggestions.

Approach:

When you refer to information, differentiate data generated by your own studies from other available information. Present work done by specific persons (including you) in past tense.

Describe generally acknowledged facts and main beliefs in present tense.

The Administration Rules

Administration Rules to Be Strictly Followed before Submitting Your Research Paper to Global Journals Inc.

Please read the following rules and regulations carefully before submitting your research paper to Global Journals Inc. to avoid rejection.

Segment draft and final research paper: You have to strictly follow the template of a research paper, failing which your paper may get rejected. You are expected to write each part of the paper wholly on your own. The peer reviewers need to identify your own perspective of the concepts in your own terms. Please do not extract straight from any other source, and do not rephrase someone else's analysis. Do not allow anyone else to proofread your manuscript.

Written material: You may discuss this with your guides and key sources. Do not copy anyone else's paper, even if this is only imitation, otherwise it will be rejected on the grounds of plagiarism, which is illegal. Various methods to avoid plagiarism are strictly applied by us to every paper, and, if found guilty, you may be blacklisted, which could affect your career adversely. To guard yourself and others from possible illegal use, please do not permit anyone to use or even read your paper and file.

Criterion for Grading a Research Paper (Compilation) by Global Journals

Please note that following table is only a Grading of "Paper Compilation" and not on "Performed/Stated Research" whose grading solely depends on Individual Assigned Peer Reviewer and Editorial Board Member. These can be available only on request and after decision of Paper. This report will be the property of Global Journals.

Topics	Grades		
	A-B	**C-D**	**E-F**
Abstract	Clear and concise with appropriate content, Correct format. 200 words or below	Unclear summary and no specific data, Incorrect form Above 200 words	No specific data with ambiguous information Above 250 words
Introduction	Containing all background details with clear goal and appropriate details, flow specification, no grammar and spelling mistake, well organized sentence and paragraph, reference cited	Unclear and confusing data, appropriate format, grammar and spelling errors with unorganized matter	Out of place depth and content, hazy format
Methods and Procedures	Clear and to the point with well arranged paragraph, precision and accuracy of facts and figures, well organized subheads	Difficult to comprehend with embarrassed text, too much explanation but completed	Incorrect and unorganized structure with hazy meaning
Result	Well organized, Clear and specific, Correct units with precision, correct data, well structuring of paragraph, no grammar and spelling mistake	Complete and embarrassed text, difficult to comprehend	Irregular format with wrong facts and figures
Discussion	Well organized, meaningful specification, sound conclusion, logical and concise explanation, highly structured paragraph reference cited	Wordy, unclear conclusion, spurious	Conclusion is not cited, unorganized, difficult to comprehend
References	Complete and correct format, well organized	Beside the point, Incomplete	Wrong format and structuring

Index

A

Ablation · 28
Abscissa · 9, 55, 58
Alleviates · 28
Annihilation · 10, 3, 2, 4

C

Collisions · 27, 28
Contradicts · 21

D

Dilemma · 13, 14

H

Helical · 24, 26, 27, 28, 1, 51

I

Illusion · 4
Impedance · 28, 31, 37, 40, 42, 43, 44
Intercalation · 6, 16

M

Milestones · 1

P

Paradoxical · 20, 21
Pellets · 24, 26, 27, 28
Percolation · 3
Poincare · 2, 11, 13, 14
Precision · 5, 10, 11

S

Spatiotemporal · 24, 26

T

Triumph · 2, 23

V

Vorticity · 47, 49, 53, 56

Global Journal of Science Frontier Research

Visit us on the Web at www.GlobalJournals.org | www.JournalofScience.org
or email us at helpdesk@globaljournals.org

ISSN 9755896